A carbon deposition and sulphur poisoning study of new pyrochlore catalysts for methane reforming

A thesis submitted to Keele University in partial fulfilment of the requirements for the degree of Doctor of Philosophy

By

Zainab K. Alfatlawi

School of Chemistry and Physics

June 2019

Abstract: -

Reforming of landfill gases for the production of syngas that leads to the generation of heat or electricity is a very promising pathway considering the increasing price of oil. The dry reforming technique is a very interesting approach to reduce the greenhouse effect and convert these gases into valuable syngas. A key factor for the success of the dry reforming process is selecting a catalyst that shows high stability and activity toward dry reforming conditions as well as resistance to carbon deposition and sulphur poisoning.

This work aims to prepare a new pyrochlore catalyst as an alternative to Ni supported catalysts that suffer from deactivation because of carbon deposition and sulphur poisoning.

Several essentials factors were changed to produce a promising catalyst for methane reforming including a) the preparation method, b) the ratio of Ni doped and c) the kind of the metal doped.

The $LaCeZrNiO_7$ was prepared by the hydrothermal and the Pechini methods. The performance of the Ni-doped pyrochlore catalysts were compared with a noble metal (Ru) pyrochlore under different dry reforming conditions.

All new prepared pyrochlore catalysts were characterized using XRD, BET, SEM and TPR techniques. The pyrochlore phase was seen in all prepared materials; however an additional $La/CeZrO_4$ phase was also seen in all the hydrothermal Ni catalysts.

Generally, no significant carbon deposition was seen on all materials at temperatures above 750^{o} C and an almost complete conversion was observed at high temperatures without deactivation for both the Ni and Ru catalysts under the conditions of stoichiometric and methane-rich dry reforming.

At low temperatures, the hydrothermal 1Ni-LCZ pyrochlore catalyst, showed a significant increase in carbon deposition compared with that synthesised by the Pechini method.

However, the low hydrothermal Ni loading pyrochlore catalyst showed low carbon deposition with high activity at 650°C.

The performance of the catalysts in the presence of H_2S (10-30 ppm) was investigated under the methane-rich dry reforming and at temperatures between 700 and 1000° C. All Ni catalysts showed high resistance and complete conversion for more than 40 hours with 10 ppm of H_2S at 850°C. The Ru catalyst was however the only one to show excellent activity without complete deactivation at 30 ppm at 700°C. At a temperature of 900°C and above, no deactivation was observed even when the H_2S concentration increased for all catalysts.

Acknowledgements: -

First, I would like to thank my almighty God for showering his blessing on me.

I would like to thank my PhD supervisors, Professor Mark Ormerod and Dr Richard Darton for encouraging my research and for allowing me to grow as a researcher scientist.

My gratitude also goes to Dr John Staniforth for providing technical support for advice and for fixing devices whenever it was needed.

I would like to thank my friends in the Lennard-jones building for academic and emotional support.

I would like to acknowledge the Iraqi cultural attaché and ministry of higher education for awarding me this PhD scholarship and support me financially.

I would like to express appreciation to my beloved husband, Ghaith who stood by my side through this journey and taking care of my lovely kids Fatima and Mariam.

My beloved brothers Mohammed, Ahmed, Ali, Hussain and my sweetheart sister Zahra, words cannot express how grateful I am. Your continuous supports, appreciations and prayers of days and nights made me able to get such successes and honours.

This work is humbly dedicated to the memory of my mum Ghaidaa and my dad Kadhem who always believed in my ability to be successful in my academic area. You are gone but your belief in me has made this journey possible.

Contents

1-INTRODUCTION

Petroleum fuels have had a great influence on human success and they are currently one of the primary sources of energy. With a significantly increasing dependency on limited oil, and greenhouse gas emission expanding continuously due to the combustion of fossil fuel leading to environmental impacts on major scientific, technical and industrial sectors, these issues have led to the investigation of ways to utilize alternative and available sources of energy such as natural gas to produce useful and clean chemical fuel and consequently electrical power.[1,2,5] Natural gas reserves will help the global economy and biogas as a part of natural gas can be generated by the aerobic decomposition of organic material and contains approximately equal amount of methane and carbon dioxide.[6] Landfill sites and sewage treatment plants are another vital source of biogas .[3] Because the majority of natural gas is methane which has the ability to react with carbon dioxide the amount of greenhouse gases could be reduced by turning them into useful chemical feedstocks (synthesis gases).[2] This issue has become increasingly important in recent studies.

1-1 FUEL CELLS

The chemical energy from fossil fuels can be converted effectively in to electricity by fuel cells.[7]

Fuel cells are electrochemical instruments that have the ability to produce electricity from chemical energy directly. When comparing against the traditional power generation techniques, fuel cell technology is cleaner and more efficient. [2, 8]

Several types of fuel cell exist and each type is characterized by the electrolyte materials, the operation temperature and ionic species they transport.

All types of fuel cells have the same operating principle as illustrated in fig -1-

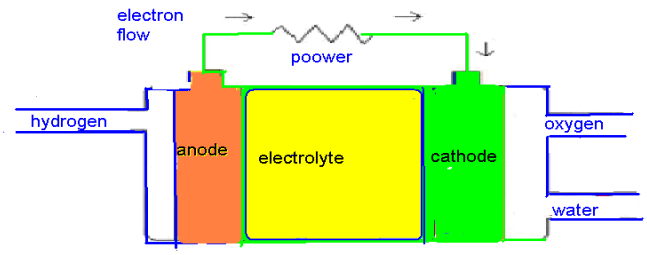

Fig.1. The general operating principles of a fuel cell

Hydrogen as the fuel is oxidized at the anode and generates proton and electrons. At the cathode oxygen is reduced to oxide ions and these oxide ions react with the protons to form water. Proton or oxide species travel through the electrolyte depending on its kind and electrons transport around an electrical circuit, producing electrical energy. [6]

In the case of commercial applications researchers are investigating both polymer electrolyte membrane fuel cells which have lower operation temperatures (80 $^{\circ}$C), require hydrogen as the fuel and the electrodes are made from carbon with a platinum electrocatalyst; and the solid oxide fuel cell which uses a solid oxide as the electrolyte, requiring elevated temperature operation (750-1000 $^{\circ}$C) using hydrocarbons as a fuel and air as the oxidant. [9]

Fuel cells which require hydrogen–rich gas streams as a fuel are potentially extremely expensive, as there is no hydrogen infrastructure present to deliver hydrogen fuel and developing this network would be a costly solution. Solid oxide fuel cells have been shown to be a promising technology that allows the utilization of a range of fuels such as petrol thanks to the high operation temperature. [6]In addition solid oxide fuel cells offer the combination of heat and power applications that increase their efficiency and also provide clean energy.[8,9]
Recently methane –based fuels have attracted huge attention and both the fundamental and technology aspects have developed significantly. For example solid oxide fuel cell (SOFC) that are fed by biogas mixture have been considered with a power efficiency of about 48.7%, whereas traditional electrical generation efficiency via a gas turbine is around 41.5 %.[9, 27)

1-2 REFORMING REACTIONS

The conversion of hydrocarbon fuels into synthesis gas (H_2+CO) can be achieved by three main chemical methods. [1, 3, 10] Steam reforming (eq 1), carbon dioxide reforming (eq 2) and partial oxidation reforming (eq 3)

$CH_4 + H_2O \longrightarrow 3H_2 + CO$ .....eq (1)

$CH_4 + CO_2 \longrightarrow 2H_2 + 2\,CO$ .....eq(2)

$CH_4 + 1/2O_2 \longrightarrow 2H_2 + CO$ .....eq(3)

The difference in the reforming roles is due to the oxidising agent, the ratio of H_2/CO, kinetics and energetics of the reaction.[1] Choice of reforming method depends on the application. For example, partial oxidation is useful for small portable systems where high efficiencies are required, whereas a high hydrogen content requires steam reforming.[2] However, in spite of the deactivation issues, when compared to the other reforming reactions, dry reforming has a 20% lower operation cost. [55]

Recently, large volumes of research have been reported focusing on hydrogen generation by methane reforming. [1, 3, 9]

1-2-1 Partial oxidation:-

Because of the rapid start-up, simpler set-up of the reformer that does not require optimizing for heat transfer thanks to its exothermic nature, the partial oxidation process has becomes useful in small portable systems. [1,2] In addition, no requirement for a water delivery system makes partial oxidation reforming less expensive, more simple and suitable for remote location which may suffer from lack of water availability. [7]However some of the associated problems with partial oxidation (POX) is the ability to undergo total oxidation (eq 4) or catalyst deactivation due to carbon deposition through methane decomposition (eq 5)

$CH_4 + 2O_2 \longrightarrow 2H_2O + CO_2$ .....eq(4)

$CH_4 \longrightarrow 2H_2 + C$ .....eq(5)

In order to overcome these difficulties, the catalysts are required to have significantly better selectivity towards synthesis gas (H_2+CO) than carbon dioxide and water.[8]

Generally POX catalysts contain Ni. The Ni anode may play dual roles: catalyze the methane reforming reaction and encourage electrochemical oxidation of H_2, CO and CH_4.[6,9] However quick carbon formations on Ni surfaces and re-oxidation of Ni lead to decreased in the performance of fuel cells. This carbon deposition becomes worse at high temperatures due to the tendency of Ni to sinter and agglomerate in to large particles. [4]

1-2-2 Steam reforming (SRM):

The most common oxidant for converting hydrocarbons to CO and H_2 is steam;[1] Although some of the CO is converted to CO_2 via water gas shift reaction(eq 6) depending on the temperature and ratio of the steam to methane:

$CO + H_2O \longrightarrow H_2 + CO_2$.....eq(6)

To achieve maximum conversion, high temperatures, low pressures and high steam to hydrocarbon ratios are required. An increased cooling effect because of the endothermic reaction at the cell inlet is one of the major problems with steam reforming which is very difficult to control and causes anode cracking.

Steam reforming catalysts encounter four main challenges:

1-Sulphur poising, even at a ppb levels block the active sites.

2- Carbon formation which crush the catalyst and block the active surface.3- Sintering due to high temperatures and high pressure of steam that may make the metal particles in the catalyst grow during the operation.

4- Activity, with the main reasons for low activity being sulphur poising or sintering that result in higher tube temperatures and even carbon formation.

More information about catalyst limits, improvement of catalysts, the process and information at the atomic level of catalysts are required for overcoming these difficulties.[13]

1-2-3 Dry reforming(DRM):-

The importance of methane dry reforming has been widely studied. This reaction produces syngas from two important greenhouse gases and can reduce the net emission of these gases.[1,4] In addition this reaction is also used to generate a wide range of products. For example, it can be used to produce higher alkenes (eq9) via Fisher-Tropsch (FT,eqn) (eq7) [15] which requires H_2:CO≈2:1 ratio and this feed ratio is provided by dry reforming and can then be combined with the reserve water-gas shift reaction (eq8) to increase the selectivity toward long chain hydrocarbons.

$(2n + 1)\ H_2 + nCO \rightarrow C_nH_{(2n+2)} + nH_2O$.....eq(7)

$nCO + nH_2O \rightarrow nCO_2 + nH_2$ .....eq(8)

The overall process is:-

$2\ nCO + (n + 1)H_2 \rightarrow C_nH_{(2n+2)} + nCO_2$.....eq(9)

Dry reforming (eq 2) is a highly endothermic reaction and requires high temperatures to reach high equilibrium syngas yields.[54]

$CH_4 + CO_2 \rightarrow 2CO + 2H_2 \quad \Delta H=247$ kJ/mol.....eq(2)

Examples to drive the endothermic reaction forward are using the heat from solar-chemical energy.[53]Tomishighe et al. also suggested utilizing partial (eq3) or complete oxidation (eq 4) due to their exothermic nature.[52]

$CH_4 + 1/2O_2 \rightarrow 2H_2 + CO \quad \Delta H = -36$ kJ/mol .....eq(3)

$CH_4 + 2O_2 \rightarrow 2H_2O + CO_2 \quad \Delta H = -803$ kJ/mol.....eq(4)

In addition the CO_2 and H_2O act as co-reactants in steam and dry reforming.

Deactivation of the catalyst because of carbon formation is one of the major problems associated with DRM. [16] Moreover, due to the endothermic nature of the reaction at high conversion, severe temperature gradients occur which leads to catalyst cracking. [14] Thus, catalyst development requires a high deactivation resistance to overcome sintering and carbon deposition. [1]

In order to eliminate high energy demand for SRM and DRM reactions, authothermal reforming (ATR) technology that is a combination both of exothermic (POM) and endothermic (SRM or DRM) reaction was developed. The ATR process can be achieved by adjusting the molar ratio of the reactants; however, the main drawback of the ATR process is the high cost of oxygen separation [52]

$7CH_4 + 3O_2 + H_2O \rightarrow 7CO + 15H_2 + CO_2 \quad \Delta H = -6.8$ kJ/mol……..eq (10)

$2CH_4 + O_2 + CO_2 \rightarrow 3H_2 + 3CO + H_2O$ ……..eq (11)

Tri-reforming process (TRM) is an endothermic process which reduces the distinct disadvantages of DRM, SRM and POM processes besides increasing both the catalyst life and process efficiency.

$20CH_4 + H_2O + 9O_2 + CO_2 \rightarrow 21CO + 41H_2 \quad \Delta H = 12.9$ kJ/mol….eq (12)

The big issue in TRM is controlling all three feeds together, as an unbalanced feed can result in the opposite effect on the catalyst. The presence of a large number of reagents causes a large number of side reactions, making the chemistry of the reforming process hard to study. [53]

1-3 Development of catalyst properties

Many current studies have been devoted to developing solid oxide fuel cells to run on hydrocarbons at low temperature, which have several advantages including being suitable for residential power generation, reducing the system cost and increasing long-term component stability .[6,9] However, cell performance decreases because the ionic conductivity reduces at low temperature. [9]Furthermore, by direct hydrocarbon feeding, rapid deactivation due to carbon deposition remains another issue for reduced-temperatures. [1]

Carbon can react directly with the catalyst and reduces the number of active site or destroys the microstructure by deposition within the metal porous structure. In addition, carbon blocks the flow of reactive gases in the system mechanically. [3]The significant issue with carbon deposition is no reaction temperature gives a completely carbon free system thermodynamically. [4] At low temperature the Boudouard reaction is favoured (eq 13))

$2CO_{(g)} \rightarrow CO_{2(g)}+C_{(S)}$ $\Delta H = -172$ kJ/mol .....eq(13)

And at higher temperatures, methane decomposition occurs (eq 5)

$CH_{4(g)} \rightarrow C_{(s)}+2H_{2(g)}$ $\Delta H = 19$ kJ/mol .....eq(5)

Developing a material to give high ionic conductivity without deleterious carbon build-up at low temperatures has been the subject of many recent studies.

Currently nickel/Yttria-Stabilized Zirconia (YSZ) is used for methane conversation. [8]

Although the nickel-based anodes have been shown to have good conductivity and catalyst activity, nickel catalysts promote carbon deposition which leads to performance degradation.[4]

In addition, nickel cermet anodes are prone to re oxidation by the oxidant which may affect the cell efficiency. Many studies have been devoted to improving redox stability and coking resistance. For example, Run and Shao [9] have reviewed the anode materials for SOFCs and the development of practical nickel based cermet anodes which utilize hydrocarbons directly.

To increase the coking resistance several strategies have been extensively investigated including:-

1-3- 1 Addition of steam /oxidant into the fuel gas to increase O/C ratio.

A steam:methane ratio of around 2.5 is used in commercial steam reforming effectively to avoiding coke formation.[45] Although steam introduction into the fuel gas can reduced coke formation, King et.al found that conversion of methane over a Ni-YSZ anode was significantly reduced from 78% to 9% after 120 hours operation at 700 °C under steam reforming conditions.[28] This deactivation was because of sintering, where small particles of Ni grow in size and thus reduce the total active surface area.

Several studies of adding O_2 or CO_2 into the methane fuel gas to prevent coke formation over nickel anode have been done, [29] but this is problematic, as it leads to a decrease in the power density due to polarization resistance which increases with increasing amounts of oxidant. These results demonstrate that the majority of Ni anodes exhibit low catalytic activity and proper modification is required.

1-3-2 Effect of polarization current:

Under polarization condition in the fuel cell, the oxygen ions (O^{-2}) move from the cathode to the anode and by increasing the polarization current, the flux of O^{-2} increases which implies the conversion of fuels as methane into CO, CO_2, H_2 and H_2O will increase.[30] Some researchers have demonstrated that polarization inhibits coke formation. For example, Koh et.al found that by applying current densities greater than 85 m A cm^{-2} coke formation could be supressed, because the carbon reacted with O^{2-} as soon as it was formed.[31]

1-3-3 Application of anode catalyst layer:

catalyst layers limit direct exposure of anode to the hydrocarbon and so reduce the coke formation process. Ru-CeO_2 was used first by Zhan and Barnet due to lower sensitivity to coking in an internal reforming.[32] This thin layer of catalyst converts hydrocarbon into syngas under current density condition . Over this catalyst layer, CH_4 and O_2 have been converted into CO and H_2. Power, H_2O and CO_2 are produced from electrochemical oxidation process during diffusion syntheses gas to the anode. The layer of catalyst by providing CO and H_2 which have higher electrochemical activity than methane, improve the performance of the cell. [33]However the anode catalyst layer reduces the diffusion rates of reactants and products because it acts as a diffusion barrier and so decreases the power output. [34] Improvements in the microstructure of the catalyst layer can enhance the cell performance. Several studies in order to improve the anode catalyst layer have been made. The optimization of the Ni content in the anode by changing preparation methods, surface acidity modification and conductivity improvement are very important functions to enhance the fuel cell performance. [9] However ,Ni based catalyst layer in spite of its lower cost could not be ideal material at reduced temperature due to low catalytic activity for hydrocarbon conversion, thus more modifications are still required.

1-3-4 Modification of the anode surface by introducing another metal:

Catalytic activity against carbon deposition can be increased by providing a small quantity of another metal as a separate phase on the surface of the Ni particles in a nickel based anode. For example, the presence of a small amount of Au effectively inhibits the decomposition of methane. [35] Results have indicated that Au prevents the dissociative adsorption of methane or the hydrogenation reaction step which causes carbon formation. However, the stability of the Au after high temperature thermal treatment decreases due to coarsening of the nanosize particles during long operation times. Other metals, such as Cu, Ru and Rh have also been used as additives. [9]Although several Ru and Rh based catalysts have been shown to have low

carbon formation ratios, these materials are prohibitively expensive [9, 56]. In addition to Au, copper is inert toward carbon deposition and shows high electronic conductivity [36]. Because carbon atoms energetically prefer the Ni (111) and Cu (111) sites, the adsorption energy of carbon could be at lower level during addition of Cu into Ni due to less overlap occurring between the C2p and the metallic 3d orbitals.

To add Cu into the Ni-based anode several methods have been reported. Wet impregnation has been used to improve dramatically the cell stability and decrease the coke formation; however, it is difficult to control the microstructure of the deposited components and the process is time consuming. [37] Another method to add active metals in to the Ni anode structure is electrochemical deposition which can control the morphology. This technique uses a direct current electro-plating method to add copper to porous electrode structures, but it is difficult to control the exact amount of electroplated copper. [38] Because of these limitations, microwave irradiation has recently been used for the synthesis of metal and metal oxide nanoparticles, however, the long term stability of this anode has still been the crucial issue up to now.[39]

1-3-5 Modification of anode surface with other oxides(s):

For practical applications, conventional Ni anodes are preferred due to their low cost, high electronic and ionic conductivity and high stability under fuel cell conditions. Many strategies have been applied to prevent the Ni surface from being directly exposed to hydrocarbon fuels to reduce carbon deposition and sintering. Oxide modifications have been extensively used to improve the anode performance via increasing coking resistance. For example, the addition of small amounts (1%) of CeO_2 to Ni-YSZ suppressed the carbon formation and exhibited high performance for steam reforming of methane, [40] however CeO_2 concentrations in excess of this limit deactivate the Ni catalyst. Some oxygen ion conducting ceria materials such as $Sm_{0.2}(Ce_{1-x}Ti_x)_{0.8}O_{1.9}$ (SCT_X) modified Ni-YSZ have been utilized for direct methane reforming and have shown significant performance improvement by 60% as compared to unmodified cell and the

authors attributed this improvement to rapid redox equilibria which reduces the amount of carbon deposition and improves the stability of SOFCs.[41] Some studies demonstrated that the addition of proton conducting oxides such as $SrZr_{0.95}Y_{0.05}O_3$ promoted dramatically Ni-YSZ anodes and improved the coking resistance because of increasing local O/C ratio on the surface of the catalyst in the anode.[42]

1-4 Alternative anode materials

Mixed metal oxides have been used as alternative anode materials because of their electronic and ionic conduction ability as well as their catalytic properties. [8] The ability to substitute different metals into their structures makes the catalysts less sensitive to deactivation. For example, perovskite materials with the general formula ABO_3 greatly reduce carbon formation at lower cost than noble metals. One study in this field is $Sr_{0.2}La_{0.8}CoO_3$ while showed potential as a catalyst which can be used in vehicle exhausts. [44] Several perovskites have been reported which have the ability to be alternative catalyst materials instead of traditional Ni anodes for methane reforming. However one important drawback of perovskite is their low electrical conductivity under anode atmospheres. [9] Several attempts to incorporate Ni into perovskite based catalyst have been made for increasing perovskite catalyst ability toward conductivity and reforming. A nickel doped $SrZrO_3$ has been shown to be very efficient toward methane conversion at low temperature. [3] The catalyst displayed significantly lower tendency to carbon deposition compared to conventional supported nickel catalysts. To increase the catalyst activity, lower valence elements (typically rare earth metals) can be substituted in to the structure. For example, the addition of Ce to Ni perovskite ($La_{0.6}Ce_{0.4}Fe_{(1-x)}Ni_xO_3$) reduced the carbon accumulation dramatically due to creating oxygen vacancies which increased oxygen ion mobility and consequently oxidized adsorbed carbon. [43]

1-5 Pyrochlore structure:

Pyrochlores are other important types of mixed oxides. They are crystalline thermally stable mixed metal oxides with a cubic unit cell and the general empirical formula $A_2B_2O_7$. [11, 14] The pyrochlore structure (fig 2) is derived from the simple fluorite structure AO_2 (fig3). The difference is that the pyrochlore has two cation sites and one of the eight O anions absent. The A site is usually occupied by a large cation typically rare-earth trivalent metal such as La and is coordinated with eight oxygen anions and the B site cation is occupied by a smaller tetravalent transition metal such as Zr and it is coordinated with six oxygen atoms.[1,10]

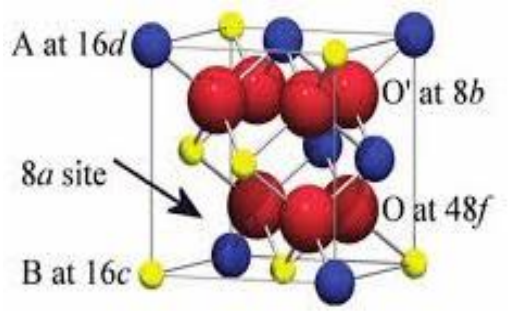

Fig 2-structure of Pyrochlore, Blue atoms A^{3+}, yellow B^{4+} and red O^{2-}

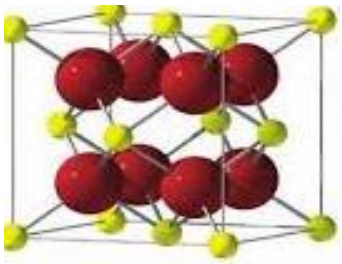

Fig. 3: Unit cell of fluorite, yellow atoms (A^{4+}) and the red O^{2-}.

Pyrochlores are interesting for reactions that require thermal stability at high temperature such as dry reforming (DRM). [14] Using pyrochlore in dry reforming was first studied by Ashcroft et.al.[1] Two important properties make them interesting for this reaction. Firstly; oxygen ion conductivity due to oxygen vacancies in the structure which improves the oxide mobility as a result, limiting carbon deposition formed by CH_4 dissociation. Secondly; isomorphic substitution of catalytically active transition metals like Ru in the B site where they do not sinter under DRM conditions. [11,16]

There are two rules for forming a stable pyrochlore: first: the ratio of the ionic radius at A and B site must be between 1.46 and 1.80 because if the ratio was above of 1.8 a perovskite phase

will be formed and if the ratio was under 1.4 a fluorite structure will formed. The second: total chemical valences of A and B ions must be in balance with the O ions.[17]

Because of the thermal stability at reaction conditions $La_2Zr_2O_7$ (LZ) pyrochlore has been considered as an appropriate material for partial oxidation reforming (POX) and has shown high ability to accommodate metals that increase the oxygen ion conductivity. [10]

For B site substitution, Ru, Rh and Pt have been considered as catalytically active transition metals. [11] In spite of economic issues for noble metals, they have greater resistance to carbon formation compared to lower cost metals such as Ni which undergoes deactivation due to carbon deposition. [15] Thus enhancing a Ni catalyst with noble metals appears to be a good idea against carbon formation. [51]

To inhibit carbon formation, the incorporation of an active metal within the pyrochlore structure leading to high oxygen mobility is considered to be an effective way in recent studies.

To reduce the deactivation, Ni (3%) was substituted into the La-Sr-Zr pyrochlore (LSZN) for catalytic partial oxidation of a surrogate diesel fuel. This pyrochlore produced stable H_2 and CO and had a lower amount of carbon deposition compared to Ni/Al_2O_3 after 2 hours of reaction. The resistance to carbon deposition has been attributed to the oxygen ion conductivity of the Sr which provides a localized oxygen source from the pyrochlore lattice to react with strongly adsorbed carbon. [7] Some researchers have reported Ru and Pt substituted pyrochlores in which the lattice oxygen gasifies surface carbon and the amount of carbon deposition is reduced dramatically.[50] $La_{(2-x)}Sr_xRh_yZr_{(2-y)}O_7$ showed a high resistance to deactivation by sulphur, aromatics and carbon deposition compared to $La_2Zr_2O_7$. Rh metal has shown high selectivity toward H_2 and CO with low carbon formation,[48] but because of the Rh cost some researchers substituted Ru as an alternative active metal in the pyrochlore structure with improvement in the catalytic activity demonstrated. [46, 12] Ashcroft in his study observed that ($Ln_2Ru_2O_7$: Ln is a lanthanide) are extremely active for partial oxidation and dry reforming of methane. However

the Ru pyrochlore was not stable under reforming conditions. [47] The decomposition of the pyrochlore occurred when bulk Ru-metal was created under reducing reaction conditions. The stability of Ru catalysts can be improved by partially substituting Ru into the structure of lanthanium-stronium-zirconat which is more stable and results showed that the LSRZ accumulated less carbon on the structure due to greater oxygen ion conductivity of the Sr-containing pyrochlore. Ru substitution creates a less expensive catalyst that has high resistance to sulphur and aromatic deactivation. In addition it has comparable activity to the Rh substituted catalyst. [2]

In the case of A site substitution, Gaur et al. substituted Ca at the La site in LRZ leading to an increase in stability and a reduction in the carbon deposition. [14] This substitution creates oxygen vacancy and probably decreased the bond-energy of La-O and Zr-O bonds as during DRM these bonds break and O^{2-} is released from the structure, but the lattice oxygen is not depleted from the pyrochlore because it is replenished from two sources. The first, from dissociation of CO_2 and the second from the steam which is formed during the reaction. [1,14] The ionic radius ratio $r(A^{3+})/r(B^{4+})$ has an important role in the crystal structure. Low activation energy and high mobile vacancies concentration are necessary to obtain high conductivity, and these two functions are related to the lattice structure. Generally pyrochlore oxides can be anion conductors, because the O^{2-} ions are at the 8b and 48f sites and in the completely ordered pyrochlore the 8b site is vacant. Therefore they have low activation energy. [14] On other hand, because the ionic radius ratio is higher than 1.46 they have low concentrations of mobile vacancies. Reducing in $r(A^{3+})/r(B^{4+})$ causes O^{2-} occupies partially the 8b site vacant, as a result oxygen vacancies will formed at the 48f site. However, due to cation disordering the activation energy will increase and the fluorite –type structure will be produced.[1,14] Many studies have reported that the highest ionic conductivity is obtained at the phase boundary between pyrochlore and fluorite phases due to lattice distortion, which acts as a driving force. This

property is obtained by doping elements into A, B and both sites. The effect of doping on the ionic conductivity in series of $(La_{1-x}Y_x)_2Zr_2O_7(0<x<1)$ was reported by F.Yang et al. [18] To achieve the highest improvement in conductivity there should be as many phase boundaries as possible and the two phase components should have similar conductivity to prevent phase boundary mixing by the less conductive second phase. The highest conductivity is obtained when x=0.5 where two phase composites contain 82 and 18% pyrochlore and fluorite phases respectively.

1-6 other ways to increase catalyst resistance

Greater dispersion of active metal on the catalyst surface provides a larger active surface and generally limits the carbon formation. [1] Changing the properties of the support, type of metal, metal concentration, promoter and preparation method can result in a catalyst with high resistance to deactivation due to increase in dispersion ratio.

Mixed oxides catalysts for reforming have been prepared by various synthesis methods and because the preparation method affects the final catalyst properties, these appear to focus more on which parameters give ideal catalysts and these are high purity, small average particle size and large surface area.[5]

The solid state synthesis method requires a series of heating cycles at high temperature, often in excess of 800 $^{\circ}$C, but the products suffer from low surface area because of agglomeration and compositionally contain multiple unwanted phases. [3,11] Cao et al. in their study reported that proper addition of ceria by using solid state route at 1873 K for 12 hours could largely reduce the thermal conductivity and also improve the sintering resistance of LZ pyrochlore.[19]

To prepare pure and fine nanocrystalline powder at low temperatures, Joulia et al. used an organic sol-gel (alkoxide) method and citrate synthesis to synthesise $La_2(Zr_{1-x}\ Ce_x)_2O_7$. [20] However, the sol-gel method is expensive due to using alkoxide solutions. [21]

Co-precipitation is another method for synthesizing high-purity catalysts at low temperature. In this method the nitrate or chloride is used as a precursor solution that is added into a strong base solution under constant string at room temperature, the precipitate is then washed with water, ethanol or a mixture of both solvents and finally dried at 120°C overnight. [20]Several pyrochlore and perovskite compounds are formed from this method.[5,20] Although co-precipitation and sol-gel produce fine powders with high phase purity, calcination at high temperature is necessary for crystallization.[22] In contrast to the other synthesis techniques the hydrothermal method has great potential to prepare complex oxides with high quality and high surface area at relatively low temperature.[23] In addition it is easy to control the reaction kinetically.[24] The compositional homogeneity and extra small grain size are achieved because of elimination of calcinations step.[25] Phase-pure lanthanum stannate pyrochlore ($Ln_2Sn_2O_7$) has been fabricated by several methods and only by the hydrothermal route showed nanosphere morphology, large surface area and improved redox properties. [17]Arbag et al. synthesized Ni substituted silicate mesoporous MCM-41 catalyst and promoted it with Rh by using both a hydrothermal and an impregnation method and they observed that the hydrothermal method made a catalyst which showed lower selectivity for reverse water gas shift (RWGS) as compared to the other route. [1] The hydrothermal method uses a sealed vessel like an autoclave to increase the autogenous pressure that leads to an increase in the temperature of solvent higher than the boiling point .It also produces pure phase materials and avoids poor stoichiometry by changing in the condition of reaction. [26]Besides preparation method, the nature of counter-cation and the solvent are also other parameters which influence the structural phase of the compound. The effect of chloride and nitrate precursor on the properties of LZ showed that the low polarisable counter-cation (chloride) favoured the formation of another phase. [20] Crisafull et al. studied the effect of precursor of Ru in Ni-Ru on SiO_2 catalyst and observed higher dispersion with nitrate as compared to chloride which means smaller Ni particles are formed and thus greater resistance

to deactivation.[49] Furthermore the Cl^- blocked the active site and decreased the activation. Energy nature of the solvent had an impact on the particle size. Organic solvents permitted the formation of large particles than aqueous solvent which have strong interactions which lead to smaller particle size. [20]

1-7 H_2S Poisoning:-

Liquid hydrocarbons mostly contain sulphur impurities up to 3000 ppm by weight, and even deep desulfurization treatment cannot wholly remove H_2S contaminants. To purify the feed to a low level of sulphur a high percentage of operating costs is required; therefore, the development of a catalyst that maintains their activity in the presence of sulphur compounds is preferred. The reactivity of sulphur is related to the number of electron pairs present for bonding therefore; toxicity increases in the order of SO_4^{2-}, SO_2 and H_2S[54]. Metal catalysts are affected by trace levels of H_2S because of strong sulphur –metal bonding. The chemisorbed sulphur on the metal catalyst involves the s and p orbitals of the sulphur interacting with the d orbital of the metal. Sulphur can decrease the availability of electrons in the d orbitals and thus withdraw charge from metals and therefore reduce the connection probability between the metal and reactants. Besides the formation of metal sulphides, the catalyst can also be deactivated by the formation of sulphates on the support by changing the crystal arrangement.

1-8 Mechanism of H_2S poisoning:-

According to the recent literature there are three primary types of poisoning mechanism called 1-sulphidation, 2-alteration and 3-coke formation by which sulphur compounds can affect the performance of a catalyst[55,56].

Sulphidation mechanism is related to the interaction between sulphur and catalyst active sites. In this process, metal sulphides form by reacting hydrogen sulphide gas with the active metal sites, and then the catalyst loses its reforming activity for producing syngas from

hydrocarbons[57]. Deactivation here depends on the temperature and H_2S concentration in the feed gas[58]. At low concentrations of H_2S, sulphur will be adsorbed on to the catalyst surface while at the higher concentration subsequent sulphidation reaction occurs and sulphur will be adsorbed into the catalyst material to form metal sulphides resulting in a permanent loss in activity[59, 60]. In general, raising the temperature or reducing the sulphur content can regenerate the catalyst that was deactivated by adsorption of sulphur on to the surface which blocked off the access to the metal sites[61,62]. To suppress the formation of strong sulphide bonds in the structure, slightly oxidising environment from the lattice structure of the catalyst or from the feed gas will be helpful to convert sulphide into SO_2 species[63].

In the second mechanism, sulphur poisoning alters the catalyst functionality by affecting the reaction pathways of adsorbing reactants on the surface of metal sites. This phenomenon is reported in catalysts that have heterogeneity in their material structure[64]. For example in the ethane partial oxidation system and in the presence of SO_2, the selectivity of Pt and Rh catalysts toward steam reforming reduce due to the SO_2 enhanced ethylene production[65].

The third mechanism suggests sulphur compounds help carbonaceous coke growth on the catalyst in alkane reforming reactions. In this mechanism, sulphur atoms interact with alkyl radicals to form R-S species. The R-S species rapidly dehydrogenate to give very stable coke deposits on the active sites of the catalyst[66-68]. Many studies report that the presence of a small amount of H_2S reduces the amount of carbon formation by deactiving some of the metal sites that reduce the rate of coke formation[69].

1-9 Improving tolerance toward H_2S poisoning:-

One approach to enhanced sulphur resistance in reforming systems is by improving the catalyst materials. This improvement can be obtained through elemental additives that increase the sulphur resistance of reforming catalysts [70,71]. In addition to incorporating elemental

components into the catalyst material, the development of a sulphur resistant catalyst structure also enhances catalyst performances[72].

1-9-1 Elemental additives:

1-9-1-1 Sulphur prevention elements:-

A few elements such as cerium and alkaline species can prevent sulphur build-up on reforming catalysts. For example cerium, by increasing oxygen mobility in the lattice of the catalyst structure, results in the formation of sulphur oxides on the active metal sites that are more easily removed at high temperature instead of the formation deposited sulphur[73,74]. Postle studied the interaction of sulphur with a commercial $Ce_{0.9}Gd_{0.1}O_{2-x}$ catalyst and its influence on H_2 production from CH_4/H_2O. The study showed that the activity improved on substitution of oxygen sites in the ceria lattice with sulphur anions, producing new catalytic sites which increased methane conversion[75]. Alkaline components are beneficial due to reacting with sulphur compounds before reaching the active metal sites to prevent catalyst poisoning[76]. Barium oxide has been used to prevent sulphide formation on the catalyst by generation of Ba-S instead of the formation of nickel sulphides[77]. Other studies have shown that potassium influences the Ni-S bond and prevents permanent poisoning[78].

1-9-1-2 Sulphur tolerance elements:-

Noble metals have similar catalytic properties to transition metals but are more resistant to sulphur poisoning. Kantservo showed that the presence of a small amount of Pd or Pt enhances the stability of Ni species in the presence of sulphur for the tri-reforming of methane. TRM reaction applied at 800°C on the mixture containing 3500 ppm H_2S over 10 min was equivalent to 58 hours in a natural gas containing 10 ppm H_2S[79]. Mata prepared a Ru perovskite with Sr partial substitution. This study showed a high and stable yield toward hydrogen production at 850°C under auto-thermal reforming of methane in the presence 50ppm H_2S over 24 hours[80].

1-9-1-3 Synergistic combinations:-

Synergistic effects can be seen when two components that individually are not tolerant to sulphur are combined and improve the catalyst tolerance to sulphur poisoning. In Gaillard's study, molybdenum incorporated into Ni catalysts improved the reducibility and helped in the removal of carbon and sulphur deposition from the surface of the catalyst[81]. In Nikolaos study, the doping of Au shifts the equilibrium of sulphur reactions toward H_2S formation by changing the electronic properties of the catalyst[82]. Cobalt also shows the same role as Au doping in Ni catalysts. Moreover, cobalt prevents the deactivation of the Ni sites by reacting with the sulphur content in the feed[83].

1-9-2 Structural Modification:

1-9-2-1 Pyrochlore, perovskite and metallic alloys:-

Pyrochlore and perovskite materials are a class of metal oxides with a general formula of $A_2B_2O_7$ and ABO_3 respectively that are interesting adductors to avoid sulphur poisoning. An essential property of these materials is that catalytically active metals can be substituted into the structure which imparts specific properties against sulphur compounds[84, 85-54]. This material by providing labile lattice oxygen atoms, minimises the negative effect of sulphur from the catalyst. The group of Spivey have worked extensively on pyrochlore materials[86, 87]. For example, they found that La/Sr/Zr/Rh pyrochlores lose some activity at the initial stages of reforming in the presence of 50 ppm dibenzothiophene without continuous deactivation with time on stream. They suggest that the poisoning occurred on the catalyst surface and when sulphur was removed from the stream almost full activity was seen[88].

Alloys of Ni also have certain sulphur resistant properties. Alloying by reducing the rate of the most destructive bond such as carbon-carbon and metal-sulphur bond and increasing the rate of competing reactions such as carbon and sulphur oxidation, improve the tolerance of catalysts. Nickel can be alloyed with several metals such as iron, cobalt, manganese and others[89, 90].

Huq showed that due to the foam structure of a nickel-tin alloy, the catalyst had excellent resistance in the presence of 200 ppm H_2S at 850°C. Tin enhanced both carbon deposition resistance and sulphur tolerance by acting as a site blocker avoiding the Ni interacting with the sulphur and therefore improving the stability of the reforming catalyst [91]. The addition of Mo and W to Ni-based catalysts reduces deactivation in steam reforming. In the presence of any sulphur species, Mo tends to form MoS_2 and the active sites of the Ni would not be affected. Ni catalysts doped with Mo are more sulphur resistant than Ni catalysts alone in the presence of 10 ppm H_2S[92, 93]

1-9-2-2 Core- shell structure:-

Coating metal active sites with inert materials forming core-shell structures isolate unwanted sulphur and allow reactants to enter the core side for reaction. Hua et al.[94] demonstrated, Ce/ZrO_2 shell by coating with Ni-Cu nanoclusters enhanced the conversion of methane in dry reforming in the presence of 500 ppm H_2S at 800°C. The cell had a maximum power density of 1.05 W cm^{-2}. Tosodkov showed that by incorporing Fe_2O_3 into the shell structure this reduced the impact of sulphur by increasing H_2S conversion into elemental sulphur in steam reforming[95].

1-9-2-3 Adjusting synthesis method and catalyst structures:-

Researchers have shown that adjusting the conventional synthesis method can enhance the sulphur resistance properties of a catalyst. Postal et al. used the wet impregnation method to obtain iridium and cerium-based catalysts. They compared the resistance of this catalyst with the same adjusted catalyst where iridium was oxidised at 300°C followed by reduction at 500°C. The adjusted catalyst recovered its activity when sulphur was removed from the feed stream[96].

Misture et al reported that the presence of defective spinel oxide sites has an essential role in providing oxygen which helps to remove deposited sulphur on the catalyst which results in

additional reaction sites. They found that the Ni/Co ratio and the synthesis temperature of the starting spinel affects the reforming activity and sulphur tolerance[97].

Shakouri studied the effect of preparation method, Ni/Co ratio and reduction temperature on Ni-Co/AlMgOX catalyst. The catalyst with higher Ni content showed higher resistance to H_2S poisoning. Also, Ni was easier to reduce than cobalt, and the reforming activity of the catalyst prepared by impregnation preparation method was better than the coprecipitation method. They also showed that a reduction at 850 °C produced larger particle sizes than at a lower temperature[98].

1-10 Regeneration of sulphur-poisoned catalysts:-

Since most of the catalysts are expensive and the lifetime of reforming systems depends on the catalyst performance, therefore the ability of the catalyst to recover itself is one of the critical properties that the industrial sector are looking for it. Catalyst regeneration usually requires harsher conditions than the standard operating conditions in a reactor.

The regeneration method, generally involves thermal treatment in oxygen, hydrogen or steam atmosphere. The regeneration step also consumes a significant amount of energy which makes the researcher's interest in this field to reduce the cost of the reforming process[54,85]

Yong investigated the deactivation and regeneration of Ni-Ce catalysts supported on alumina under steam reforming conditions during sulphur poisoning. The study showed that the deactivating behaviour remarkably depends on the operating temperature and the H_2S concentration. The regeneration of the catalyst was studied under conditions of H_2S removal, increasing the temperature and by steam treatment. The results showed that the catalyst could not regenerate itself at low temperature while at high temperature due to the mechanism of H_2S adsorption; the catalyst could recover its activity easily. The complete catalyst regeneration occurred within three hours of the stream treatment following by three hours of H_2 reduction, even after low-temperature poisoning, [99].

Other commercial treatments were reported by Izquiredo et al and included oxidizing sulphur deposits into sulphate species and then thermally decomposing into SO_2 gas. Metal oxides can then be reduced back, to be recycled. The study suggests that the incorporation of ceria may help the regeneration process by enhancing oxygen mobility promoted by the Ce^{3+}/Ce^{4+} redox mechanism[100].

Complete activity recovery of a Ni-ceria based catalyst after poisoning to 7400 ppm of thiophene was obtained by thermal treatment at 800°C in O_2/N_2 50:50 mixtures. The need for a reduction step before rerunning the reaction is one drawback of this treatment, which is necessary after oxidising the nickel sites. The catalyst may deactivate by thermal degradation and/or phase transferring of the active components due to the exothermicity associated with the oxidative treatment. Therefore this application cannot be used as a general regeneration procedure.[101] Oxidative treatment is however useful when the catalyst structure does not change at high oxidation temperatures. Some authors have used diluted oxygen at high temperature to reactivate Ni/Al_2O_3 but the irreversible formation of the inactive spinel $NiAl_2O_4$ occurred[102].

Reactivation of sulphur-contaminated catalysts in steam instead of oxygen treatment was studied by Rostrup-Nielsen[103]. Steam can remove sulphur as hydrogen sulphide via:-

$NiS + H_2O \rightarrow NiO + H_2S$

90% of the sulphur can be removed using this treatment at temperatures between 800 and 900°C. Complete sulphur removal from the catalyst surface after steam treatment was indicated in the study by Oudghiri-Hassani et al. However alterations of the catalyst structure due to Ni oxidation were identified by infrared spectroscopic analysis. The H_2O may produce some oxidation of reduced Ni by $Ni+H_2O \rightarrow NiO+H_2$[104].

1-11 Aim of this PhD thesis:-

This PhD thesis aimed to:-

- Prepare new pyrochlore with Ni incorporation and compare the performance with Ru incorporation.
- Study the effect of the Pechini and hydrothermal preparation methods on the performance of the catalyst.
- Characterise the catalyst by various techniques (XRD, SEM, BET and TPR).
- Study the effect of methane dry reforming in a 2:1 and 1:1 CH_4: CO_2 ratio on catalyst performance and at the various temperatures.
- Determine the quantity and quality of carbon deposition on each catalyst.
- Determine the stability of the catalyst under H_2S poisoning
- Study the regeneration ability of the catalyst after H_2S poisoning

1-12 References:-

1- Pakhare, D., Shaw, C., Haynes, D., Shekhawat, D. and Spivey, J., 2013. Effect of reaction temperature on activity of Pt-and Ru-substituted lanthanum zirconate pyrochlores (La2Zr2O7) for dry (CO2) reforming of methane (DRM). Journal of CO_2 Utilization, 1, pp.37-42.

2- Haynes, D.J., Campos, A., Berry, D.A., Shekhawat, D., Roy, A. and Spivey, J.J., 2010. Catalytic partial oxidation of a diesel surrogate fuel using an Ru-substituted pyrochlore. Catalysis Today, 155(1-2), pp.84-91.

3- Evans, S.E., Good, O.J., Staniforth, J.Z., Ormerod, R.M. and Darton, R.J., 2014. Overcoming carbon deactivation in biogas reforming using a hydrothermally synthesised nickel perovskite catalyst. RSC Advances, 4(58), pp.30816-30819. ``

4- Evans, S.E., Staniforth, J.Z., Darton, R.J. and Ormerod, R.M., 2014. A nickel doped perovskite catalyst for reforming methane rich biogas with minimal carbon deposition. Green Chemistry, 16(10), pp.4587-4594.

5- Richardson, R.A., Cotton, J.W. and Ormerod, R.M., 2004. Influence of synthesis route on the properties of doped lanthanum cobaltite and its performance as an electrochemical reactor for the partial oxidation of natural gas. Dalton Transactions, (19), pp.3110-3115.

6- Ormerod, R.M., 2003. Solid oxide fuel cells. Chemical Society Reviews, 32(1), pp.17-28.

7-D.H.Haynes, A. Campos, MW Smith, D Shekhawat, JJ Spivey - Catalysis Today, **2010** , 154, 210-216

8- Staniforth, J., Evans, S.E., Good, O.J., Darton, R.J. and Ormerod, R.M., 2014. A novel perovskite based catalyst with high selectivity and activity for partial oxidation of methane for fuel cell applications. Dalton Transactions, 43(40), pp.15022-15027.

9- Wang, W., Su, C., Wu, Y., Ran, R. and Shao, Z., 2013. Progress in solid oxide fuel cells with nickel-based anodes operating on methane and related fuels. Chemical reviews, 113(10), pp.8104-8151.

10- Haynes, D.J., Berry, D.A., Shekhawat, D. and Spivey, J.J., 2008. Catalytic partial oxidation of n-tetradecane using pyrochlores: effect of Rh and Sr substitution. Catalysis Today, 136(3-4), pp.206-213.

11- Pakhare, D., Schwartz, V., Abdelsayed, V., Haynes, D., Shekhawat, D., Poston, J. and Spivey, J., 2014. Kinetic and mechanistic study of dry (CO2) reforming of methane over Rh-substituted La2Zr2O7 pyrochlores. Journal of Catalysis, 316, pp.78-92.

12- Haynes, D., 2007. The catalytic partial oxidation of n-tetradecane on Rh and Sr substituted pyrochlores.13- J. Sehested, Catal. Today, **2006**, 111, 103–110

14- S.Gaura, D.J.Haynes and J.J.Spiveya.Catal.A-Gen, **2011**,403, 142-151

15- Pakhare, D., Haynes, D., Shekhawat, D. and Spivey, J., 2012. Role of metal substitution in lanthanum zirconate pyrochlores (La 2 Zr 2 O 7) for dry (CO 2) reforming of methane (DRM). Applied Petrochemical Research, 2(1-2), pp.27-35.

16- Pakhare, D., Shaw, C., Haynes, D., Shekhawat, D. and Spivey, J., 2013. Effect of reaction temperature on activity of Pt-and Ru-substituted lanthanum zirconate pyrochlores (La2Zr2O7) for dry (CO2) reforming of methane (DRM). Journal of CO2 Utilization, 1, pp.37-42.

17-X.X Liu, P.Lu, L. Wang, Z.Zhang, Xiuju Wang, and Z.Wang. The scientific world .**2015** , 1-8

18- Yang, F., Wang, Y., Zhao, X. and Xiao, P., 2015. Enhanced ionic conductivity in pyrochlore and fluorite mixed phase yttrium-doped lanthanum zirconate. Journal of Power Sources, 273, pp.290-297.

19- Xu, Z., He, L., Zhong, X., Zhang, J., Chen, X., Ma, H. and Cao, X., 2009. Effects of Y2O3 addition on the phase evolution and thermophysical properties of lanthanum zirconate. Journal of Alloys and Compounds, 480(2), pp.220-224.

20-W.Duarte, A.Meguekam, M.Colas, S.Rossignol.J Matersci, **2015**, 50,463-475

21-oulia A, Vardelle M, Rossignol S. J Eur Ceram Soc, 2013, 33. 2633–2644

22- Chen, D. and Xu, R., 1998. Hydrothermal synthesis and characterization of La2M2O7 (M= Ti, Zr) powders. Materials research bulletin, 33(3), pp.409-417.

23- Zeng, J., Wang, H., Zhang, Y., Zhu, M.K. and Yan, H., 2007. Hydrothermal synthesis and photocatalytic properties of pyrochlore La2Sn2O7 nanocubes. The Journal of Physical Chemistry C, 111(32), pp.11879-11887.

24- Farid, M.A., Asghar, M.A., Ashiq, M.N., Ehsan, M.F. and Athar, M., 2014. Hydrothermal synthesis of doped lanthanum zirconate nanomaterials and the effect of V–Ge substitution on their structural, electrical and dielectric properties. Materials Research Bulletin, 59, pp.405-410

25- Wang, C., Wang, Y., Cheng, Y., Huang, W., Khan, Z.S., Fan, X., Wang, Y., Zou, B. and Cao, X., 2012. Preparation and thermophysical properties of nano-sized Ln2Zr2O7 (Ln= La, Nd, Sm, and Gd) ceramics with pyrochlore structure. Journal of Materials Science, 47(10), pp.4392-4399.

26-Riman, R.E., Suchanek, W.L. and Lencka, M.M., 2002, November. Hydrothermal crystallization of ceramics. In Annales de Chimie Science des Materiaux (Vol. 27, No. 6, pp. 15-36). No longer published by Elsevier.

27- Maréchal, F., Leuenberger, S., Membrez, Y., Bucheli, O. and Favrat, D., 2004. Process flow model of solid oxide fuel cell system supplied with sewage biogas. Journal of Power Sources, 131(1-2), pp.127-141.

28-King, D.L., Strohm, J.J., Wang, X., Roh, H.S., Wang, C., Chin, Y.H., Wang, Y., Lin, Y., Rozmiarek, R. and Singh, P., 2008. Effect of nickel microstructure on methane steam-reforming activity of Ni–YSZ cermet anode catalyst. journal of Catalysis, 258(2), pp.356-365.

29- Goula, G., Kiousis, V., Nalbandian, L. and Yentekakis, I.V., 2006. Catalytic and electrocatalytic behavior of Ni-based cermet anodes under internal dry reforming of CH4+ CO2 mixtures in SOFCs. Solid State Ionics, 177(19-25), pp.2119-2123.

30- Park, S., Vohs, J.M. and Gorte, R.J., 2000. Direct oxidation of hydrocarbons in a solid-oxide fuel cell. Nature, 404(6775), p.265.

31- Koh, J.H., Yoo, Y.S., Park, J.W. and Lim, H.C., 2002. Carbon deposition and cell performance of Ni-YSZ anode support SOFC with methane fuel. Solid State Ionics, 149(3-4), pp.157-166.32-Zhan, Z. L.; Barnett, S. A. Science **2005**, 308, 844

33- Zhu, H., Colclasure, A.M., Kee, R.J., Lin, Y. and Barnett, S.A., 2006. Anode barrier layers for tubular solid-oxide fuel cells with methane fuel streams. Journal of Power Sources, 161(1), pp.413-419.

34- Lin, Y., Zhan, Z. and Barnett, S.A., 2006. Improving the stability of direct-methane solid oxide fuel cells using anode barrier layers. Journal of power sources, 158(2), pp.1313-1316.

35- Park, S., Vohs, J.M. and Gorte, R.J., 2000. Direct oxidation of hydrocarbons in a solid-oxide fuel cell. Nature, 404(6775), p.265.

36-Jia, L. C.; Wang, X.; Hua, B; Pu, J.; Yuan, S. L.; Li, J. Int. J. Hydrogen Energy **2012**, 37, 11941

37- Wang, Z., Weng, W., Cheng, K., Du, P., Shen, G. and Han, G., 2008. Catalytic modification of Ni–Sm-doped ceria anodes with copper for direct utilization of dry methane in low-temperature solid oxide fuel cells. Journal of Power Sources, 179(2), pp.541-546.

38- Park, E.W., Moon, H., Park, M.S. and Hyun, S.H., 2009. Fabrication and characterization of Cu–Ni–YSZ SOFC anodes for direct use of methane via Cu-electroplating. International journal of hydrogen energy, 34(13), pp.5537-5545.39-Islam, S.; Hill, J. M. J. Power Sources **2011**, 196, 5091

40-He, B. B.; Zhao, L.; Wang, W. D.; Chen, F. L.; Xia, C. R. Electrochem. Commun. **2011**, 13,194

41- Chen, Y., Chen, F., Wang, W., Ding, D. and Gao, J., 2011. Sm0. 2 (Ce1− xTix) 0.8 O1. 9 modified Ni–yttria-stabilized zirconia anode for direct methane fuel cell. Journal of Power Sources, 196(11), pp.4987-4991.

42- Jin, Y., Saito, H., Yamahara, K. and Ihara, M., 2009. Improvement in durability and performance of nickel cermet anode with SrZr0. 95Y0. 05O3-α in dry methane fuel. Electrochemical and Solid-State Letters, 12(2), pp.B8-B10.

43- Erri, P., Dinka, P. and Varma, A., 2006. Novel perovskite-based catalysts for autothermal JP-8 fuel reforming. Chemical engineering science, 61(16), pp.5328-5333

44- Evans, S.E., Staniforth, J.Z., Darton, R.J. and Ormerod, R.M., 2014. A nickel doped perovskite catalyst for reforming methane rich biogas with minimal carbon deposition. Green Chemistry, 16(10), pp.4587-4594.

45- Takahashi, H., Takeguchi, T., Yamamoto, N., Matsuda, M., Kobayashi, E. and Ueda, W., 2011. Effect of interaction between Ni and YSZ on coke deposition during steam reforming of methane on Ni/YSZ anode catalysts for an IR-SOFC. Journal of Molecular Catalysis A: Chemical, 350(1-2), pp.69-74.

46- Haynes, D.J., Berry, D.A., Shekhawat, D. and Spivey, J.J., 2008. Catalytic partial oxidation of n-tetradecane using pyrochlores: effect of Rh and Sr substitution. Catalysis Today, 136(3-4), pp.206-213.

47-Ashcroft, A.T., Cheetham, A.K., Jones, R.H., Natarajan, S., Thomas, J.M., Waller, D. and Clark, S.M., 1993. An in situ, energy-dispersive x-ray diffraction study of natural gas conversion by carbon dioxide reforming. The Journal of Physical Chemistry, 97(13), pp.3355-3358.

48- Shekhawat, D., Gardner, T.H., Berry, D.A., Salazar, M., Haynes, D.J. and Spivey, J.J., 2006. Catalytic partial oxidation of n-tetradecane in the presence of sulfur or polynuclear aromatics: Effects of support and metal. Applied Catalysis A: General, 311, pp.8-16.

49- Crisafulli, C., Scire, S., Maggiore, R., Minico, S. and Galvagno, S., 1999. CO 2 reforming of methane over Ni–Ru and Ni–Pd bimetallic catalysts. Catalysis Letters, 59(1), pp.21-26.

50-S. M. Stagg-Williams, R. Soares, E. Romero, W. E. Alvarez and D. E. Resasco, in Stud. Surf. Sci. Catal., ed. F. V. M. S. M. Avelino Corma and G. F. José Luis, Elsevier, **2000**, vol. 130, pp. 3663–3668

51- García-Diéguez, M., Pieta, I.S., Herrera, M.C., Larrubia, M.A. and Alemany, L.J., 2011. RhNi nanocatalysts for the CO2 and CO2+ H2O reforming of methane. Catalysis Today, 172(1), pp.136-142.

52- J.R. Rostrup-Nielsen, Catal Today, **2000**, 63,159-164.

53- Debek, R. and Dębek, R., 2016. Novel catalysts for chemical CO2 utilization (Doctoral dissertation, Université Pierre et Marie Curie-Paris VI).

54-Boldrin, P., Ruiz-Trejo, E., Mermelstein, J., Bermúdez Menéndez, J.M., Ramírez Reina, T. and Brandon, N.P., 2016. Strategies for carbon and sulfur tolerant solid oxide fuel cell materials, incorporating lessons from heterogeneous catalysis. Chemical reviews, 116(22), pp.13633-13684.

55-Wierzbicki, T.A., Lee, I.C. and Gupta, A.K., 2016. Recent advances in catalytic oxidation and reformation of jet fuels. Applied Energy, 165, pp.904-918.

56-Niakolas, D.K., 2014. Sulfur poisoning of Ni-based anodes for solid oxide fuel cells in H/C-based fuels. Applied Catalysis A: General, 486, pp.123-142.

57-Lorenzi, G., Lanzini, A. and Santarelli, M., 2015. Digester gas upgrading to synthetic natural gas in solid oxide electrolysis cells. Energy & Fuels, 29(3), pp.1641-1652.

58-González, A.V., Rostrup-Nielsen, J., Engvall, K. and Pettersson, L.J., 2015. Promoted RhPt bimetallic catalyst supported on δ-Al2O3 and CeO2–ZrO2 during full-scale autothermal reforming for automotive applications: post-mortem characterization. Applied Catalysis A: General, 491, pp.8-16.

59-Khan, M.S., Lee, S.B., Song, R.H., Lee, J.W., Lim, T.H. and Park, S.J., 2016. Fundamental mechanisms involved in the degradation of nickel–yttria stabilized zirconia (Ni–YSZ) anode during solid oxide fuel cells operation: a review. Ceramics International, 42(1), pp.35-48.

60-Chen, X., Jiang, J., Yan, F., Li, K., Tian, S., Gao, Y. and Zhou, H., 2017. Dry reforming of model biogas on a Ni/SiO2 catalyst: overall performance and mechanisms of sulfur poisoning and regeneration. ACS Sustainable Chemistry & Engineering, 5(11), pp.10248-10257.

61-Rhyner, U., Edinger, P., Schildhauer, T.J. and Biollaz, S.M., 2014. Applied kinetics for modeling of reactive hot gas filters. Applied Energy, 113, pp.766-780.

62-Riegraf, M., Hoerlein, M.P., Costa, R., Schiller, G. and Friedrich, K.A., 2017. Sulfur Poisoning of Electrochemical Reformate Conversion on Nickel/Gadolinium-Doped Ceria Electrodes. ACS Catalysis, 7(11), pp.7760-7771.

63-Ocsachoque, M.A., Russman, J.I.E., Irigoyen, B., Gazzoli, D. and González, M.G., 2016. Experimental and theoretical study about sulfur deactivation of Ni/CeO2 and Rh/CeO2 catalysts. Materials Chemistry and Physics, 172, pp.69-76.

64-McCue, A.J. and Anderson, J.A., 2014. Sulfur as a catalyst promoter or selectivity modifier in heterogeneous catalysis. Catalysis Science & Technology, 4(2), pp.272-294.

65-Cimino, S., Mancino, G. and Lisi, L., 2014. Ethane catalytic partial oxidation to ethylene with sulphur and hydrogen addition over Rh and Pt honeycombs. Catalysis Today, 228, pp.131-137.

66-Krcha, M.D., Dooley, K.M. and Janik, M.J., 2015. Alkane reforming on partially sulfided CeO 2 (111) surfaces. Journal of Catalysis, 330, pp.167-176.

67-Gillan, C., Fowles, M., French, S. and Jackson, S.D., 2013. Ethane steam reforming over a platinum/alumina catalyst: effect of Sulfur poisoning. Industrial & Engineering Chemistry Research, 52(37), pp.13350-13356.

68-Cimino, S., Lisi, L. and Mancino, G., 2017. Effect of phosphorous addition to Rh-supported catalysts for the dry reforming of methane. International Journal of Hydrogen Energy, 42(37), pp.23587-23598.

69-Neubert, M., Treiber, P., Krier, C., Hackel, M., Hellriegel, T., Dillig, M. and Karl, J., 2017. Influence of hydrocarbons and thiophene on catalytic fixed bed methanation. Fuel, 207, pp.253-261.

70-Lee, J., Li, R., Janik, M.J. and Dooley, K.M., 2018. Rare Earth/Transition Metal Oxides for Syngas Tar Reforming: A Model Compound Study. Industrial & Engineering Chemistry Research, 57(18), pp.6131-6140.

71-Chattanathan, S.A., Adhikari, S., McVey, M. and Fasina, O., 2014. Hydrogen production from biogas reforming and the effect of H 2 S on CH 4 conversion. International Journal of Hydrogen Energy, 39(35), pp.19905-19911.

72-Gür, T.M., 2016. Comprehensive review of methane conversion in solid oxide fuel cells: prospects for efficient electricity generation from natural gas. Progress in Energy and Combustion Science, 54, pp.1-64.

73-Savuto, E., Navarro, R.M., Mota, N., Di Carlo, A., Bocci, E., Carlini, M. and Fierro, J.L.G., 2018. Steam reforming of tar model compounds over Ni/Mayenite catalysts: effect of Ce addition. Fuel, 224, pp.676-686.

74-Li, R., Roy, A., Bridges, J. and Dooley, K.M., 2014. Tar Reforming in model gasifier effluents: transition metal/rare earth oxide catalysts. Industrial & Engineering Chemistry Research, 53(19), pp.7999-8011.

75-Postole, G., Bosselet, F., Bergeret, G., Prakash, S. and Gelin, P., 2014. On the promoting effect of H2S on the catalytic H2 production over Gd-doped ceria from CH4/H2O mixtures for solid oxide fuel cell applications. Journal of Catalysis, 316, pp.149-163.

76-Tribalis, A., Panagiotou, G.D., Bourikas, K., Sygellou, L., Kennou, S., Ladas, S., Lycourghiotis, A. and Kordulis, C., 2016. Ni catalysts supported on modified alumina for diesel steam reforming. Catalysts, 6(1), p.11.

77-da Silva, A.L. and Heck, N.C., 2015. Oxide incorporation into Ni-based solid oxide fuel cell anodes for enhanced sulfur tolerance during operation on hydrogen or biogas fuels: A comprehensive thermodynamic study. International Journal of Hydrogen Energy, 40(5), pp.2334-2353.

78-Moud, P.H., Andersson, K.J., Lanza, R. and Engvall, K., 2016. Equilibrium potassium coverage and its effect on a Ni tar reforming catalyst in alkali-and sulfur-laden biomass gasification gases. Applied Catalysis B: Environmental, 190, pp.137-146.

79-Kantserova, M.R., Orlyk, S.M. and Vasylyev, O.D., 2018. Catalytic Activity and Resistance to Sulfur Poisoning of Nickel-Containing Composites Based on Stabilized Zirconia in Tri-reforming of Methane. Theoretical and Experimental Chemistry, 53(6), pp.387-394.

80-Mota, N., Ismagilov, I.Z., Matus, E.V., Kuznetsov, V.V., Kerzhentsev, M.A., Ismagilov, Z.R., Navarro, R.M. and Fierro, J.L.G., 2016. Hydrogen production by autothermal reforming of methane over lanthanum chromites modified with Ru and Sr. International journal of hydrogen energy, 41(42), pp.19373-19381.

81-Gaillard, M., Virginie, M. and Khodakov, A.Y., 2017. New molybdenum-based catalysts for dry reforming of methane in presence of sulfur: A promising way for biogas valorization. Catalysis Today, 289, pp.143-150.

82-Sapountzi, F.M., Zhao, C., Boréave, A., Retailleau-Mevel, L., Niakolas, D., Neofytidis, C. and Vernoux, P., 2018. Sulphur tolerance of Au-modified Ni/GDC during catalytic methane steam reforming. Catalysis Science & Technology, 8(6), pp.1578-1588.

83-Saha, B., Khan, A., Ibrahim, H. and Idem, R., 2014. Evaluating the performance of non-precious metal based catalysts for sulfur-tolerance during the dry reforming of biogas. Fuel, 120, pp.202-217.

84-Hbaieb, K., Rashid, K.K.A. and Kooli, F., 2017. Hydrogen production by autothermal reforming of dodecane over strontium titanate based perovskite catalysts. international journal of hydrogen energy, 42(8), pp.5114-5124.

85-Yeo, T.Y., Ashok, J. and Kawi, S., 2019. Recent developments in sulphur-resilient catalytic systems for syngas production. Renewable and Sustainable Energy Reviews, 100, pp.52-70.

86-Pakhare, D. and Spivey, J., 2014. A review of dry (CO 2) reforming of methane over noble metal catalysts. Chemical Society Reviews, 43(22), pp.7813-7837.

87-Abdelsayed, V., Shekhawat, D., Poston Jr, J.A. and Spivey, J.J., 2013. Synthesis, characterization, and catalytic activity of Rh-based lanthanum zirconate pyrochlores for higher alcohol synthesis. Catalysis today, 207, pp.65-73.

88-Haynes, D.J., Berry, D.A., Shekhawat, D. and Spivey, J.J., 2009. Catalytic partial oxidation of n-tetradecane using Rh and Sr substituted pyrochlores: Effects of sulfur. Catalysis Today, 145(1-2), pp.121-126.

89-Tsai, H.C., Morozov, S.I., Yu, T.H., Merinov, B.V. and Goddard III, W.A., 2015. First-principles modeling of Ni4M (M= Co, Fe, and Mn) alloys as solid oxide fuel cell anode catalyst for methane reforming. The Journal of Physical Chemistry C, 120(1), pp.207-214.

90-Jung, S.Y., Ju, D.G., Lim, E.J., Lee, S.C., Hwang, B.W. and Kim, J.C., 2015. Study of sulfur-resistant Ni–Al-based catalysts for autothermal reforming of dodecane. International Journal of Hydrogen Energy, 40(39), pp.13412-13422.

91-Rodriguez, J.A. and Hrbek, J., 1999. Interaction of sulfur with well-defined metal and oxide surfaces: unraveling the mysteries behind catalyst poisoning and desulfurization. Accounts of Chemical Research, 32(9), pp.719-728.

92-Bartholomew, C.H., Weatherbee, G.D. and Jarvi, G.A., 1979. Sulfur poisoning of nickel methanation catalysts: I. in situ deactivation by H2S of nickel and nickel bimetallics. Journal of Catalysis, 60(2), pp.257-269.

93-Rodriguez, J.A. and Hrbek, J., 1999. Interaction of sulfur with well-defined metal and oxide surfaces: unraveling the mysteries behind catalyst poisoning and desulfurization. Accounts of Chemical Research, 32(9), pp.719-728.

94-Hua, B., Yan, N., Li, M., Sun, Y.F., Chen, J., Zhang, Y.Q., Li, J., Etsell, T., Sarkar, P. and Luo, J.L., 2016. Toward highly efficient in situ dry reforming of H 2 S contaminated methane in solid oxide fuel cells via incorporating a coke/sulfur resistant bimetallic catalyst layer. Journal of Materials Chemistry A, 4(23), pp.9080-9087.

95-Tsodikov, M.V., Kurdymov, S.S., Konstantinov, G.I., Murzin, V.Y., Bukhtenko, O.V. and Maksimov, Y.V., 2015. Core-shell bifunctional catalyst for steam methane reforming resistant to H2S: Activity and structure evolution. International Journal of Hydrogen Energy, 40(7), pp.2963-2970.

96-Postole, G., Nguyen, T.S., Aouine, M., Gélin, P., Cardenas, L. and Piccolo, L., 2015. Efficient hydrogen production from methane over iridium-doped ceria catalysts synthesized by solution combustion. Applied Catalysis B: Environmental, 166, pp.580-591.

97-Misture, S.T., McDevitt, K.M., Glass, K.C., Edwards, D.D., Howe, J.Y., Rector, K.D., He, H. and Vogel, S.C., 2015. Sulfur-resistant and regenerable Ni/Co spinel-based catalysts for methane dry reforming. Catalysis Science & Technology, 5(9), pp.4565-4574.

98-Shakouri, M., 2011. Effects of preparation, Ni/Co ratio and sulfure poisoning of Ni-Co bimetallic catalysts for dry reforming reaction (Doctoral dissertation, University of Saskatchewan.)

99-Yang, X., 2017. An experimental investigation on the deactivation and regeneration of a steam reforming catalyst. Renewable Energy, 112, pp.17-24.

100-Izquierdo, U., García-García, I., Gutierrez, Á.M., Arraibi, J.R., Barrio, V.L., Cambra, J.F. and Arias, P.L., 2018. Catalyst Deactivation and Regeneration Processes in Biogas Tri-Reforming Process. The Effect of Hydrogen Sulfide Addition. Catalysts, 8(1), p.12.

101-Spivey, J.J., 2011. Deactivation of reforming catalysts. In Fuel Cells: Technologies for fuel processing (pp. 285-315).

102-Ashrafi, M., Pfeifer, C., Pröll, T. and Hofbauer, H., 2008. Experimental study of model biogas catalytic steam reforming: 2. Impact of sulfur on the deactivation and regeneration of Ni-based catalysts. Energy & Fuels, 22(6), pp.4190-4195.

103-Rostrup-Nielsen, J.R., 1971. Some principles relating to the regeneration of sulfur-poisoned nickel catalyst. Journal of Catalysis, 21(2), pp.171-178.

104-Oudghiri-Hassani, H., Abatzoglou, N., Rakass, S. and Rowntree, P., 2007. Regeneration of an n-decanethiol-poisoned nickel catalyst. Journal of Power Sources, 171(2), pp.811-817

2. Experimental

2-1. Catalyst preparation:

2-1-1. 0.5Ru-LCZ (Hydrothermal method)

The $LaCeRu_{0.5}Zr_{1.5}O_7$ oxide was prepared by the hydrothermal method using salts of [$La(NO_3)_3.6H_2O$], [$ZrOCl_4.8H_2O$], [$Ce(NO_3)_3.6H_2O$] and [$RuCl_3$] as precursors. 0.5 mol of each salt was dissolved in 40 ml of deionised water and then 3 ml of [$La(NO_3)_3.6H_2O$], 3 ml of [$Ce(NO_3)_3.6H_2O$], 4.5 ml of [$ZrOCl_4.8H_2O$] and 1.5 ml of [$RuCl_3$] were transferred into a 23 ml Teflon-lined stainless steel autoclave. NaOH solution (pH=10) which act as mineraliser, was dropped into the above solution. It was stirred by hand to form a thick gel. The autoclave was kept at 210°C for 72h. Then the autoclave was cooled to ambient temperature naturally. The resulting product was recovered by three cycles of centrifuging at 5000 rpm for 15 minutes and washed with distilled water before being dried at 60^{o} C overnight. Finally, the resulting material was ground to form a fine powder and was calcined 2h at 800^{o} C before characterisation.

2-1-2. Ni-LCZ (Hydrothermal method)

The $LaCeNi_xZr_{2-x}O_7$(x=0.25, 0.5, 1) samples were prepared by the hydrothermal method using salts of ($ZrOCl_2.8H_2O$), ($Ni(NO_3)_2.6H_2O$), ($Ce(NO_3)_3.6H_2O$) and ($La(NO_3)_3 \cdot 6H_2O$) as precursors. 0.5 mol of each metallic precursor was separately dissolved in 40 ml of deionized water. The appropriate amount of each salt solution as shown in table below was transferred into a Teflon lined stainless steel autoclave, and then NaOH which act as mineraliser was added in the above solution. This was stirred by hand to form a thick gel. The autoclave was heated in an oven at 150 °C for 96 hours. The autoclave was then cooled to ambient temperature naturally. The resulting product was washed with ultra-pure water and recovered

using several cycles of centrifuging at 5000 rpm, then the sample was dried and ground to form a powder used for characterization and catalyst testing.

Table 2.1: Quantity of reagents in pyrochlore samples

Pyrochlore Catalysts	$La(NO_3)_3{\cdot}6H_2O$	$Ce(NO_3)_3.\ 6H_2O$	$Ni(NO_3)_2.6H_2O$	$ZrOCl_2.8H_2O$	NaOH
$LaCeNiZrO_7$	3 ml	3 ml	3 ml	3 ml	0.44 g
$LaCeNi_{0.5}Zr_{1.5}O_7$	2.5 ml	2.5 ml	1.25 ml	3.75 ml	0.46 g
$LaCeNi_{0.25}Zr_{1.75}O_7$	2.5 ml	2.5 ml	0.6 ml	4.3 ml	0.46 g

2-1-3. Ni-LCZ (Pechini method)

$LaCeNi_xZr_{2-x}O_7$ (x= 0.25, 1) was prepared by the Pechini method. The precursors used were $ZrOCl_2.8H_2O$, $Ni(NO_3)_2.6H_2O$, $Ce(NO_3)_3.6H_2O$ and $La(NO_3)_3{\cdot}6H_2O$. 1 mol of each salt was separately dissolved in de-ionized water. 2.5 ml of each salt solution were mixed together and then 12 ml of citric acid was added to the mixture of 10 ml salts. To ensure complete metal complexation, the solution was continuously stirred and heated to 75^{o}C. 12 ml of ethylene glycol was added to the above solution at 75^{o}C. A viscous gel was obtained after the solution had been kept stirring and the water evaporated. The resulting foam was placed in an oven at 110^{o}C to dry overnight and then calcined at 1000^{o}C for 8 hours to burn off the organic precursors and form the pyrochlore catalyst.

2.2 Characterisation:-

The synthesized samples were characterized using powder x-ray diffraction (XRD), scanning electron microscopy (SEM), and Bruner-Emmett-Teller (BET) surface area analysis.

2.2.1 Powder X-ray diffraction:-

Powder X-ray diffraction is an essential tool for structure characterisation during methane reforming because of: 1-Determination of the structure of a catalyst by the peak positions, as two different materials show different X-rar diffraction patterns .2- Periodically arranged atoms in a crystalline material provide a series of a sharp peak, while, amorphous materials due to the random nature of the arrangement of atoms produce broad, noisy background. 3- identify the material changes due to the reforming reaction e.g. changes in the structure of composition may be lead to the deactivation of the catalyst.

To perform powder X-ray diffraction (PXRD) analysis, the ground catalyst is placed into a sample holder with diameter 25 mm and depth of 1 mm. A smooth surface was achieved by pressing a glass slide against the sample. Then, the sample holder was placed into a Bruker D8 Advance powder X-ray diffractometer which used Cu $K\alpha_1$ radiation with a wavelength of 1.5406 Å at 40 KV and 40 mA tube voltage and current respectively. Patterns were collected between 10 and 90° (2θ). The patterns as raw files were then converted to Excel files for analysis. The international centre for diffraction data PDF-2 database was used for peak identification by referencing peaks to existing powder XRD patterns.

2.2.2 Scanning electron microscopy

Scanning electron microscopy (SEM) is one of the main analytical techniques used for analysing the morphology and composition of a catalyst. SEM gives a high magnification image with good depth of field and excellent resolution. The EDS analysis was used to check homogeneity of the tested materials as this gave the elemental composition.

For scanning electron microscopy (SEM), samples were dispersed onto a conductive carbon tab that was placed onto a 15 mm stainless steel stub (Hitachi), coated with a thin layer of gold and are then mounted on to a special stub, then the stub was mounted to a pedestal

within a high resolution (1.5 nm) field emission SEM, (the Hitachi S4500) and the imaging chamber was evacuated.

2.2.3 Bruner, Emmett and Teller (BET) analysis:-

Measuring the BET surface area is an essential property for many materials. The concept of the theory is based on isothermal adsorption of nitrogen at a set temperature and pressure. A surface of catalyst will adsorb a set quantity of gas, and by using the BET equation (1), the surface area will be determined.

$$\frac{p}{n_a(p_0 - p)} s_{total} = \frac{1}{n_m C} + \frac{(C-1)}{n_m C} \cdot \frac{p}{p_0} \qquad \text{.....Equation1}$$

- The equilibrium (p) and the saturation (p_0) pressure of adsorbates at the temperature of adsorption.
- The adsorbed gas quantity (n_a) (for example, in volume units)
- n_m is the monolayer capacity
- The BET constant is, C.
- S_{total} is the total surface area

An Autosorb-1- series analyser was used to perform BET measurments. 0.2 g of sample was measured and then placed into a 12 mm sample cell, which was attached to the Autosorb with a Swagelock fitting. To remove water and other contaminants from the sample, the sample was outgassed under vacuum. At the same time, the temperature of the sample was increased to 350^{o}C with a temperature programme of 1^{o}C min^{-1} and then a held for 2h. After that, the cell was cooled to room temperature before submersion in liquid nitrogen to -196^{o} C. To determine desorption and adsorption isotherm, the adsorbates gas of nitrogen was used and the surface area was determined by using AUTOSORB Software.

2.3 Experimental Set-Up of Catalyst Testing

Three types of experiments were performed during the dry reforming reaction. To find the most active catalyst among the prepared catalyst, and to determine the durability of catalyst, and to find the poisoning resistance and regeneration trend of the catalyst, the activity test, long-term stability and catalyst poisoning tests were performed respectively.

Catalyst testing was performed by placing 20±0.5 g of the catalyst in a quartz reactor tube between two pieces of quartz wool. This reactor was placed in a Eurotherm controlled electric furnace and the temperature monitored with a k-type thermocouple. A gas manifold delivered reactant gases to the furnace, and was controlled by mass flow controllers, and each gas could be turned on or off independently. The gas mix was sent through the catalyst within the quartz reactor tube. The product gases were delivered to a quadrupole mass spectrometer (QMS) where up to 12 separate mass fragments can be analysed in virtually real time.

2-3-1.Catalyst Reduction

The catalyst was reduced before each reaction to activate the catalyst prior to reforming. Experiments used 20% of H_2 in a Helium carrier with flow rates of 2 ml min^{-1} and 18 ml min^{-1} respectively. The reduction was done by using a temperature programme at a rate of 10 ^{o}C min^{-1} from room temperature to 900 ^{o}C to ensure complete reduction of the sample. The sample was then cooled under helium flow to the desired temperature of isothermal reaction.

Temperature-programmed- reduction (TPR) is one of the best, quickest and economical methods for catalyst characterisation particularly when using a new or modified catalyst.

TPR is widely used for providing a qualitative picture of the reproducibility of the catalyst surface by integrating the peaks for hydrogen consumption and water evolution as well as its high sensitivity to chemical changes.[7]

2-3-2. Reforming Reactions

2-3-2-1. Catalyst Activity Test

To find the best catalyst from the prepared catalysts, the temperature programmed reaction surface (TPRS) technique was applied after reduction experiment.

The TPSR technique is used for comparing and screening different catalysts under various conditions. The samples were reduced to 900^{o}C and cooled back to room temperature to perform TPSR. During cooling time, the appropriate reactant gases were measured until the mixture had established. The TPSR followed an up cycle and down cycle of increasing and decreasing temperature to determine any hysteresis effect. The samples were heated at the rate of 5^{o}Cmin^{-1} to 900^{o}C and cooled down to 300^{o}C by the rate of 10^{o}C min^{-1} with the reactant gases passing over the catalyst. All reactants of a complete cycle were monitored by QMS with a scan rate of 12 seconds. The space velocity in all cases was approximately 60000 mL hr^{-1} g$_{cat}$ $^{-1}$

2-3-2-2. Long Term Stability Test

To determine the stability of the catalyst, the chosen catalyst was reduced, and the temperature was adjusted at the desired temperature with the flow of pure helium passed through the sample. The appropriate flow rate of the reactant gases was established, and after 5 min of initial reading by the QMS, the reactant gases were passed over the catalyst, and QMS recorded produced gases during the designated reaction period. A flow of pure helium is re-established after turning off all reactant gases and then the furnace allowed to cool down.

2-3-2-3. H_2S Poisoning Test:-

H_2S poisoning test was performed to study the resistance of the catalyst towards the H_2S. The test was the same as for the long-term stability test, but the difference was in adding sulphur from a 10 ppm cylinder. The period of reaction was dependent on the resistance of the

catalyst toward H_2S. 10ppm H_2S was chosen and tested on 1-Ni-LCZ (Hy) at 850°C to obtain the best concentration to start with. As this catalyst showed long-term stability for 72 hours, the amount of 30 ppm as the highest concentration was selected to decrease the lifetime and study the poisoning behaviour faster. The concentration of H_2S was kept at 30 ppm, and the experiments were performed at various temperatures to study the perfect temperature. As the amount of H_2S was too low, the QMS cannot detect any H_2S fragments.

2-3-2-4. Sulphur Poisoning Recovery

The recovery from the H_2S poisoning experiment was performed by removing the H_2S feed and increasing the helium flow to maintain a total flow of 20 ml min^{-1}. The recovery was investigated in two ways.

1- The effect of initial H_2S concentration on recovery:-the experiment was performed after poisoning the catalyst with 10, 20 and 30 ppm H_2S, then the H_2S was removed from the reaction stream, and the temperature was increased to 900°C

2- The effect of temperature on recovery:-after poisoning with 10 ppm H_2S at 850°C, the poisoning factor was removed and the temperature was changed after 20 hours to 800°C and after 45 hours increased to 900°C.

The recovery was monitored as in section 2-3-2-2 before cooling under inert helium flow ready for TPO.

2-3-3 Temperature Programmed Oxidation

The amount of deposited carbon on the catalyst after each reforming reaction was quantified by temperature programmed oxidation (TPO) with 10% O_2 in He and total flow rate of 20ml min^{-1}. The experiment was performed by raising the temperature to 900° C and with temperature programme of 10°C min^{-1}. The deposited carbon is oxidised to CO and CO_2 and

then passed to QMS for analysis. The carbon desorption is monitored and quantified using predetermined calibration to find a mass of carbon deposition during reaction.

2-4. Data analysis procedures:-

MKS spectra mini lab provides the signal of ion fragments. Sensitivity value was determined by using oxygen as a reference gas due to its ionisation ability to account for other mass fragments. Then sensitivity relative to oxygen was calculated by the following formula:

$$\frac{flow\ rate\ of\ oxygen}{flow\ rate\ of\ gas} \times \frac{reading\ for\ gas\ fragment}{reading\ for\ oxygen\ molecolar\ ion}$$

The flow rate is accurately measured using pre-calibrated mass flow meters.

To convert the signal to the mole of gas, firstly, the correction factor was determined. Helium was used as inert and unaffected gas to account for the difference in gas ionisation as a result of redox behaviour at the filament. The intensity correction factor was calculated by dividing the first value of helium into each subsequent value. Then, the next formula was used to determine product gases corrected signal strength:

$$\frac{signal\ intensity}{sensitivity} \times intensity\ correctionnfactor$$

The above formula is without units and only shows the relative amount of each gas, but by using the ideal gas law this value can be converted in to the moles. As at the same temperature, pressure and volume the same number of moles is available, an average value of methane before passing over the catalyst was taken, and all corrected value were divided by this amount to obtain the number of moles for each gas relative to moles of methane.

2-5 Results and discussion:-

2-5-1-1 - *X-ray diffraction (XRD) of $LaCeZr_{2-x}Ni_x O_7$ prepared by the hydrothermal method*

To confirm that a pyrochlore phase has successfully formed, the catalysts were analysed using XRD. The XRD profile for the non-Ni containing LCZ showed a crystalline pattern that is indicative of the cubic $La_2Zr_2O_7$ pyrochlore phase with typical intense diffraction peaks of the pyrochlore structure at $2\theta=28.74^o$, 33.31^o, 47.83^o and 56.76^o (fig 2-1). The peaks are sharp indicating an increase in crystal grain growth [1]. Doping Ni in to the B site introduces typical diffraction peaks of NiO at 37.68^o and 43.06^o.

The XRD patterns of spent catalysts show peak splitting which suggests the mixed structure of cubic La/Ce ZrO_4 oxide phase with space group P213 and Pyrochlore Ce/La Zr_2O_7 with space group Fd-3m are in this composition rather than the fluorite phase (CeO_2) which is also typical for these materials[11,12]. This composite structure is composed of coarse Ce-rich fluorite and fine Zr-rich pyrochlore grains and the structure is not purely cubic. [8] Metallic Ni was detected in reduced 1-Ni catalyst pattern at 44^o and 50^o, which indicates that NiO reacts with H_2 during the reduction process. By decreasing the amount of Ni, the splitting in the peak become more evident and ZrO_2 emerged obviously in the structure. In the as-prepared 0.5-Ni and 0.25Ni two peaks of La/$CeZrO_4$ and ZrO_2 was observed instead of one peak of La Ce ZrO_7 in the used and reduced catalyst. Increasing the amount of Ni improves the insertion of Ce that is present in the fluorite phase into the structure of the catalyst. Free Ni metal was not observed clearly in the reduced catalyst pattern of 0.25Ni at 50^o, as low amount of Ni leads to intensity of peak being low. As reduced and used samples were tested after H_2S poisoning, a peak of Ce_2O_2S was observed at around $\theta=20^o$.

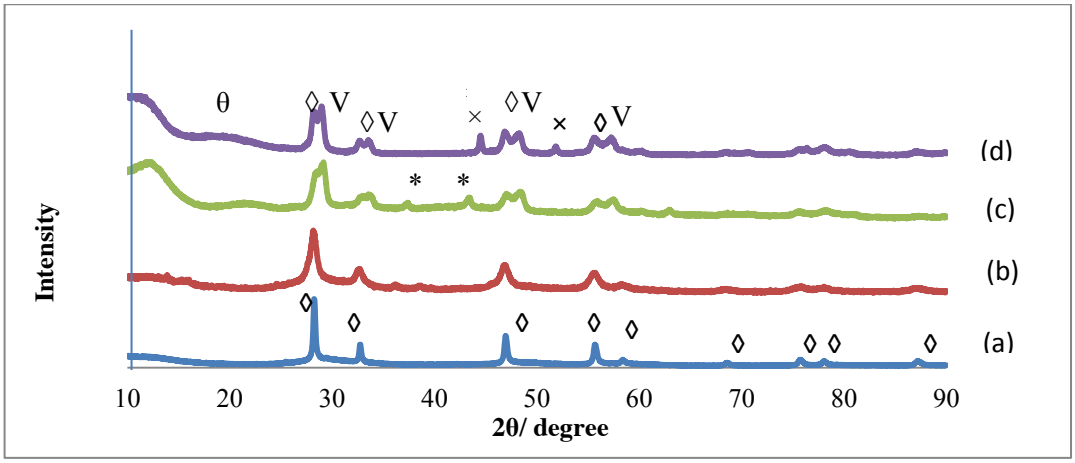

Fig 2-1: XRD patterns for a) LCZ, b) 1-NiLCZ, c) spent 1-NiLCZ and d) reduced used 1-NiLCZ La/Ce Zr_2O_7 ◊, Ce/La ZrO_4V, Ce/La O_2S θ , NiO*, Ni ×,

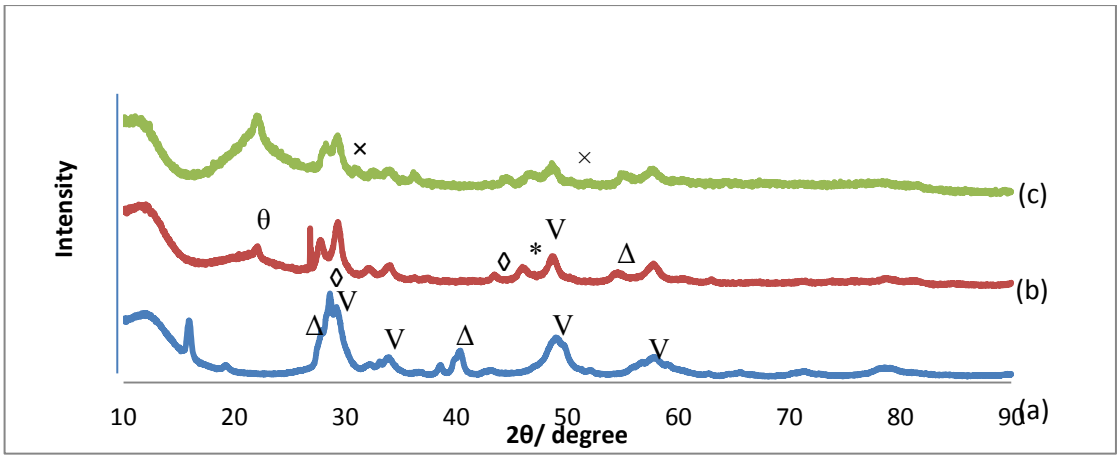

Fig 2-2: XRD patterns for a) as-prepared 0.5-Ni LCZ b) spent 0.5-Ni LCZ and c) reduced used 0.5-Ni LCZ Δ ZrO_2 , La/Ce Zr_2 O_7 ◊, La/Ce ZrO_4 V, Ce/La O_2S θ, Ni O *, Ni ×

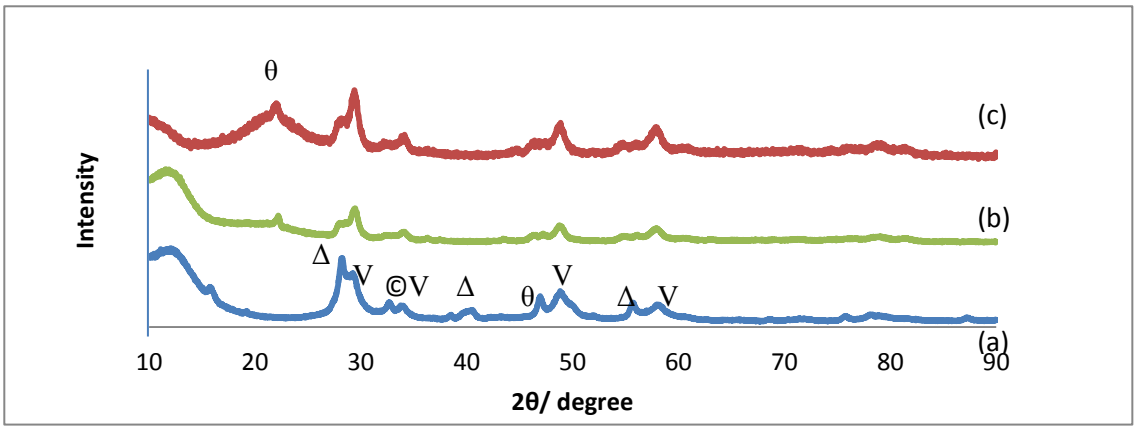

Fig 2-3: XRD patterns for a) as-prepared 0.25-Ni LCZ b) spent 0.25-Ni LCZ and c) reduced used 0.25-Ni LCZ La/Ce ZrO_4 V Ce/La O_2S θ, ZrO_2 Δ, $LaNiO_4$ ©

2-5-1-2 - X-ray diffraction (XRD) of $LaCeZr_{1.5}Ru_{0.5}O_7$ prepared by hydrothermal method

Fig 2-4 presents the XRD patterns of $LaCeZr_{1.5}Ru_{0.5}O_7$ as-synthesised, after TPO and after reduction. Peaks corresponding to the pyrochlore $La_2Zr_2O_7$ phase were detected in the as-prepared structure. A small peak belonging to La Ru O was detected at 29°. As reduced and used samples were tested after H_2S poisoning, a peak of Ce_2O_2S was observed at around θ=20°. After TPO of the long-term stability test and reduction of the spent catalyst, the XRD pattern does not show a significant difference in peak position. This suggests this catalyst has thermal and chemical stability under reaction temperature and reducing conditions during DRM.

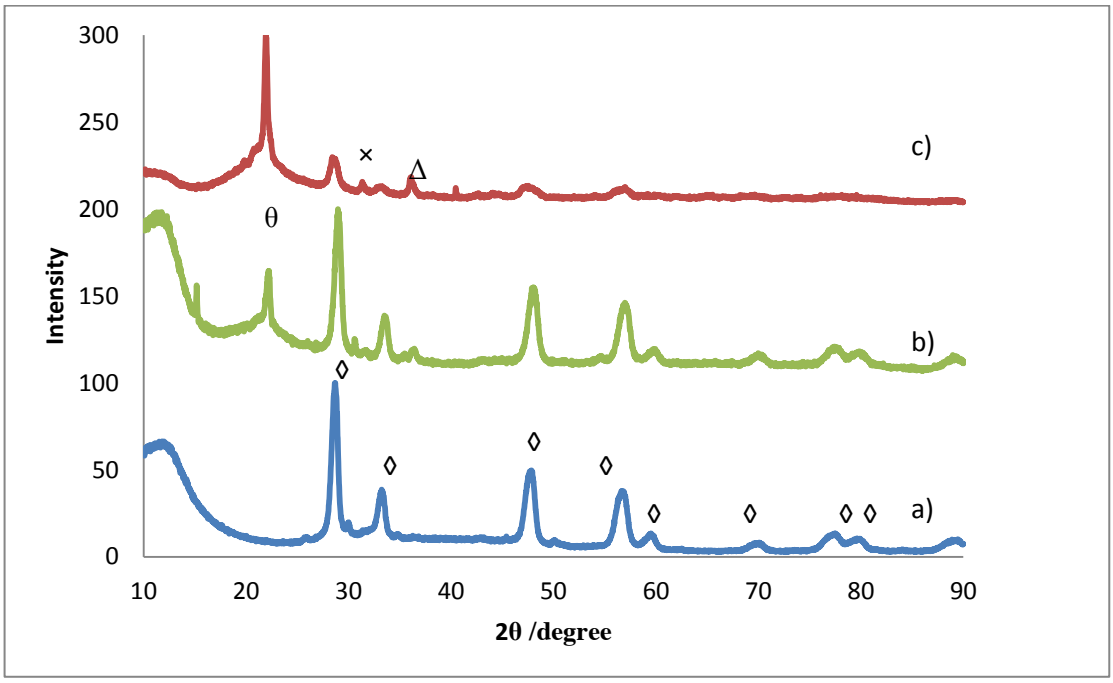

Fig 2-4: XRD patterns for a) as-prepared 0.5-Ru LCZ b) spent 0.5-Ru LCZ and c) reduced used 0.5-Ru LCZ, $La_2Zr_2O_7$ ◊, La Ru O ×, Ce/La O_2S θ, ZrO_2 Δ

2-5-1-3 - X-ray diffraction (XRD) of $LaCeZrNiO_7$ prepared by Pechini method

The XRD spectra for the as-synthesised, TPO after long-term stability test and the reduction after TPO of $LaCeZrNiO_7$ are shown in fig 2- 5. The typical diffraction peaks of NiO can be observed at 36 °, and 41.7° besides the initial diffraction peaks belonging to the pyrochlore phase. The obvious different between the as-prepared and used catalyst was in the large back ground peak at around 20 degree that refers to the Ce/La O_2S θ as it was tested after H_2S poisoning.

The pyrochlore structure was unchanged after the post experiments and the reduction conditions (b,c), and was extremely stable.

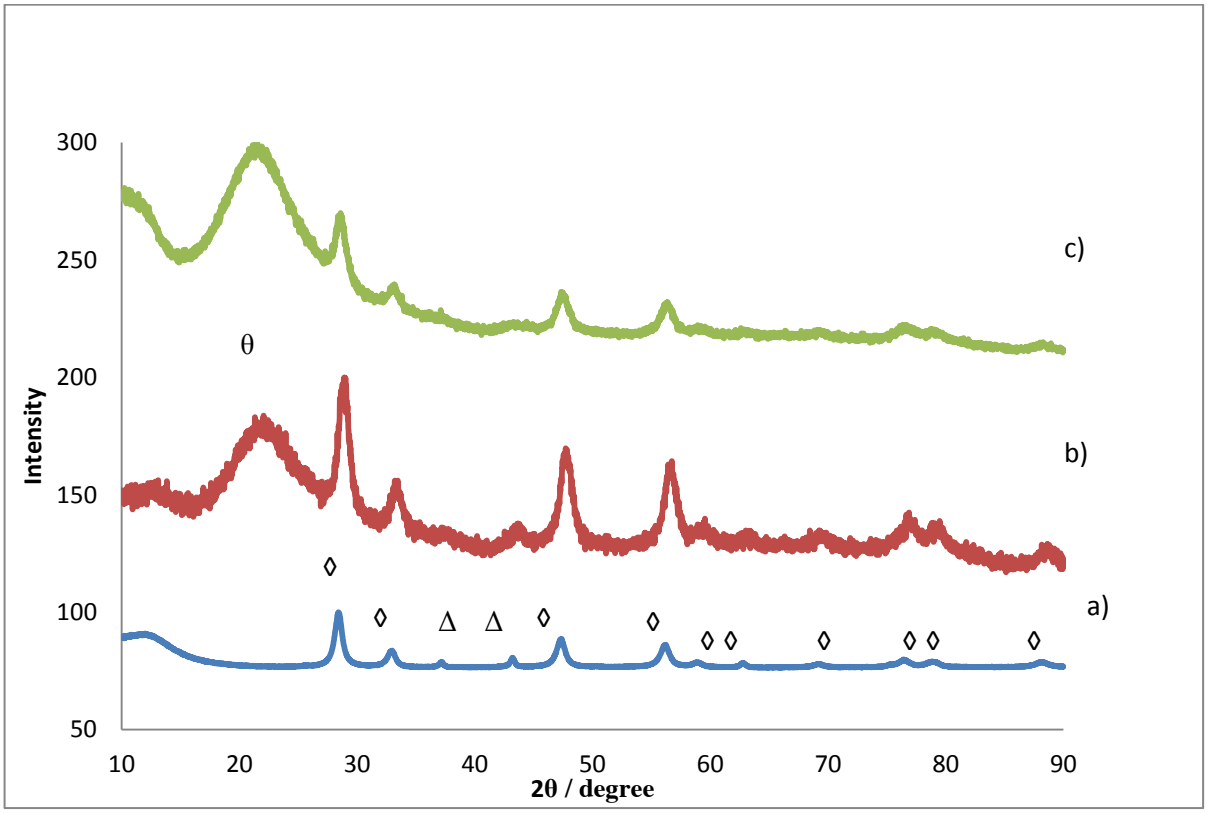

Fig 2-5: XRD patterns for a) as-prepared LCNZ b) spent LCNZ and c) reduced used LCNZ $La_2Zr_2O_7$ ◊, NiO Δ , Ce/La O_2S θ

2-5-2-1 – Temperature programmed reduction of $LaCeZr_{2-x}Ni_xO_7$ prepared by hydrothermal method

The H_2-TPR profiles obtained from LCZN with various levels of Ni-doping before and after DRM reaction are presented in fig 2- 6 to 8.

According to the literature, pure NiO phase is reduced at temperatures between 220 and 420 °C, [4]with the first reduction for all three catalysts nearly similar. As the catalyst was produced by the hydrothermal method and no high temperature calcination was applied, therefore some Ni in the form of hydroxides remained in the structure of the catalyst and had weaker interaction. The second peak at 300 °C can be attributed to the reduction of bulk NiO and the third reduction peak corresponds to the reduction of NiO species having interaction with the Pyrochlore support which occurs at higher temperature at 390 °C.[1]

Only one wide reduction peak centred around 420 °C can be observed for the used catalyst, which indicates the presence of strong interaction between Ni and surrounding lattice species. No reduction peak was observed for the un-doped Ni-catalyst due to absence of any reducible metal in the structure.

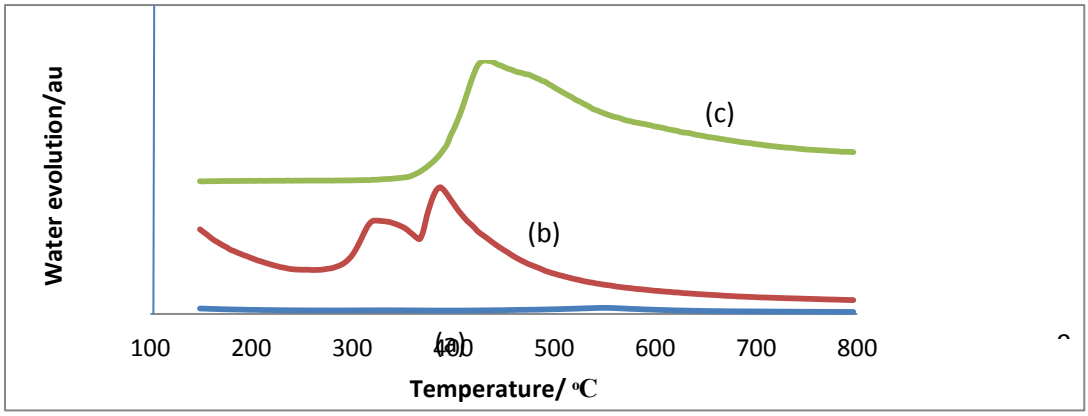

Fig 2-6: H_2-TPR profiles of a) LCZ, b) as-prepared LCNZ and c) used LCNZ

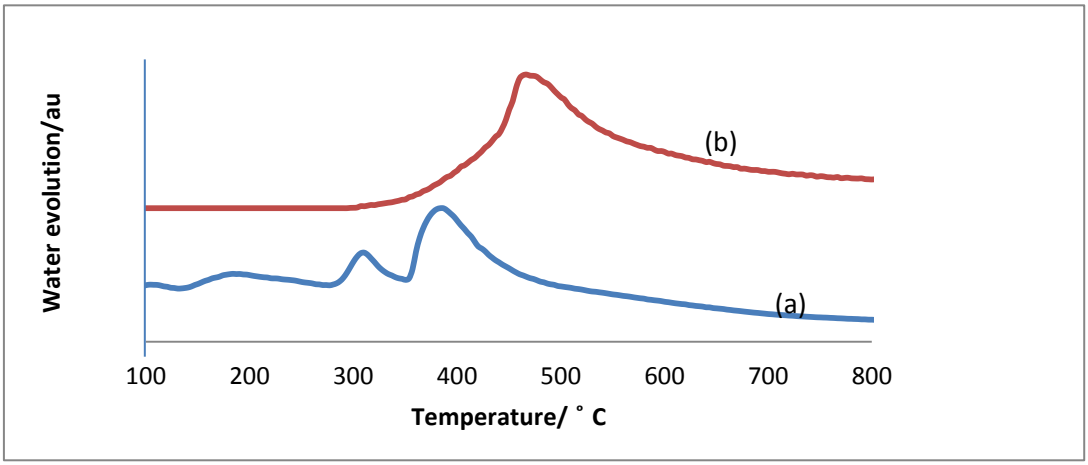

Fig 2-7: H_2-TPR profiles of 0.25-Ni a) as-prepared b) used catalyst

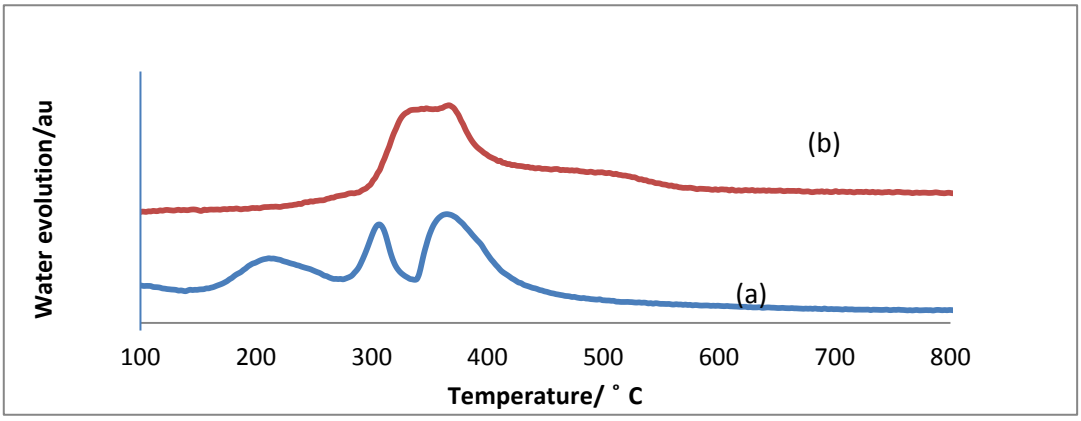

Fig 2-8: H_2-TPR profiles of 0.5-Ni a) as-prepared b) used catalyst

2-5-2-2 – Temperature programmed reduction of $LaCeZr_{1.5}Ru_{0.5}O_7$ prepared by the hydrothermal method

TPR of LCRuZ shows multiple reduction peaks at 100, 238 and 350 °C before DRM reaction. Pakhare in his study showed the reduction peaks of LRuZ located at 100, 238, 450 and 551 °C. They suggested that the peak at 100 °C was due to a small amount of Ru at the pyrochlore surface that is not strongly bond to the pyrochlore structure, and the peak at 238 °C is assigned to the reduction of Ru substituted into the pyrochlore structure and those at 450 and 551° C, are attributed to the reduction of the lanthanum zirconate Pyrochlore.[5] In the study of ruthenium catalyst supported on high-surface-area zirconia , the author showed that a broad reduction peak at around 330 °C can been attributed to the strong metal-support interaction of Ru/ZrO_2 [6]. After DRM reaction, only one broad TPR peak was observed that was shifted to lower temperature.

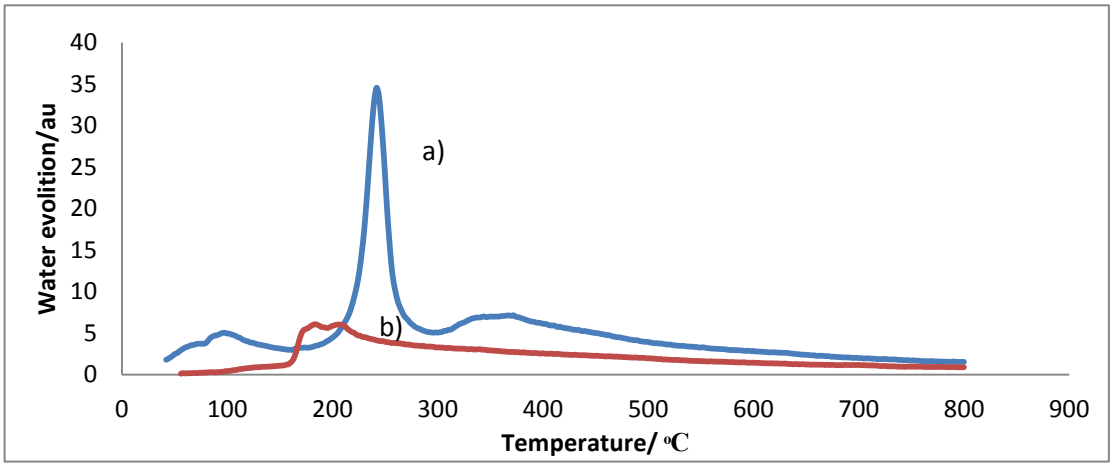

Fig 2-9: H_2-TPR profiles of 0.5-RuLCZ a) as-prepared b) used catalyst

2-5-2-3 – Temperature programmed reduction of $LaCeZrNiO_7$ prepared by Pechini method

Fig 2-10 shows the reduction profile before and after dry reforming at 30 ppm H_2S with a TPO step i- between for LCZN that was prepared by the Pechini method. Before the reforming reaction, the catalyst had a broad-wide peak reduction in the range of 385 °C to 644 °C that contains three individual small peaks at 432, 496 and 592 °C. After reforming, the

third peak (592°C) disappeared, and a decrease in reduction temperature was observed from 642 to 520°C. The decrease in reduction temperature is due to the sintering that results in an increase in the size of Ni particles with the monotonic distribution that made the interaction between the Ni and pyrochlore weaker.[1]

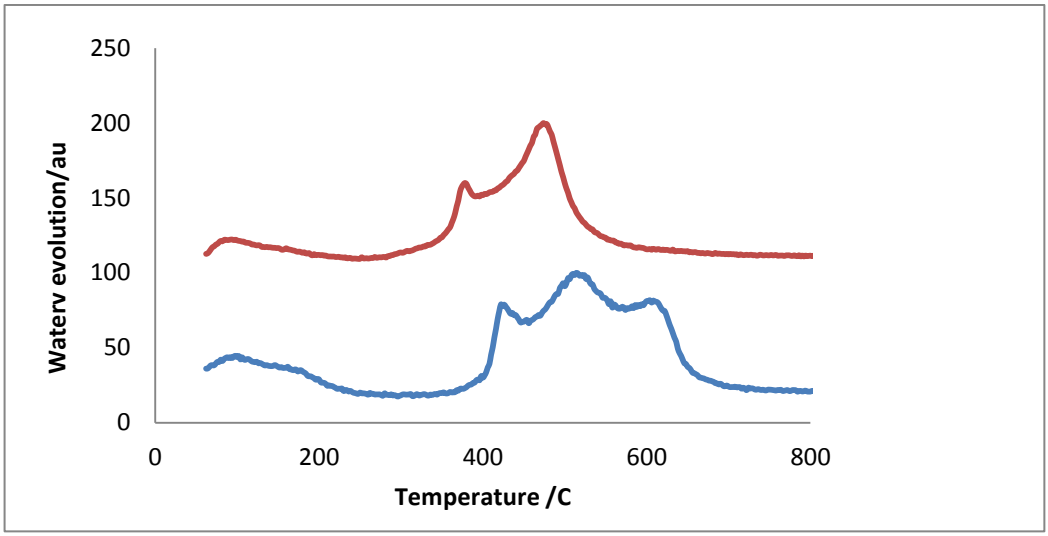

Fig 2-10: H_2-TPR profiles of a) as-prepared LCNZ and b) used LCNZ

2-5-3-1 Scanning electron microscopy analysis of $LaCeZr_{2-x}Ni_xO_7$ prepared by the hydrothermal method

To study the morphology and surface changes of the catalyst, the SEM images of $LaCeZr_{2-x}Ni_xO_7$ before and after reaction in the absence and presence of H_2S, in the reduced state and after recovery have been investigated and are shown in fig 2-11.

As seen from the as-prepared catalyst at different magnifications (a), the $LaCeNiZrO_7$ (x=1) comprise two different shapes, the nano sheets are relatively abundant in Ce, whereas fine grains are rich in Zr. Ce rich sheets are the fluorite phase, while the fine Zr rich grains are the pyrochlore phase [8]. Therefore, the structure of $LaCeNiZrO_7$ would be better reflected as a fluorite-pyrochlore composite structure. After 20 hours of dry reforming at 850°C and doing TPO, no significant change occurred except a slight increase in size as displayed in (b). The morphology of the catalyst at 700°C with continuous addition of 30 ppm H_2S shows that the

structure of the catalyst is entirely covered with filamentous coke(c). After making a recovery by H_2S removal, it can be seen that no filamentous coke is left on the surface, instead granular coke can be observed (d). The surfaces of the used reduced catalyst consists of agglomerated crystalline powders with an irregular hole which is assigned to the re-oxidation of the reduced metallic Ni-active species [9,10](e).

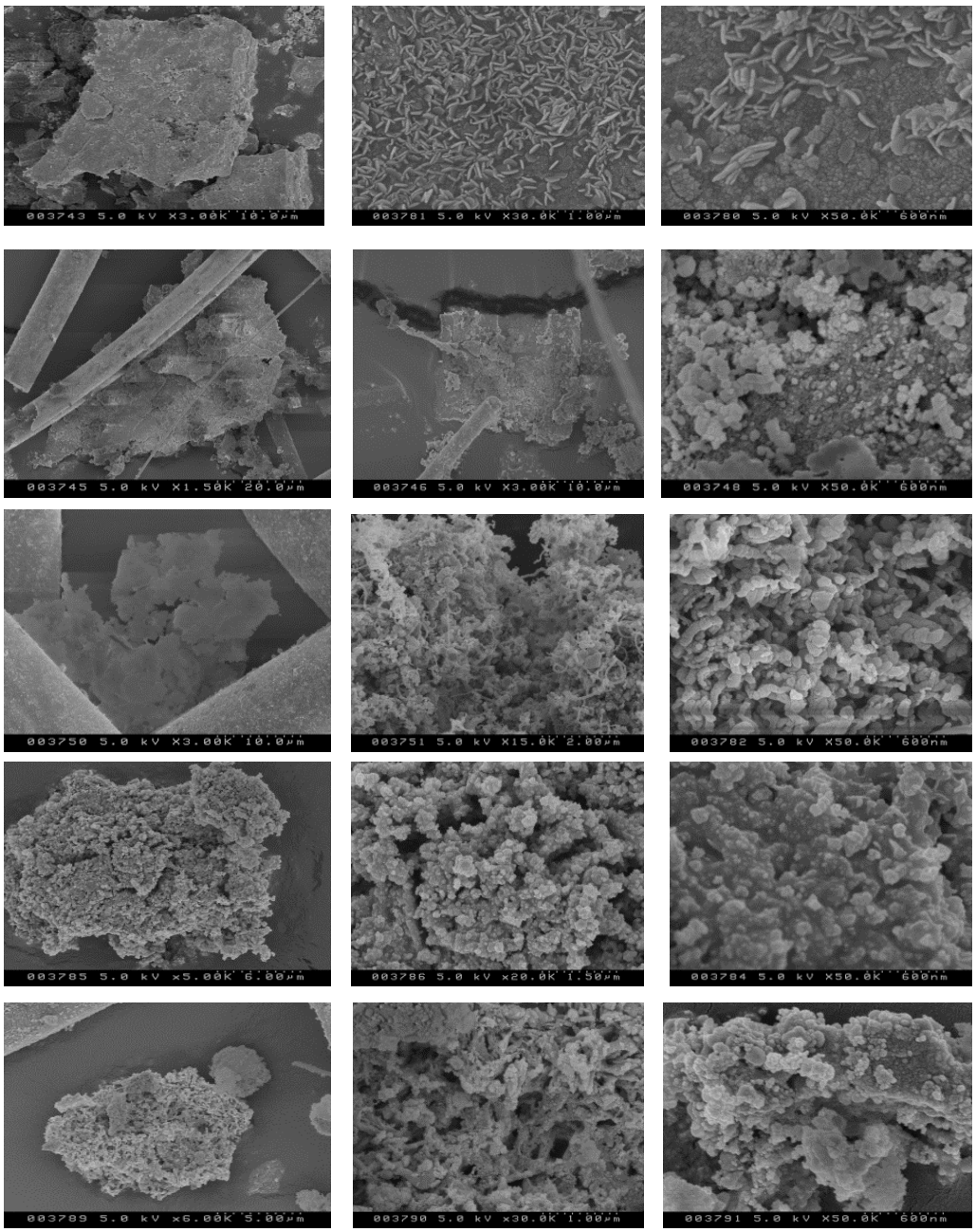

Fig 2-11: SEM images of as-synthesised (a) ,spent after long term stability without H_2S (b), spent after long term stability with H_2S (c), recovered catalyst (d) and used reduced catalyst (e).

As can be seen from fig 2-12, the morphology of x= 0.25-Ni and x= 0.5-Ni in the as-prepared state are very similar to the morphology of the used catalyst of 1-Ni LCZ and this was confirmed by XRD.

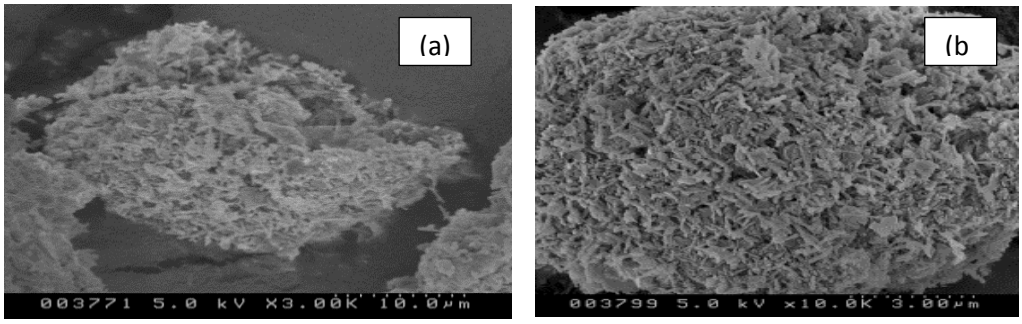

Fig 2-12: SEM images of as-prepared (a) x= 0.25-Ni and (b) x= 0.5-Ni LCZ

2-5-3-2 Scanning electron microscopy analysis of $LaCeZr_{1.5}Ru_{0.5}O_7$ prepared by hydrothermal method

SEM of RuLCZ demonstrates aggregation of particles consisting of many smaller spherical particles. The nanoparticles are well separated, and particle boundaries are clearly visible.

No significant difference was observed between the morphological features of the RuLCZ before and after the reforming reaction.

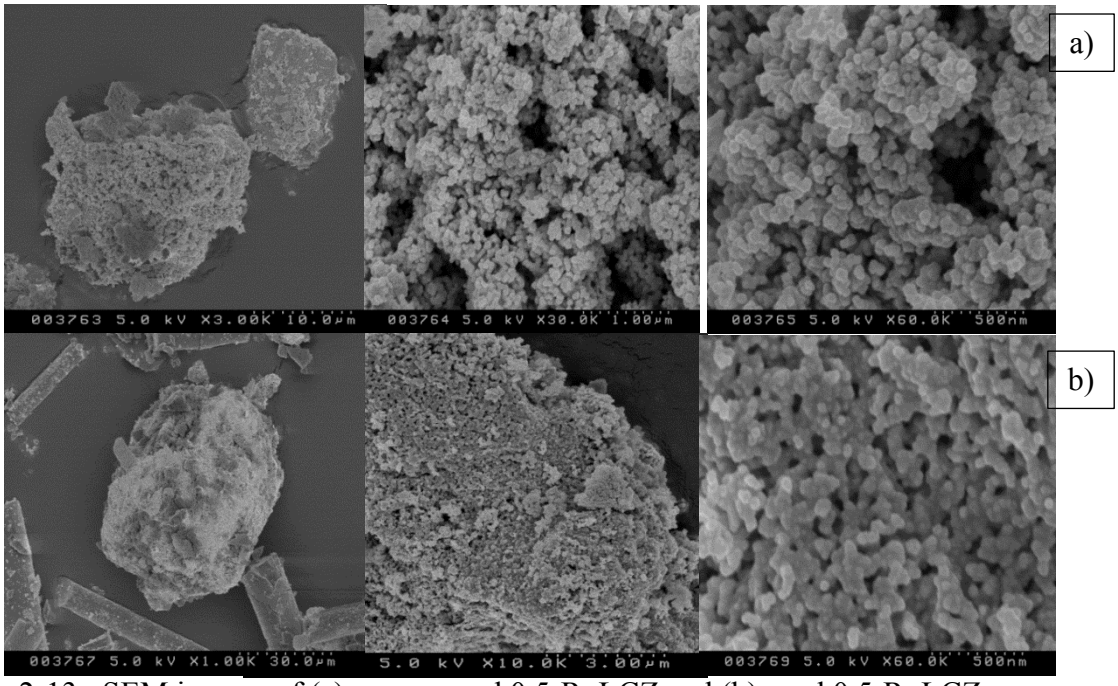

Fig 2-13: SEM images of (a) as-prepared 0.5-RuLCZ and (b) used 0.5-RuLCZ

2-5-3-3 Scanning electron microscopy analysis of $LaCeZrNiO_7$ prepared by the Pechini method

Fig 2-14 shows SEM of the sample prepared by the Pechini method. As can be seen, the catalyst consists of an irregular rigid triangle plate-shaped agglomerates. Relatively fine uniform spherical particles that were distributed regularly can also be observed. No significant changes in the microstructure were noted after DRM reaction.

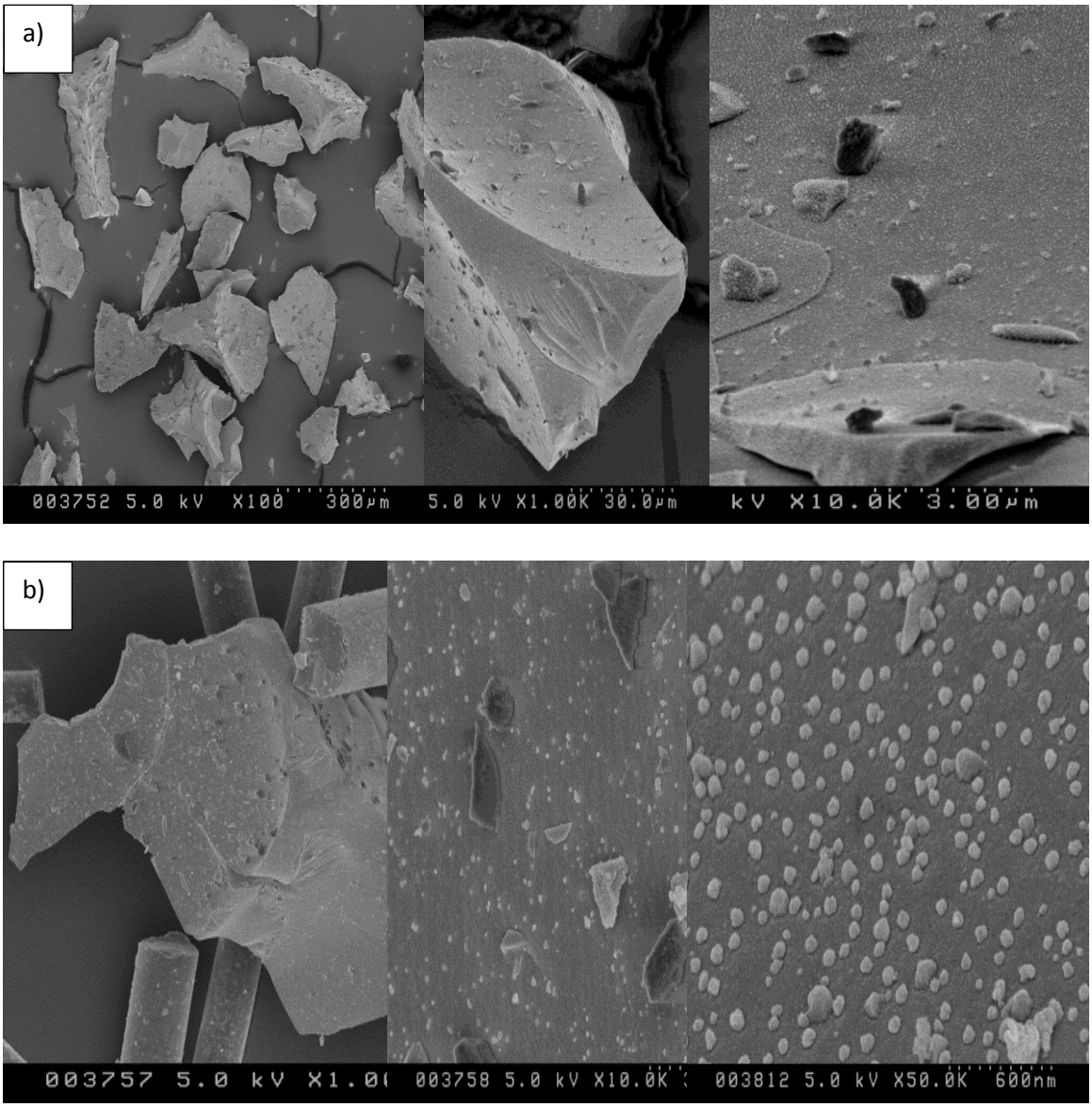

Fig 2-14: SEM images of (a) as-prepared Ni-LCZ and (b) used Ni-LCZ

2-5-4 Bruner–Emmett–Teller (BET) Analysis:-

BET calculation was applied to determine the surface area of the catalyst. The results are shown in table 2-2. As can be seen, the Ru containing catalyst had the smallest surface area. The surface area of the nickel containing catalysts prepared by the hydrothermal method increased with an increase in Ni loading. The surface area of the Pechini method nickel containing catalyst was close to half the surface area of the hydrothermal method, which had the same amount of nickel.

Table 2-2 Surface area of several Pyrochlore catalysts

Sample	**Surface area / m^2g^{-1}**
$LaCeZr_{1.5}Ru_{0.5}O_7$	17.30
$LaCeZr_{1.75}Ni_{0.25}O_7$	62.13
$LaCeZr_{1.5}Ni_{0.5}O_7$	63.38
$LaCeZrNiO_7$	86.99
$LaCeZrNiO_7$ (Pechini)	45.36

2-6 Conclusions:-

From the XRD results it can be concluded that all of the four catalysts contain a pyrochlore phase in their structures. However, the Ni pyrochlore catalysts prepared by the hydrothermal method showed spilt peaks that belonged to the mixture of pyrochlore ($La/Ce_2Zr_2O_7$) and $La/CeZrO_4$ oxide phases. All Ni pyrochlore catalysts showed impurity in the form of NiO which increased with the amount of Ni loading. The Ru catalyst, unlike the hydrothermal Ni catalyst, did not show $La/CeZrO_4$ oxide phase in its profile.

TPR analysis showed all four catalysts are reducible and when comparing the as-synthesised catalysts, the reduction peak was shifted to higher temperatures in the case of the hydrothermal Ni catalysts, whilst in the Pechini method the reduction peak shifted to lower temperature indicating some level of sintering. In comparison with as-prepared catalyst, Ru in the used Ru Pyrochlore had the widest peak instead of sharp peak that was shifted to the lower temperature.

BET analysis showed that the Ni hydrothermal catalysts have the larger surface area in comparison with Pechini method and the Ru catalyst has the biggest particle size with the lowest surface area.

From SEM analysis, it was found that the hydrothermal method produces irregular agglomerate particles while the Pechini method generates rigid triangel plate particles with regular spherical uniform particles on the surface indicating that Ni is incorporated on the mixed structure and they are quite small and well dispersed.

2-7 References:-

1- Haynes, D.J., Shekhawat, D., Berry, D.A., Zondlo, J., Roy, A. and Spivey, J.J., 2017. Characterization of calcination temperature on a Ni-substituted lanthanum-strontium-zirconate pyrochlore. *Ceramics International*, *43*(18), pp.16744-16752.

2- Zhao, W., Zhang, K., He, Z., Xue, J., Li, W., Xie, D. and Zhang, H., 2018. Vacuum sintering of highly transparent La1. 28Yb1. 28Zr2O7. 84 ceramic using nanosized raw powders. *Ceramics International*, *44*(11), pp.12535-12538.

3- Song, C., Pan, W. and Srimat, S.T., 2002. Tri-reforming of Natural Gas Using CO 2 in Flue Gas of Power Plants without CO 2 Pre-separation for Production of Synthesis Gas with Desired H 2/CO Ratios. In *Environmental Challenges and Greenhouse Gas Control for Fossil Fuel Utilization in the 21st Century* (pp. 247-267). Springer, Boston, MA.

4- Li, C. and Chen, Y.W., 1995. Temperature-programmed-reduction studies of nickel oxide/alumina catalysts: effects of the preparation method. *Thermochimica Acta*, *256*(2), pp.457-465

5- Pakhare, D., Haynes, D., Shekhawat, D. and Spivey, J., 2012. Role of metal substitution in lanthanum zirconate pyrochlores (La 2 Zr 2 O 7) for dry (CO 2) reforming of methane (DRM). *Applied Petrochemical Research*, *2*(1-2), pp.27-35.

6- Sun, G., Xu, A., He, Y., Yang, M., Du, H. and Sun, C., 2008. Ruthenium catalysts supported on high-surface-area zirconia for the catalytic wet oxidation of N, N-dimethyl formamide. *Journal of hazardous materials*, *156*(1-3), pp.335-341.

7- http://www.micromeritics.com/Repository/Files/appnote120.pdf

8- Kwak, K.H., Shim, B.C., Lee, S.M., Oh, Y.S., Kim, H.T., Jang, B.K. and Kim, S., 2011. Formation and thermal properties of fluorite-pyrochlore composite structure in La2 (ZrxCe1−x) 2O7 oxide system. *Materials Letters*, *65*(19-20), pp.2937-2940.

9- Haynes, D.J., Shekhawat, D., Berry, D.A., Zondlo, J., Roy, A. and Spivey, J.J., 2017. Characterization of calcination temperature on a Ni-substituted lanthanum-strontium-zirconate pyrochlore. *Ceramics International*, *43*(18), pp.16744-16752.

10- Fang, X., Zhang, X., Guo, Y., Chen, M., Liu, W., Xu, X., Peng, H., Gao, Z., Wang, X. and Li, C., 2016. Highly active and stable Ni/Y2Zr2O7 catalysts for methane steam reforming: On the nature and effective preparation method of the pyrochlore support. *international journal of hydrogen energy*, *41*(26), pp.11141-11153.

11- Chen, H., Gao, Y., Liu, Y. and Luo, H., 2009. Coprecipitation synthesis and thermal conductivity of La2Zr2O7. *Journal of Alloys and Compounds*, *480*(2), pp.843-848.

12- Le Saché, E., Pastor-Pérez, L., Watson, D., Sepúlveda-Escribano, A. and Reina, T.R., 2018. Ni stabilised on inorganic complex structures: superior catalysts for chemical CO2 recycling via dry reforming of methane. *Applied Catalysis B: Environmental*, *236*, pp.458-465.

3. Methane Rich Dry Reforming Over Pyrochlore Catalysts

3.1 Introduction

3.1.1 Thermodynamics of dry reforming reaction: -

Dry reforming is a more appropriate reforming process for landfill biogas conversion into clean fuels due to no requirement for CO_2 separation steps.[1]

Dry reforming of methane is a highly endothermic reaction, but there are several possible side reactions that may occur during the DRM process[2] including: -

1) Reverse water gas shift reaction (RWGS), which can occur across the whole temperature range

$CO_2 + H_2 \leftrightarrow H_2O + CO$ $\Delta H = +41$ kJ mol^{-1}…….eq1

2) Carbon forming reactions including: - a) methane decomposition favourable at high temperatures (eq2) b) Boudouard reaction favoured at low temperatures (eq3) c) hydrogenation of CO and CO_2 eq (4, 5)

$CH_4 \leftrightarrow C + 2H_2$ $\Delta H = 74.9$ kJ mol^{-1}…….eq2

$2CO \leftrightarrow CO_2 + C$ $\Delta H = -172.4$ kJ mol^{-1}…..……eq3

$CO + H_2 \leftrightarrow H_2O + C$ $\Delta H = -131.3$ kJ mol^{-1}……..eq4

$CO_2 + 2H_2 \leftrightarrow 2H_2O + C$ $\Delta H = -90$ kJ mol^{-1}…….……eq5

3) Oxidative coupling of methane that occurs at high temperatures (eq 6, 7)

$2\ CH_4 + CO_2 \leftrightarrow C_2H_6 + CO + H_2O$ $\Delta H = 106$ kJ mol^{-1}…….……eq6

$2CH_4 + 2CO_2 \leftrightarrow C_2H_4 + 2CO + 2H_2O$ $\Delta H = 284$ kJ mol^{-1}……eq7

To limit side reactions, DRM has to be performed at high temperatures. However, from the economic and technical prospects, it would be more beneficial to perform this process at low temperatures (<700 °C). Therefore, a stable, active and selective catalyst is required which can promote the DRM reaction at low temperatures and at the same time inhibit carbon formation.[3]

Most active catalysts belong to group VIII and can be divided in to a) earth abundant transition metals and b) noble metals.

The low reaction rate for CH_4 decomposition[4], the low ability of carbon to dissolve into the Ru crystalline lattice[5], high resistance in high-temperature applications and its significant reaction energy reduction[6] makes Ru a promising catalytically metal for DRM reaction. However, its high cost still challenges the industrial sector.

Ni metal catalysts due to their high activity and market price are frequently used for dry reforming. However, Ni catalysts are highly sensitive to carbon deposition. Recently, the addition of Ce as promoters has been shown to be one way to enhance carbon resistance properties of Ni-based catalysts.[3]

3.1.2 The effect of ceria on reforming and carbon deposition: -

Cerium with electronic conFigure3-uration of [Xe] $4f^2 5d^0 6s^2$ has common oxidation states of $Ce^{+3}(Ce_2O_3)$ and $Ce^{+4}(CeO_2)$.[7] The oxidation state of cerium is dependent on the pressure of O_2 and temperature that it is exposed to.[8]

Ceria can act as a powerful redox agent which is usually referred to as the oxygen storage capacity (OSC) [9]

The Conversion between the reduced and stoichiometric state of cerium can be described as follow [7]

$Ce_2O_3 + O_2 \leftrightarrow CeO_2$ ……..eq8

Oxygen can be stored in the CeO_2 form under high pressure of O_2 and, any stored oxygen is released into the gas phase at low pressures of O_2. This form of redox behaviour increases the mobility of oxygen on the catalytic surface, resulting in increasing the rate of carbon oxidation.

Ceria also promotes the reverse Boudouard reaction in carbon dioxide reforming by increasing the reaction between CO_2 and carbon[10] as shown in equations 9 and 10.

$Ce_2O_3 + CO_2 \leftrightarrow 2CeO_2 + CO$ …….. eq9

$2CeO_2 + C \leftrightarrow Ce_2O_3 + CO$ ……..eq10

Other beneficial effects of ceria are increasing the catalytic surface area by increasing dispersion of Ni, minimising sintering effect and improving the selectivity of reactant conversion.[10,11]

3.2 Carbon Dioxide Reforming of Methane for Ni-LCZ Prepared by the Hydrothermal Method

The aim of this section is to compare the dry reforming performance of a LCZ pyrochlore catalyst that has been prepared by the hydrothermal methods with different amounts of Ni doping. Initial tests were achieved using a 2:1 mixture of methane and carbon dioxide. The samples were prereduced in the same manner using a temperature programme of $10^{o}C\ min^{-1}$ up to $900^{o}C$ under 10% hydrogen. Temperature programmed reactions were carried out over (0.125Ni-LCZ, 0.25Ni-LCZ, 0.5Ni-LCZ and 1Ni-LCZ). The reactions were followed by QMS and converted to mole equivalent of methane. At the end of each reaction, temperature programmed oxidation was performed to determine the kind and the amount of deposited carbon. After this step, each sample was tested isothermally at varying temperatures from

650°C to 850°C and the deposited carbon analysed using post reaction TPO. The relationship between time on stream and carbon deposited was investigated for all Ni doped catalysts under 2:1 mixture of methane and carbon dioxide.

3.2.1 Temperature Programmed Surface Reaction during CH_4:CO_2=2:1 (TPSR)

TPSR for 0.125Ni-LCZ, 0.25Ni-LCZ, 0.5Ni-LCZ and 1Ni-LCZ under methane rich conditions are shown in Figure3- 1, 2, 3 and 4 respectively.

TPSR of 0.125Ni-LCZ (Figure3-1) shows that no reaction is observed until ~760°C. At this point CO formation begins while CO_2 and CH_4 are consumed. It can be seen that some water is beginning to form as a result of the reverse water gas shift reaction. However, syngas formation is negligible even at the end of the reaction.

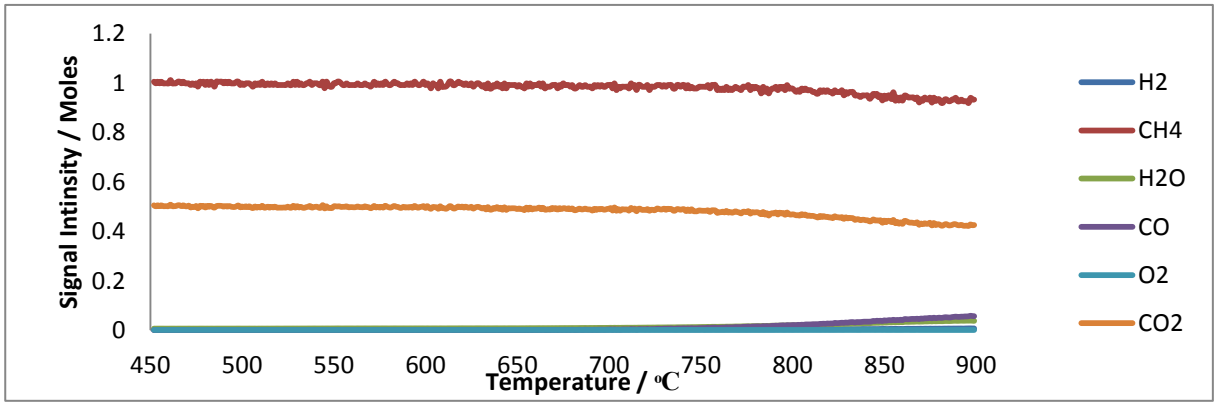

Figure3- 1- reaction profile for a 2:1 CH_4/CO_2 mixture passed over 0.125Ni-LCZ

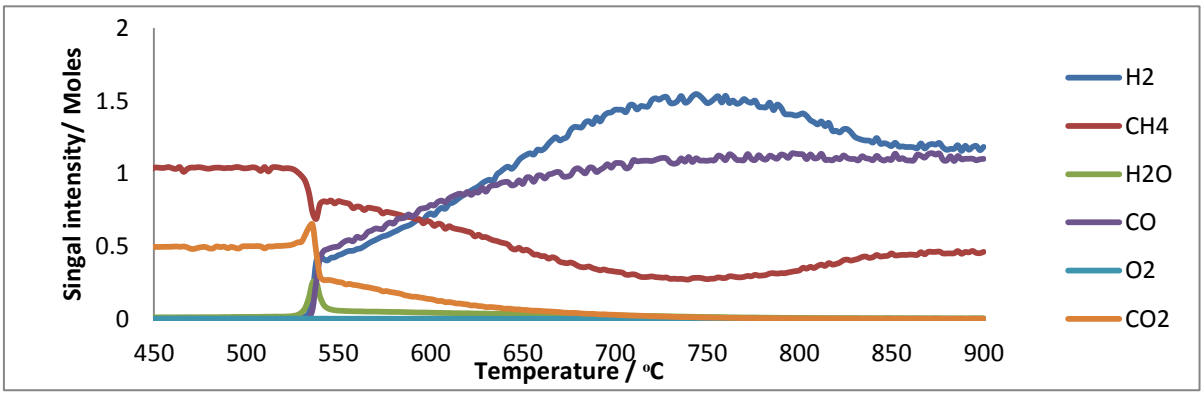

Figure3- 2- reaction profile for a 2:1 CH_4/CO_2 mixture passed over 0.25Ni-LCZ

As can be seen from Figure3- 2, by doubling the amount of Ni to 0.25, syngas production happened sooner and at 534°C. From this point, syngas production increased linearly and the ratio of H_2:CO became almost 1:1 until 630 °C. After this temperature the ratio began to exceed 1:1 with an increase in the amount of methane decomposition because of the Boudouard reaction. At this temperature the carbon monoxide is recombined to form carbon dioxide and in consequence reformed with methane resulting in greater methane conversion and hydrogen formation. When the temperature increased, the Boudouard reaction became less thermodynamically favourable resulting in a falling off the H_2: CO ratio and this stabilised at 1:1 by 850°C.[25]

The presence of ceria in the structure also could be the reason for increasing the amount of methane conversion[12-16]. Ceria increases the activity through increasing metal dispersion and therefore increasing surface area[19-22]. In addition, ceria has been shown to be active for methane reforming and also aids CO and H_2 formation through CO_2 and H_2O dissociation[13,17,18] as illustrated in the following reactions:

$2CeO_2 + CH_4 \leftrightarrow Ce_2O_3 + CO + 2H_2$ ……eq11

$Ce_2O_3 + CO_2 \leftrightarrow 2CeO_2 + CO$ ……...…….eq12

$Ce_2O_3 + H_2O \leftrightarrow 2CeO_2 + H_2$ ..……..eq13

By increasing the amount of nickel to 0.5, the reaction started later than for 0.25-Ni by 75°C. (Figure3-3). A low level of water production can be seen due to the occurrence of the reverse water gas shift reaction. At 730°C the CO_2 is converted completely, and the composition of the synthesis gas formed changes and becomes more hydrogen rich.

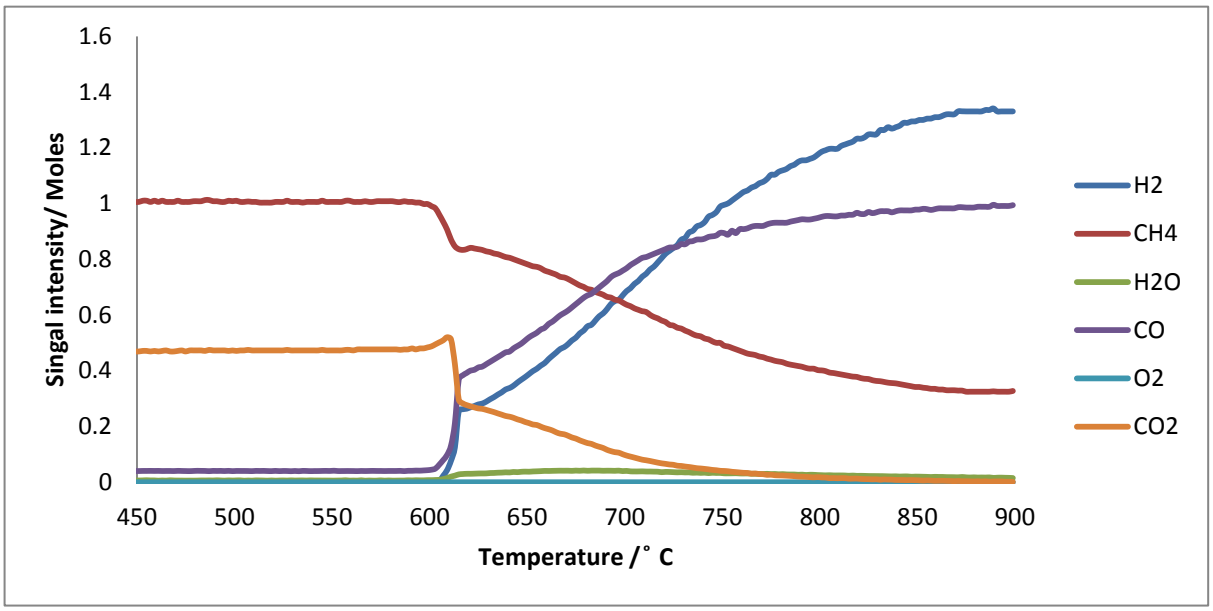

Figure3- 3- reaction profile for a 2:1 CH_4/CO_2 mixture passed over 0.5Ni-LCZ

Figure3- 4 shows the biogas reforming reaction profile for 1Ni-LCZ. As can be observed, the temperature that reforming began, is similar to 0.5Ni-LCZ and interestingly the shape of the profile is similar to 0.25 Ni-LCZ except for the sharp drop in the amount of CO_2 and CH_4. The Boudouard reaction has an effective impact on 1Ni-LCZ at the low temperatures and becomes less favourable at higher temperatures resulting in a falling ratio of H_2: CO to reach the stoichiometric DRM level. However, the presence of ceria also had an essential role in the methane and carbon dioxide conversion, as was explained previously.

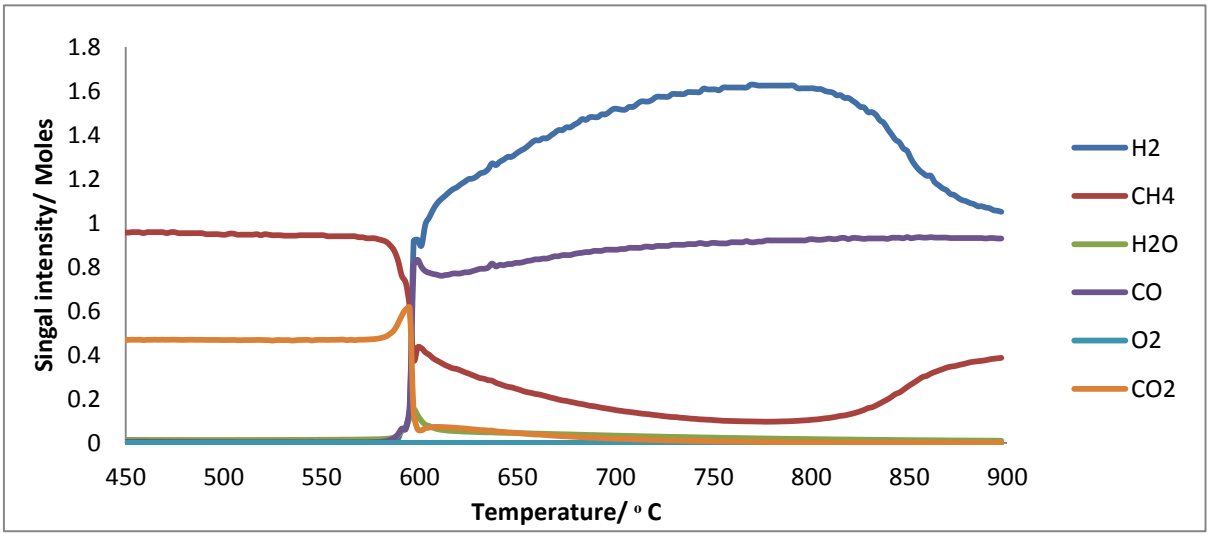

Figure3- 4- reaction profile for a 2:1 CH_4/CO_2 mixture passed over 1Ni-LCZ

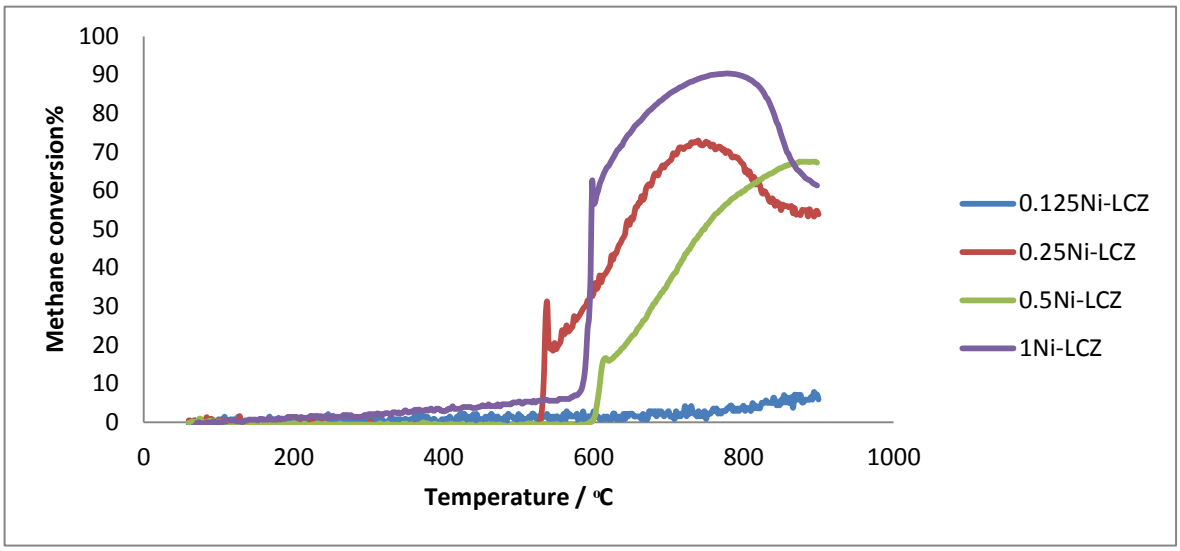

Figure3- 5- percentage methane conversion for a 2:1 CH_4/CO_2 mixture passed over various nickel doped $LaCeZr_{2-x}Ni_xO_7$(x=0.125,0.25,0.5,1)

The percentage methane conversion of various Ni doped pyrochlore catalysts during temperature programmed reactions are shown in Figure 3- 5. Because of the lack of active site availability, the methane conversion rate of the 0.125Ni-LCZ catalyst is negligible even at high temperature.

The starting temperature is lower for 0.25Ni-LCZ and this can be attributed to CeO_2 acting to encourage methane decomposition through distribution of oxygen across the catalyst surface. The reason for this is that the effective amount of CeO_2 in 0.25NI-LCZ is higher than for the other catalysts, due to the lower amount of Ni in the structure of the catalyst. As the size and dispersion of Ni crystallites affect the activity of the DRM catalyst, therefore, the amount of carbon deposited should increase with higher loading of Ni if large crystallites of the active phase are formed[28]. Literature data show that large Ni particle size limited removal of carbon deposition by preventing contact with lattice oxygen[29-31].

At high temperature (870 ° C), the catalyst activity decreased by reducing the amount of nickel in the structure. The reason could be due to the greater H_2:CO_2 and CO:CO_2 ratios resulting in the reduction of the CeO_2 to Ce_2O_3. Low CO_2 concentration decreases the ability of Ce_2O_3 oxidation to CeO_2 and therefore Ce_2O_3 does not encourage methane reforming[13,23]. With increasing nickel doping, the level of Boudouard reaction increased in the middle step of the reaction.

3.2.2 Isothermal Dry Reforming of Methane

In this section, the isothermal reforming of the three Ni-doped LCZ Pyrochlore catalysts during methane-rich dry reforming was investigated at various temperatures ranging from 650 ° C -850 °C. At the end of each reaction, the amount of carbon deposited on the catalyst was quantified. As was discussed before, the three catalysts of La Ce Ni $_x$ Zr $_{1-x}$ O_7 with x=0.25, 0.5, and 1Ni, were stable and did not show loss of reforming activity in the form of total oxidation product.

3.2.2.1.1 Isothermal dry reforming of rich- methane over 0.25 Ni -LCZ

For about 3 hours of reaction, high levels of methane decomposition were observed at the temperature of 650 ° C as shown in Figure3- 6 (a). The decomposition was then suppressed and reached the theoretical value of 50% conversion as adsorbed species occupy active sites and as a consequence the amount of H_2 and water formation decreased. Some small levels of cycling due to the redox properties of ceria can be seen after 15 hours of reaction. The presence of some H_2O for the rest of the reaction can be attributed to the following reaction[24]: -

$$CeO_2 + CH_4 \leftrightarrow Ce_2O_3 + CO_2 + H_2O \quad \text{……..eq14}$$

The percentage of CO_2 conversion was lower than expected by approximately 10% by the end of the reaction time. The probability of Boudouard reaction is too high at this temperature, leading to increase in the amount of CO_2 in the reaction. After two hours of reaction, the

amount of hydrogen compared to CO, reduced due to the reverse water gas shift reaction. By increasing the temperature to 700^{o}C, some excess consumption of methane was seen in the initial period of reaction but decreased instantly to the theoretical value. Low cycling behaviour started earlier than 650^{o}C and the amount of CO did not correlate with the CO_2 conversion and was lower than expected by 10%. It can be suggested that at this temperature the possibility of the Boudouard reaction occurring is very high. The reverse water gas shift reaction could be the reason for the amount of CO being higher than H_2 at all periods of the reaction. The CO_2 conversion was 10% higher at a temperature of 750^{o}C and this greater conversion of CO_2 compared with CH_4 is may be due to the lower activation energy of CO_2 or because of the following reaction: -

$Ce_2O_3 + CO_2 \leftrightarrow 2CeO_2 + CO$……..eq12

At 800^{o}C, although CO_2 and CH_4 conversion almost reached its stoichiometric ratio of reforming, both the hydrogen and carbon monoxide yields were lower than expected by 10%.

Finally, at 850^{o}C a steady production of synthesis gas with a ratio of H_2:CO=1 was seen and all the CO_2 was consumed leading to an inability for the reverse water gas shift reaction to occur.

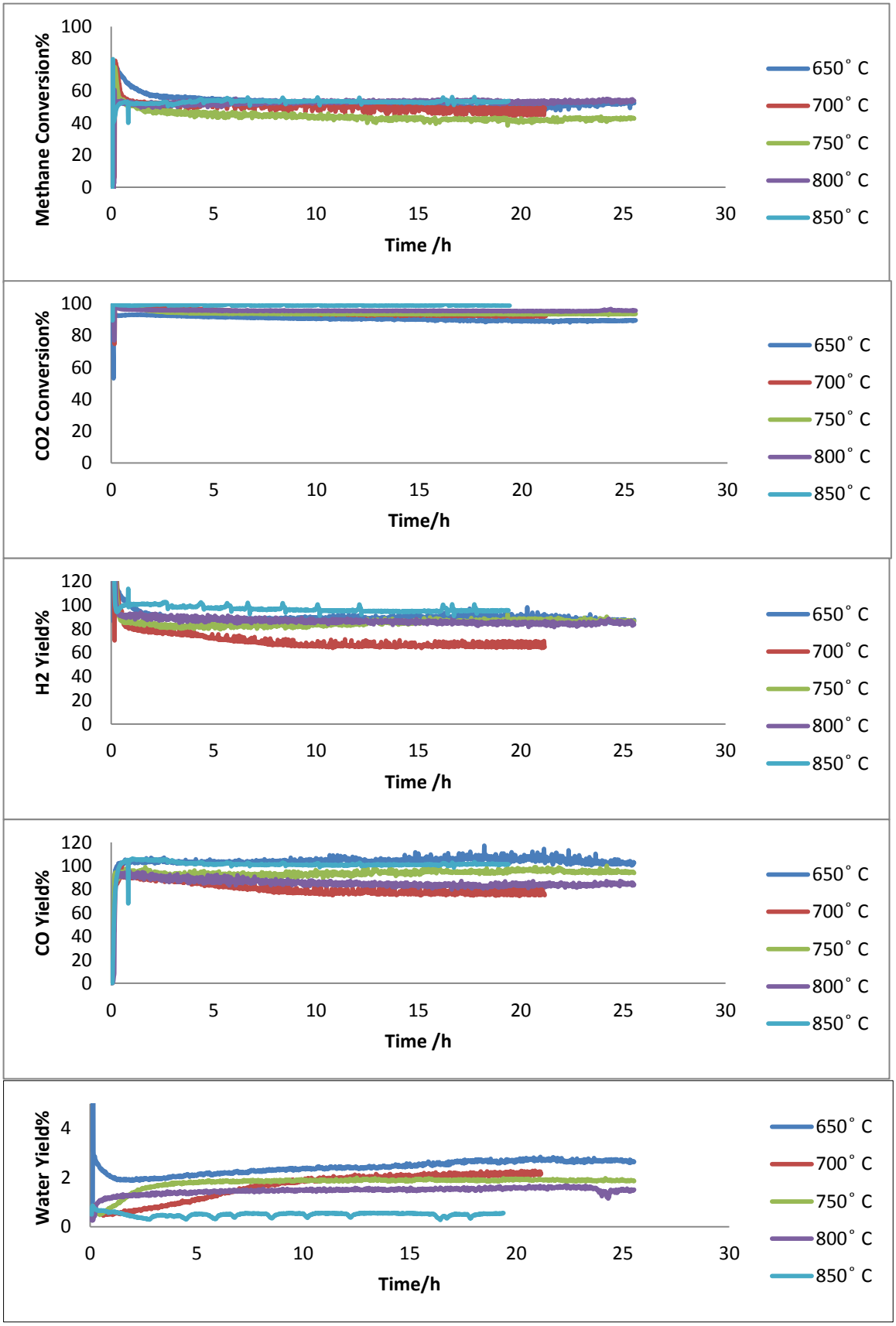

Figure3- 6- isothermal dry reforming of methane at various temperature over 0.25Ni-LCZ with CH_4:CO_2 =2:1 a)CH_4 conversion b)CO_2conversion c)H_2 yield d)CO yield e)water production

3.2.2.1.2 Carbon deposition: -

Temperature programmed oxidation (TPO) was performed to find the nature and the amount of carbon species on the catalysts. Deactivation by coking due to coverage of the active sites during DRM is the most probable reason for catalyst deactivation. In dry reforming, carbon deposits on the surface occur because of CH_4 disproportionation and the Boudouard reaction[28].

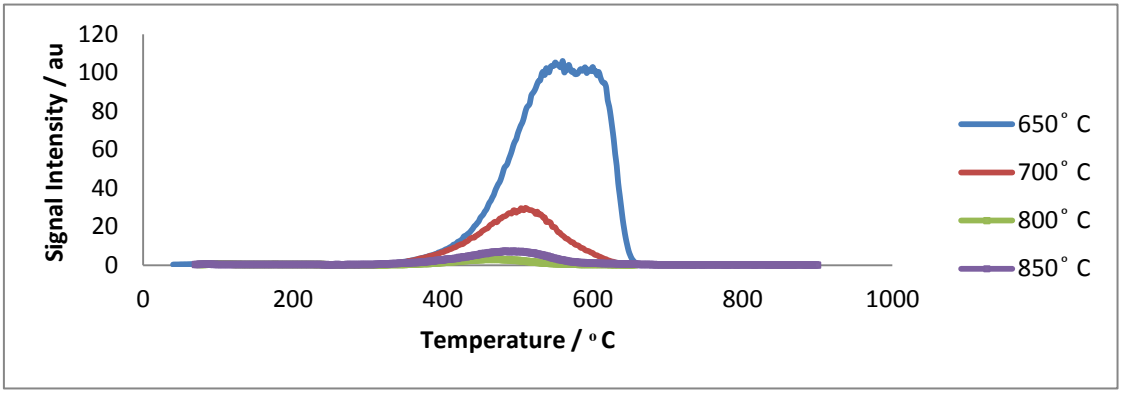

Figure3- 7-post reaction TPO profiles of isothermal methane rich dry reforming over 0.25 Ni-LCZ at various temperature

As shown in Figure3- 7, the amount of carbon deposition decreased by increasing the temperature. The highest amount of carbon was deposited at 650° C because of both the Boudouard reaction and methane decomposition which is shown by two distinct peaks on the TPO profile. By increasing the temperature to 700° C, the secondary carbon peak disappeared whilst the primary peak remained. At 800° C, the amount of carbon deposition was at the lowest level. This suppression in the amount of carbon can be attributed to the methane coupling resulted in the formation of ethane, ethane or ethyne. In this case the amount of carbon deposition decreased due to low probability of conversion of methane by the pyrolysis reaction[25].

It can be concluded, that the secondary peak at 650° C can be assigned to carbon formed during the Boudouard reaction and the initial peak which decreased by increasing the temperature corresponds to methane decomposition.

3.2.2.2.1 Isothermal dry reforming of rich- methane over 0.5 Ni -LCZ

As can be seen from Figure3- 8, some excess consumption of methane was seen at the beginning of the reaction at 650°C and 700°C. After the initial spike in methane conversion, the conversion falls from 80% to 43% for 2 hours. The reason for this suppression of methane conversion could be due to the surface becoming dirty as adsorbed species occupy active sites. The ratio of H_2:CO falls below 1:1 due to the presence of unreformed CO_2 and the consumption some H_2 via the reverse water gas shift reaction. The production of water in the reaction profile can also be attributed to this reaction. At 750°C, the dry reforming profile is like the profile of 0.25Ni-LCZ at 800°C. Nearly complete methane and CO_2 conversion was seen combined by a decrease in the amount of CO and H_2 production. Increasing the temperature to 800°C decreased the CH_4 and CO_2 conversion with an increasing level of H_2O formation. At 850° C and 900° C, the reaction reached the theoretical value in the form of cycling. No evidence of water from the reverse water gas shift reaction can be seen at 900°C, although some gradual increase in water formation in the form of cycling can be observed after 15 hours of reaction at 850°C.

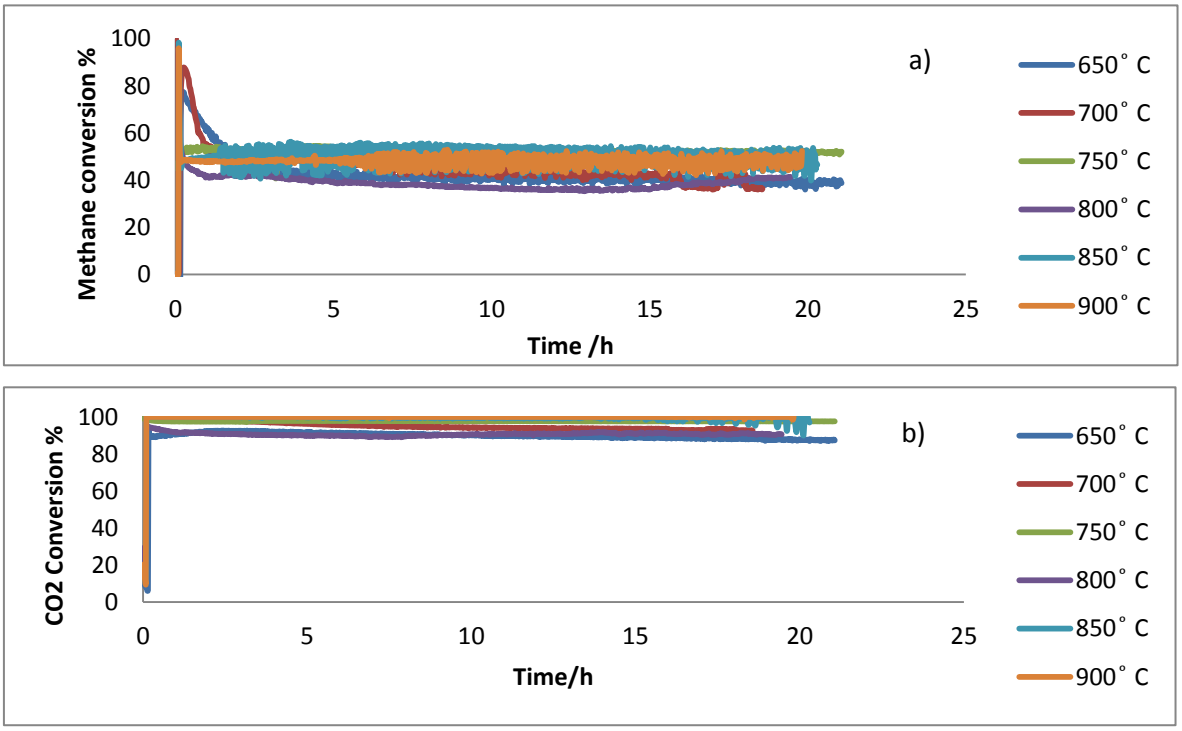

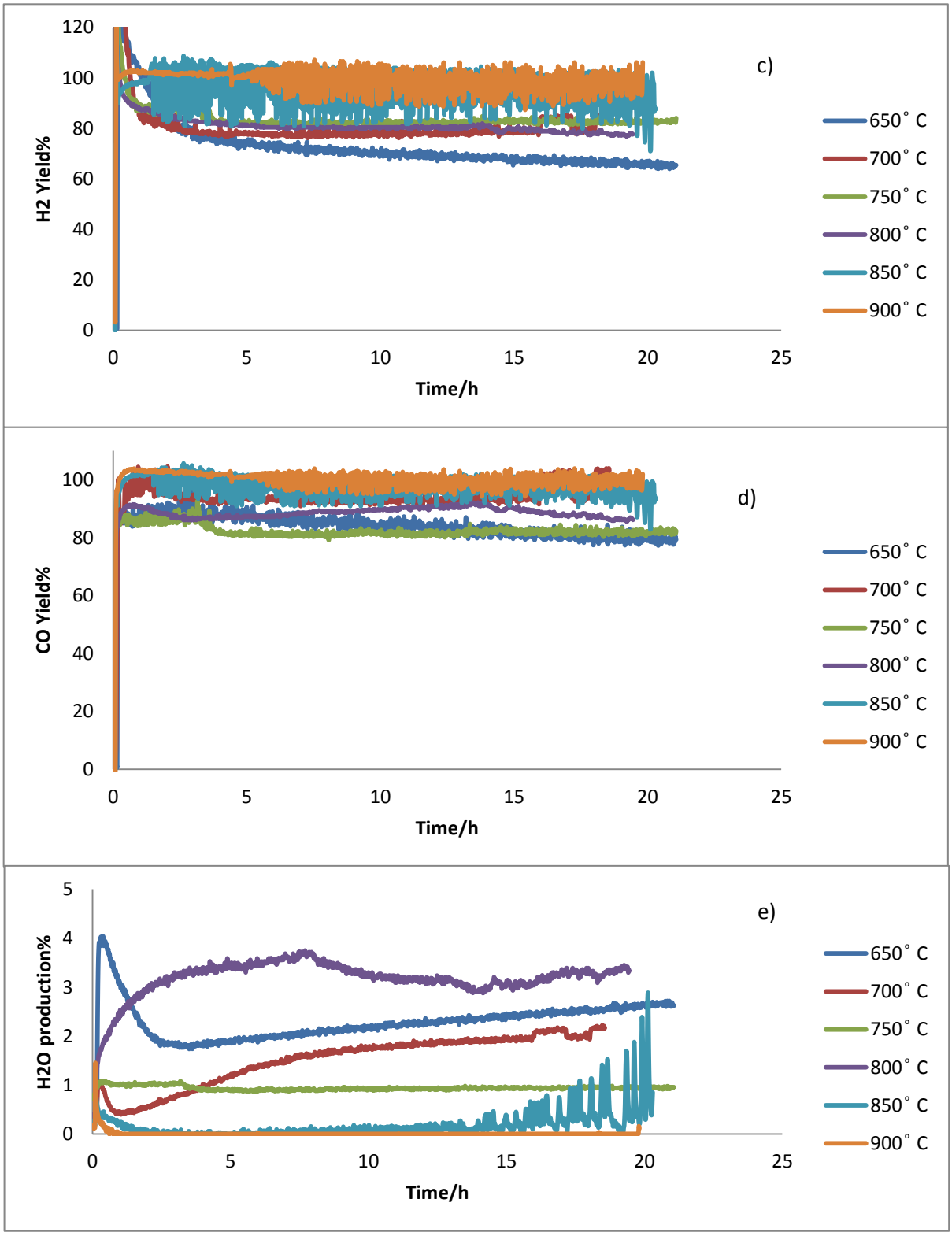

Figure3- 8- isothermal dry reforming of methane at various temperature over 0.25Ni-LCZ with CH_4:CO_2 =2:1 a)CH_4 conversion b)CO_2 conversion c)H_2 yield d)CO yield e)water production

3.2.2.2.2 Carbon deposition: -

As two different mass spectrometers were used for this series of dry reforming reactions, each with a different CO_2 signal intensity, two charts for the TPO were obtained.

As can be seen from Figure 3- 9, by increasing the temperature, the amount of carbon deposition significantly decreased especially from 650°C to 750°C. Unlike at other reforming temperatures that show a gradual increase in the water formation, at 750°C and 900°C, the amount of water formation did not show an increasing trend over time and therefore, at these two temperatures, the TPO peaks are located in the same temperature range suggesting that the same kind of carbon was deposited on the surface of the catalysts. The TPO peak at the higher temperature within the TPO profile has another kind of deposited carbon.

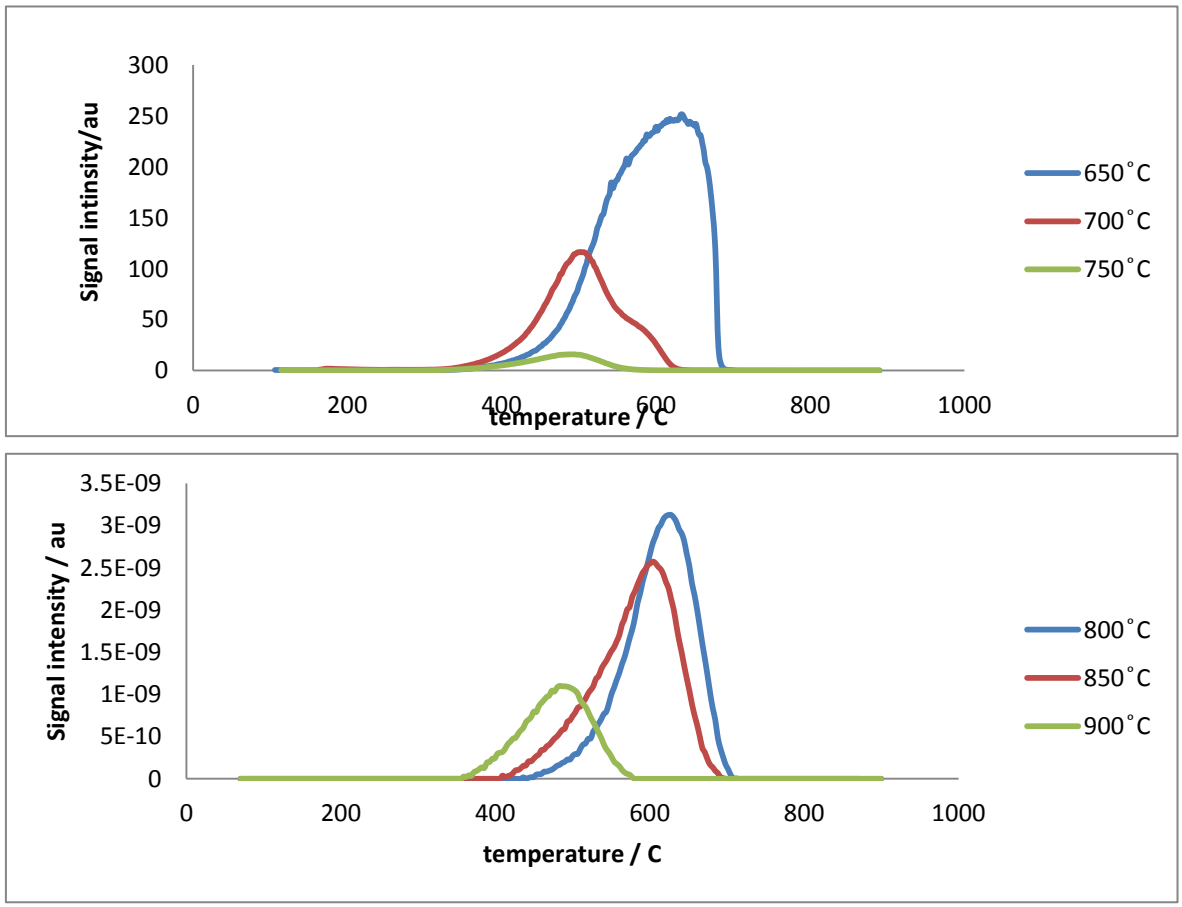

Figure 3- 9-post reaction TPO profiles of isothermal methane rich dry reforming over 0.5 Ni-LCZ at various temperature

3.2.2.3.1 Isothermal dry reforming of rich- methane over 1 Ni -LCZ

Some cycling of the methane conversion at varying temperature was seen for 1- NiLCZ. This was correlated with an increased activity at the lower temperature resulting in higher methane conversion. During the initial period of reaction, as the temperature increased the methane conversion was more than what could be achieved by a pure DRM reaction. The presence of ceria in the structure encourages the dry reforming of methane through the dissociation of CO_2 and distribution of oxygen to encourage methane partial oxidation. Lower H_2 and CO yields were seen at a temperature of 650°C, potentially due to CO reduction (CO-R): $CO + H_2 \leftrightarrow C + H_2O$ in addition to the Boudouard reaction, which can be seen through the lesser CO_2 conversion and greater water formation. As the temperature increased, methane conversion showed no increase over time and at 700 °C, similar behaviour for the CO_2 conversion was observed at 750 °C, 800 °C and 850 °C. However, differences were visible after 5 hours of reaction with the trend showing a reduction in the amount of CO_2 conversion and consequently a decrease in H_2 and CO production. The decrease in the CO_2 level was comparable with the level which was seen at 650°C. Interestingly at 700°C even the CO_2 and CH_4 conversion were at the same level as at 650°C, but the yield of H_2 and CO were greater by 20%.

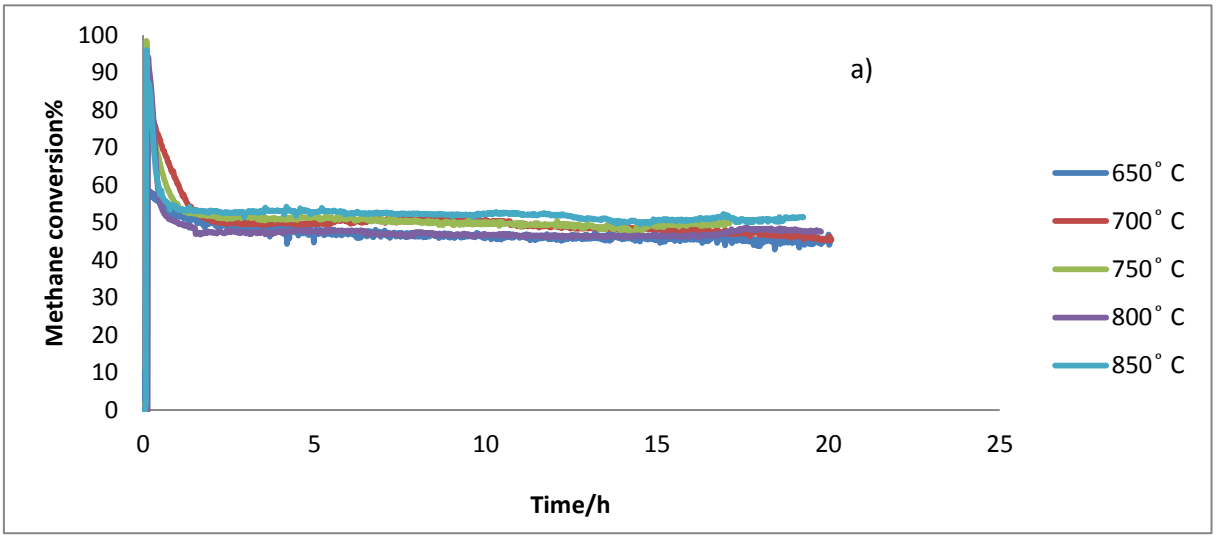

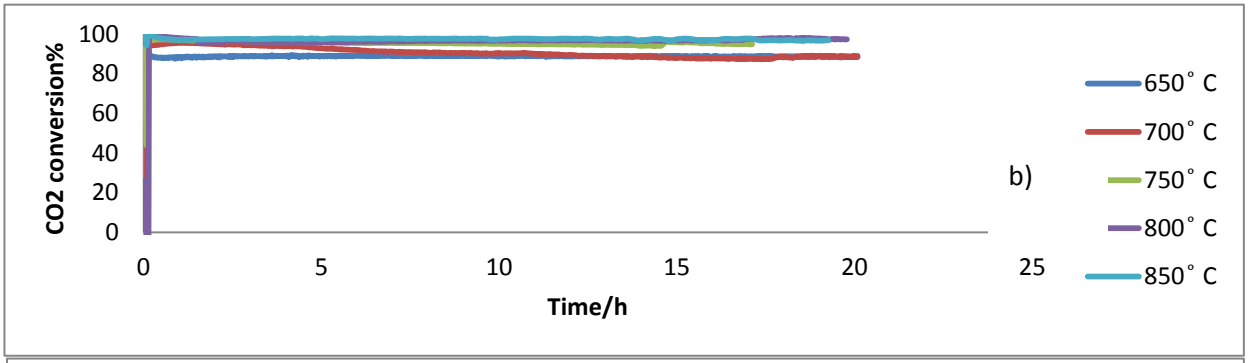

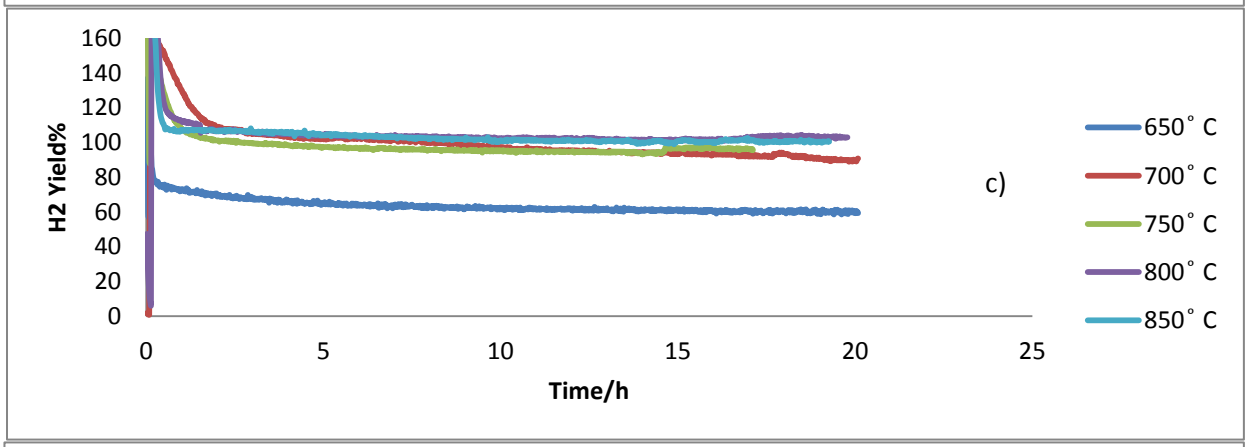

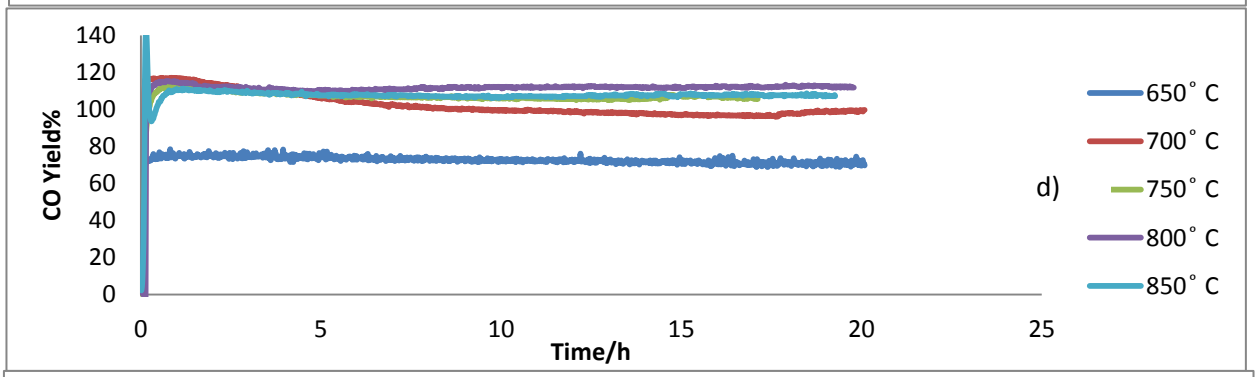

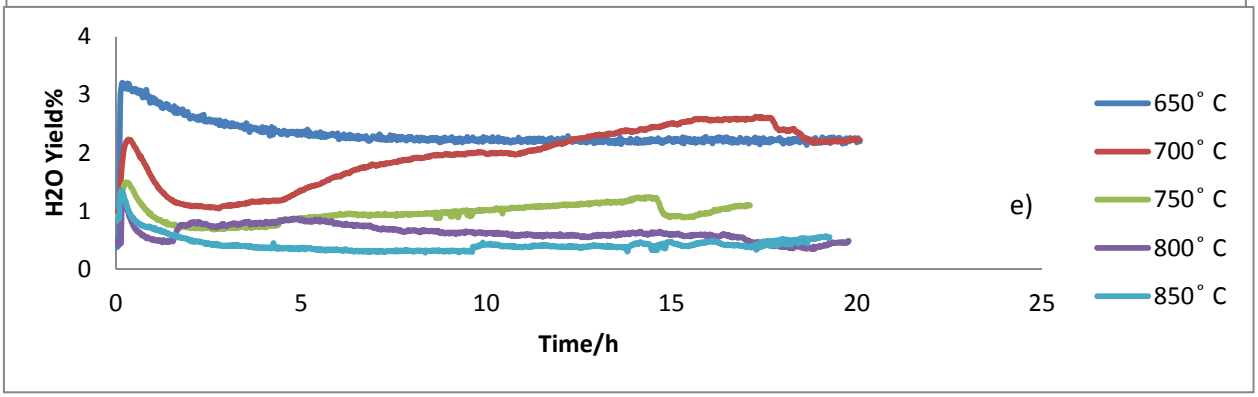

Figure 3- 10 isothermal dry reforming of methane at various temperature over 1Ni-LCZ with CH_4:CO_2 =2:1 a) CH_4 conversion b) CO_2 conversion c) H_2 yield d) CO yield e) water production

3.2.2.3.2 Carbon deposition

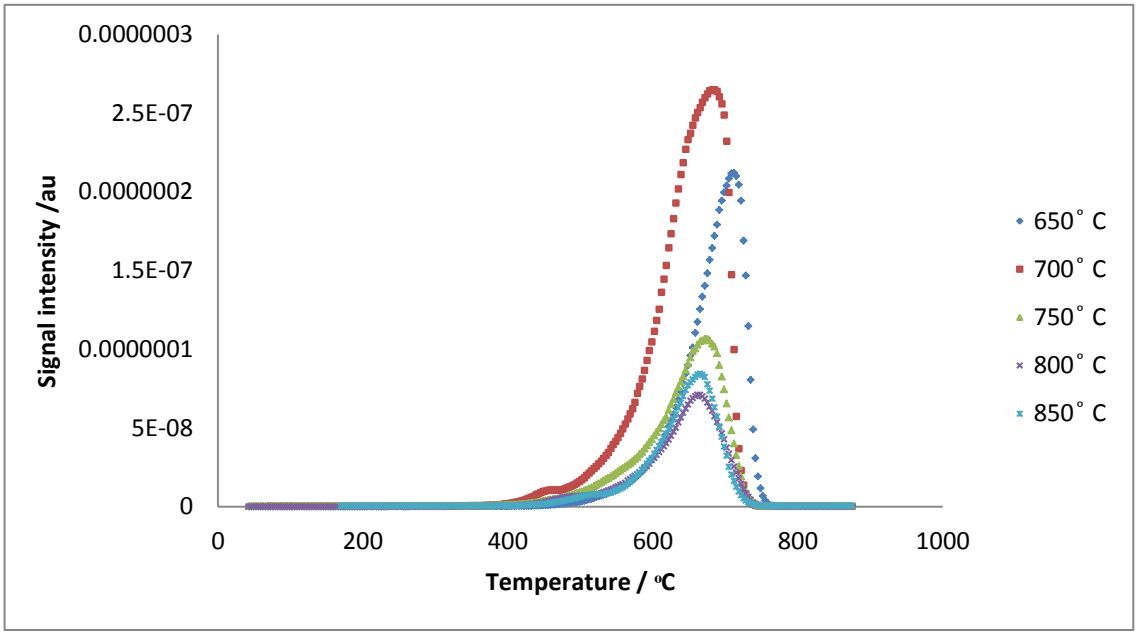

Figure 3- 11-post reaction TPO profiles of isothermal methane rich dry reforming over 1 Ni-LCZ at various temperature

At 650° C, because of the Boudouard reaction, the TPO peak was slightly shifted to higher temperature. As was seen previously in the DRM profile, the H_2 and CO yields were lower than expected in comparison with CH_4 and CO_2 conversion, therefore, the deposited carbon is a result of both the Boudouard and CO reduction reactions. It was clearly seen that at the temperature of 650° C the amount of carbon deposition was lower than 700° C and the TPO peak was shifted to the lower temperature. In addition, the TPO profile of 700° C shows another carbon peak at 460° C .The greater amount of carbon deposition at this temperature could be attributed to the total oxidation reaction. The presence of CeO_2 directly encouraged the total oxidation of methane reaction which was accompanied by an increase in water formation ($CH_4+2O_2 \leftrightarrow 2H_2O+CO_2$). At 750° C and above, the amount of carbon deposition was significantly decreased and only one peak on the TPO profile was observed suggesting one type of carbon was being formed.

3.2.3 Summary comparison of CH_4, CO_2 conversion and product selectivity for LCZ catalysts with different nickel contents during methane-rich dry reforming

3.2.3.1 -Methane and carbon dioxide conversion: -

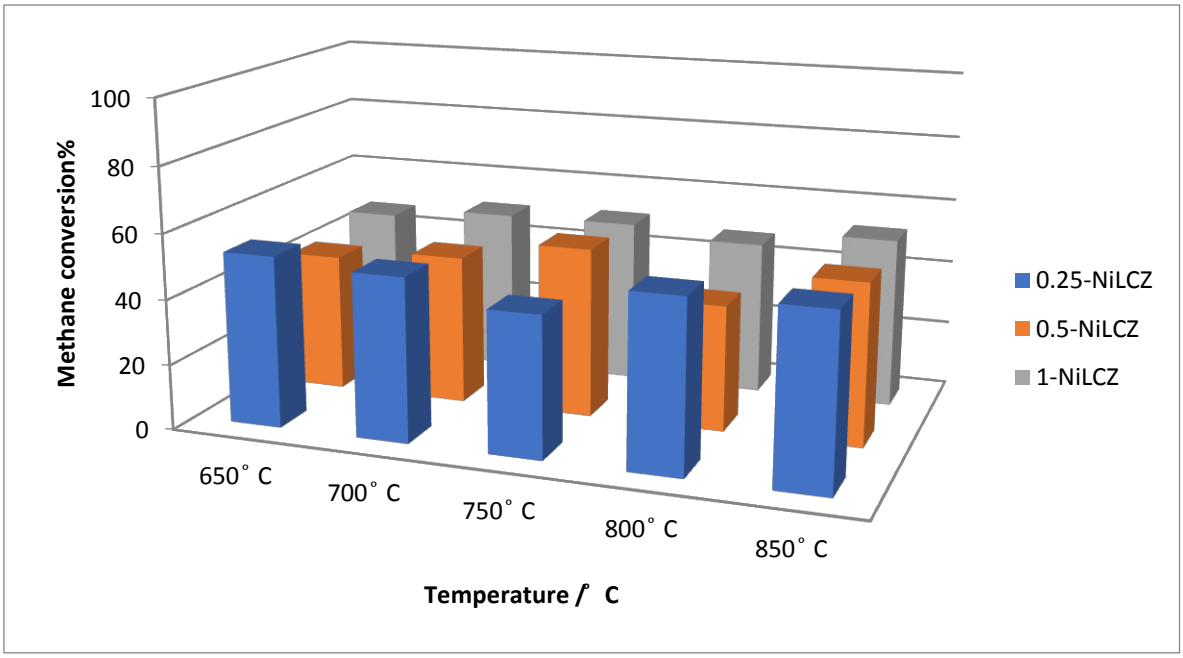

Figure 3-12-Average methane conversion for various Ni doped $LaCeZr_{2-x}Ni_xO_7$ at different temperatures for 2:1 CH_4:CO_2 dry reforming reaction

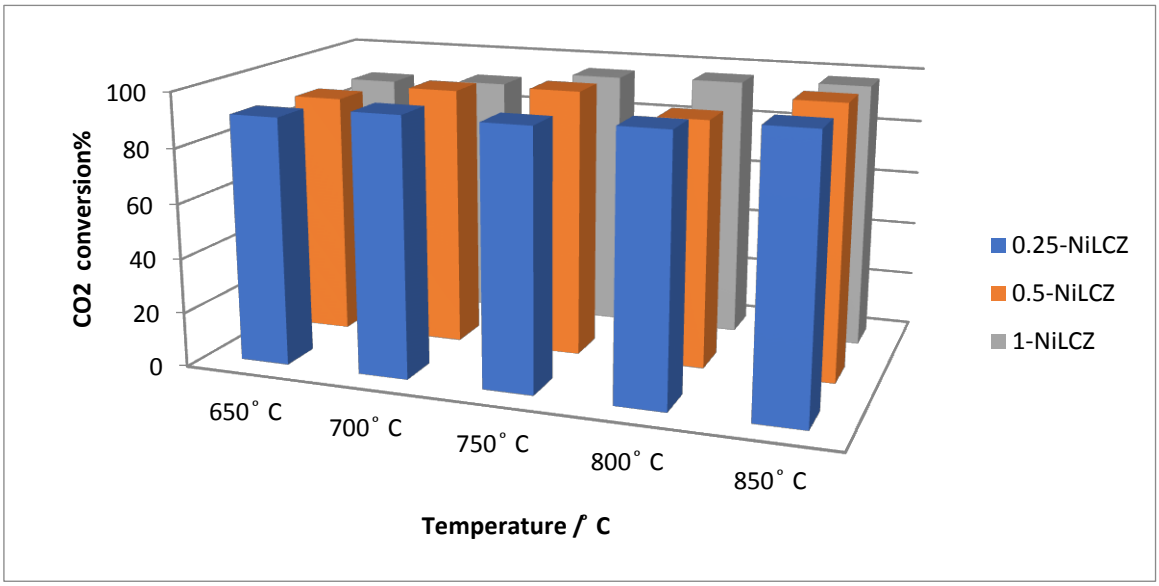

Figure 3-13-Average carbon dioxide conversion for various Ni doped $LaCeZr_{2-x}Ni_xO_7$ at different temperatures for 2:1 CH_4:CO_2 dry reforming reaction

As can be seen from Figure3- 12, there was no increasing or decreasing trend in the methane conversion by increasing the amount of Ni. At low-temperature, 0.25-NiLCZ displayed conversion of methane in excess of what could be achieved by a 2:1 CH_4: CO_2 reforming reaction. This can be attributed to the presence of a high concentration of CeO_2 in the catalyst. Ceria has been shown to be active for methane reforming ($CeO_2+CH_4 \leftrightarrow Ce_2O_3+CO+H_2O$). As the temperature is increased (700 ^{o} C) all Ni-doped LCZ catalysts show nearly the same amount of conversion. At 750 ^{o} C, since the reduced form of ceria (Ce_2O_3) becomes more favourable, the level of methane conversion decreased as compared with other higher Ni concentrations. There was an increasing trend in methane conversion above 800 ^{o} C, and at 850 ^{o} C, with all three catalysts displayed a stoichiometric conversion of methane resulting in 50% conversion.

Increasing the nickel doping has very little overall effect on the reforming process especially at 700 ^{o} C and 850 ^{o} C and the presence of ceria in various forms in the structure has an essential role in methane conversion. 1NiLCZ showed a flatter methane conversion profile compared to other catalysts.

In general, CO_2 conversion was associated with methane conversion. Although 0.25NiLCZ exceeded the equivalent amount of methane conversion at 650 ° C, the CO_2 conversion was the same as for the other catalysts. This similarity confirms the effect of ceria in a free form in the structure of the catalyst. It is worth mentioning that because of the increased thermodynamically potential for DRM at increased temperatures of reaction, the influence of ceria becomes less essential.

3.2.3.2 Product selectivity

As ceria played an important role during methane conversion by forming various forms in the presence different amount of Ni, therefore, analysis of product selectivity will be an important

and useful tool for the distinguishing the difference in performance of the catalyst. Figure 3-14 shows hydrogen yield with varying temperature. At 650°C, as the amount of Ni increased, the H_2 yield decreased from 103 % to 73%. This is due to the presence of side reaction which gives special distinguishing properties during the reforming process. By increasing the temperature to 700° C, 1-NiLCZ, showed an instant increase reaching almost 100% yield while 0.25-NiLCZ displayed a sharp decrease to 80% at this reforming temperature. By increasing the temperature, the H_2 yield exceeds 100% due to the greater amount of active Ni site available in the structure of 1-NiLCZ .At 850°C all three catalysts reached almost 100% hydrogen yield.

It can be confirmed from this observation that at 850° C, the reaction kinetics becomes the limiting factor rather than the amount of available nickel in the catalyst.

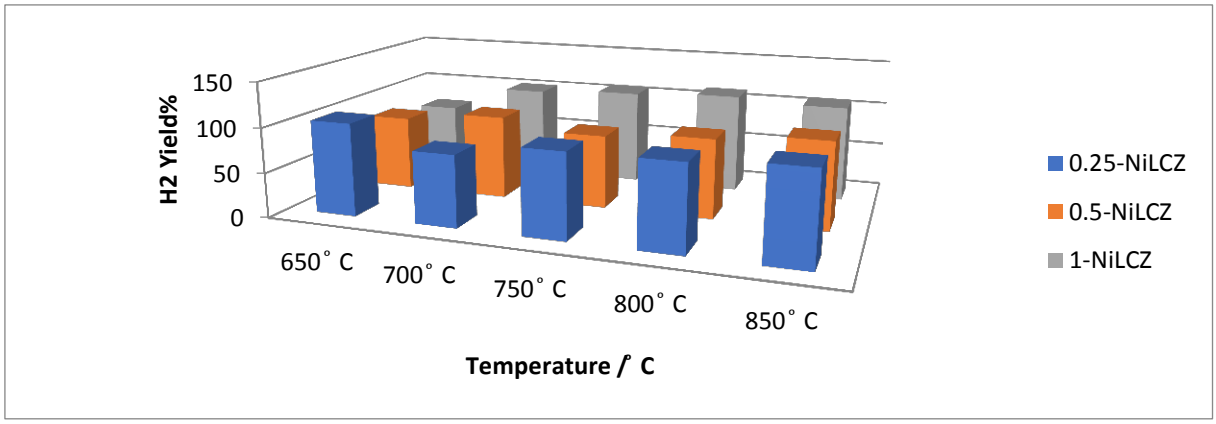

Figure 3-15-Average hydrogen yield for various Ni doped $LaCeZr_{2-x}$ Ni_xO_7 at different temperatures for 2:1 CH_4:CO_2 dry reforming reaction

In the 2:1 CH_4: CO_2 dry reforming reaction, the yield of CO has to correlate with the partial pressure of CO_2. As the CO_2 is almost fully consumed, the carbon monoxide yield displayed a flattened profile as was clear in 1-NiLCZ in Figure3- 16. The CO yield, at the higher temperature in both 0.25 and 0.5-NiLCZ catalysts did not correlate with the CO_2 conversion. The decrease in the amount of CO by about 15% in comparison with 1-NiLCZ could be

because of some side reaction e.g. CO reduction (CO-R): $CO + H_2 \leftrightarrow C + H_2O$ in addition to the Boudouard reaction. At 850°C as DRM became more thermodynamically favourable the yield of CO from the 0.25 and 0.5 NiLCZ became higher, giving almost 100% yields.

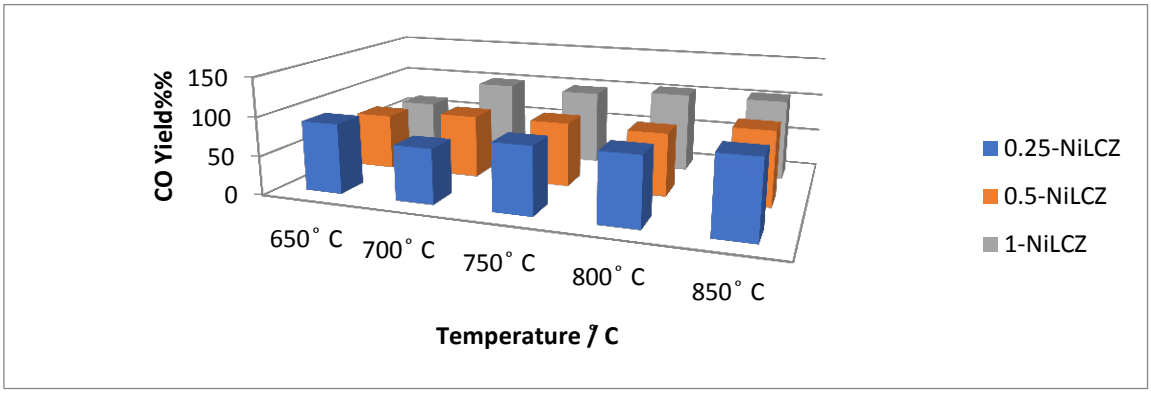

Figure 3-16-Average carbon monoxide yield for various Ni doped $LaCeZr_{2-x}$ Ni_xO_7 at different temperatures for 2:1 CH_4:CO_2 dry reforming reaction

As can be seen from Figure3- 17, 1-NiLCZ displayed a negative correlation between the temperature of reaction and the formation of water because of a decrease in the reverse water gas shift reaction. All three catalysts showed similar H_2O production at a temperature of 650° C which could be attributed to H_2 oxidation by CeO_2 .As the temperature increased, 0.25 NiLCZ showed a spike in water formation at 750 and 800° C while 0.5 NiLCZ showed only one sharp increasing peak at 800° C. This could be because of side reactions as total oxidation.

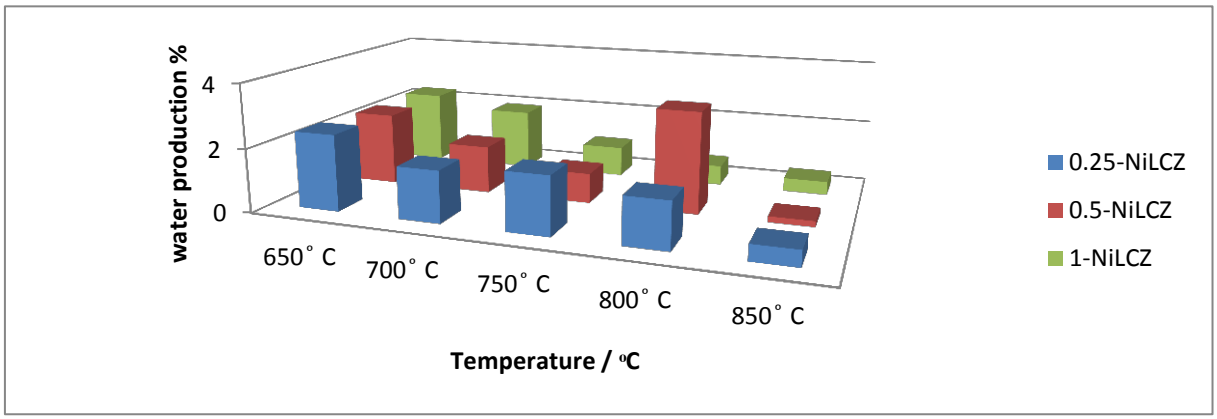

Figure 3-17-Average water yield for various Ni doped $LaCeZr_{2-x}$ Ni_xO_7 at different temperatures for 2:1 CH_4:CO_2 dry reforming reaction

3.2.3.3 Carbon deposition

The comparison of the mass of carbon deposited during 2:1 methane to carbon dioxide reforming over each catalyst is shown in Figure3- 18.

As CO hydrogenation and the Boudouard reaction are thermodynamically favourable at lower temperatures, all three catalysts show a decrease in carbon deposition with temperature.

At low temperatures, a significant difference in the amount of deposited carbon was seen by increasing the amount of Ni. 0.25-NiLCZ had the lowest amount of deposited carbon and the reason for this is attributed to more nickel sites present for reaction with more carbon formed as a result of the Boudouard reaction. In addition, the presence of CeO_2 increases the ability of the catalyst to oxidise carbon at the lower temperature. At higher temperatures >700°C, the deposited carbon was suppressed significantly, and the amount of nickel had no significant impact on carbon deposition. The presence of ceria increases the potential for carbon oxidation through increased oxygen availability.

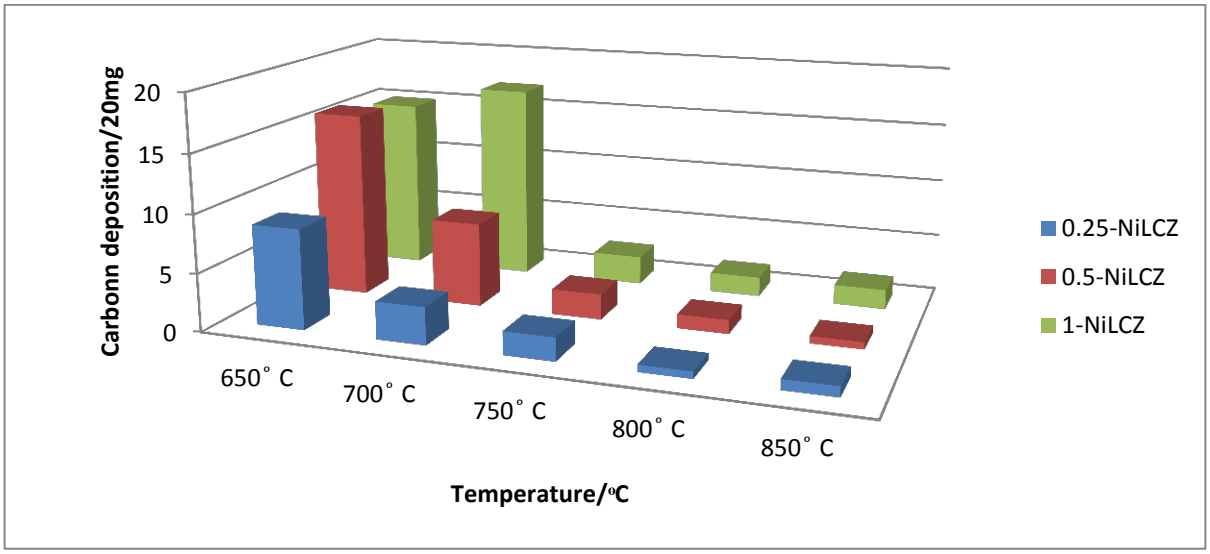

Figure3-18-carbon deposition from reactions at various Ni doped $LaCeZr_{2-x}$ Ni_xO_7 with different temperatures during 2:1 CH_4:CO_2 dry reforming reaction

3.2.4.1 Long term stability of 0.25-NiLCZ and 1-NiLCZ for methane rich DRM at 750 °C

Figures 3-19 and 20 show the profiles of isothermal dry reforming over 0.25 and 1-NiLCZ including moles of product per mole of converted methane estimated. As can be seen the amount of CH_4 and CO_2 conversion was close to the stoichiometric ratio in both catalysts. After consumption of mobile oxygen of cerium –zirconium oxide, the level of methane conversion decreases slightly below the stationary state[26]. During the DRM, the amount of H_2 was lower than CO because of the reverse water gas shift reaction. The main difference between 0.25- NiLCZ and 1-NiLCZ was in the amount of syngas emission where it was higher by nearly 20% in 1-Ni-LCZ. The decrease in the amount of CO and H_2 in comparison with 1-NiLCZ could be because of some side reactions, such as CO reduction (CO-R): $CO + H_2 \leftrightarrow C + H_2O$. In addition, ceria can chemisorb large amount of H_2 and CO. Both catalysts showed stability in performance without any deactivation within 3 days of reaction.

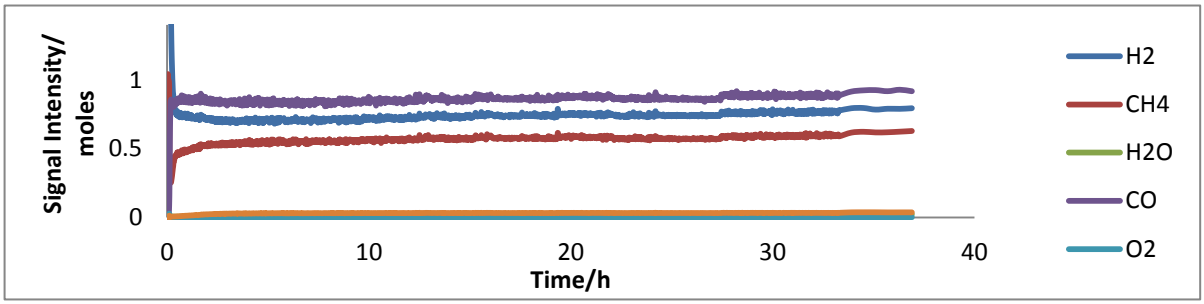

Figure3- 19-Isothermal dry reforming reaction for 2:1 CH_4:CO_2 over 0.25Ni-LCZ for 3 days at 750°C

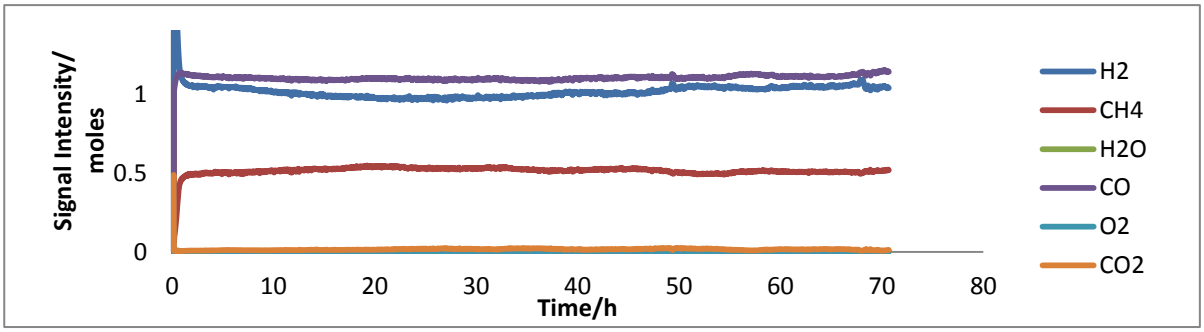

Figure 3- 20-Isothermal dry reforming reaction for 2:1 CH_4:CO_2 over 1Ni-LCZ for 3 days at 750°C

3.2.4.2 Carbon deposition: -

The amount of carbon deposited for 2:1 CH_4:CO_2 over 0.25 and 1-NiLCZ for one and three days was compared and is shown in Figures 3- 21 and 22.The amount of carbon deposition over 0.25-NiLCZ after 20h and 72h was 2 and 2.1 mg/20mg_{cat} respectively, while it was 2.5 and 3mg/20mg_{cat} over 1-NiLCZ.

One visible difference between the two catalysts is the carbon peak shifts to higher temperature in 1-Ni-LCZ indicating the presence of traces of carbonaceous species which are oxidised between 500 and 700 °C, while one major TPO peak at 500 °C corresponds to a soft type of carbon since it can be oxidised under relatively mild conditions. The presence of soft carbon supports the hypothesis leading to small Ni domains available at the catalyst surface during reaction. Therefore, the Ni particles of 0.25-NiLCZ remain small and well dispersed on the surface. The agglomeration of Ni clusters would lead to more graphitic carbon.

The amount of carbon deposition does not really increase with time for both catalysts and increasing the quantity of Ni at this temperature also showed no real effect on the quantity of deposited carbon. It can be concluded that the presence of ceria releasing oxygen under oxygen-poor environments and quick reoxidation under oxygen-rich environment plays a key role in carbon suppression.

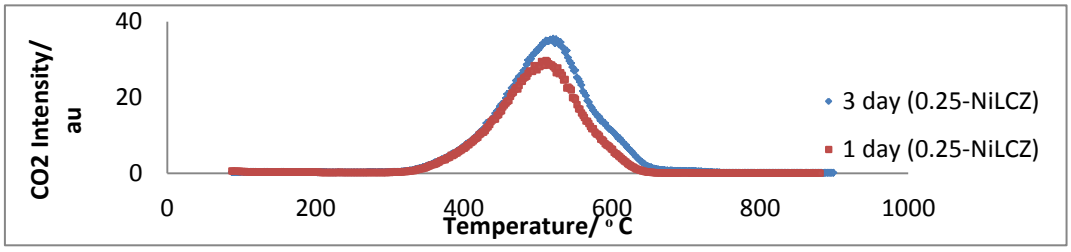

Figure 3- 21- TPO profiles of 0.25Ni-LCZ after DRM during 20 h and after 72 h at 750 °C

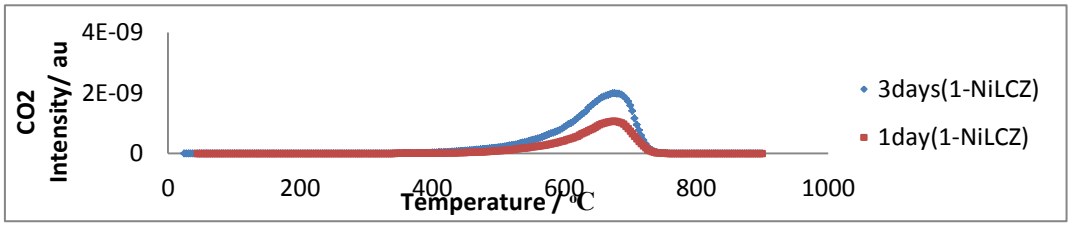

Figure 3- 22- TPO profiles of 1Ni-LCZ after DRM during 20 h and after 72 h at 750 °C

3.3 Carbon Dioxide Reforming of Methane for Ni-LCZ Prepared by Pechini Method

As the preparation method has an impact on catalyst performance in the case of activity, stability and selectivity, in this part of the thesis, the effect of Pechini preparation method has been investigated on dry reforming under the conditions of 2:1 CH_4: CO_2 at various temperatures.

3.3.1 Temperature programmed biogas reformation.

As can be seen from Figure3- 23, the reaction started at around 488° C with a gradual decrease in methane and carbon dioxide correlating with the production of H_2 and CO. A low level of H_2O production because of the reaction of hydrogen with the unreacted carbon dioxide (reverse water gas shift reaction) was noticeable until 800°C. After the temperature of 800° C, the reactant and products reached its thermodynamic equilibrium value and did not change significantly. As the hydrogen and carbon monoxide are at a maximum, it can be suggested that the DRM should be performed at around this temperature.

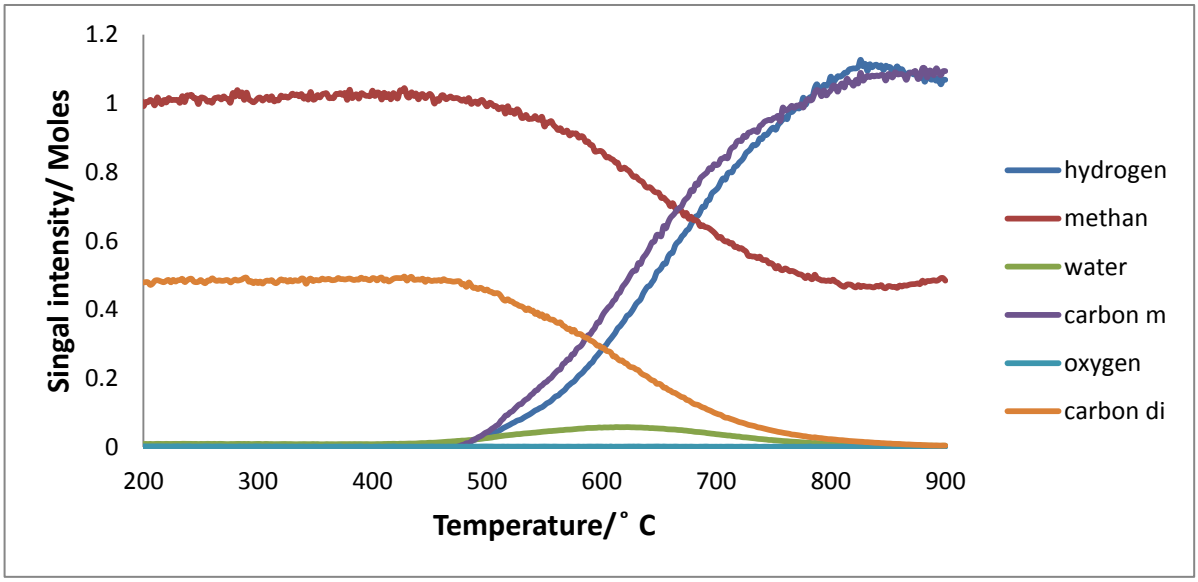

Figure 3- 23- reaction profile for a 2:1 CH_4/CO_2 mixture passed over 1Ni-LCZ prepared by Pechini method

3.3.2.1 Isothermal Dry Reforming Of Methane

The catalytic activity of the Pechini prepared catalyst Ni-LCZ in the temperature range of 650°C-850°C with a CH_4/CO_2 =2:1 has been investigated and is shown in Figure 3- 24.

As can be seen from Figure 3- 24, the conversion of CO_2 and CH_4 were almost similar to the same value as the equilibrium limit at temperatures higher than 750°C. In the case of H_2 and CO production, there were some side reactions which made the amount of H_2 and CO lower than expected at temperatures lower than 850°C.

Generally, because of the reverse water gas shift reaction, the amount of H_2 was lower than CO and the presence of cerium in the structure of the catalyst may play an essential role in increasing the amount of CO in the synthesis gas by reaction with any deposited carbon ($2CeO_2+C\leftrightarrow Ce_2O_3+CO$). The lowest level of CO can be seen at a temperature of 700°C due to the Boudouard reaction. The level of CO_2 conversion was lower than CH_4 conversion because of the water gas shift reaction at the temperature of 650°C and 700°C.

The presence of two distinct regions of H_2O production at temperatures lower than 850°C may suggest another source of water occurring during the dry reforming reaction. As the amount of H_2 and CO reduced in the same trend, the reaction of $H_2+ CO\leftrightarrow H_2O+ C$ could be responsible for this source of water, which appears as a second level of water in Figure 3-24(e).

At the temperature of 850°C, the amount of hydrogen increased by 5% which was acceptable because of methane decomposition, but surprising there was not an excess of methane conversion. Higher consumption of water because of the following reaction $Ce_2O_3+H_2O\leftrightarrow 2CeO_2+H_2$ may be the reason for this increasing H_2 yield.

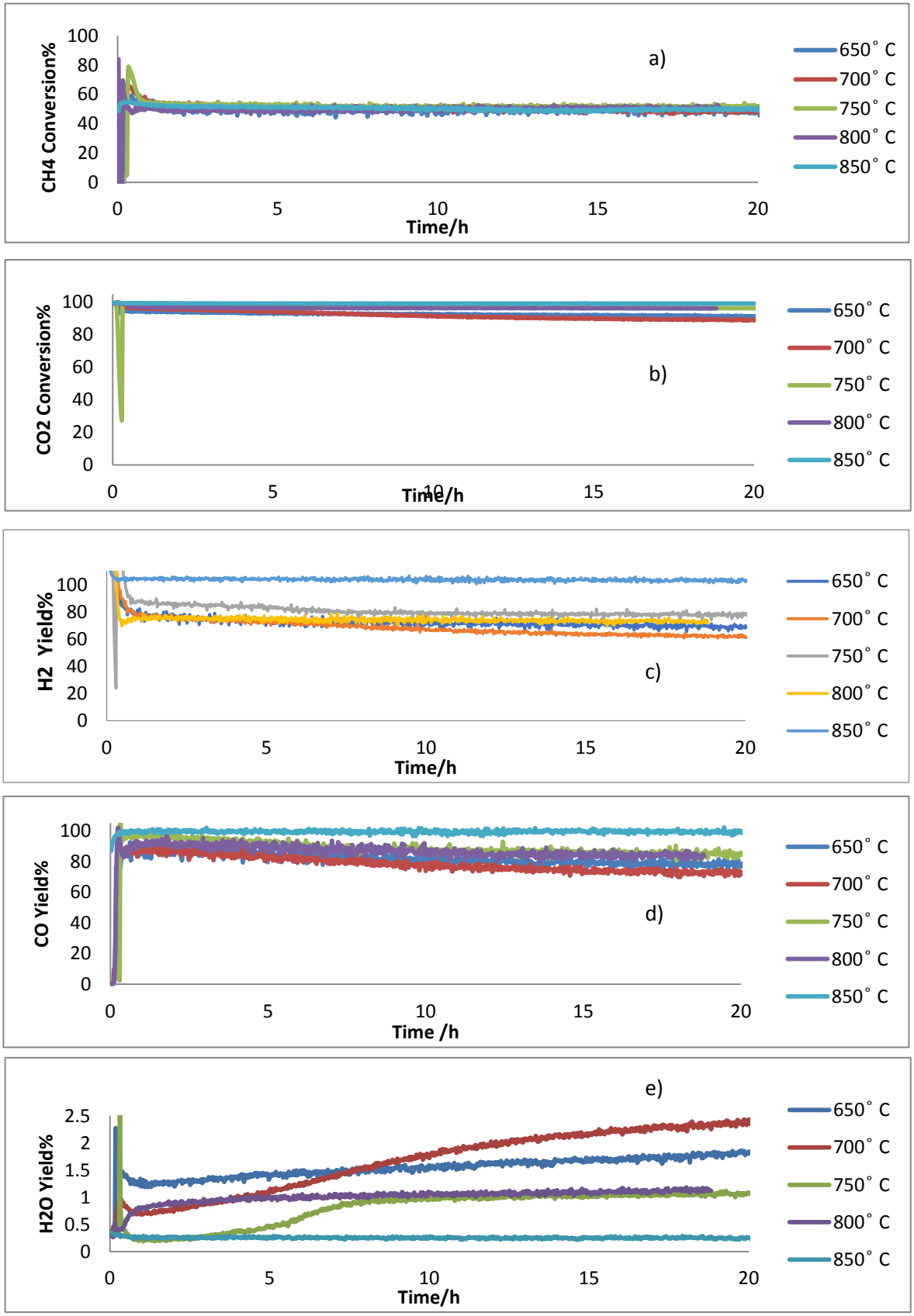

Figure 3- 24- isothermal dry reforming of methane at various temperature over 1Ni-LCZ with CH_4:CO_2 =2:1 a) CH_4 conversion b) CO_2 conversion c) H_2 yield d) CO yield e) water production

3.3.2.2 Carbon deposition:-

As carbon formation can easily block the active centres of the catalyst besides destroying the reactor as a result of blocking the reactor tube, it is desirable to predict under which conditions the carbon formation is not thermodynamically favourable.

As can be seen from Figure3- 25; the highest amount of carbon was formed at 700 ° C as a result of the Boudouard reaction. At temperatures of 800 ° C and 850 ° C, the TPO peak has shifted to lower temperatures and can be attributed to polymeric carbon species. At a temperature of 650 ° C and 700 ° C, another carbon species is observed at a higher temperature. As was explained previously, the source of this carbon could be due to the reaction of $H_2+CO \leftrightarrow H_2O+C$ which is thermodynamically favourable at a lower temperature. As this carbon peak is located at high temperature within the TPO, it can be considered the less reactive carbon species exist on the catalyst as the form of dehydrogenated carbon[27].

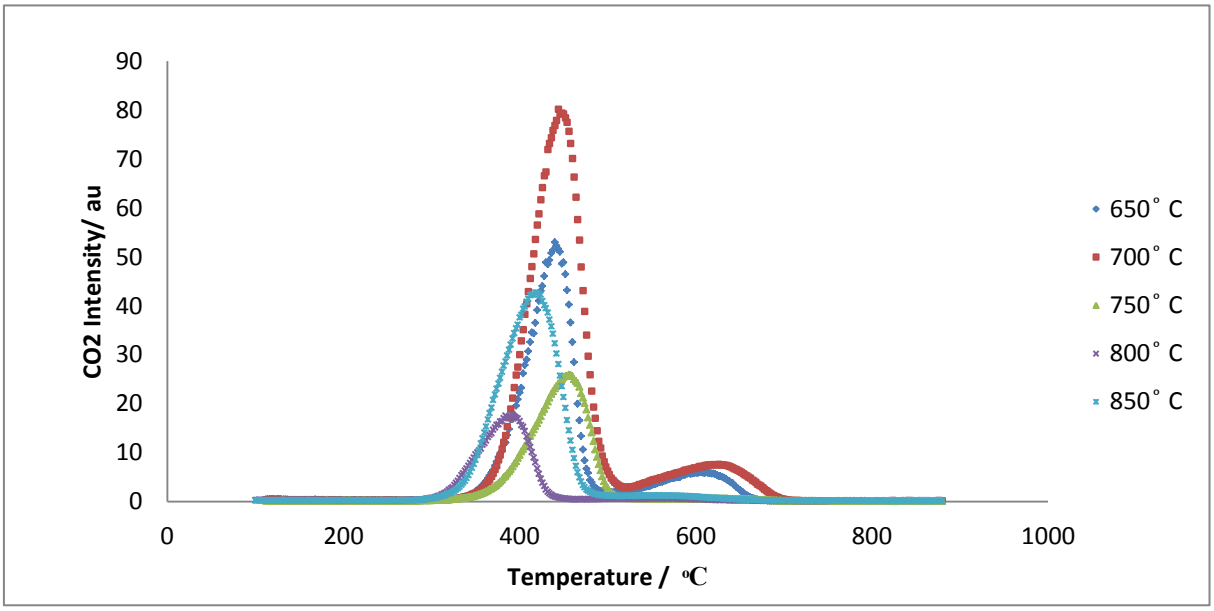

Figure 3- 25-post reaction TPO profiles of isothermal methane rich dry reforming over 1Ni-LCZ prepared by Pechini method at various temperature

3.3.3 Long term stability of Pechini prepared catalyst 1-NiLCZ for methane rich DRM at 750 °C

To investigate the impact of preparation method on catalyst stability for an extended period, the experiment was performed for three days under the conditions of CH_4:CO_2=2:1 at 750 °C.

After 12 h of gradual decrease in activity, the catalyst showed constant stability for the remainder of the reaction. However, the decline in activity at the beginning was not sharp, and it was only about 7% in the case of the H_2 yield. As the decrease in activity was stopped after 12 h of the reaction, it is unlikely that the deactivation is due to carbon formation. As can be seen from TPO profile, the increase in carbon formation is too low.

It is suggested that the presence of cerium in the catalyst structure suppresses the deposition of carbon.

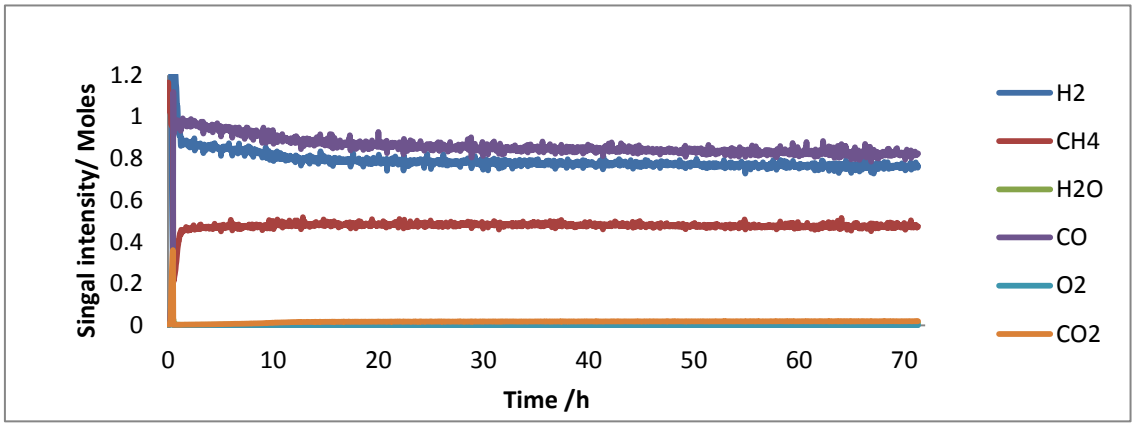

Figure 3- 26-Isothermal dry reforming reaction for 2:1 CH_4:CO_2 over 1Ni-LCZ for 72 h at 750 °C

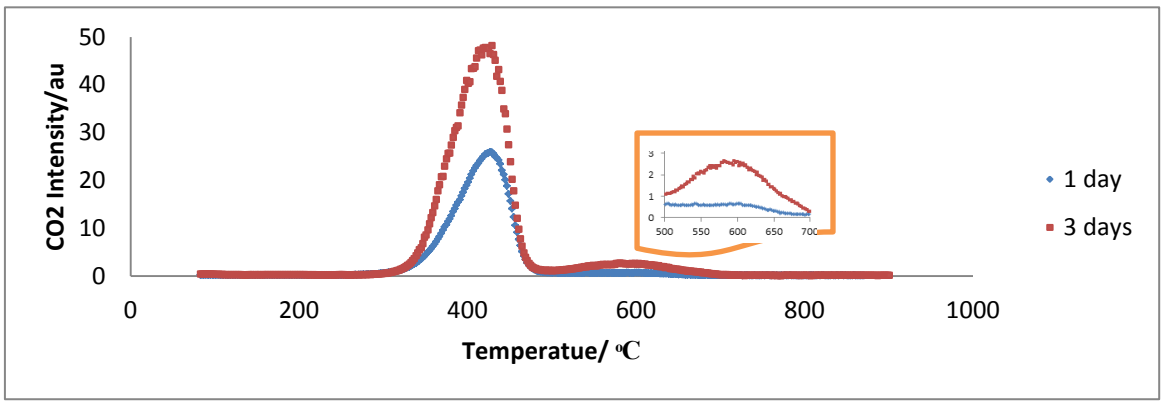

Figure 3- 27- TPO profiles of 1Ni-LCZ after DRM for 20 h and 72 h at 750 °C

3.4 Carbon Dioxide Reforming of Methane for Ru-LCZ Prepared By Hydrothermal Method

Noble metals have shown high activity towards DRM besides their resistance to carbon formation. In this section, the effect of Ru catalyst has been investigated on dry reforming during the condition of 2:1 CH_4: CO_2 at various temperatures.

3.4.1 Temperature programmed biogas reformation.

As can be seen from Figure 3- 28, the light off temperature of Ru-LCZ is 460 ◦ C. At this temperature, the CO formation begins while CO_2 is consumed. At a temperature of around 500 ◦ C, the H_2 starts to appear and a low level of H_2O is produced as a result of the reverse water gas shift reaction making the ratio of H_2/CO lower than one. At a temperature of 725 ◦ C, the reaction reaches its equilibrium limit and the concentration of H_2 slightly increases above this temperature and correlates with methane decomposition.

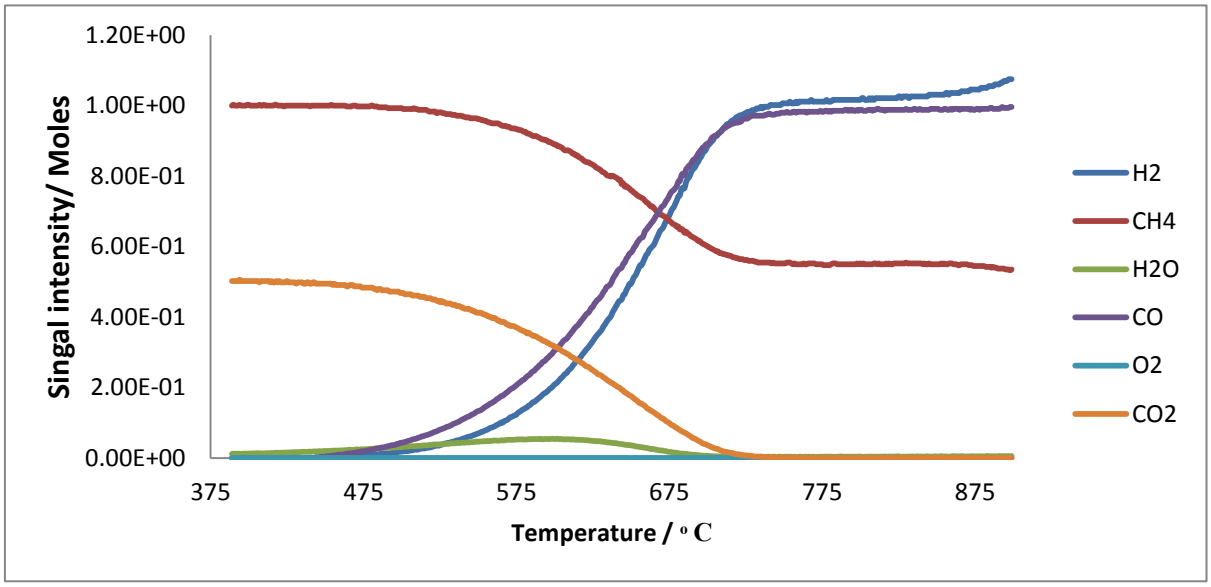

Figure 3- 28- reaction profile for a 2:1 CH_4/CO_2 mixture passed over 0.5Ru-LCZ prepared by hydrothermal method

3.4.2.1 Isothermal Dry Reforming of Methane

Reactant conversion and product selectivity are shown in Figure 3- 29. High CH_4 and CO_2 conversion are observed at temperatures above 750° C. At 850° C, the methane conversion was higher than the equilibrium conversion due to methane decomposition which results in the higher amount of H_2 (6%). However, this amount of H_2 decreased and remained constant at 95% after 10h of reaction. At temperatures lower than 750° C, because of the reverse water gas shift reaction, the CO_2 conversion and H_2 yield decreased by 7% and the presence of water at these two temperatures confirm this reaction.

Generally, the catalysts showed nearly constant activity at all temperatures.

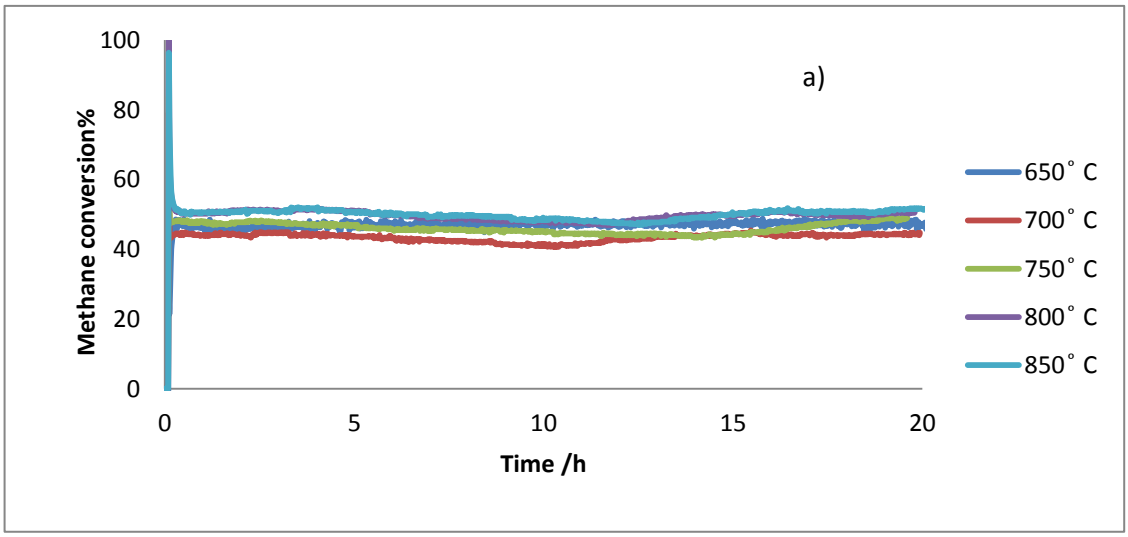

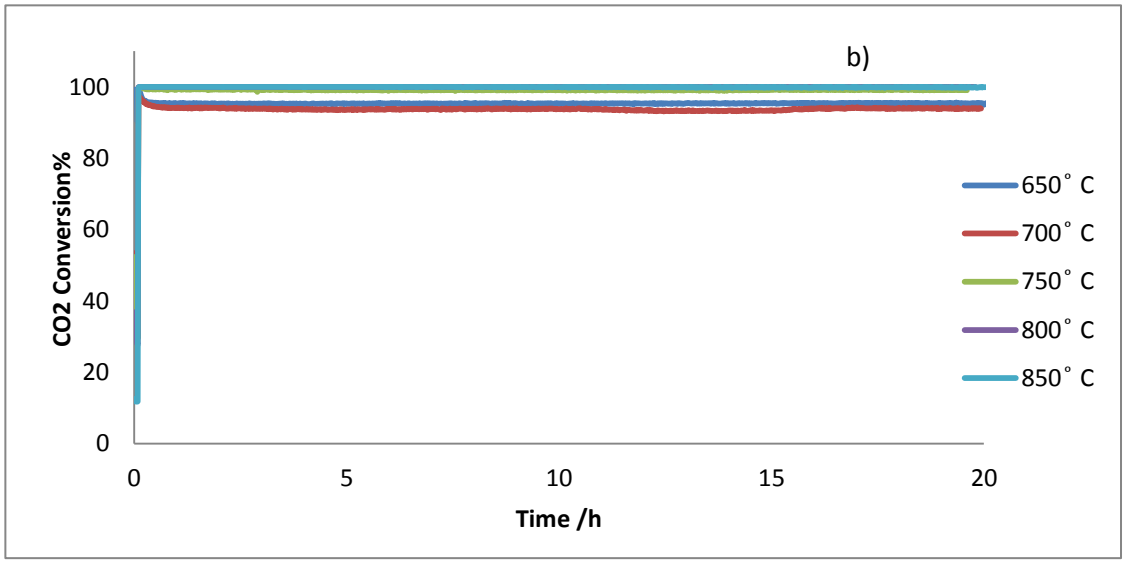

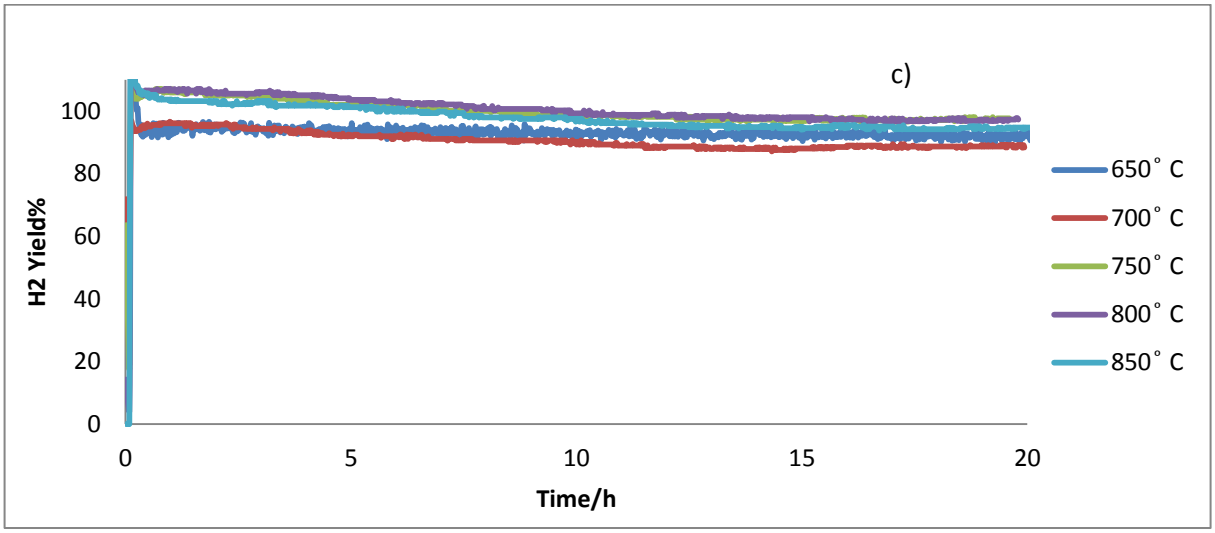

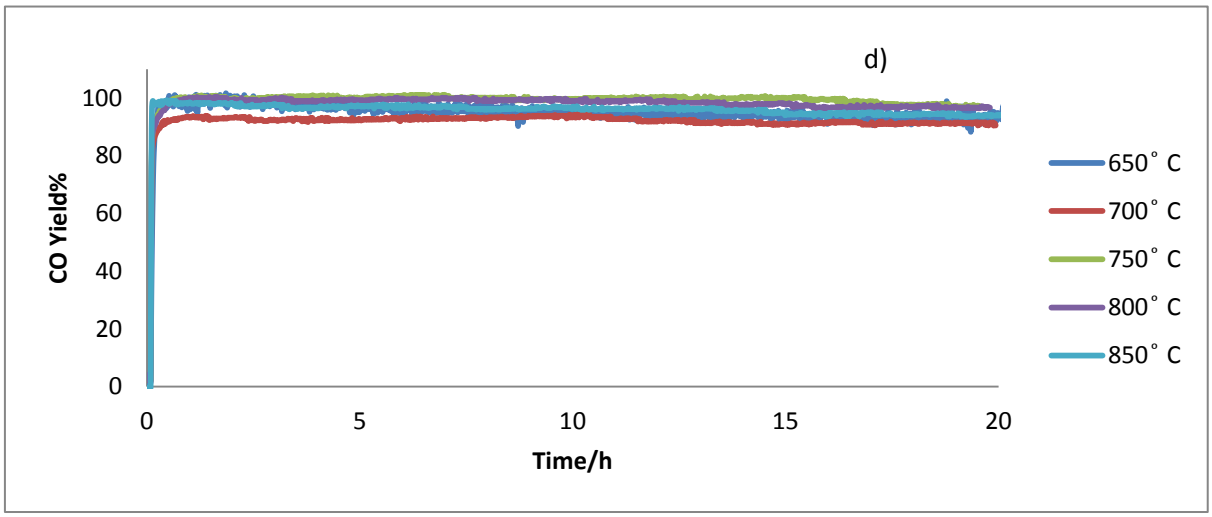

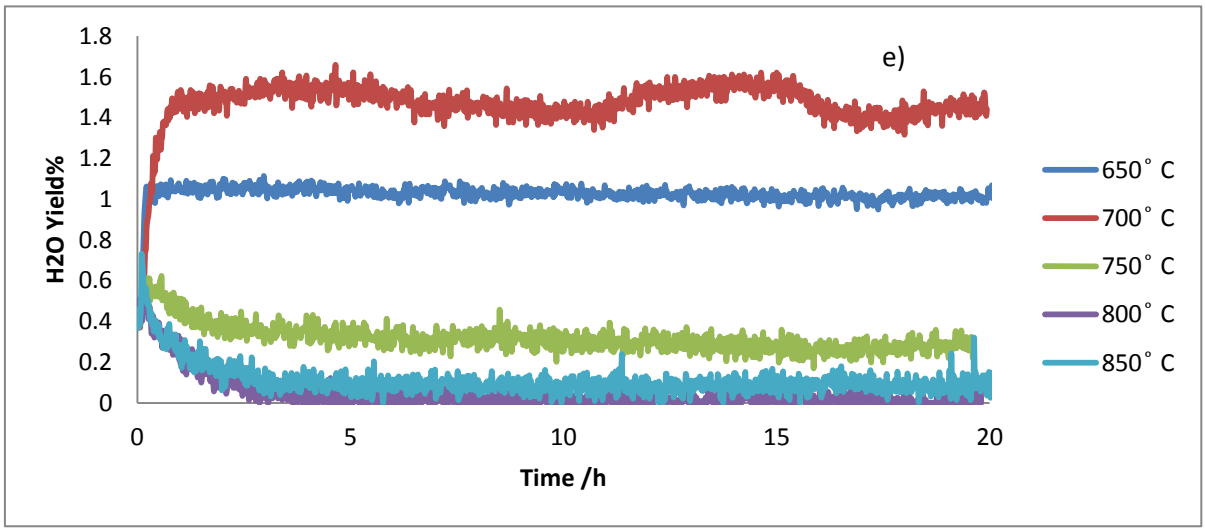

Figure 3- 29- isothermal dry reforming of methane at various temperature over 0.5Ru-LCZ with CH_4:CO_2 =2:1 a) CH_4 conversion b) CO_2 conversion c) H_2 yield d) CO yield e) water production

3.4.2.2 Carbon deposition: -

To determine the quantity and nature of the carbon species on the catalyst surface, TPO was performed after the DRM reactions.

As can be seen from Figure 3- 30, the highest level of accumulated carbon was at a temperature of 850° C due to methane decomposition. Carbon species form atom by the Boudouard reaction is unlikely because of the absence of a CO_2 peak at a temperature higher than 600°C. The 350°C peak can be attributed to highly reactive coke.

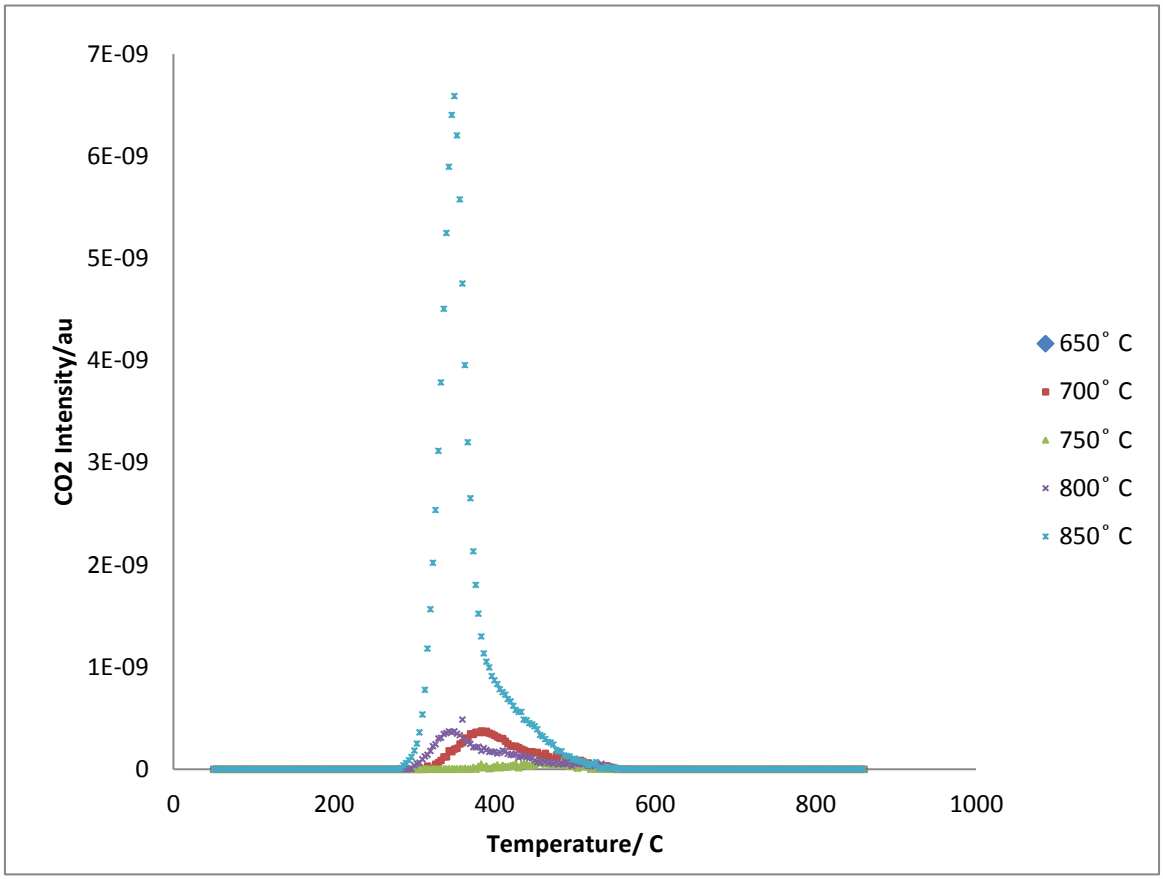

Figure 3- 30-post reaction TPO profiles of isothermal methane rich dry reforming over 0.5Ru-LCZ at various temperature

3.5 Summarising the effect of preparation method and doped metal on dry reforming (2:1 CH_4:CO_2)

3.5.1 Methane and carbon dioxide conversion: -

CH_4 and CO_2 conversion after 20h reforming reaction on 0.5 Ru-LCZ, Ni-LCZ (HY) and Ni-LCZ (Pechini) catalysts at different temperature are shown in Figure 3- 31a and 31b. As can be seen, both Ni catalysts showed slightly higher CH_4 conversions than the Ru catalyst at the lower temperature. At temperatures above 800 ° C, all three catalysts showed similar CH_4 conversions. As the CO_2 conversion for both Ni catalysts decreased at the lower temperature, it suggests the Boudouard reaction is occurring more on the Ni catalysts than the Ru catalyst. As the amount of CO_2 increased due to the Boudouard reaction, the probability of methane conversion increased at the lower temperature.

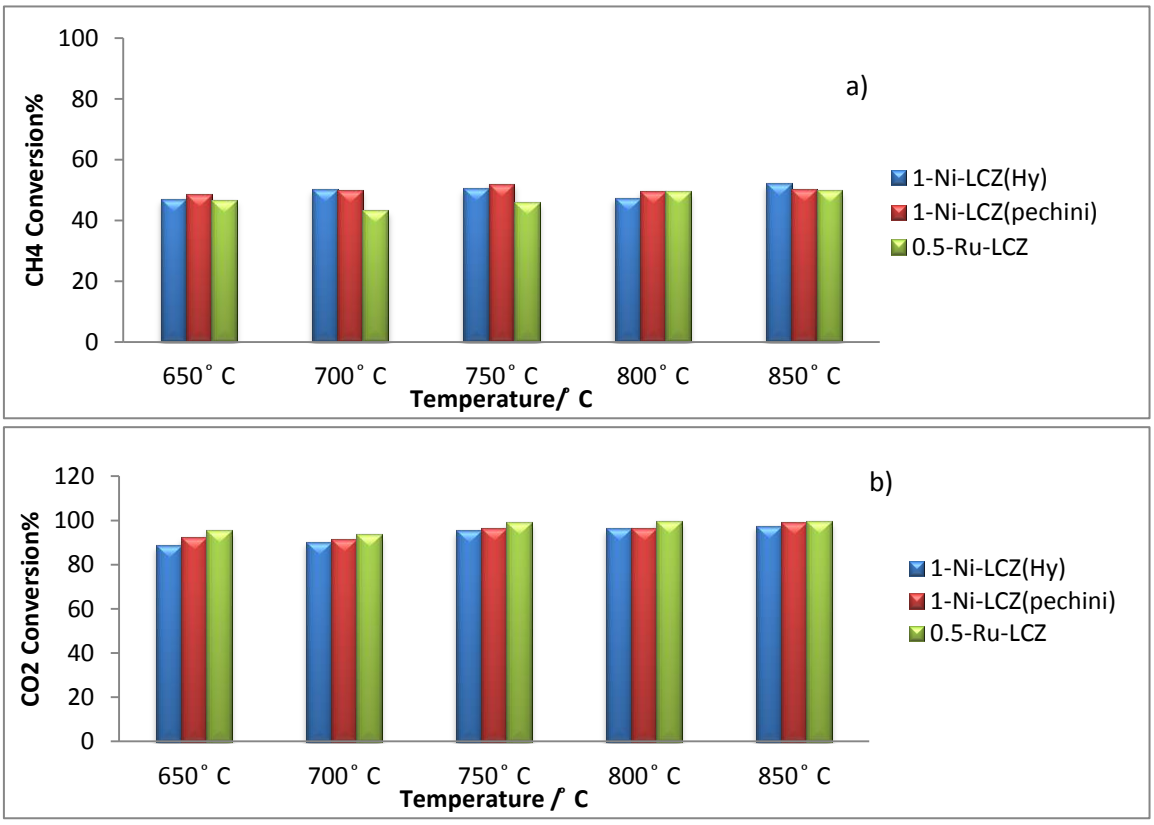

Figure3-31-average a) methane and b) carbon dioxide conversion for various catalysts at different temperatures for 2:1 CH_4:CO_2 dry reforming reaction.

3.5.2 Product selectivity

As can be seen from Figure 3- 32a and 32b, the selectivity of H_2 and CO in both Ni catalysts is lower than for the Ru catalyst at 650° C. For the hydrothermally synthesised catalyst, in addition to the Boudouard reaction, some CO reduction is occurring causing an increase in water production beside water gas shift reaction. As the amount of CO was higher than H_2, the water gas shift reaction is more likely besides CO reduction reaction for the Pechini synthesised catalyst. Almost no water gas shift reaction can be seen for the Ru catalyst at 650° C, whilst the Ni catalyst prepared by the hydrothermal method has a higher H_2 and CO selectivity at temperatures of 700° C and above. The Ni catalyst prepared by the Pechini method showed the lowest syngas selectivity at moderate temperatures, whilst the Ru catalyst showed a 3% reduction in selectivity at 850° C in contrast with other Ni catalysts that showed an increase in selectivity.

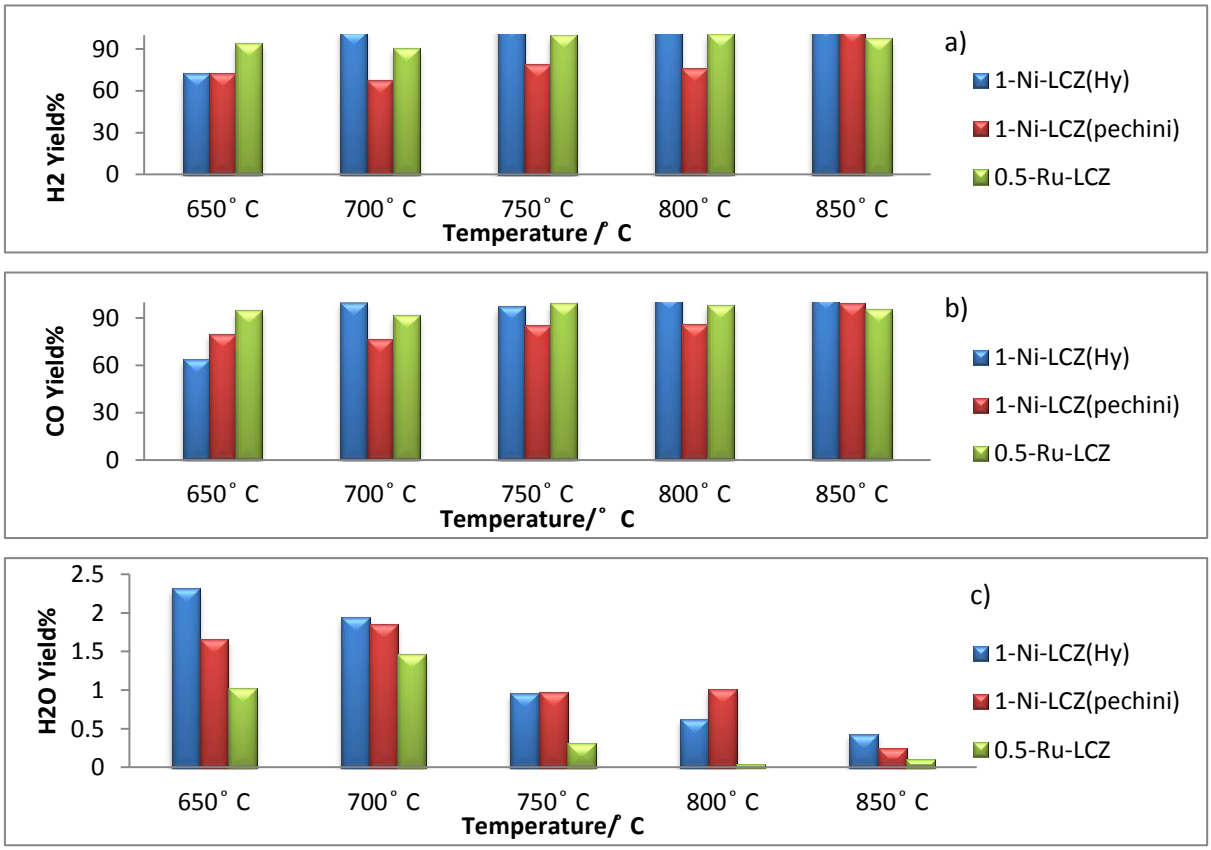

Figure 3-33-Average a) H_2, b) CO and c) H_2O selectivity for various catalysts at different temperatures for 2:1 CH_4:CO_2 dry reforming reaction

3.5.3 Carbon deposition

As can see from Figure 3- 34, Ni-LCZ (HY) has the highest amount of carbon deposition because of the Boudouard reaction and hydrogenation of CO at the lower temperatures. The amount of carbon deposition was not significantly different at various temperatures on the Ni catalyst prepared by the Pechini method. At 850 ° C, the Ru catalyst showed a low level of carbon deposition due to methane decomposition which affects catalyst activity, but even the highest levels of deposited carbon did not affect the Ni catalysts activity. It can be concluded that the amount of Ni that is not incorporated within the pyrochlore structure in the hydrothermal method was the reason for supporting the Boudouard reaction and high activity of the catalyst at the middle temperatures. The presence of cerium and the form and structure of the catalyst play an essential role in catalyst activity. The Ru catalyst support methane decomposition and Ni catalyst supports the Boudouard and CO reduction reaction.

By decreasing the ratio of Ni on LCZ catalyst (HY), the amount of carbon deposition has decreased, and it can be said that the hydrothermal preparation method did not have an adverse effect at the lower temperature. However, the Ni quantity needs to be carefully controlled for the best results.

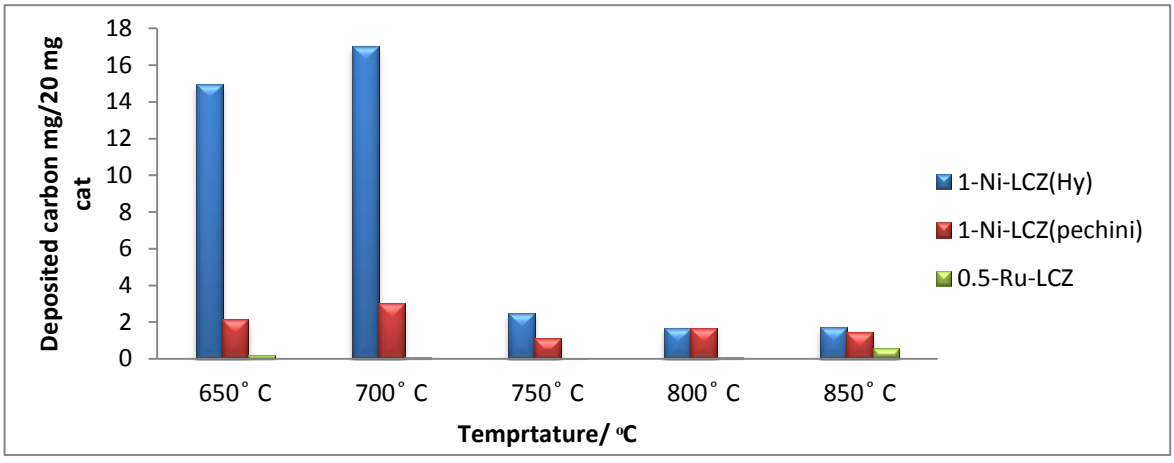

Figure 3-34-carbon deposition for various catalysts at different temperatures during 2:1 CH_4:CO_2 dry reforming reaction

3.6 Conclusion: -

The temperature programmed reaction for the methane-rich dry reforming conditions showed that the 0.25Ni-LCZ has a lower starting temperature in comparison with the 0.5 and 1Ni ratio by about 100 ℃. This was similar to both Ni-Pechini and Ru doped pyrochlore catalysts. In terms of the isothermal study at the temperature between 650 and 900 ℃,the 0.25-Ni catalyst showed high activity at 650 ℃ and conversion of methane was in excess of what could be achieved by a 2:1 methane to carbon dioxide ratio. Higher methane conversion in the low Ni catalyst was likely due to the reaction of ceria with methane suggested that Ceria showed the specific effect on lower Ni loading condition at the low temperature.

Generally, Ni-hydrothermal catalysts showed cycling behaviour in its dry reforming profiles. However, this behaviour decreased at the low reforming temperatures <800℃, and at the high ratio of Ni-doped (1Ni-LCZ). The amount of hydrogen increased with increasing the temperature and the amount of Ni in the catalyst due to the thermodynamic favourability and higher number of activating sites for CH_4 conversion. CO reduction as a side reaction plays a significant role in decreasing the amount of H_2 at the low temperatures in both the 0.25 and 0.5 Ni-LCZ catalysts. At 850^{o}C, as DRM became more thermodynamically favourable, the yields became higher, giving almost 100% yields for all the Ni-hydrothermal catalysts.

All three catalysts showed a decrease in carbon deposition trend with temperature, as CO hydrogenation and the Boudouard reaction are thermodynamically more favourable at the lower temperatures.

At the low temperatures, a significant difference in the amount of deposited carbon was seen by increasing the amount of Ni in the pyrochlore structure. The 0.25-NiLCZ pyrochlore had the lowest amount of deposited carbon due to fewer nickel sites present for reaction with carbon, that formed because of Boudouard reaction. In addition, the presence of higher effective CeO_2 increases the ability of the catalyst to oxidise carbon at the lower temperatures.

At higher temperatures >700 °C, the deposited carbon was suppressed significantly, and the amount of nickel had no significant impact on carbon deposition. The presence of ceria increases the potential for carbon oxidation through increased oxygen availability.

In terms of the long stability experiments at 750 ℃ under methane-rich dry reforming conditions, the amount of CH_4 and CO_2 conversion were close to the stoichiometric ratio for both the 0.25 and 1-Ni hydrothermal pyrochlore catalysts. The main difference between 0.25-NiLCZ and 1-NiLCZ was in the amount of syngas emission, where it was higher by nearly 20% for 1-Ni-LCZ. The decrease in the amount of CO and H_2 in comparison with 1-NiLCZ could be because of some side reactions as CO reduction (CO-R). During the DRM, the amount of H_2 was lower than CO because of the reverse water gas shift reaction. In addition, ceria can chemisorb large amounts of H_2 and CO. Both catalysts showed stability in performance without any deactivation over 3 days of reaction.

The amount of carbon deposition showed no real increase with time for both 0.25 and 1-Ni-LCZ catalysts, increasing the amount of Ni at 750^{o}C did not show any effect on deposited carbon. One visible difference between the two catalysts is that the carbon peak shifts to higher temperature for 1-Ni-LCZ, indicating the presence of traces of carbonaceous species, while one major TPO peak at 500 °C for 0.25 -NiLCZ corresponds to a soft type of carbon since it can be oxidised under relatively mild conditions. This presence of soft carbon supports the hypothesis leading to small Ni domains available at the catalyst surface during the reaction. Therefore, the Ni particles of 0.25-NiLCZ remain small and well dispersed on the surface. The agglomeration of Ni clusters would lead to more graphitic carbon.

In the methane-rich dry reforming, both the hydrothermal and the Pechini Ni catalysts showed slightly higher CH_4 conversions than the Ru catalyst at the lower temperature. As the CO_2 conversion for both Ni catalysts decreased at the lower temperature, it suggests that the Boudouard reaction is occurring and is more likely on Ni catalysts than the Ru catalyst. As

the amount of CO_2 increased due to the Boudouard reaction, the probability of methane conversion increased at the lower temperature. The selectivity of H_2 and CO in both Ni catalysts is lower than for the Ru catalyst at 650°C due to the Boudouard reaction and CO reduction reaction causing an increase in water production. Ni catalysts prepared by the Pechini method showed the lowest syngas selectivity at the middle temperature. Ru catalyst showed a 3% reduction in selectivity at 850°C in contrast with other Ni catalysts due to the carbon deposition.

The hydrothermal 1Ni-LCZ pyrochlore catalyst has the highest amount of carbon deposition because of the Boudouard reaction and hydrogenation of CO at the lower temperature. The amount of carbon deposition was not significantly different at various temperatures on the Ni catalysts prepared by the Pechini method. At 850°C, the Ru catalyst showed a low level of carbon deposition due to methane decomposition which affects catalyst activity. The highest level of deposited carbon did not affect the Ni catalysts activity. It can be concluded that the amount of Ni that is not incorporated within the pyrochlore structure in the hydrothermal method was the reason for promotion of the Boudouard reaction and high activity of the catalyst at the middle temperature. The presence of cerium and the form and structure of the catalyst play an essential role in catalyst activity. Ru catalysts support methane decomposition and Ni catalyst support the Boudouard and CO reduction reactions. By decreasing the ratio of Ni in the hydrothermal LCZ catalysts, the amount of carbon deposition decreased, and it can be said that the hydrothermal preparation method had no adverse effect at the lower temperature, however controlling the Ni amount has to be done carefully to achieve the best results.

3.7 References: -

1-De Falco, M., Iaquaniello, G. and Centi, G. eds., 2013. *CO2: a valuable source of carbon* (p. 194). London: Springer.

2-M.K. Nikoo, N.A.S. Amin, Thermodynamic analysis of carbon dioxide reforming of methane in view of solid carbon formation, Fuel Processing Technology, 92 (2011) 678-691.

3-Debek, R. and Dębek, R., 2016. *Novel catalysts for chemical CO2 utilization* (Doctoral dissertation, Université Pierre et Marie Curie-Paris VI).

4-Pen, M.A., Gomez, J.P. and Fierro, J.G., 1996. New catalytic routes for syngas and hydrogen production. *Applied Catalysis A: General*, *144*(1-2), pp.7-57.

5-Verykios, X.E., 2003. Mechanistic aspects of the reaction of CO2 reforming of methane over Rh/Al2O3 catalyst. *Applied Catalysis A: General*, *255*(1), pp.101-111.

6-Djinović, P., Črnivec, I.G.O., Batista, J., Levec, J. and Pintar, A., 2011. Catalytic syngas production from greenhouse gasses: Performance comparison of Ru-Al2O3 and Rh-CeO2 catalysts. *Chemical Engineering and Processing: Process Intensification*, *50*(10), pp.1054-1062.

7-Alessandro, T., 2002. *Catalysis by ceria and related materials* (Vol. 2). World Scientific.

8-Lohsoontorn, P., Brett, D.J.L. and Brandon, N.P., 2008. Thermodynamic predictions of the impact of fuel composition on the propensity of sulphur to interact with Ni and ceria-based anodes for solid oxide fuel cells. *Journal of Power Sources*, *175*(1), pp.60-67.

9-Jun, K.W., Roh, H.S. and Chary, K.V., 2007. Structure and catalytic properties of ceria-based nickel catalysts for CO2 reforming of methane. *Catalysis Surveys from Asia*, *11*(3), pp.97-113.

10-Rezaei, M., Alavi, S.M., Sahebdelfar, S. and Yan, Z.F., 2009. A highly stable catalyst in methane reforming with carbon dioxide. *Scripta Materialia*, *61*(2), pp.173-176.

11-Livermore, S.J., Cotton, J.W. and Ormerod, R.M., 2000. Fuel reforming and electrical performance studies in intermediate temperature ceria–gadolinia-based SOFCs. *Journal of power sources*, *86*(1-2), pp.411-416.

12-Dong, W.S., Jun, K.W., Roh, H.S., Liu, Z.W. and Park, S.E., 2002. Comparative study on partial oxidation of methane over Ni/ZrO2, Ni/CeO2 and Ni/Ce–ZrO2 catalysts. *Catalysis letters*, *78*(1-4), pp.215-222.

13-Laosiripojana, N. and Assabumrungrat, S., 2005. Catalytic dry reforming of methane over high surface area ceria. *Applied Catalysis B: Environmental*, *60*(1-2), pp.107-116

14-Eriksson, S., Rojas, S., Boutonnet, M. and Fierro, J.L.G., 2007. Effect of Ce-doping on Rh/ZrO2 catalysts for partial oxidation of methane. *Applied Catalysis A: General*, *326*(1), pp.8-16.

15-He, H. and Hill, J.M., 2007. Carbon deposition on Ni/YSZ composites exposed to humidified methane. *Applied Catalysis A: General*, *317*(2), pp.284-292.

16-Laosiripojana, N., Sutthisripok, W. and Assabumrungrat, S., 2005. Synthesis gas production from dry reforming of methane over CeO2 doped Ni/Al2O3: Influence of the doping ceria on the resistance toward carbon formation. *Chemical Engineering Journal*, *112*(1-3), pp.13-22.

17-Koo, K.Y., Roh, H.S., Jung, U.H. and Yoon, W.L., 2009. CeO 2 promoted Ni/Al 2 O 3 catalyst in combined steam and carbon dioxide reforming of methane for gas to liquid (GTL) process. *Catalysis letters*, *130*(1-2), p.217.

18-Xu, C., Zondlo, J.W., Gong, M., Elizalde-Blancas, F., Liu, X. and Celik, I.B., 2010. Tolerance tests of H2S-laden biogas fuel on solid oxide fuel cells. *Journal of Power Sources*, *195*(15), pp.4583-4592.

19-Rezaei, M., Alavi, S.M., Sahebdelfar, S. and Yan, Z.F., 2009. A highly stable catalyst in methane reforming with carbon dioxide. *Scripta Materialia*, *61*(2), pp.173-176.

20-Passos, F.B., de Oliveira, E.R., Mattos, L.V. and Noronha, F.B., 2005. Partial oxidation of methane to synthesis gas on Pt/CexZr1− xO2 catalysts: the effect of the support reducibility and of the metal dispersion on the stability of the catalysts. *Catalysis Today*, *101*(1), pp.23-30.

21-Roh, H.S., Potdar, H.S. and Jun, K.W., 2004. Carbon dioxide reforming of methane over co-precipitated Ni–CeO2, Ni–ZrO2 and Ni–Ce–ZrO2 catalysts. *Catalysis Today*, *93*, pp.39-44.

22-Pompeo, F., Gazzoli, D. and Nichio, N.N., 2009. Stability improvements of Ni/α-Al2O3 catalysts to obtain hydrogen from methane reforming. *International journal of hydrogen energy*, *34*(5), pp.2260-2268.

23-Mamontov, E., Egami, T., Brezny, R., Koranne, M. and Tyagi, S., 2000. Lattice defects and oxygen storage capacity of nanocrystalline ceria and ceria-zirconia. *The Journal of Physical Chemistry B*, *104*(47), pp.11110-11116.

24-Trovarelli, A., de Leitenburg, C., Boaro, M. and Dolcetti, G., 1999. The utilization of ceria in industrial catalysis. *Catalysis today*, *50*(2), pp.353-367.

25-Evans, S.E., 2017. *Catalytic reforming of biogas using nickel-based perovskite materials* (Doctoral dissertation, Keele University).

26-Simonov, M.N., Rogov, V.A., Smirnova, M.Y. and Sadykov, V.A., 2017. Pulse Microcalorimetry Study of Methane Dry Reforming Reaction on Ni/Ceria-Zirconia Catalyst. *Catalysts*, *7*(9), p.268.

27-Haynes, D.J., Campos, A., Berry, D.A., Shekhawat, D., Roy, A. and Spivey, J.J., 2010. Catalytic partial oxidation of a diesel surrogate fuel using an Ru-substituted pyrochlore. *Catalysis Today*, *155*(1-2), pp.84-91.

28-Radlik, M., Adamowska-Teyssier, M., Krztoń, A., Kozieł, K., Krajewski, W., Turek, W. and Da Costa, P., 2015. Dry reforming of methane over Ni/Ce0. 62Zr0. 38O2 catalysts: Effect of Ni loading on the catalytic activity and on H2/CO production. *Comptes Rendus Chimie*, *18*(11), pp.1242-1249

29- Zanganeh, R., Rezaei, M. and Zamaniyan, A., 2013. Dry reforming of methane to synthesis gas on NiO–MgO nanocrystalline solid solution catalysts. *International Journal of Hydrogen Energy*, *38*(7), pp.3012-3018.

30- Odedairo, T., Chen, J. and Zhu, Z., 2013. Metal–support interface of a novel Ni–CeO2 catalyst for dry reforming of methane. *Catalysis Communications*, *31*, pp.25-31.

31- Bobin, A.S., Sadykov, V.A., Rogov, V.A., Mezentseva, N.V., Alikina, G.M., Sadovskaya, E.M., Glazneva, T.S., Sazonova, N.N., Smirnova, M.Y., Veniaminov, S.A. and Mirodatos, C., 2013. Mechanism of CH 4 Dry Reforming on Nanocrystalline Doped Ceria-Zirconia with Supported Pt, Ru, Ni, and Ni–Ru. *Topics in Catalysis*, *56*(11), pp.958-968.

4. Dry reforming of methane over pyrochlore catalysts under stoichiometric conditions: -

This section of the thesis will demonstrate the effect of stoichiometric conditions on various catalyst's activity with differing Ni loading, preparation method and active metal.

4.1.1 Effect of different Ni loadings on the LCZ catalysts: -

The reactions over time at different temperatures under stoichiometric conditions for 0.25, 0.5 and 1Ni-LCZ are shown in figure 4-1.

As can be seen, the profiles of all three catalysts are almost identical, and the initial reaction occurred by increasing the synthesis gas at around 450° C. Due to the reverse water gas shift reaction the amount of CO was higher than H_2 at all temperatures. On increasing the temperature, the ratio of H_2:CO almost becomes one for higher Ni loading catalysts. 0.25 NiLCZ did not however show unity in the H_2/CO ratio. The presence of free ceria in the structure of the catalyst could be the reason for the reverse water gas shift reaction and as a result this gives a lower H_2/CO production ratio.

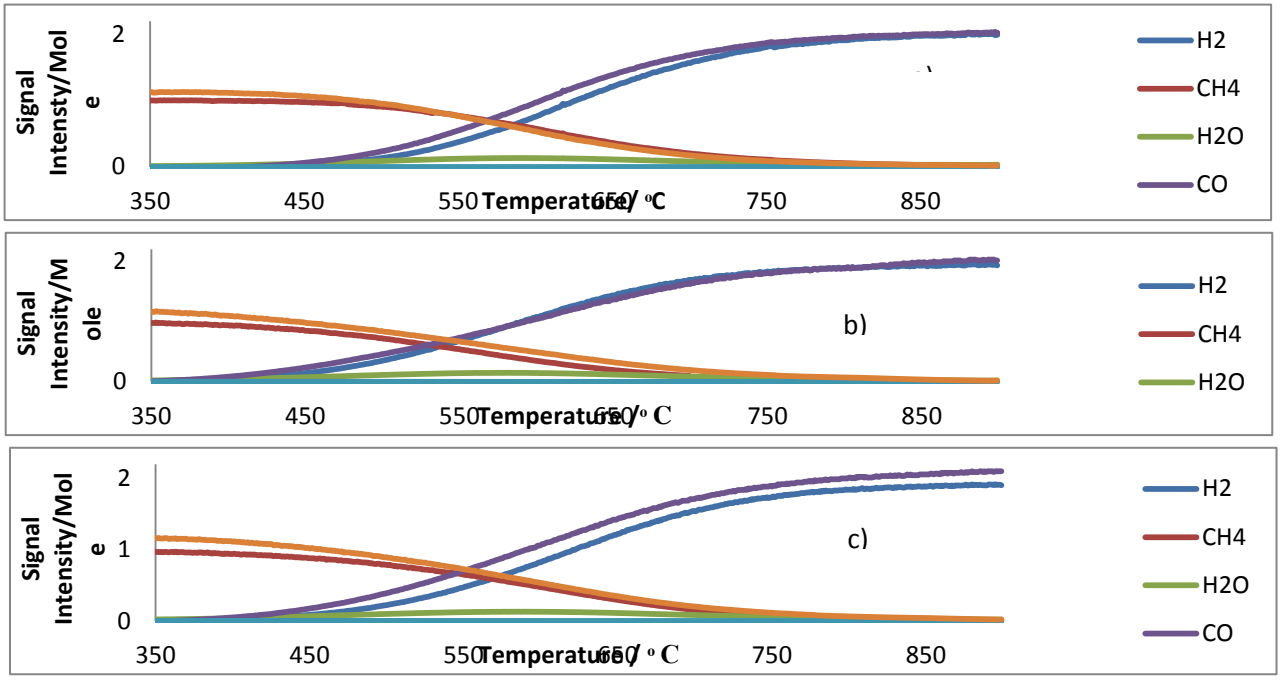

Figure4- 2-1- Reaction profile for 1:1 CH_4/CO_2 mixture passed over a) 1-NiLCZ, b) 0.5-Ni LCZ and c) 0.25Ni-LCZ

4.1.2 Isothermal of stoichiometric dry reforming over different Ni loadings

The activity and stability of various Ni loading in the La Ce Zr $_{2-x}$Ni $_{x}$O $_{7}$ catalyst (x=0.25, 0.5 and 1) has been investigated using stoichiometric conditions. The dry reforming reaction was performed at different temperatures for around 20 h. and to determine the carbon deposition, a TPO experiment was conducted at the end of each reforming experiment

4.1.2.1.1 Low loading of Ni (0.25Ni-LCZ):-

The lowest conversion was seen at 650 °C due to the endothermic nature of dry reforming which is preferred at a higher temperature[6]. As can be seen from figure 4- 2; the CH_4 conversion was lower than the CO_2 conversion by 8% at 650^{o} C. In contrast, due to the reverse water gas shift reaction, the level of H_2O was higher in comparison with the other higher temperatures. Moreover, the CO yield was less than the CO_2 conversion by 8% suggesting that the Boudouard reaction was occurring that increased the amount of CO_2. As the amount of H_2 was lower than expected by 20%, the reaction of carbon deposition via $CO_2+2H_2 \leftrightarrow C+2H_2O$ could be the cause of this reduction[8] in addition to the water gas shift reaction. At 800^{o}C, due to the water gas shift reaction, the methane conversion ratio becomes higher than the CO_2 conversion.

Interestingly the H_2 and CO yields did not correlate with the CH_4 and CO_2 conversions, and even they were lower than the synthesis gas yield at 750^{o}C. In addition, the amount of H_2O was smaller than was seen at 750^{o} C. Therefore, the reverse water gas shift reaction and methane coupling could not be the reason for this 15 to 20% reduction and the amount of CO was higher than H_2 because of the reverse water gas shift reaction at 750^{o}C.

Generally, it can be said that the CH_4 and CO_2 conversion increased by increasing the temperature and in contrast, the amount of water decreased. At 750^{o}C and 800^{o}C, the H_2: CO ratio reached unity, however, the amount of synthesis gas was higher at 750^{o}C.

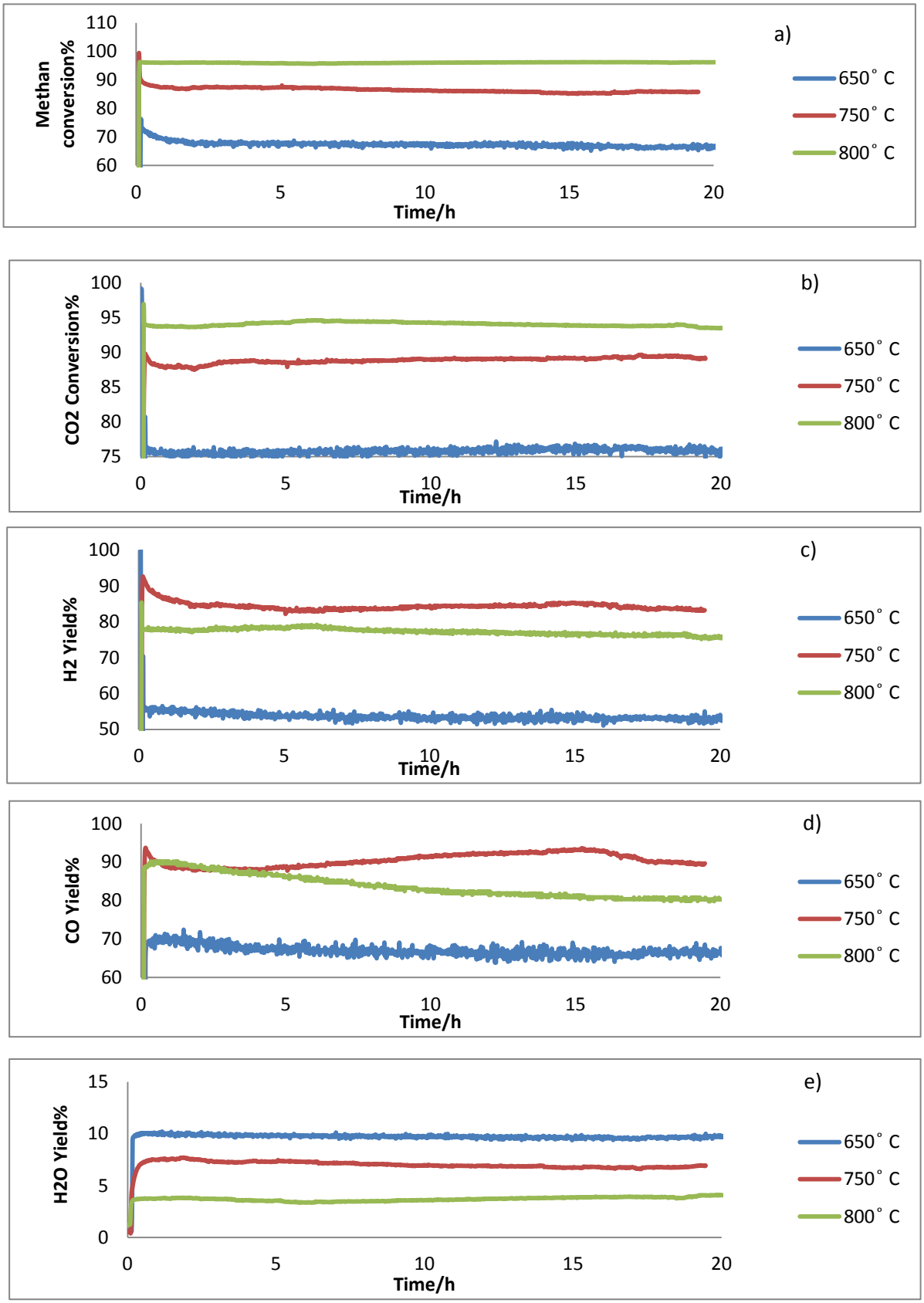

figure 4- 2- isothermal dry reforming of methane at various temperature over 1Ni-LCZ with CH_4:CO_2 =1:1 a) CH_4 conversion b) CO_2 conversion c) H_2 yield d) CO yield e) water production.

4.1.2.1.2 Carbon deposition: -

Figure4- 3 shows the CO_2 production profile of 0.25-NiLCZ after 20h reaction at different temperatures in the temperature programmed oxidation experiment. As carbon deposition is a factor for DRM deactivation, the critical aim in catalyst development is avoiding the hard carbon formation.

The profile of 0.25Ni-LCZ at 750 and 650^{o}C indicate the presence of a soft type of carbon that oxidises under mild conditions of 400 and 700^{o}C. It can also be observed that the amount of deposited carbon at 650^{o}C is five times more than the carbon formation at 750^{o}C. As the CO yield at 650 °C was lower by about 20% in comparison with 750^{o} C, therefore the Boudouard reaction could be taking place and may account for this significant amount of carbon at 650^{o}C. At 800^{o}C, the CO_2 peak shifted to lower temperature and the amount of carbon deposition showed no significant difference in comparison with 750^{o}C. The reason is due to the thermodynamic equilibrium of carbon formation which is favourable at a low temperature[1]. The small broad peak at 300 and 500^{o}C can be attributed to amorphous, atomic carbon species that easily gasified[2-4].

It can be concluded, as carbon deposition is closely related to Ni particle size, the presence of soft carbon suggests that the Ni particles seems to remain small and well dispersed within the catalyst[5].

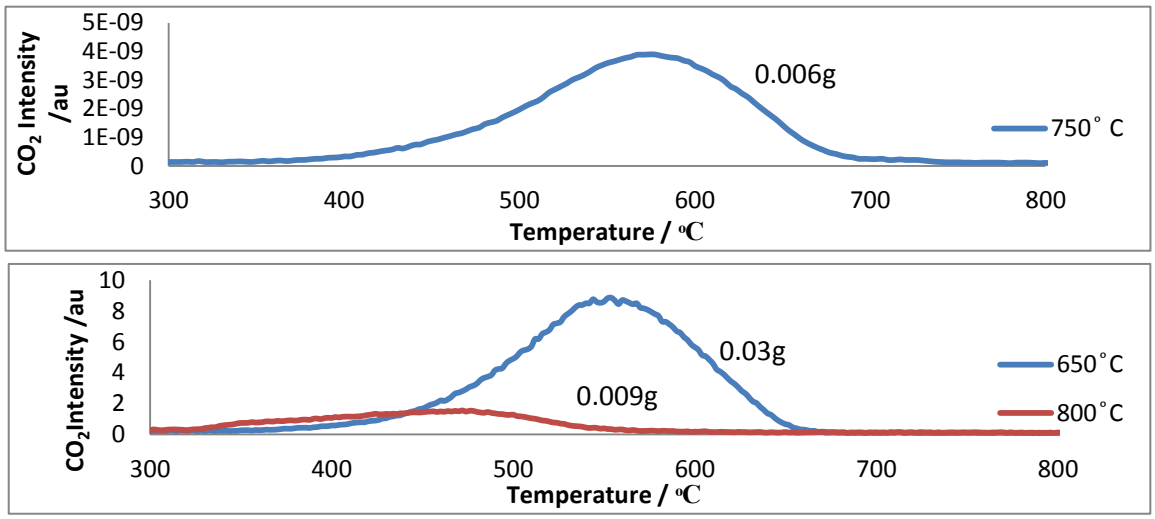

Figure 4- 3-post reaction TPO profiles of isothermal stoichiometric dry reforming over 0.25-NiLCZ at various temperatures.

4.1.2.2.1 Mid-loading of Ni (0.5Ni-LCZ):-

Almost stable catalyst activity can be observed from figure 4- 4 at all temperatures. However, a slight gradual decrease in methane conversion occurred at 650◦C. Since methane is believed to be activated by Ni, methane conversion appears to be more sensitive to deactivation than CO_2 due to carbon formation around or over the Ni particles as a result of the Boudouard reaction[5].

At 700◦ C, the reaction of carbon gasification via $CO+H_2 \leftrightarrow C+H_2O$ causes the significant reduction in H_2 yield in comparison with the CH_4 conversion[8]. The ratio of H_2/CO was lower than one due to the reverse water gas shift reaction. By increasing the temperature to 750 and 800◦ C, the level of methane conversion increased due to the endothermic nature of dry reforming which is preferred at a higher temperature. However, the amount of H_2 was lower than CO because of the reverse Boudouard and reverse water gas shift reactions.

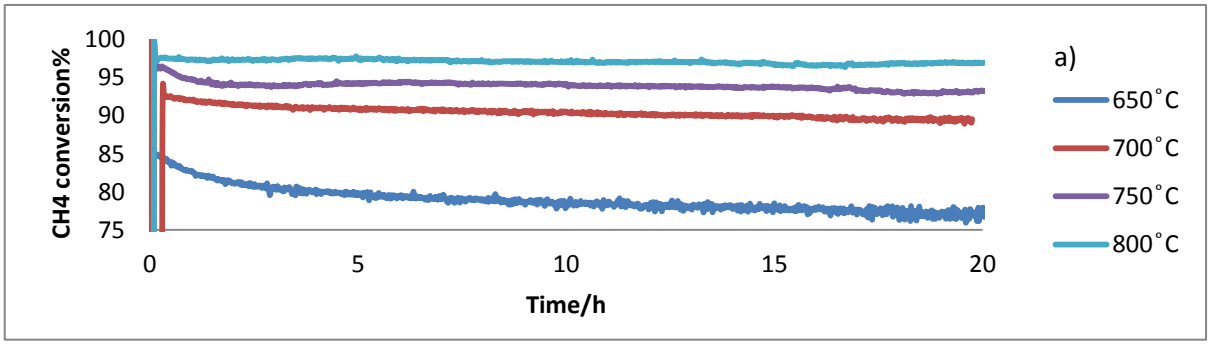

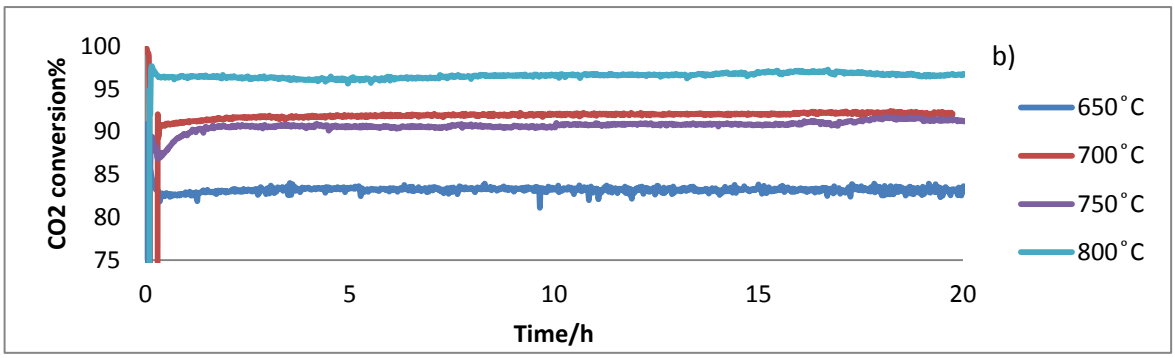

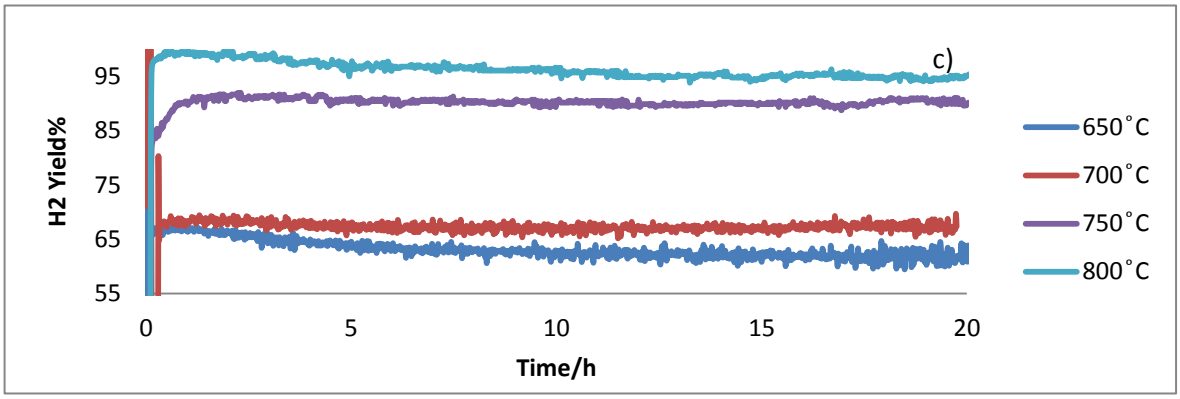

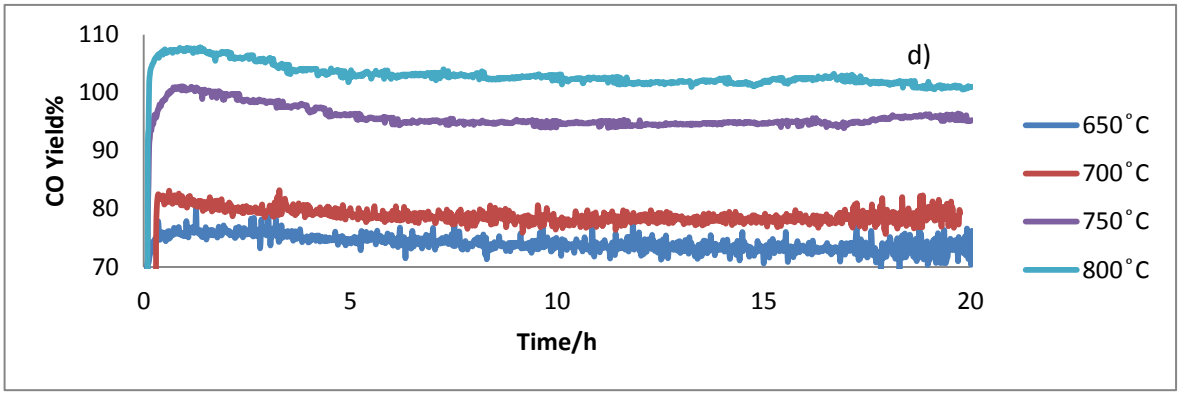

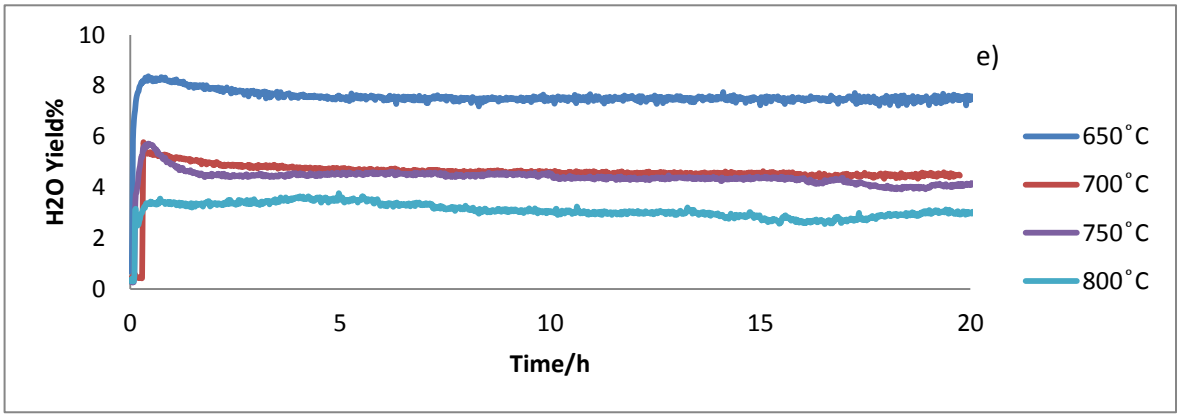

Figure 4- 4- isothermal dry reforming of methane at various temperature over 0.5Ni-LCZ with CH_4:CO_2 =1:1 a) CH_4 conversion b) CO_2 conversion c) H_2 yield d) CO yield e) water production

4.1.2.2.2 Carbon deposition:-

The post reaction profile of deposited carbon shows a reverse trend in increasing carbon deposition with temperature. This increase in carbon deposition is due to the Boudouard reaction and CO reduction that is favourable at a low temperature. The amount of deposited carbon at temperature of 750 and 800°C was lower by 86 times in comparison with 650°C.

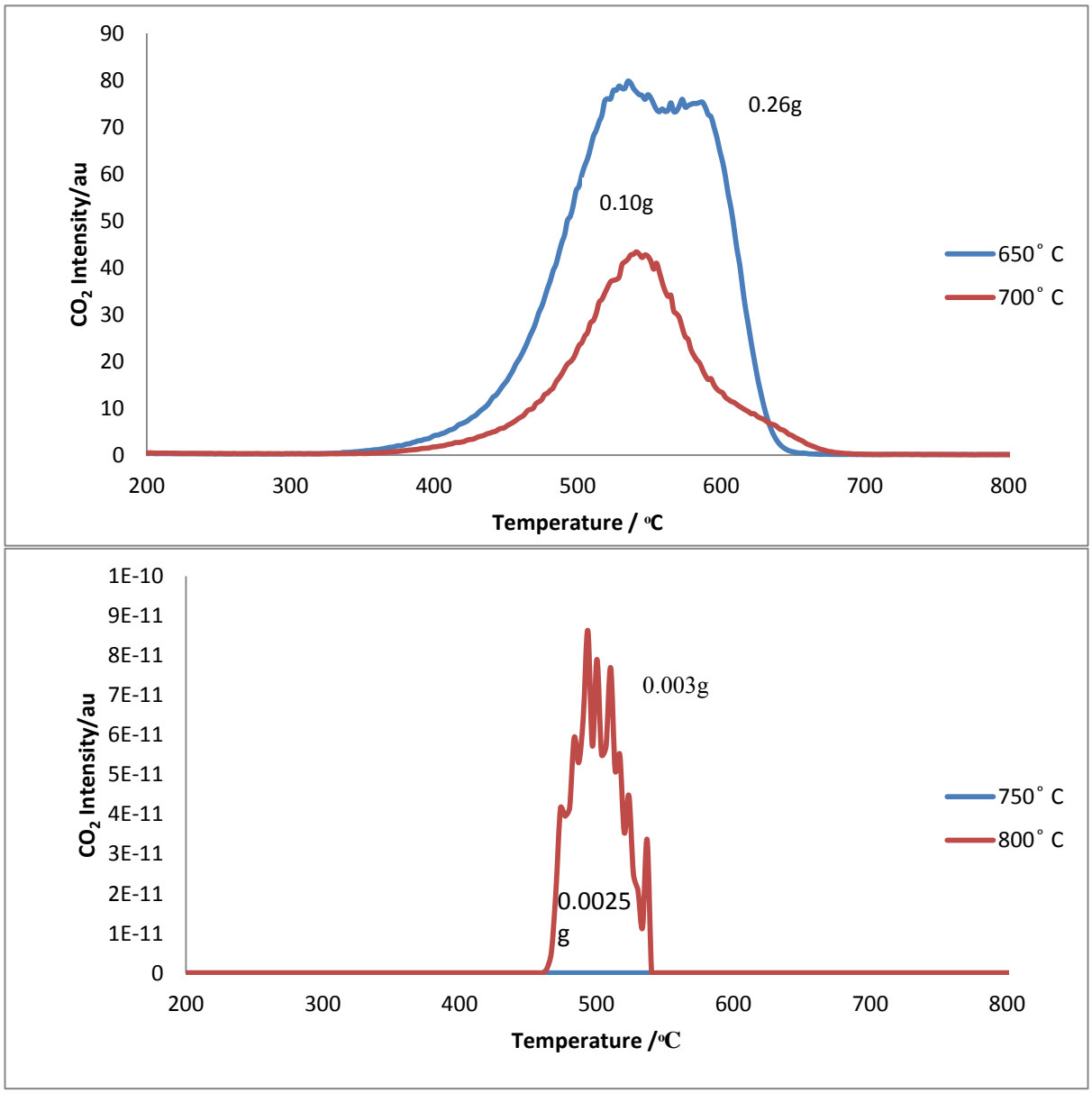

Figure 4- 5-post reaction TPO profiles of isothermal stoichiometric dry reforming over 0.5-NiLCZ at various temperatures

4.1.2.3.1 High loading of Ni (1Ni-LCZ):-

Because of carbon deposition, the CH_4 conversion showed a decreasing trend with time at 650° C, due to the loss of active Ni sites. However, this decreasing trend was not observed in the CO_2 conversion. By increasing the temperature to 850° C, the average of methane conversion increased from 72% to 96%. Some level of water formation was seen at all temperatures that makes the amount of CO larger than H_2. At 750 ° C, the reverse Boudouard reaction increased the catalyst activity. The CH_4 conversion was higher than CO_2 conversion by 5% at 850° C, while, the amount of H_2 was lower than the CO yield. Also, the amount of H_2O increased in comparison with 800° C. It can be suggested, that due to the presence of ceria in the structure of catalyst, the following reaction could be occurring $CH_4+1.5O_2 \leftrightarrow CO+2H_2O$.

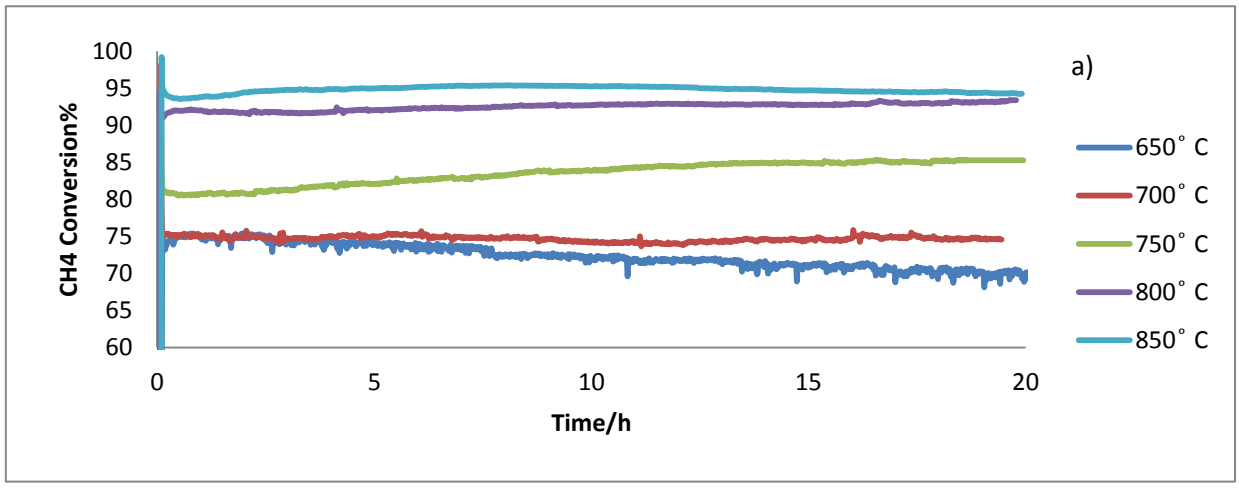

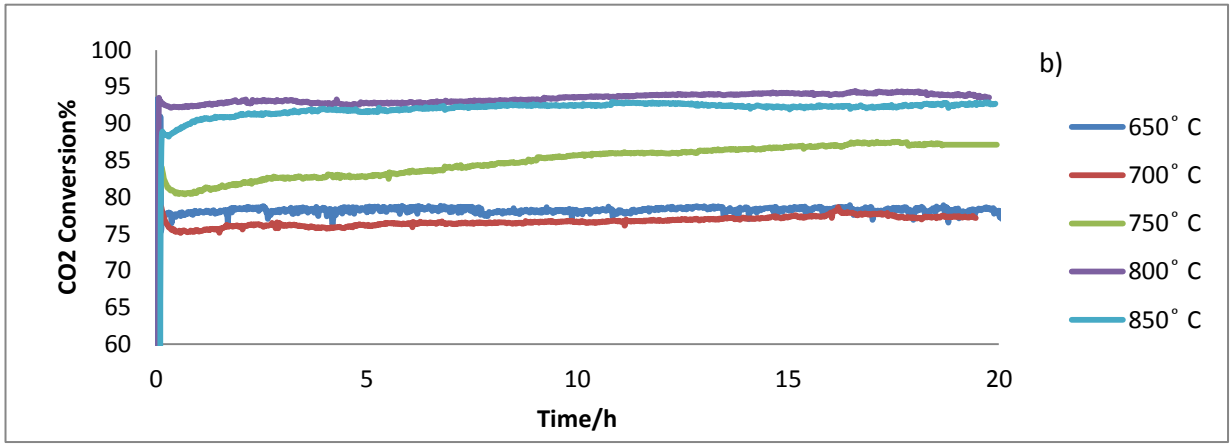

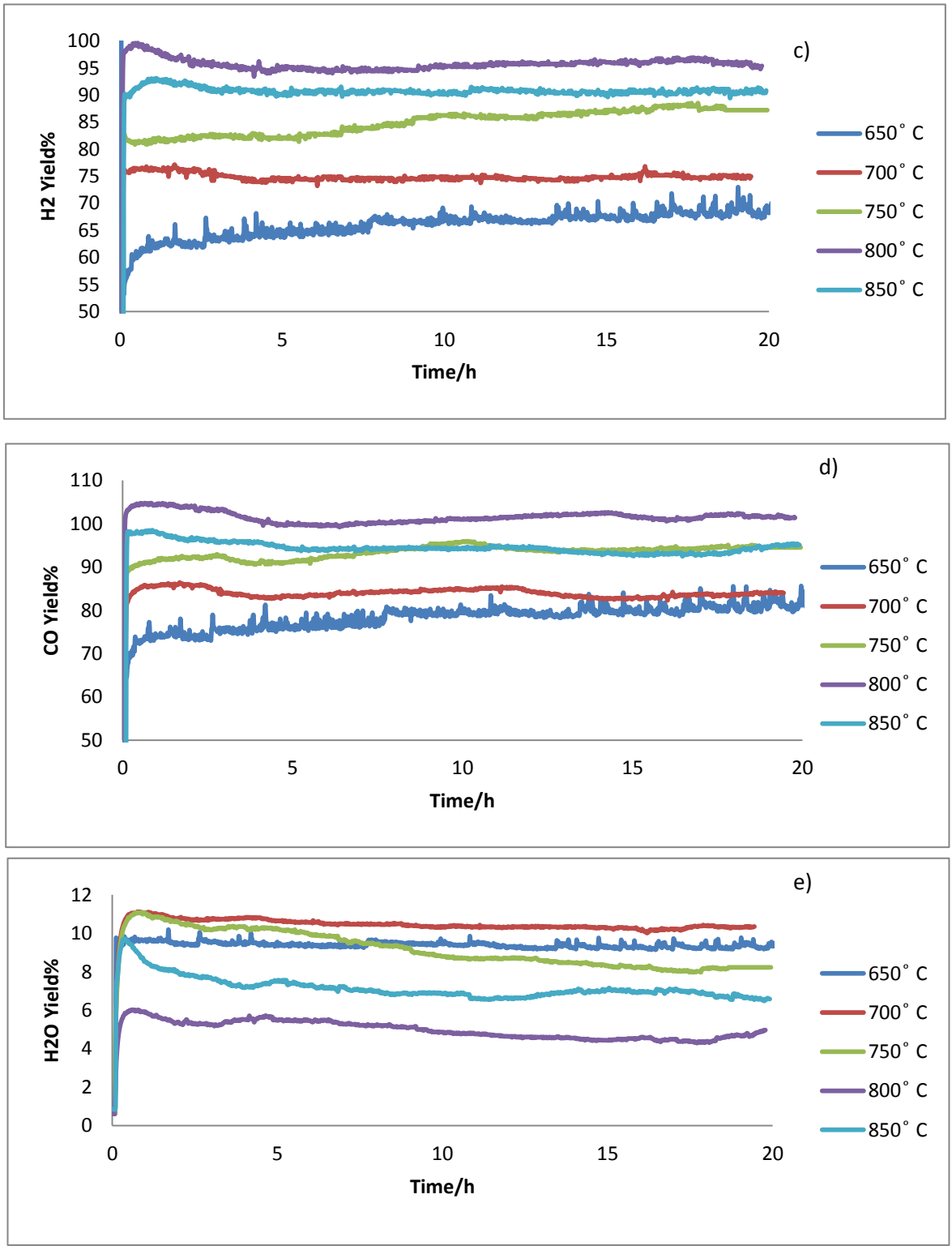

Figure 4- 6- isothermal dry reforming of methane at various temperature over 1Ni-LCZ with CH_4:CO_2 =1:1 a) CH_4 conversion b) CO_2 conversion c) H_2 yield d) CO yield e) water production

4.1.2.3.2 Carbon deposition:-

As can be seen from figure 4-7, the amount of deposited carbon increased by decreasing the temperature. In comparison with the TPO profile of the lower Ni loading, the CO_2 peak shifted to higher temperature due to the presence of more Ni species that are not within the pyrochlore structure. The agglomeration of Ni clusters would lead to more graphitic carbon that oxidised at higher temperature. The amount of deposited carbon at 850°C is 400 times lower than 650°C. This may suggest that this kind of Ni supports the Boudouard reaction.

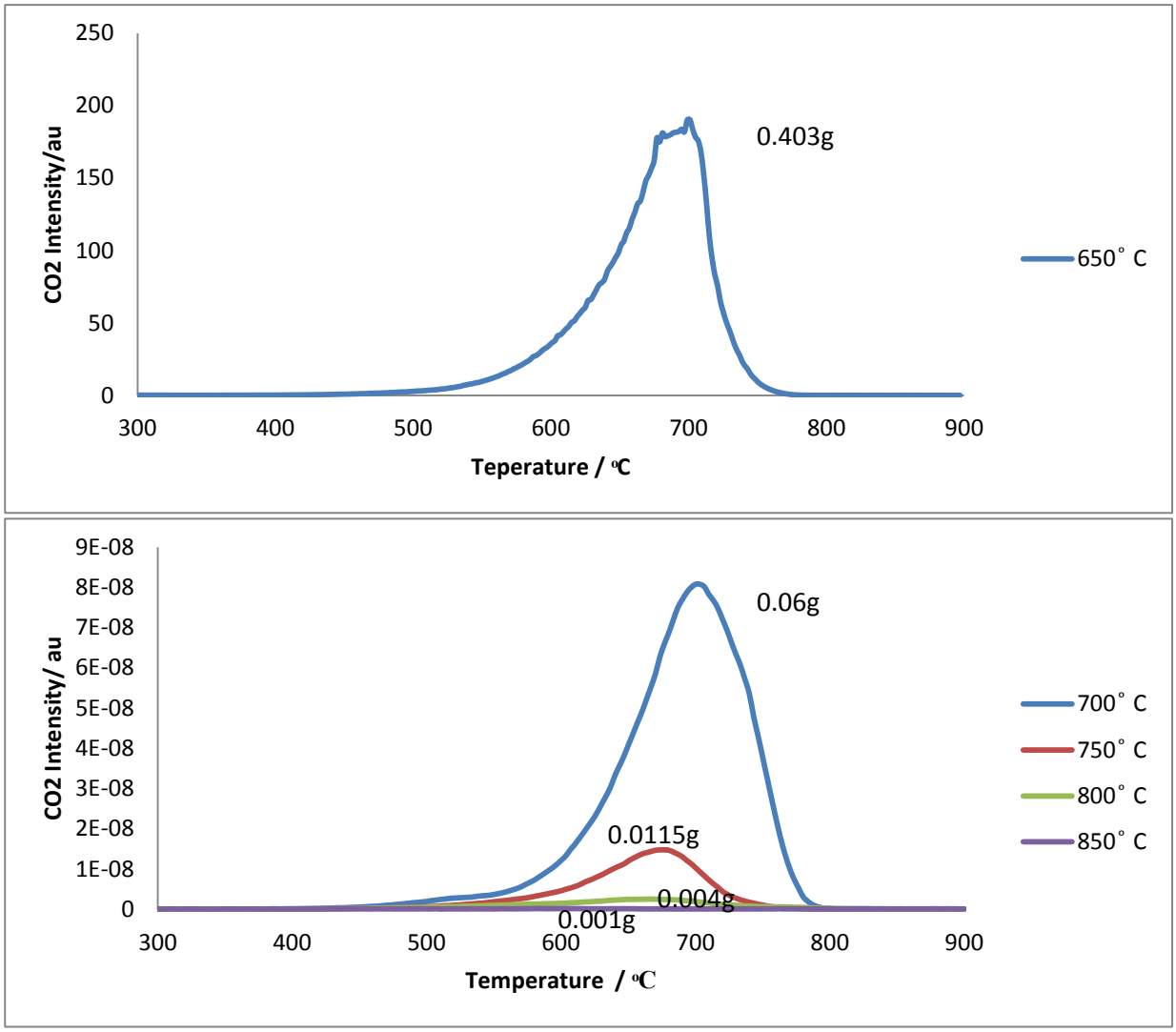

Figure 4- 7-post reaction TPO profiles of isothermal stoichiometric dry reforming over 1-NiLCZ at various temperatures

4.1.3 Comparison study of the CH_4 and CO_2 conversions, product selectivity and carbon deposition for LCZ catalysts with different nickel contents during stoichiometric methane dry reforming

Because of the low loading of Ni in 0.25 Ni-LCZ at 650° C, the CH_4 conversion was lower than other catalysts. However, 0.5 Ni-LCZ had higher conversion than 1 Ni-LCZ due to the more significant amount of deposited carbon on 1 Ni-LCZ that blocks Ni active sites.

The CO_2 conversion followed the same trend as the methane conversion at 650° C with a higher amount because of the reverse water gas shift reaction. The lower amount of H_2 in comparison with the CH_4 conversion could be due to the CO reduction that increased by the decrease in Ni loading. By increasing the temperature, the gap between CO_2 and CH_4 conversion decreased. Generally, 0.5 Ni-LCZ showed higher activity in comparison with others. At the temperature of 750° C, deposited carbon decreased significantly in the 0.5 and 1Ni-LCZ whilst the lowest loading of Ni, 0.25Ni-LCZ, had the lowest amount of deposited carbon at all temperatures.

At 800° C, despite the amount of CH_4 and CO_2 conversion in 0.25 Ni-LCZ being at the same level as other catalysts, the amount of synthesis gas showed a dramatic decrease. The water gas shift reaction could be the reason for this decrease, $CO+H_2 \leftrightarrow H_2O+C$. The presence of ceria in the catalyst structure depresses the deposited carbon and increases the amount of CO via oxidation of the carbon $C+1/2O_2 \leftrightarrow CO$.

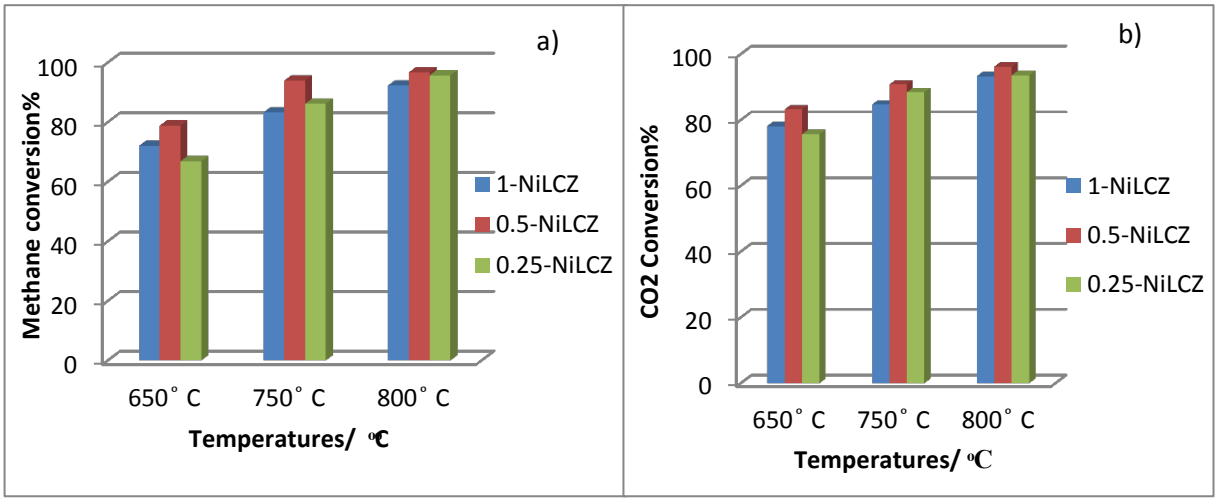

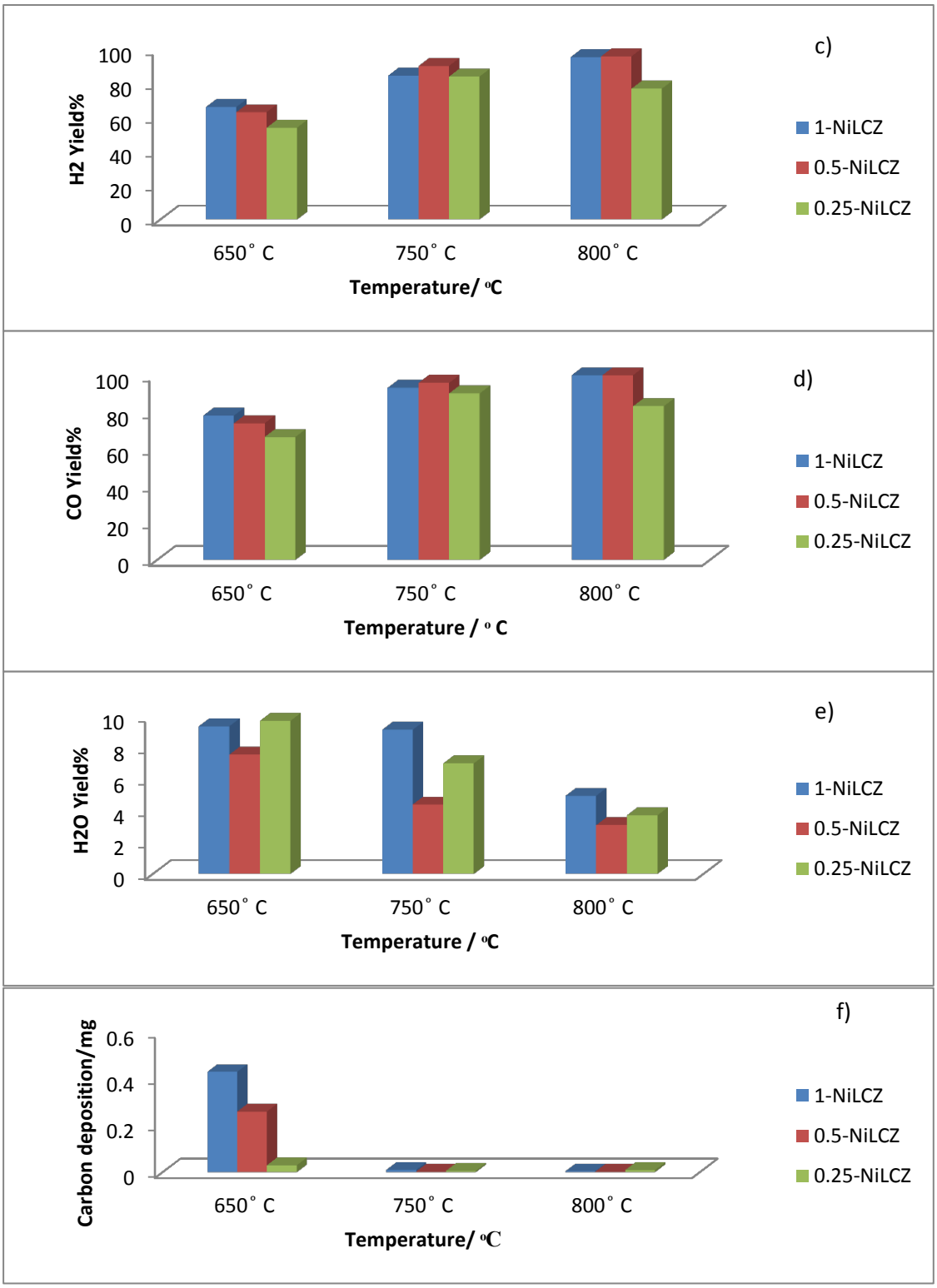

Figure 4-8- Comparison between different Ni loading LCZ at various temperatures during stoichiometric dry reforming condition a) CH_4 conversion b) CO_2 conversion c) H_2 Yield d) CO Yield e) H_2O Yield and f) carbon deposition

4.2 Effect of Pechini preparation method

4.2.1 Temperature programmed dry reforming:-

As can be seen from figure 4- 9, the conversion of reactants began at ~500°C. Because of the reverse water gas shift reaction, the amount of CO was higher than H_2 at temperatures above 500°C.

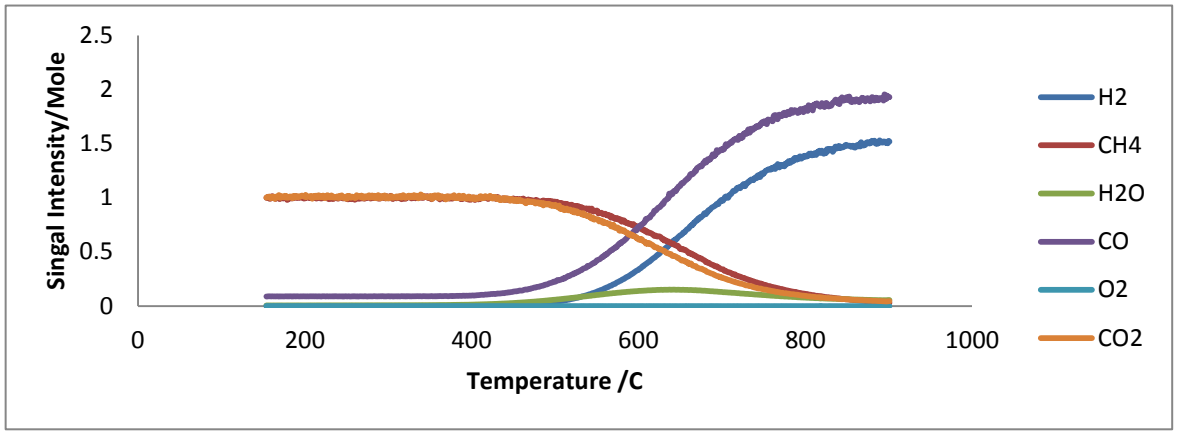

Figure4- 9- Reaction profile for 1:1 CH_4/CO_2 mixture passed over 1-NiLCZ prepared by Pechini method

4.2.2.1 Isothermal dry reforming of methane

As can be seen from figure 4- 10, the lowest level of methane conversion was at 650°C. At this temperature, the conversion decreased from 62% to 52%, which could be because of carbon deposition that blocked the active Ni sites or sintering of Ni. Due to the higher activation energy of CH_4 and the reverse water gas shift reaction, the CO_2 conversion was higher than CH_4 conversion[5]. On increasing the temperature to 750° C and 800° C, a significant increase in methane conversion was seen by 20 and 30% respectively. However, this increase was followed by a 10% reduction in conversion ratio by the end of 20h.

A lower amount of H_2 in comparison with the CH_4 conversion is due to the reverse water gas shift reaction. At 650°C because of the Boudouard reaction, the CO yield was lower than the CO_2 conversion by 10%.

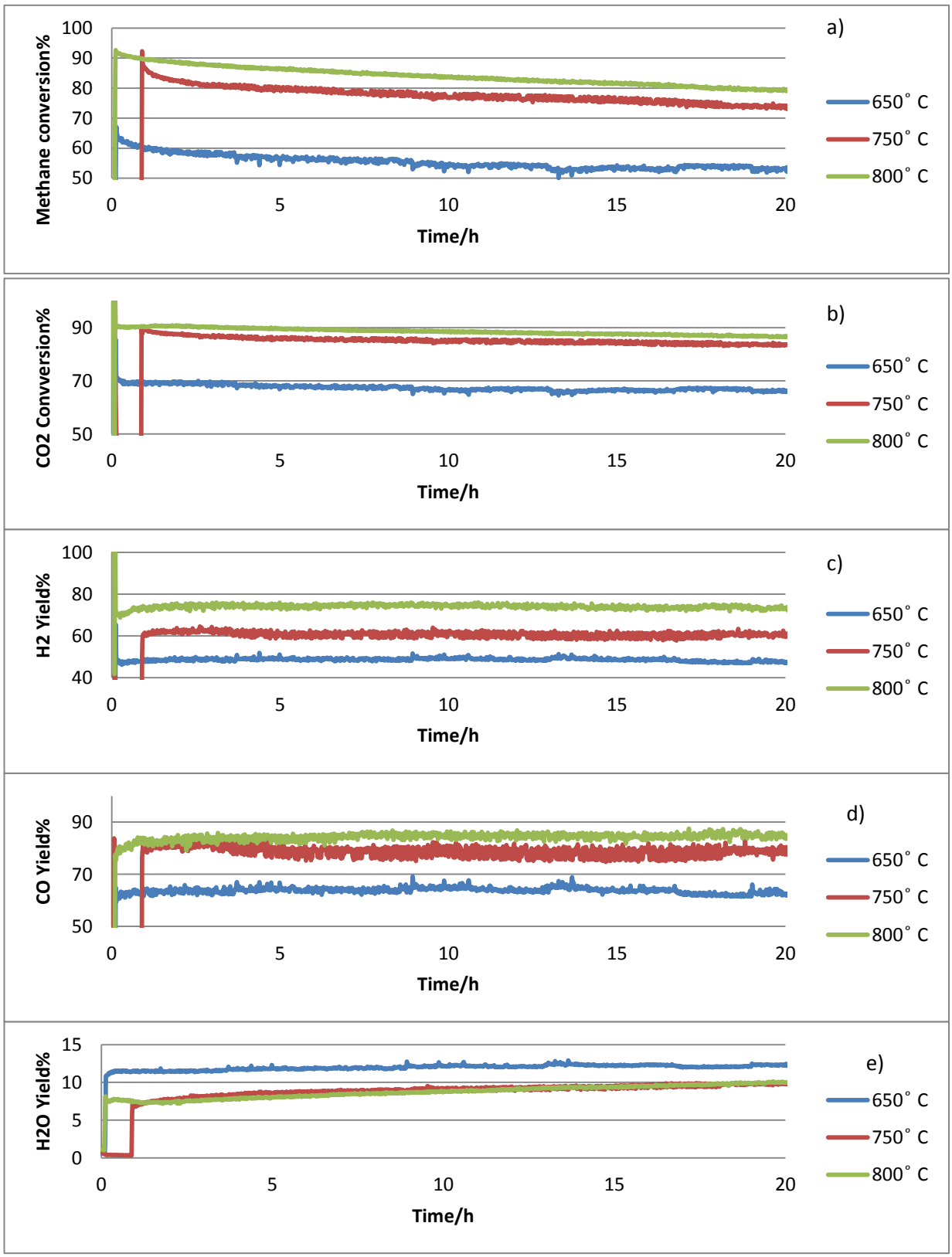

Figure 4- 10- isothermal dry reforming of methane at various temperature over 1Ni-LCZ with CH_4:CO_2 =1:1 a) CH_4 conversion b)CO_2 conversion c) H_2 yield d)CO yield e) water production

4.2.2.2 Carbon deposition:-

The carbon deposition was studied using temperature programmed oxidation (TPO) for the spent catalyst from the dry reforming reaction at various temperatures.

For all conditions, a tiny peak can be seen from figure4- 11, due to carbon which can easily oxidise at around 500°C. Even at 650°C, the amount of carbon is negligible which indicates the catalyst is resistant to carbon deposition.

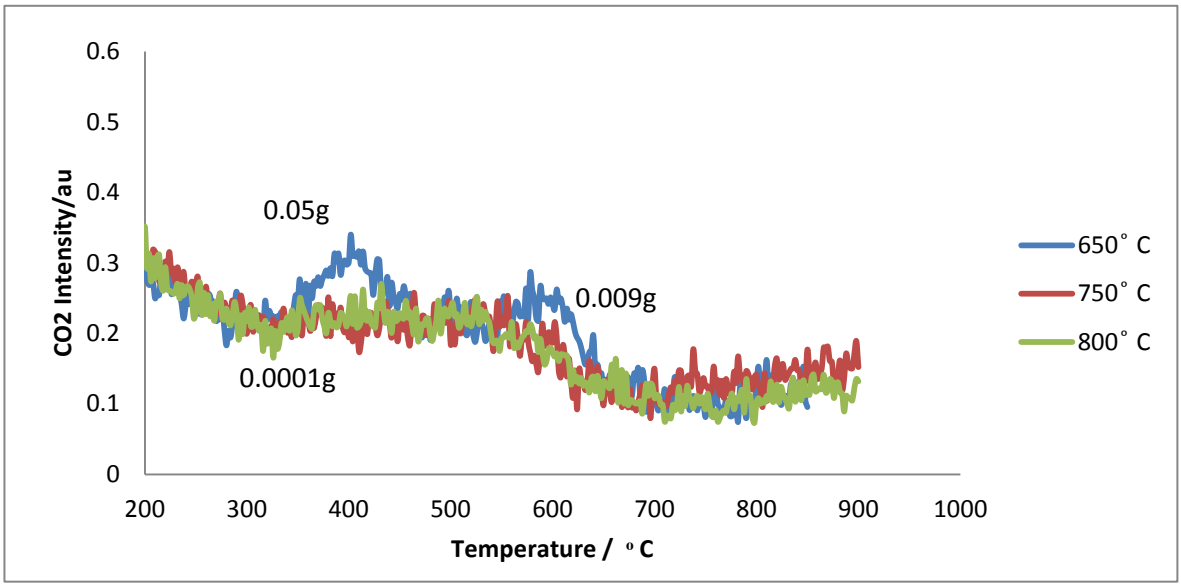

Figure 4- 11-post reaction TPO profiles of isothermal stoichiometric dry reforming over 1-NiLCZ prepared by Pechini method at various temperatures

4.3 Effect of active metal

4.3.1 Temperature programmed dry reforming:-

To study the effect of metal substitution and determine the catalyst light off temperature, a temperature programmed reaction was performed on 0.5Ru-LCZ.

Figure 4- 12 shows the reaction started at around 400°C, and as result of the RWGS reaction, a small amount of H_2O formed over the catalyst and the rate slightly increased at 575°C.

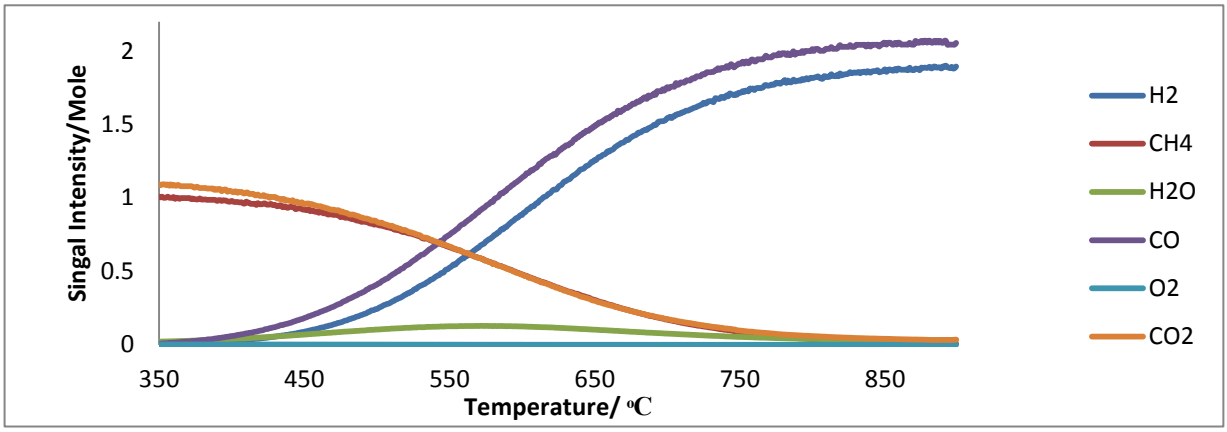

Figure 4-12- Reaction profile for 1:1 CH_4/CO_2 mixture passed over 0.5-RuLCZ catalyst prepared by the hydrothermal method

4.3.2.1 Isothermal dry reforming of methane on 0.5 Ru-LCZ

The effect of temperature and time on stream for 0.5 Ru-LCZ is shown in figure4- 13.

At all three reaction temperatures, high stability in catalyst activity can be seen. By increasing the temperature, the conversion of reactants increased due to the endothermic nature of the DRM reaction. The X_{CH4} at 650°C was about 76%, and with increasing the temperature to 800°C, the conversion increased by 20%. The CO_2 conversion also showed the same trend of methane conversion. However, a higher amount in X_{CO2}, due to the RWGS was noticeable at the lowest temperature. The H_2 yield was significantly lower than CH_4 conversion at 650°C. Therefore, the reverse water gas shift reaction would not be the only reason for this reduction as X_{CO2} did not show much difference in comparison with the CH_4 conversion. The reason could be the reduction of CO at 650°C ($CO+H_2 \leftrightarrow H_2O+C$)

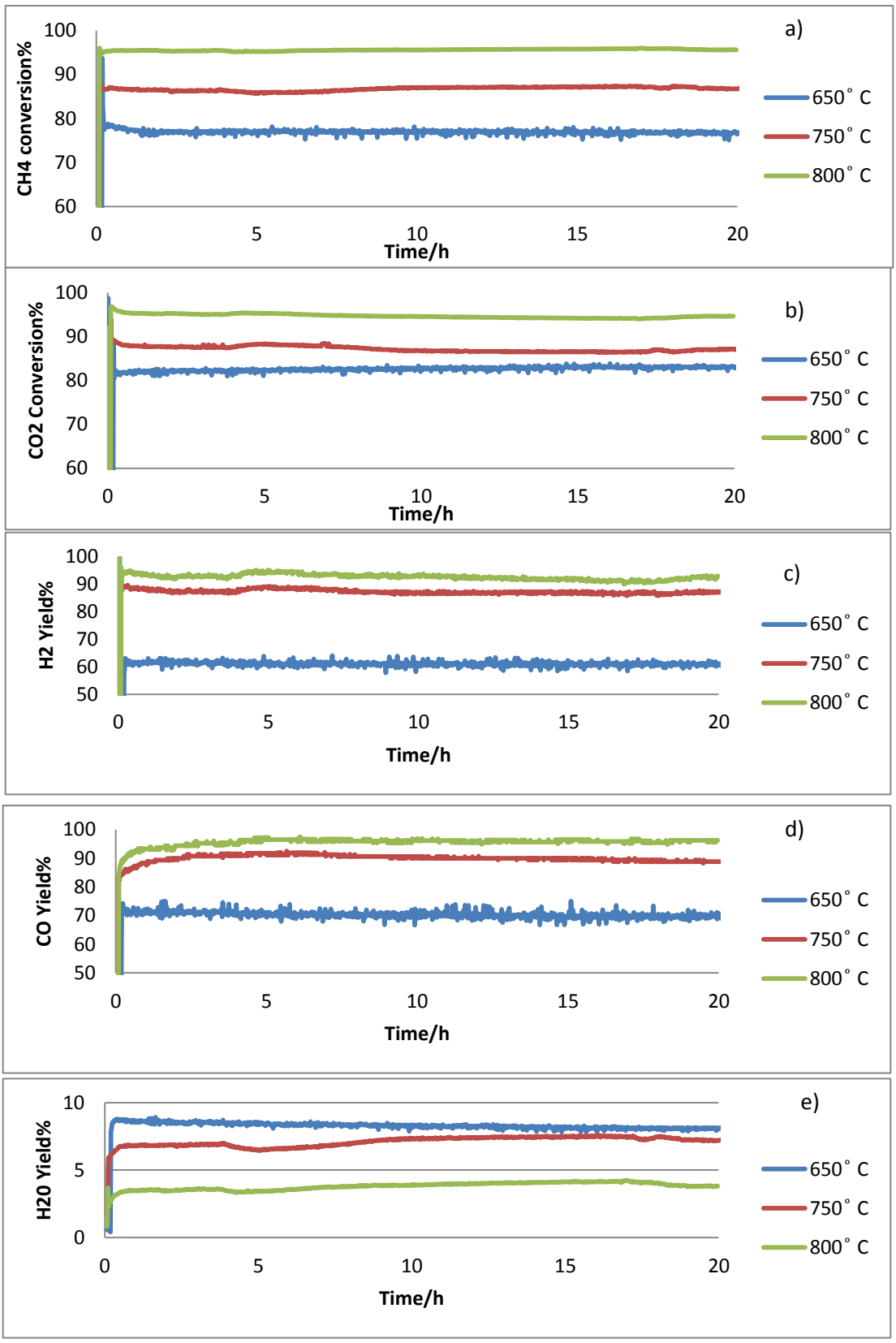

Figure 4- 13- isothermal dry reforming of methane at various temperature over 0.5Ru-LCZ catalyst with CH_4:CO_2 =1:1 a) CH_4 conversion b) CO_2 conversion c) H_2 yield d) CO yield e) water production

4.3.2.2 Carbon deposition:-

The TPO profile of 0.5 Ru-LCZ is shown in figure 4- 14. At the temperature of 650 and 750° C, the amount of carbon deposition was similar and also two peaks were observed at around 300 and 600° C. The presence of the peak at 600° C, can be attributed to the deposition of carbon on the oxide surface of the catalyst, while, a peak at a lower temperature indicates a relatively reactive carbon species which deposited on or near the active Ru sites[9,10]. At a reaction temperature of 800° C, a tiny peak could be seen that was 14 times lower than at 750° C.

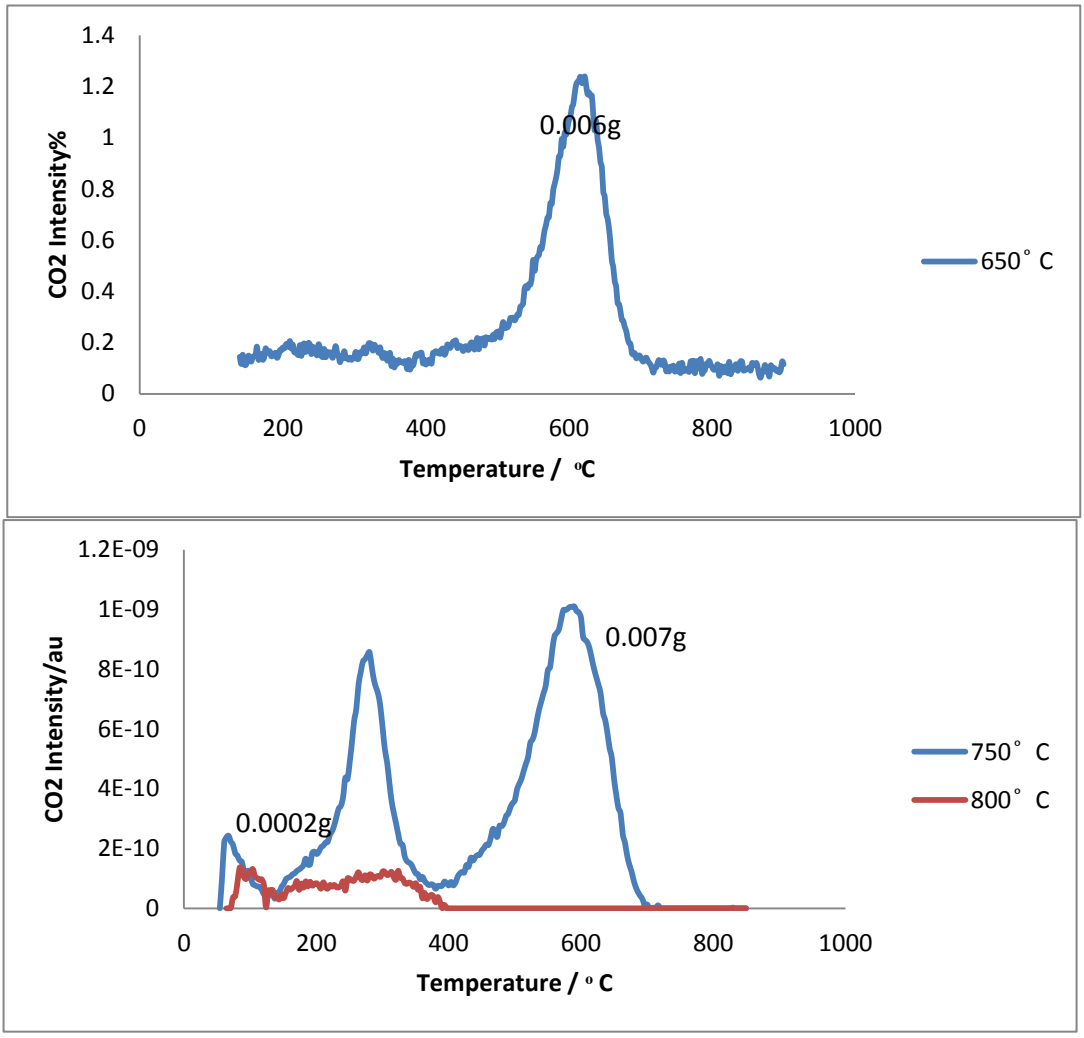

Figure 4- 14-post reaction TPO profiles of isothermal stoichiometric dry reforming over 0.5 Ru-LCZ prepared by Pechini method at various temperatures

4.4 Summary of the effect of preparation method and metal dopant on dry reforming (1:1 CH_4:CO_2)

4.4.1 Methane and carbon dioxide conversion: -

The results of average CH_4 and CO_2 conversion after 20 h at various temperatures during 1:1 CH_4:CO_2 dry reforming for 1Ni-LCZ and 0.5-Ru-LCZ prepared via the hydrothermal and Pechini methods are shown in figure4- 15.

In the case of CH_4 conversion, 1-Ni-LCZ prepared by the Pechini method had the lowest conversion especially at 650° C. In contrast, as Ru catalysts are much more resistance to carbon formation, with 0.5 Ru-LCZ showing more conversion by 20%. Interestingly, by changing the preparation method to the hydrothermal method, the conversion increased by 15% in 1-Ni-LCZ.

CO_2 conversion in Pechini method was higher than CH_4 conversion by 12%, whilst in the other two catalysts the difference was only 5%, which indicates that the Pechini method promotes the reverse water gas shift reaction. By increasing the temperature to 750 and 800° C, the difference in conversion between 1-NiLCZ (Pechini) and 0.5 Ru-LCZ decreased to 12%, while, with 1Ni-LCZ (HY) the difference was 3%.

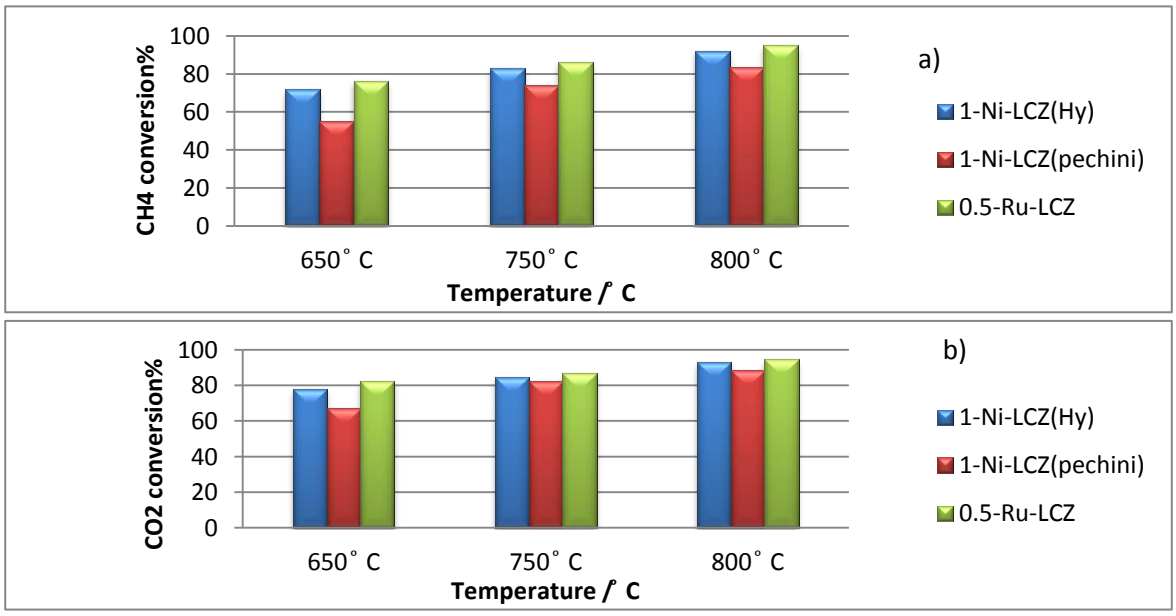

Figure 4- 15-Average a) methane and b) carbon dioxide conversion for various catalysts at different temperatures for 1:1 CH_4:CO_2 dry reforming reaction

4.4.2 Product selectivity

In comparison with the CH_4 and CO_2 conversion, 0.5Ru-LCZ had the higher reduction in H_2 and CO yield by 16 and 12% respectively. The syngas yield in 1-Ni-LCZ (HY) was in a good agreement with CH_4 and CO_2 conversion, and only a 6% reduction in H_2 yield was seen and this was similar for 1-Ni-LCZ (Pechini). The decrease in syngas yield in 0.5Ru-LCZ at 650°C could be due to the methane coupling, CO reduction reaction ($CO+H_2 \leftrightarrow H_2O+C$) and combining Boudouard and RWGS reaction. By increasing the temperature, 1-Ni-LCZ (Pechini) showed the same behaviour as 0.5Ru-LCZ at 650°C. The Ni catalyst prepared by the hydrothermal method only shows common side Boudouard reaction and reverse water gas shift reaction at the low temperature and at 800° C only the reverse Boudouard reaction occurred.

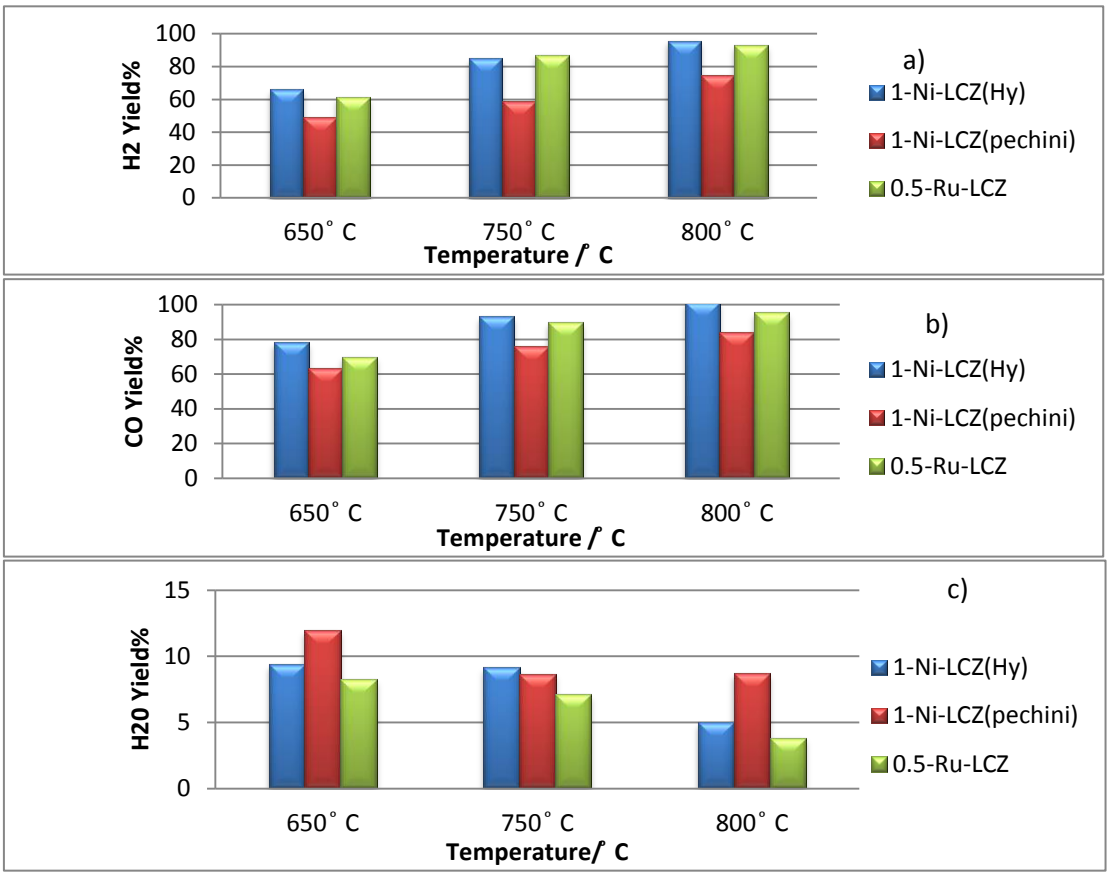

Figure 4-16-Average a) H2, b) CO and c) H_2O selectivity for various catalysts at different temperatures for 1:1 CH_4:CO_2 dry reforming reaction

4.4.3 Carbon deposition:-

As can be seen from figure 4- 17, a significant amount of carbon was deposited on 1Ni-LCZ prepared by the hydrothermal method. The Ru catalyst, as was expected showed the lowest level of carbon deposition and even at 650° C, the deposited carbon can be considered negligible. By increasing the temperature to 750° C, the level of carbon decreased dramatically over 1Ni-LCZ (Hy) and showed some similarity with other catalysts. At 800° C, all three catalysts did not show any noticeable carbon from their TPO profile.

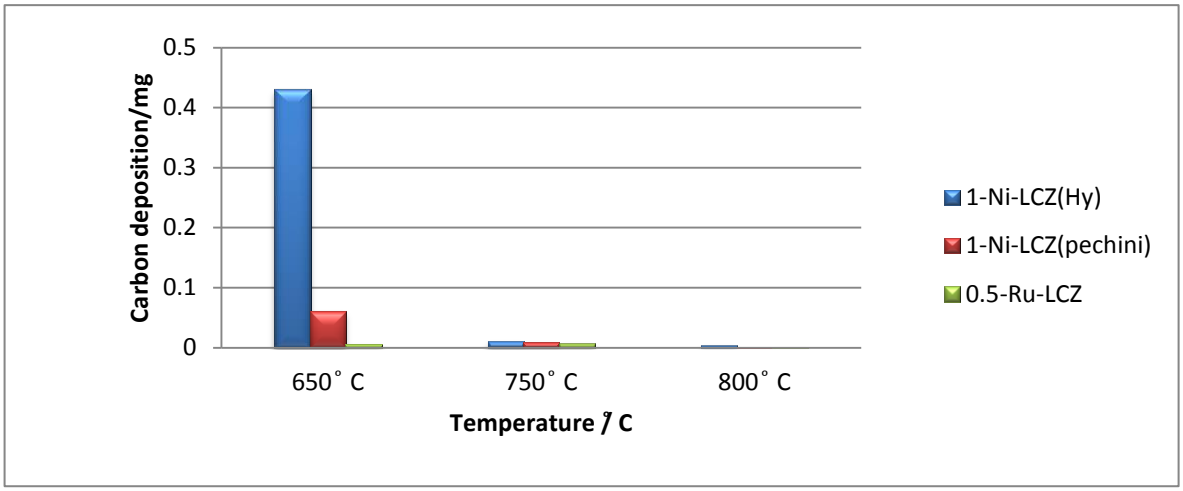

Figure 4-17-carbon deposition for various catalysts at different temperatures during 1:1 CH_4:CO_2 dry reforming reaction

4.5 Conclusions:-

The profile for temperature programmed reaction of DRM for different Ni loading on the LCZ catalyst prepared by the hydrothermal method was almost identical. The profile showed the DRM reaction began at~450℃ and CH_4 and CO_2 were fully consumed by 750℃. For the Ni containing catalyst that prepared by the Pechini method, although the reaction started at the same temperature, the ratio of H_2/CO showed a significant decrease with temperature due to the reverse water gas shift reaction and the reverse Boudouard reaction. The starting temperature point for the Ru catalyst was lower by 50℃ in comparison with other catalysts.

The isothermal study at 650℃ showed that, the 0.5NiLCZ had the highest CH_4 conversion than 0.25 and 1-NiLCZ which was attributed to the lower amount of active sites in 0.25-NiLCZ and the higher amount of deposited carbon on 1-Ni-LCZ,. At this temperature the Ni catalyst prepared by the Pechini method showed the lowest activity and the Ru containing catalyst had the highest activity. At this temperature, due to the higher activation energy of CH_4 and the reverse water gas shift reaction, CH4 conversion was lower than the CO_2 conversion for all the catalysts.

The highest level of deposited carbon on all catalysts was at 650℃, and therefore this kind of catalyst is affected by the Boudouard reaction and CO reduction. It can also be seen that the amount of Ni played significant role in carbon deposition and as was discussed in section 4.1.3, the highest level of carbon was on 1-NiLCZ which reduced the catalyst activity. Although, the 1-Ni-LCZ catalyst prepared by the Pechini method had significant lower amount of carbon deposition than 1-NiLCZ(Hy), its activity was not as good as the hydrothermal method which could be due to the loss of surface area, sintering or a poisoning mechanism[11-13.] Among all the catalysts, the Ru catalyst showed the lowest carbon deposition at 650 ℃.

The activity of all catalysts increased when temperature is increased from 650 ^{o}C to 750℃, which agrees with the endothermic nature of the reactions. However, the Ni containing catalyst prepared by the Pechini method still had the lowest reactants conversion and products selectivity and even at 800℃ showed higher water formation.

The amount of carbon deposition decreased dramatically at the temperatures of 750 and 800℃ for all Ni containing catalysts and was neglible for the Ru containing catalyst.

4.6 References:-

1-He, X. and Liu, L., 2017, December. Thermodynamic analysis on the CO2 conversion processes of methane dry reforming for hydrogen production and CO2 hydrogenation to dimethyl ether. In *IOP Conference Series: Earth and Environmental Science* (Vol. 100, No. 1, p. 012078). IOP Publishing.

2-Kumar, N., Wang, Z., Kanitkar, S. and Spivey, J.J., 2016. Methane reforming over Ni-based pyrochlore catalyst: deactivation studies for different reactions. *Applied Petrochemical Research*, *6*(3), pp.201-207.

3-Kumar, N., Shojaee, M. and Spivey, J.J., 2015. Catalytic bi-reforming of methane: from greenhouse gases to syngas. *Current opinion in chemical engineering*, *9*, pp.8-15.

4-Trimm, D.L., 1997. Coke formation and minimisation during steam reforming reactions. *Catalysis Today*, *37*(3), pp.233-238.

5-Le Saché, E., Pastor-Pérez, L., Watson, D., Sepúlveda-Escribano, A. and Reina, T.R., 2018. Ni stabilised on inorganic complex structures: superior catalysts for chemical CO2 recycling via dry reforming of methane. *Applied Catalysis B: Environmental*, *236*, pp.458-465.

6-Lavoie, J.M., 2014. Review on dry reforming of methane, a potentially more environmentally-friendly approach to the increasing natural gas exploitation. *Frontiers in chemistry*, *2*, p.81.

7-Sugiura, K., Ogo, S., Iwasaki, K., Yabe, T. and Sekine, Y., 2016. Low-temperature catalytic oxidative coupling of methane in an electric field over a Ce–W–O catalyst system. *Scientific reports*, *6*, p.25154.

8-Gaur, S., 2011. Dry reforming of methane on rhodium and nickel substituted pyrochlore catalysts.

9- Haynes, D.J., Campos, A., Berry, D.A., Shekhawat, D., Roy, A. and Spivey, J.J., 2010. Catalytic partial oxidation of a diesel surrogate fuel using an Ru-substituted pyrochlore. *Catalysis Today*, *155*(1-2), pp.84-91.

10- Haynes, D.J., Berry, D.A., Shekhawat, D. and Spivey, J.J., 2008. Catalytic partial oxidation of n-tetradecane using pyrochlores: effect of Rh and Sr substitution. *Catalysis Today*, *136*(3-4), pp.206-213.

11- Sehested, J., Gelten, J.A., Remediakis, I.N., Bengaard, H. and Nørskov, J.K., 2004. Sintering of nickel steam-reforming catalysts: effects of temperature and steam and hydrogen pressures. *Journal of Catalysis*, *223*(2), pp.432-443.

12- Sehested, J., 2006. Four challenges for nickel steam-reforming catalysts. *Catalysis Today*, *111*(1-2), pp.103-110.

13- Forzatti, P. and Lietti, L., 1999. Catalyst deactivation. *Catalysis today*, *52*(2-3), pp.165-181.

5 The effect of adding H_2S to simulate biogas on reforming activity and catalyst performance

5-1ntroduction:

Sulphur compounds are common impurities in natural gas; therefore, a sulphur resistant catalyst is required to avoid catalyst poisoning and to reduce the cost of any desulphurization stage of the reforming process. The toxicity of sulphur compounds to catalysts decreases in the order of H_2S, SO_2, and SO_3.

As ppb levels of H_2S can inhibit the catalyst activity, an important characteristic of the catalyst is its capacity to adsorb sulphur, in addition to having a certain degree of regeneration. Various variables such as sulphur composition, the composition of the catalyst and operating conditions determine sulphur toxicity.[1]

5-1-1 Sulphur chemisorption on nickel

Group 8 metal catalysts are susceptible to sulphur poisoning due to the availability of a number of electron pairs for bonding. Nickel is more sensitive to sulphide formation than other group eight metals[2]. Three factors that influence the degree of sulphur poisoning of a metal and ease of their regeneration are the nature of the metal, the sulphur-metal and sulphur –support interactions that can be influenced by preparation method[3].

Sulphur compounds can decrease the activity of a Ni-based catalyst due to: 1 strong sulphur chemisorption on active sites of catalyst to form metal sulphides which prevent reactant molecules adsorption via eq (1)

$H_2S + Ni \leftrightarrow Ni\text{-}S + H_2$……eq (1)

2 modify the chemical nature of the active sites or generate new compounds that may decrease the catalyst activity[4]. Nickel can hold sulphur until saturation[2]. At a high ratio of

H_2S/H_2, bulk sulphides are generated while at a low ratio only surface nickel sulphides can be formed. Ni_3S_2 is the most common Ni-S species that has been reported in the literature[6]. The temperature of the reaction, gas phase composition and reactor parameters can influence the formation of Ni-S species[5].

Deactivation and regeneration of several Ni-based catalysts including $Ni/ZrO_2Al_2O_3$, $Ni/CeO_2Al_2O_3$, $Ni/CeO_2/ZrO_2$ Al_2O_3 and $Rh-Ni/CeO_2$ $/Al_2O_3$ under tri-reforming reaction were investigated by Urko et al . Their study showed that when 25 ppm of H_2S was continuously added to the system at 800°C, quick deactivation and no catalyst regeneration after both self-regeneration and regeneration by oxidation process occurred in the case of $Ni/ZrO_2/$ Al_2O_3. Both Ce catalysts recovered most of their initial activity and even give higher activity than before the sulphur poisoning stage after regeneration via oxidation due to the structural modification. Rh-Ni/Ce-Zr Al_2O_3 showed higher resistance to deactivation, and it was the only catalyst which showed activity with 30% yield in the presence of 25ppm H_2S. The study suggests that focussing on the use of different support and reforming metals can help resist sulphur poisoning.[7]

5-1-2 The effect of ceria on sulphur tolerance of catalyst

It is fair to say that the discovery of the redox properties of ceria and doped Ceria's has revolutionized both catalysis and SOFC science, especially given the oxide ion and electronic conductivity of doped ceria. Ceria by acting as a store for oxygen can react with carbon and sulphur species and improve sulphur tolerence[8].

The reduced form of ceria is more reactive toward sulphur compounds than the stoichiometric form. The reaction of reduced form with H_2S is shown in (eq 2).

$Ce_2O_3 + H_2S \leftrightarrow Ce_2O_2S + H_2O$……eq 2

Oxysulphate compounds in low concentration (<100ppm) react poorly and have less reforming activity than ceria[9,10]. Ceria by delaying nickel sulphide formation improve sulphur tolerance of the catalyst [11,12]. As CO_2 concentration in dry reforming influences the ceria oxidation state (eq3), the different form of ceria will have significant effect toward sulphur poisoning.[11,13]

$Ce_2O_3 + CO_2 \leftrightarrow 2CeO_2 + CO$……eq 3

The influence of CeO_2 doping on commercial nickel catalyst (Ni/YSZ) under dry reforming condition in the presence of H_2S was investigated by Laycock et al. [14]

Due to the recent advancement in perovskites materials as a reforming catalyst, Evans investigated a 4 mole% Ni doped $SrZrO_3$ and compared its performance with doped and undoped ceria (Ni/YSZ). The perovskite showed higher resistance to sulphur poisoning than the nickel cermet materials which was attributed to the structure of the perovskite which meant sulphur faced difficulty to bond with the nickel ion.[15]

As the behaviour of pyrochlores as excellent methane dry reforming catalysts in the presence of H_2S is unknown, this part of the study focussed on looking at the influence of H_2S poisoning on these new pyrochlores at various temperatures and H_2S concentrations.

5.2 The influence of temperature on the hydrothermal Ni-LCZ pyrochlore catalyst

5.2.1.1 0.25 NiLCZ pyrochlore catalysts:

To study the effect of temperature on poisoning, the reactions were performed at variable temperature in the range of 700-1000 ^{o}C and in the presence of 30 ppm H_2S during dry

reforming of 2:1 CH_4: CO_2. Figures 5-1 to 5-5 show the behaviour and the percentage amount of each reactant and produced gases as a result of the dry reforming reaction.

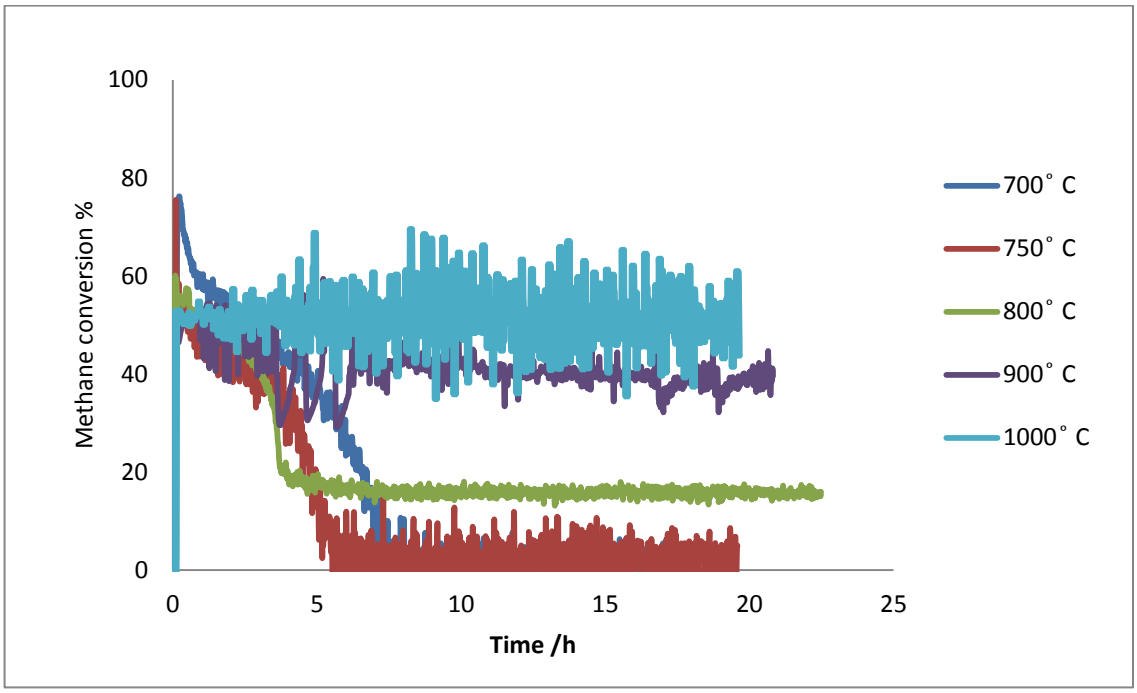

Fig 5-1 percentage of methane conversion at different temperatures during methane-rich dry reforming over 0.25Ni-LCZ in presence of 30 ppm H_2S

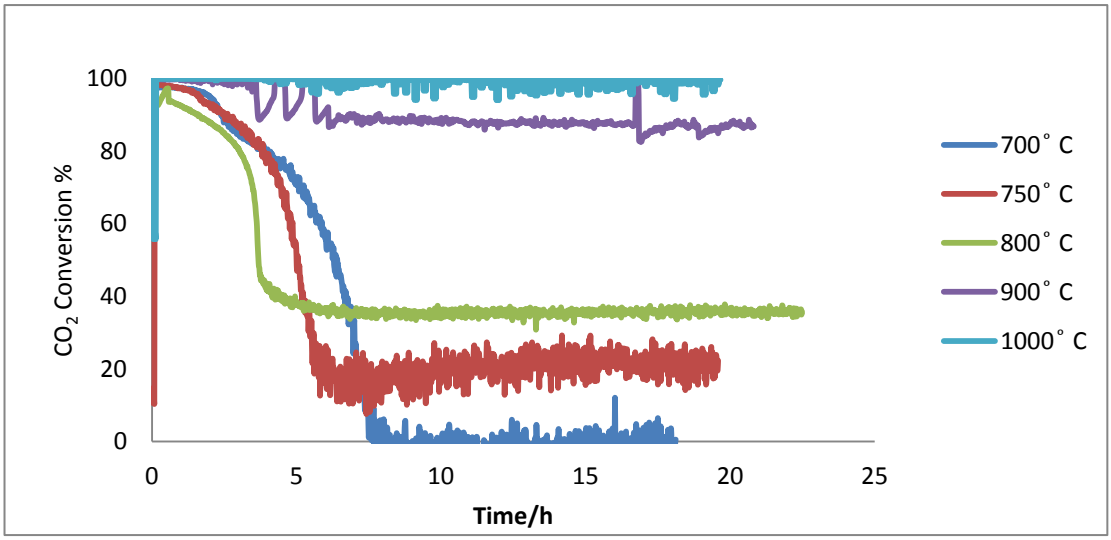

Fig 5-2 percentage of carbon dioxide conversion at different temperatures for methane-rich dry reforming over 0.25NI-LCZ in the presence of 30 ppm H_2S

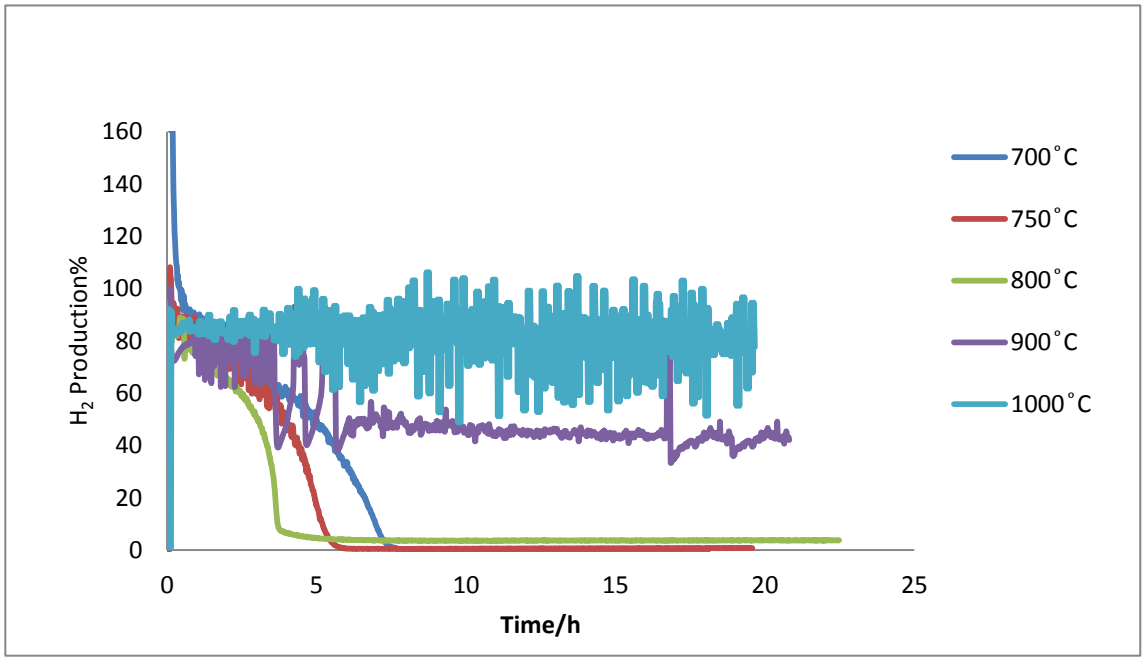

Fig 5-3 percentage of hydrogen yield at different temperatures of methane-rich dry reforming over 0.25Ni-LCZ in presence of 30 ppm H_2S

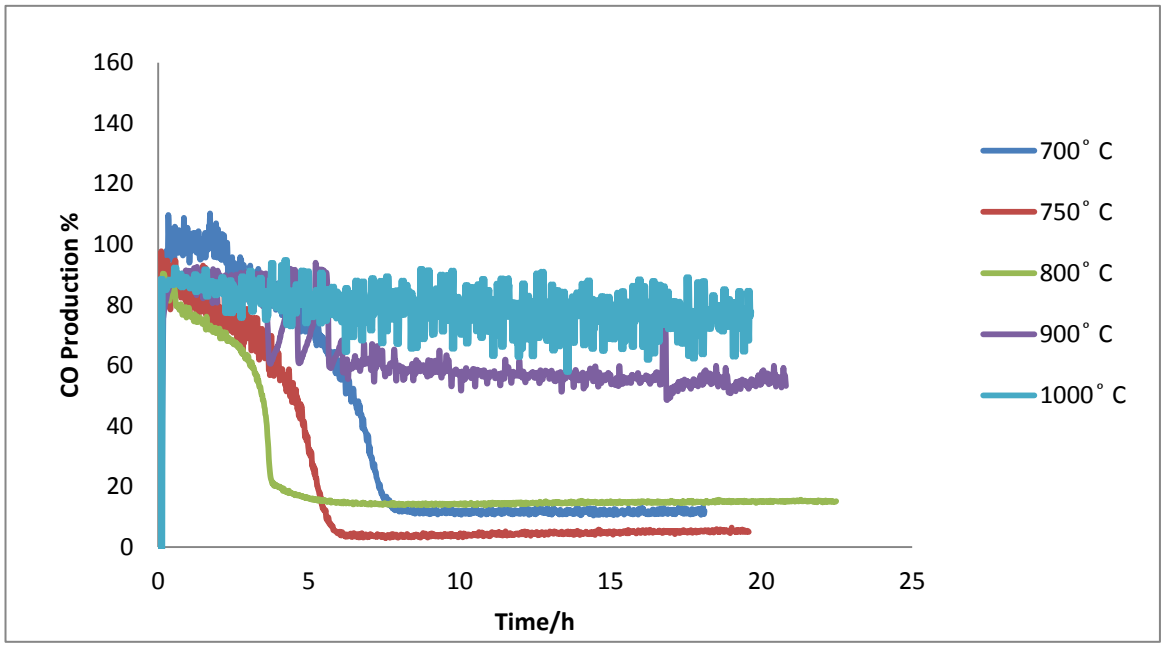

Fig 5-4 percentage of carbon monoxide yield at different temperatures of methane-rich dry reforming over 0.25Ni-LCZ in presence of 30 ppm H_2S

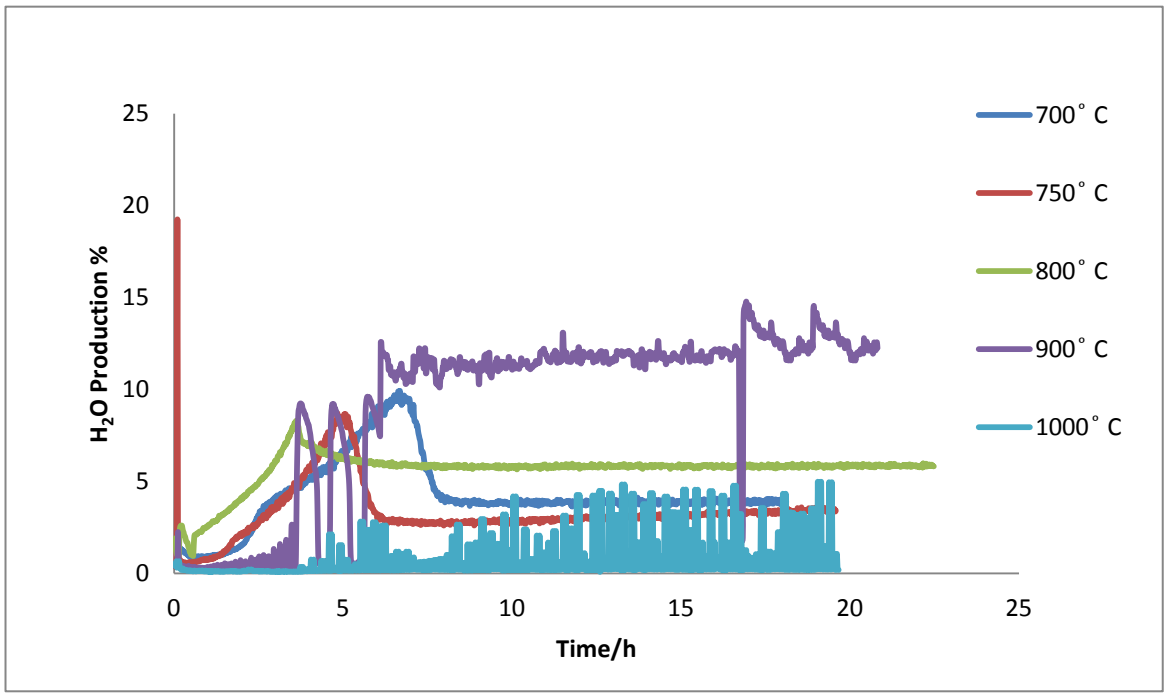

Fig 5-5 percentage of H_2O production at different temperatures of methane-rich dry reforming over 0.25Ni-LCZ in the presence of 30 ppm H_2S

At 700°C, the amount of CH_4 was at the highest level of conversion in the first 2-3h of the reaction and this amount decreased sharply resulting in complete loss of reforming activity after 7 hours. The amount of CO_2 conversion also showed the same CH_4 conversion trend. It was interesting to see water and carbon monoxide despite the absence of H_2 and CO_2 at the end of reaction.

At this temperature reaction, the deactivation occurred in two steps. The deactivation in the first region from 3 to 7h is because of the dissociative chemisorption of H_2S on active nickel sites, which at lower temperature becomes more favourable thermodynamically resulting in more deactivation of the catalytic activity. The second step of deactivation could be because of the reaction approaching steady state behaviour.

On increasing the temperature to 750°C, the same CH_4 conversion profile as at 700°C was seen, but the difference was that the first phase of deactivation happened faster although

the dissociative chemisorption of H_2S is thermodynamically favourable at the lower temperature. In comparison with the temperature of 700 °C, the amount of CO_2 conversion was higher by about 20% and again the presence of water in the absence of H_2 was clear. At 800 °C the amount of CH_4 conversion at the second phase of poisoning increased and remained constant at about 20%. The amount of CO_2 conversion showed a similar trend as for the CH_4 conversion. The presence of water and higher amounts of CO in the absence of H_2 could not be possible because of the water gas shift reaction. By increasing the temperature to higher values; the H_2S poisoning did not show any deactivation. This is because the sulphur adsorption becomes thermodynamically unfavourable at the higher temperatures. It was seen that the reaction at the higher temperatures was associated with a cycling phenomenon. This could be due to continuous oxidation and reduction of Ce and Laycock also found the phenomena of cycling in his study[14], where the catalyst activity increased when CeO_2 reduces to Ce_2O_3 through methane reforming. The activity of the catalyst decreases due to the presence of Ce_2O_3 which is inactive for methane reforming. In the presence of O_2 and CO_2, Ce_2O_3 is reoxidized resulting in an increase in catalyst activity. This process occurs continually over the reaction and the concentration of O_2 and CO_2 influence the cycling as follows:

$Ce_2O_3 + O_2 \leftrightarrow 2CeO_2$……eq 4

$Ce_2O_3 + CO_2 \leftrightarrow 2CeO_2 + CO$……..eq3

At 900 °C a period of fast cycling was seen before the catalyst showed a kind of stability. This suggests that during the lifetime of the reaction, the rate of H_2S adsorption is slightly less than the rate of desorption. Stable reforming reaction with no loss of activity was seen at 1000 °C.

The observations that can be concluded from the reforming profile of 0.25 NiLCZ are as follows: -

1- Two deactivation steps can be observed at temperatures below 900° C. The first deactivation phase accelerates with increasing reaction temperature. The reason behind this acceleration could be because of the formation of different forms of bulk nickel sulphide species where one sulphur atom can bind to four atoms of Ni (Ni_4S) and by decreasing the temperature this ability may decrease and each Ni atom will be bound by one atom of sulphur (Ni_6S_6), Therefore, the lifetime of deactivation in the first phase increases by decreasing the temperature despite the dissociative chemisorption of H_2S being more favourable at the lower temperatures.

2- the gradual increase in the rate of water formation in the first phase of deactivation is followed by a decrease because of the following reaction:

1) $H_2S + Ni \leftrightarrow H_2 + NiS$……eq1

2) $2CeO_2 \leftrightarrow Ce_2O_3 + 1/2O_2$…..... eq4

3) $H_2 + 1/2O_2 \leftrightarrow H_2O$…….....eq5

3- the presence of water at the second phase despite the absence of H_2 and an increase in the amount of water with temperature may suggest the following:

$Ce_2O_3 + H_2S \leftrightarrow Ce_2O_2S + H_2O$ ……. eq2

4- the reasons for the increasing amount of CO_2 conversion at 750° C despite the absence of methane conversion and the decrease in the amount of H_2O and CO in comparison with the temperature of 700° C may be due to the following reactions:

$H_2S + CO_2 \leftrightarrow H_2O + 1/2S_2 + CO$……. eq 6

$CO + H_2O \leftrightarrow H_2 + CO_2$……eq7

5- The reason for the increase in cycling behaviour at 900° C is due to: -

$Ce_2O_3 + H_2S \leftrightarrow Ce_2O_2S + H_2O$ ……. eq2

$Ce_2O_3 + O_2 \leftrightarrow 2CeO_2$……... eq4

5.2.1.2 Carbon deposition: -

The amount of carbon deposition was determined by temperature programmed oxidation (TPO) and the results were compared and are shown in fig 5- 6.

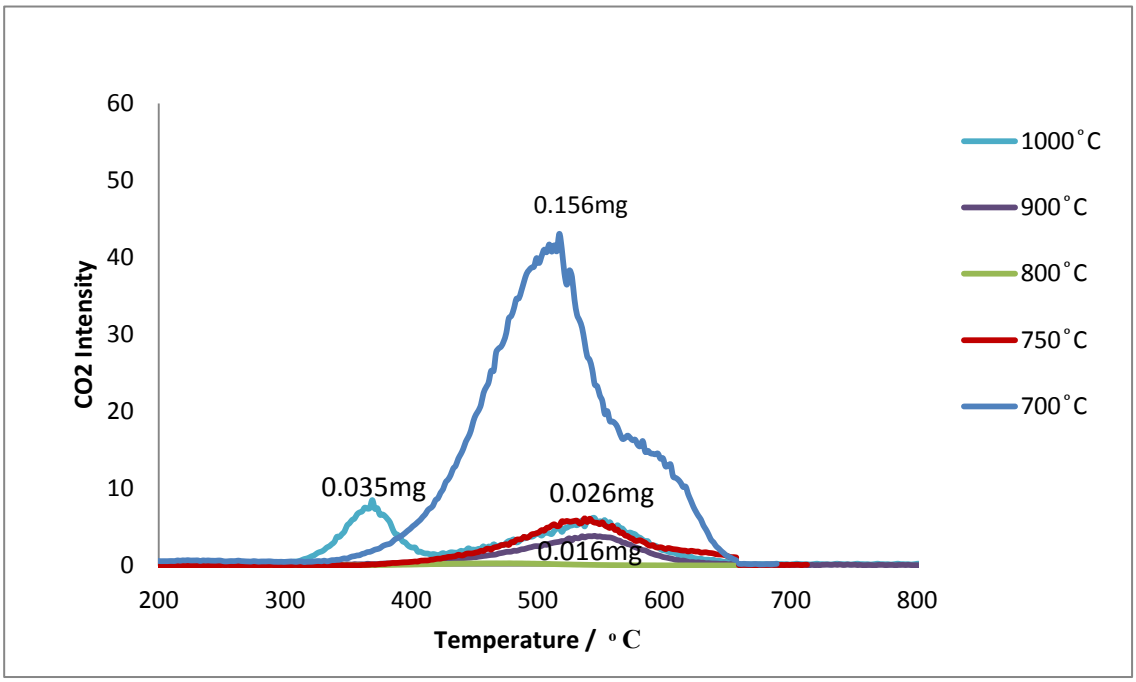

Fig 5-6- TPO profile at different temperature of methane-rich dry reforming over 0.25NI-LCZ in presence of 30 ppm H_2S

As seen from fig 5-6, the highest amount of carbon was decomposed at 700° C. At this temperature, and as was seen from CO yield profile in the previous section, the amount of CO was very high, and CO can convert to CO_2 and carbon by the Boudouard reaction.

$2CO \leftrightarrow CO_2 + C$…….eq8

This reaction is thermodynamically favoured at lower temperatures. The carbon deposition profile for the other temperatures showed no significant differences in the amount. At 1000° C, another carbon peak was observed, and this is because of the presence of several kinds of carbon that decomposed on several parts of the catalyst.

5.2.2.1 1- NI-LCZ pyrochlore catalyst (higher Ni doped):

1-Ni-LCZ pyrochlore catalyst that has the higher amount of Ni, showed a longer stability during the first region against H_2S poisoning. This longer stability was because more active sites were present on the catalyst and thus more time is needed to poison. Al the results are shown in fig 5-7 to11.

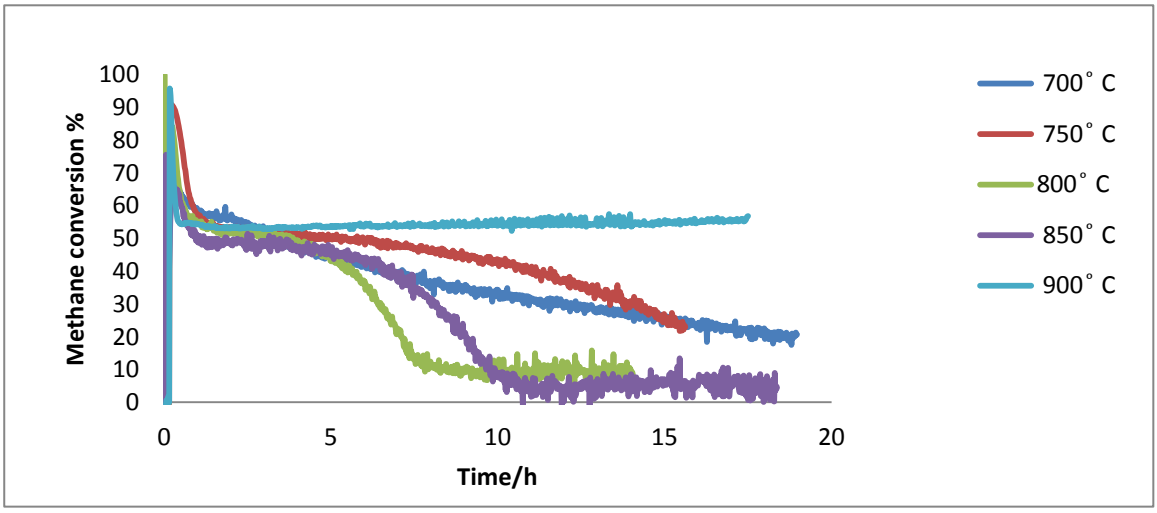

Fig 5- 7- percentage of methane conversion at different temperature methane rich dry reforming over 1-Ni-LCZ in presence of 30ppm H_2S

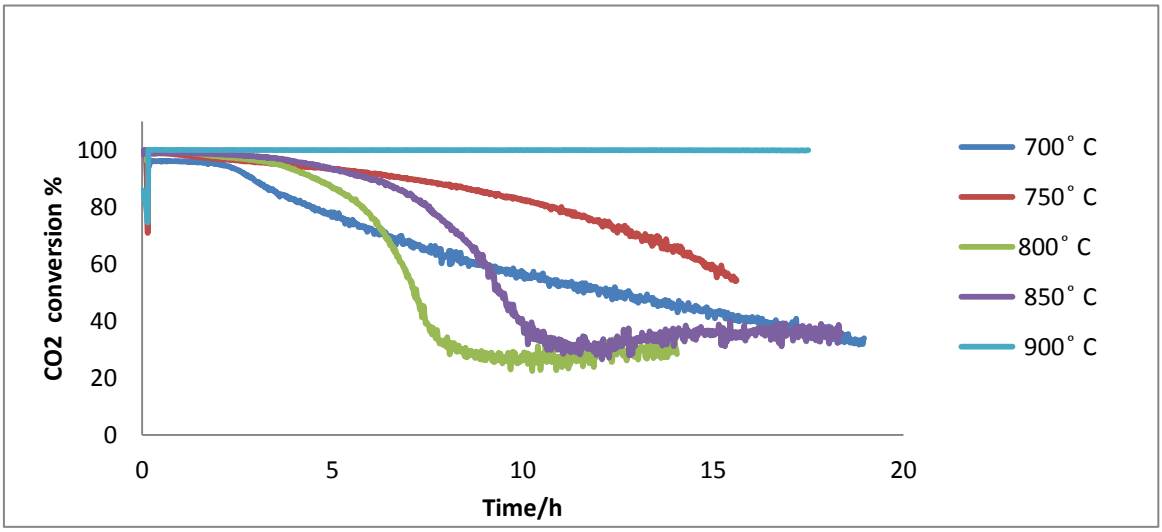

Fig 5- 8- percentage CO_2 conversion at different temperature of methane-rich dry reforming over 1-Ni-LCZ in presence of 30ppm H_2S

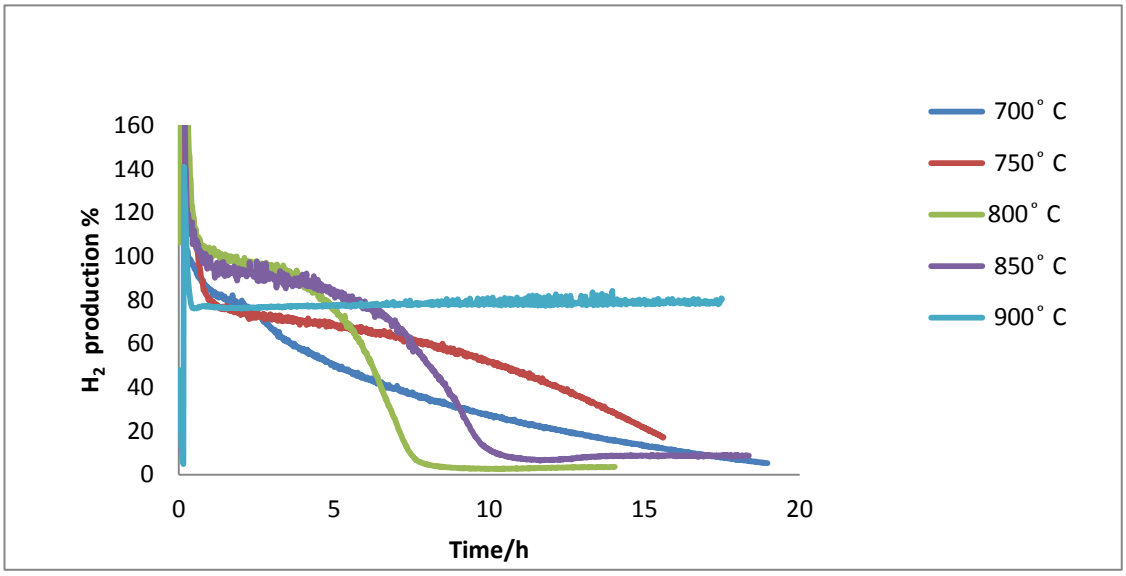

Fig 5-9- percentage of hydrogen yield at different temperature of methane-rich dry reforming over 1-Ni-LCZ in presence of 30ppm H_2S

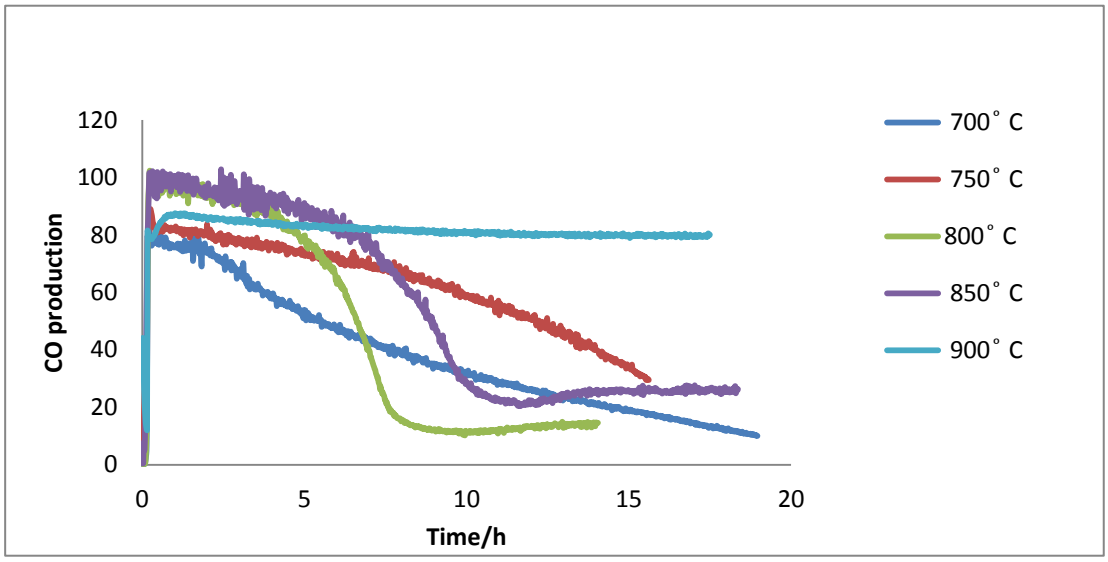

Fig 5-10- percentage of Carbon monoxide yield at different temperature of methane-rich dry reforming over 1-Ni-LCZ in presence of 30ppm H_2S

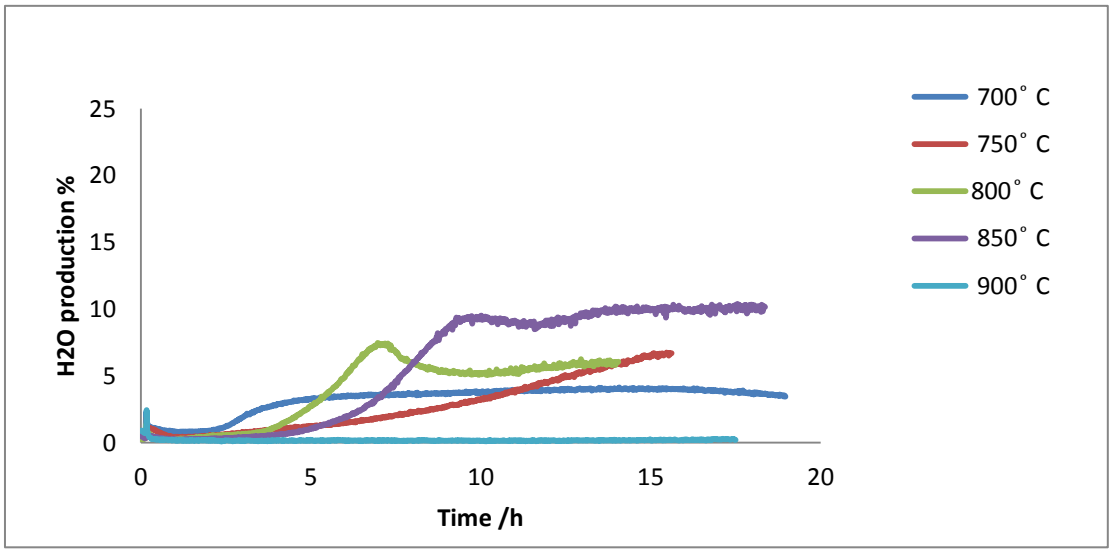

Fig 5-11- percentage of H_2O production at different temperature of methane-rich dry reforming over 1-Ni-LCZ in presence of 30ppm H_2S

At 700° C, the amount of methane conversion was at its equilibrium ratio for 2h before showing a gradual decrease in its conversion activity. The catalyst lost 30% of its activity and the ratio of CH_4 conversion was 20% at the end time of reaction. At this temperature, CO_2 conversion, H_2 and carbon monoxide yield also showed the same trend with no secondary deactivation step. It was expected from the dry reforming reaction that the amount of H_2 and CO would be twice the amount of CH_4 and CO_2, but at this temperature, the amount of CO and H_2 were lower than the CH_4 and CO_2 conversions at the end of 20h of reaction. The reason suggested is because of the CO reduction reaction:

$CO + H_2 \rightarrow C + H_2O$……eq9

that is thermodynamically favoured at the lower temperature and the existence of water in the reforming reaction can confirm this suggestion. When the poisoning temperature was increased to 750° C, the stability in CH_4 conversion extended to 10 hours. After this 10h the rate of conversion dropped faster in comparison with that at 700° C. The amount of CO_2 conversion at 750° C was in good relationship with CH_4 conversion unlike the amount

of H_2 and CO, which were lower, and the reason could be because of the CO reduction reaction. As was seen from the beginning of the reaction at 700 ^{o}C, the amount of CO was lower by 20% than expected and this decrease in the amount of CO is because of the Boudouard reaction

The secondary phase of poisoning was clear at 800^{o} C. At this temperature, the catalyst showed steady conversion for around 7h before a steep decrease in the CH_4 conversion. The percentage CH_4 conversion remained at an average of 10% and cycling was seen after 10h of reforming reaction and this could be due to desorption-adsorption of H_2S. As can been seen from the percentage of H_2O and the amount of CO in the secondary phase of poisoning, the amount of H_2O and CO_2 conversion was increasing despite the absence of H_2 and CH_4 conversion. The reason could be due to the reaction of ceria and carbon dioxide with H_2S , as was seen from equations 2 and 6.

Dissociative chemisorption of H_2S becomes less favourable when the temperature increases and at 850^{o} C the first phase of deactivation occurred at a slower rate in comparison with 800^{o}C. A similar profile of H_2, CO and CO_2 was seen at 800^{o}C and a high level of stability can be seen at 900^{o}C. The ratio of CH_4 conversion showed some low cycling behaviour after 10 h of poisoning because of adsorption-desorption or redox properties of cerium. The CO_2 conversion also showed the same trend of stability and it was in good relationship with CH_4 conversion. Methane decomposition at this temperature was impossible as the amount of H_2 did not increase. As the amount of CO was at the same level as H_2 and less than expected by 20 %, this may be due to the CO reduction reaction. There was no evidence of H_2O throughout the duration of the reaction compared with other temperatures, which could be because of the presence of ceria in form of Ce_2O_3 at this temperature, which has an essential role to absorb water.

5.2.2.2 Carbon deposition: -

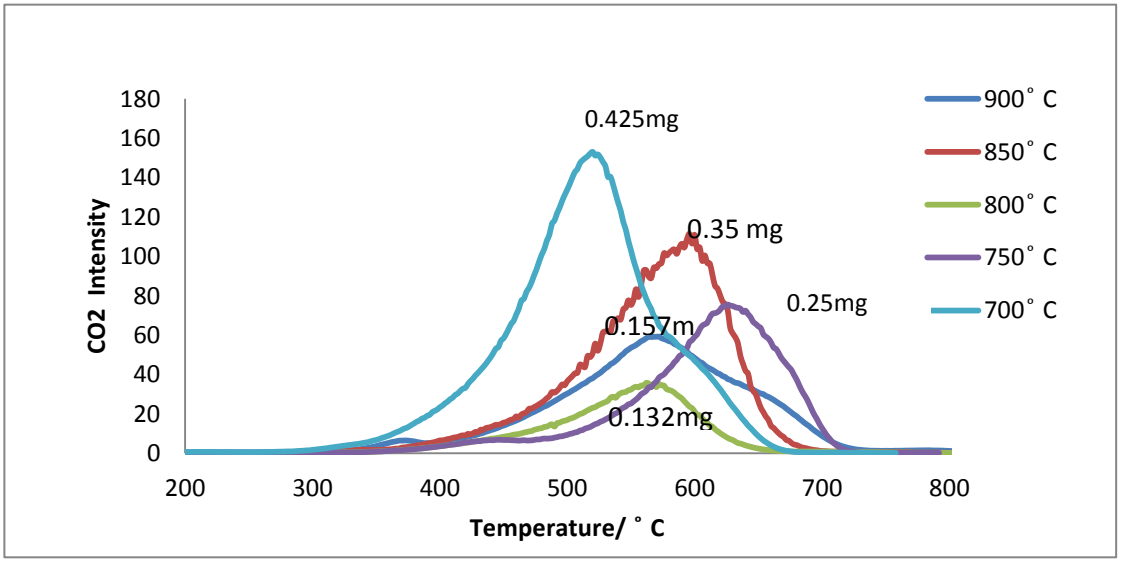

Fig 5-12- TPO profile at different temperatures of methane-rich dry reforming over 1-Ni-LCZ in presence of 30ppm H_2S

As seen in fig 5-12, and because of the Boudouard reaction, the amount of carbon deposition was seen to be at the highest level at 700°C. Overlapping shoulders can see at a temperature of 600°C which could be due to CO reduction , as discussed previously. The second highest level was at 850°C and as can be seen from fig 5-9 the amount of H_2 was at the highest level at the first 2 hours of reaction, and this is likely too due to the methane decomposition or reaction of Ce_2O_3 with CO.

$CH_4 \leftrightarrow 2H_2 + C$ ……..eq10

$Ce_2O_3 + CO \leftrightarrow 2CeO_2 + C$……eq11

At 750°C and 800°C, less carbon deposition was seen in comparison with 700°C and 850°C. The reason is due to the Boudouard reaction and methane decomposition being less favourable thermodynamically at these two temperatures. Due to the CO reduction reaction eq (9) accuring at 750°C, the amount of carbon deposition was higher than 800°C. Lower amounts of carbon deposition were seen at 900° C; despite the methane decomposition being more favourable at higher temperatures. The reason could be because the ceria suppressed the amount of carbon deposition at higher temperature, and this is because of

oxygen storage capacity of ceria and presence of oxidant in the form of CO_2 coming from the reverse water gas shift reaction.

5.3 The influence of H_2S concentration on the hydrothermal Ni-LCZ pyrochlore catalyst

5.3.1.1 The influence of H_2s concentration at 850 ℃

To study the effect of H_2S concentration on the reforming profile, the 1-NiLCZ pyrochlore catalyst was chosen and the reactions were carried out at 850° C at the various H_2S concentrations ranging from 10 ppm to 30 ppm with the results are shown in fig 5- 13 to17.

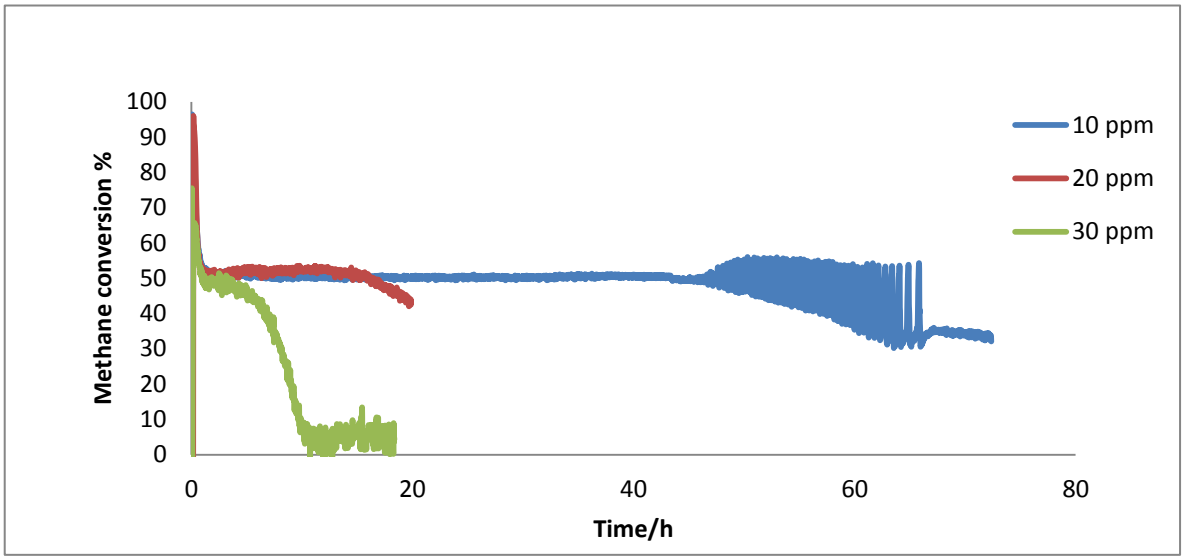

Fig 5-13- methane conversion for 2:1CH_4:CO_2 reforming reaction over 1-NiLCZ at 850°C with different concentrations of H_2S

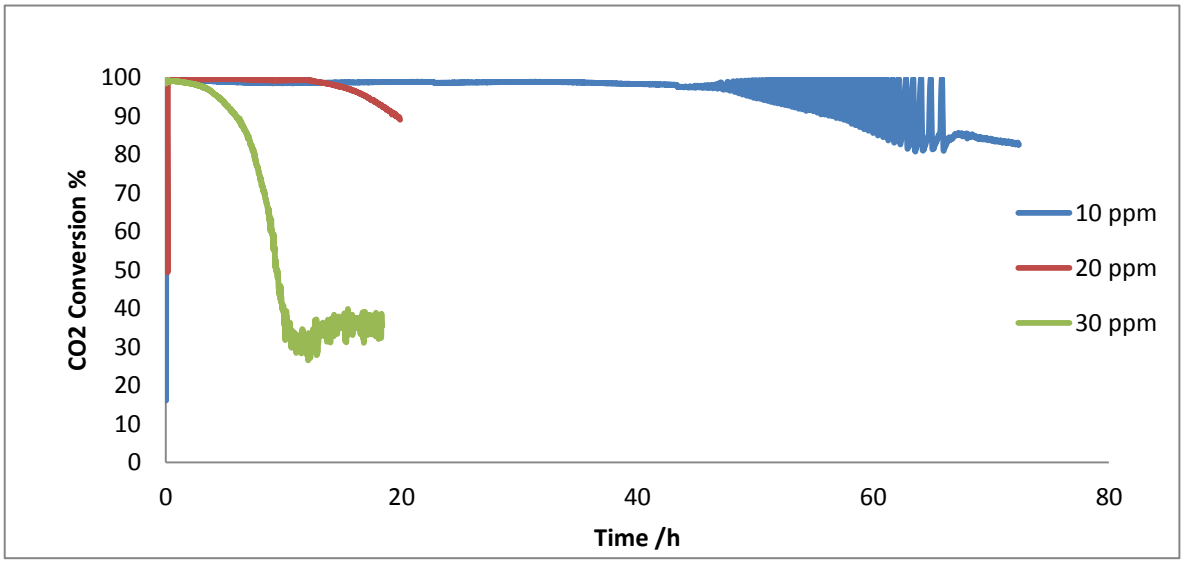

Fig 5-14- Carbon dioxide conversion for 2:1 CH_4:CO_2 reforming reaction over 1-NiLCZ at 850°C with different concentrations of H_2S

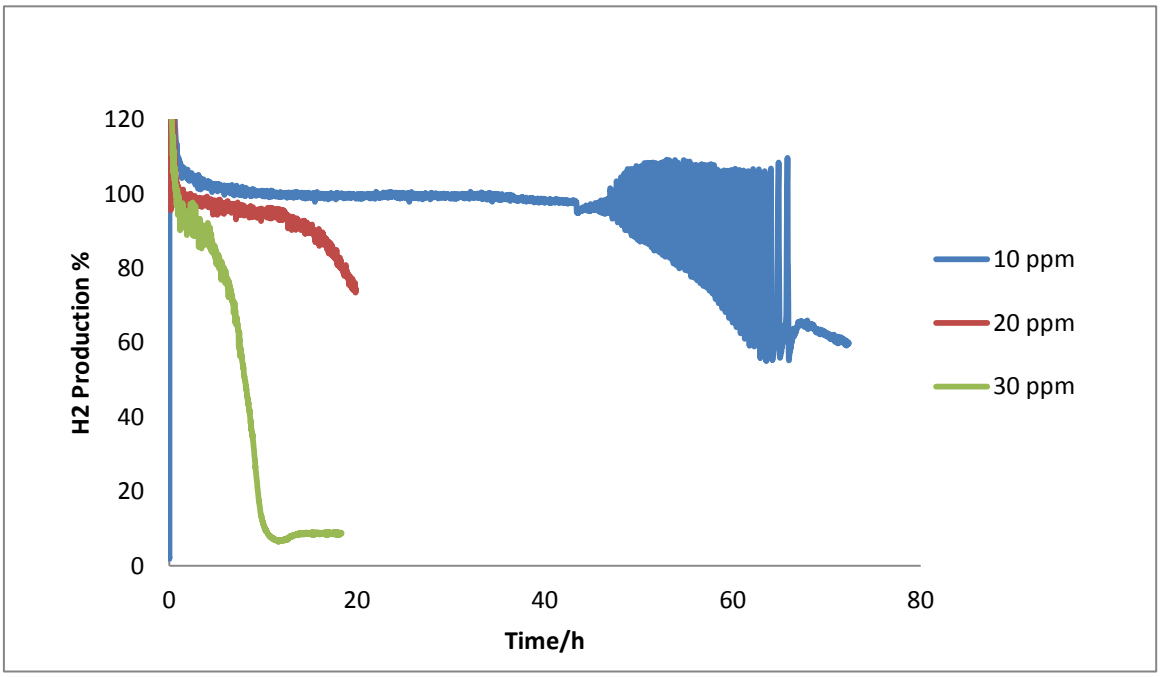

Fig 5-15- Hydrogen yield for 2:1 CH_4:CO_2 reforming reaction over 1-NiLCZ at 850° C with different concentrations of H_2S

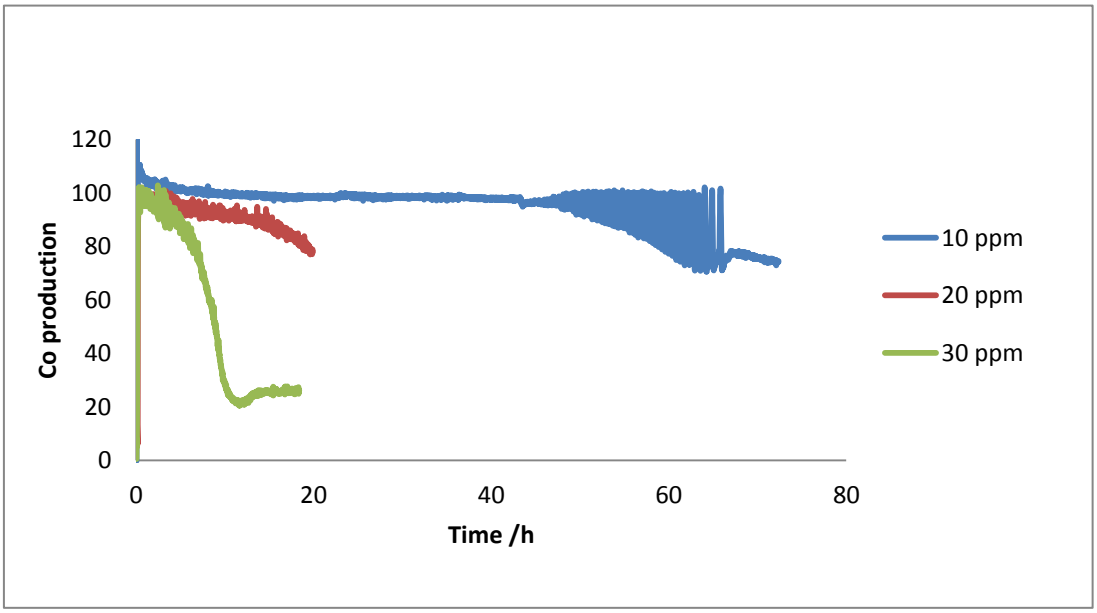

Fig 5-16- Carbon monoxide yield for 2:1 CH_4:CO_2 reforming reaction over 1-NiLCZ at 850°C with different concentrations of H_2S

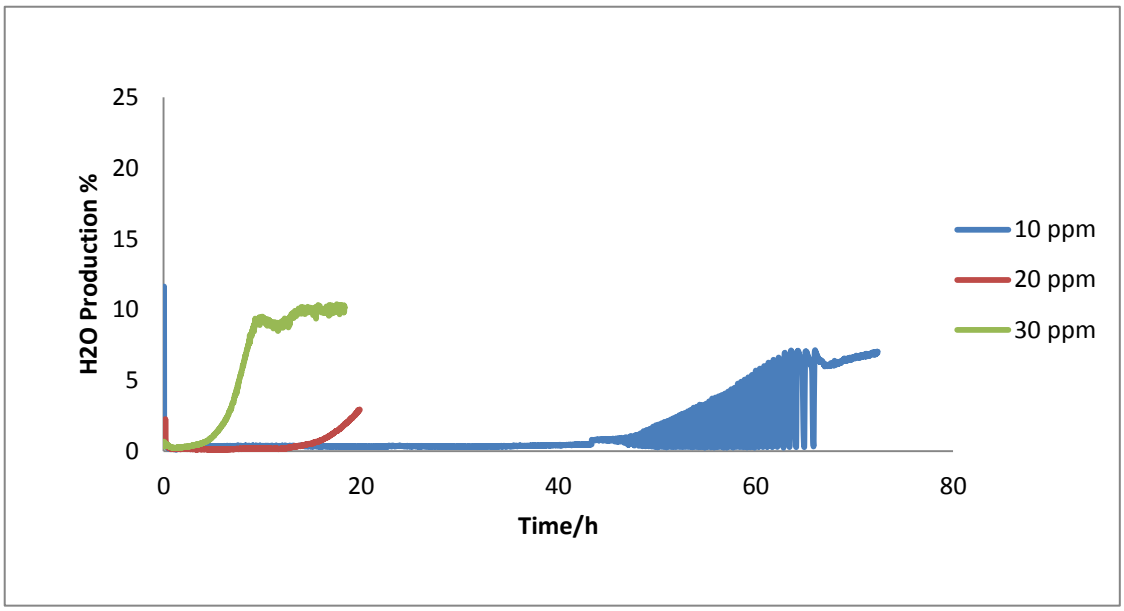

Fig 5-17- Water production for 2:1 CH_4:CO_2 reforming reaction over 1-NiLCZ at 850°C with different concentrations of H_2S

As can be seen from the result of the CH_4 conversions at various H_2S concentrations, by increasing the amount of H_2S, the rates of poisoning increase significantly. At 10 ppm of H_2S, a stable reaction at its stoichiometric ratio was seen for more than 42 hours and after

that, a period of large CH_4 conversion cycling for the next 20 hours was observed. This period of cycling decreased over time and a more linear loss of conversion occurred in the end phase of the reaction. On increasing the concentration of H_2S to 20 ppm, the loss of conversion was seen within 20 hours and at 30 ppm nearly no methane conversion was observed after 12 hours. In the case of CO_2 conversion, the conversion exhibits a relatively similar trend to the methane conversion. At 30 ppm of H_2S, the conversion of CO_2 was about 40% by the end of the reaction, while the amount of CH_4 conversion was about 5%, which was less than expected. The higher amount of CO_2 conversion in the presence of higher amounts of H_2S could be because of the reaction between H_2S and CO_2 with a production of CO, with this reaction favourable at relatively higher temperature (eq6).[16]

The existence of higher amounts of water confirms this reaction. Also, it was important to note, that the amount of carbon monoxide was very low in comparison with CO_2 conversion and this may be because of the reaction with Ce_2O_3 (eq11).

The following observations can be summarized from this section:

1-The rate of deactivation increases by increasing the H_2S concentration.

2-The rate of water formation increases by increasing the H_2S concentration. The formation of water is likely to be due to the presence of cerium in the catalyst eq (2).

3- Cycling behaviour increased on decreasing the H_2S concentration. This cycling behaviour suggested a beneficial effect for the catalyst as it reduced the extent of sulphur adsorption onto the nickel surface after this period of cycling; Ce_2O_2S acts as a protective layer which prevents the sulphur atom attacking the internal Ni sites resulting in a greater stability for the methane conversion without a decrease in activity.

4- Compared to the conversion of methane, the amount of CO_2 conversion increases with the increase in the H_2S concentration at 850 ° C (eq6)

5.3.1.2 Carbon deposition:-

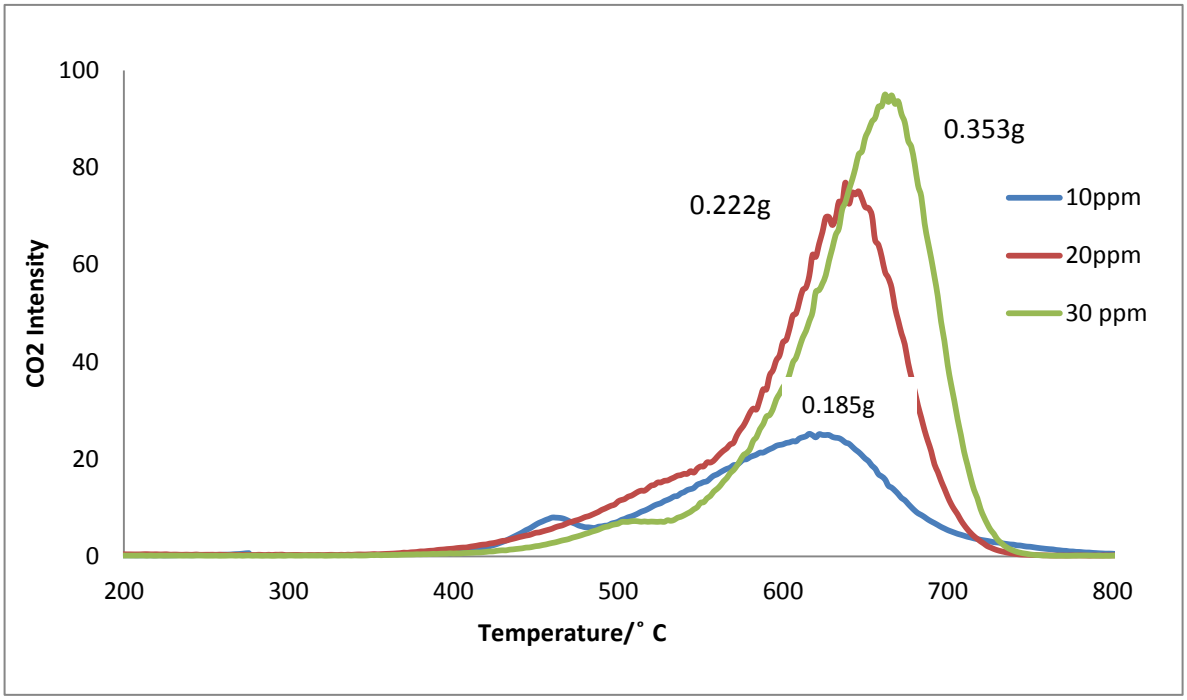

Fig 5-18- TPO for 2:1 CH_4:CO_2 reforming reaction over 1-NiLCZ at 850°C with different concentrations of H_2S

As can be seen from the fig 5- 18, the amount of carbon deposition increased on increasing the H_2S concentration. The reason could be due to the adsorbed S blocking the lattice oxygen from oxidising the deposited carbon, in addition to the occurrence of eq 11, as discussed previously. The important observation is: at 10 ppm H_2S, despite the reaction, being carried out for more than 80 hours, the amount of carbon deposition is low, and this means the catalyst has a high tolerance to carbon deposition thanks to the presence of cerium and deposition of carbon only occurring at the first stage of the reforming reaction.

5.3.2 The influence of H_2S concentration at 700 ℃

The higher H_2S concentration (30 ppm) played a significant role in CO_2 conversion at the higher temperature (850◦C) , as was discussed in the previous section, where the amount of CO_2 conversion at the end of the reaction was higher than expected in comparison with the lower H_2S concentration. For this purpose, it was interesting to know, how the behaviour of the reforming would change at a lower temperature. For that, the reactions were carried out at two concentrations of 10 ppm and 30 ppm at the temperature of 700◦C for the same catalyst and the results are shown in the fig 5- 19 to 23.

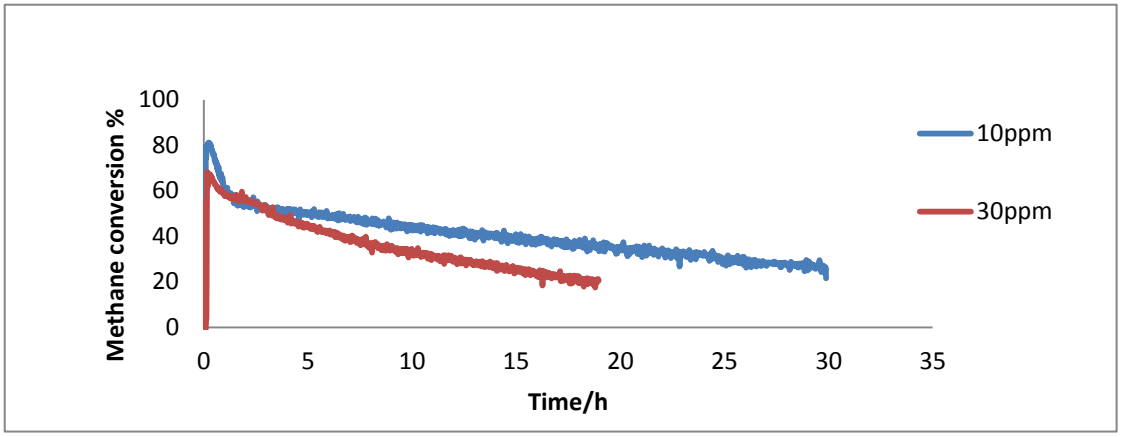

Fig 5- 19- methane conversion for 2:1CH_4:CO_2 reforming reaction over 1-NiLCZ at 700◦C with different concentrations of H_2S

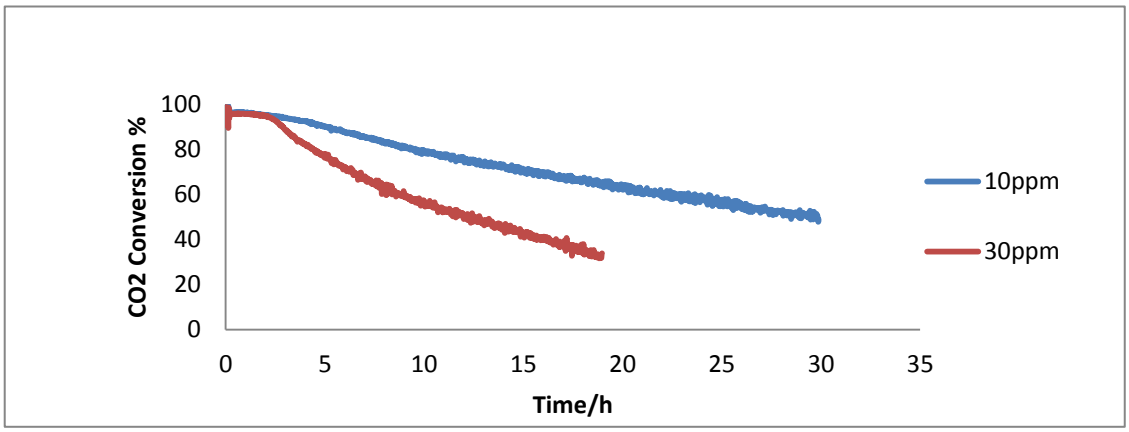

Fig 5-20- Carbon dioxide conversion for 2:1 CH_4:CO_2 reforming reaction over 1-NiLCZ at 700◦C with different concentrations of H_2S

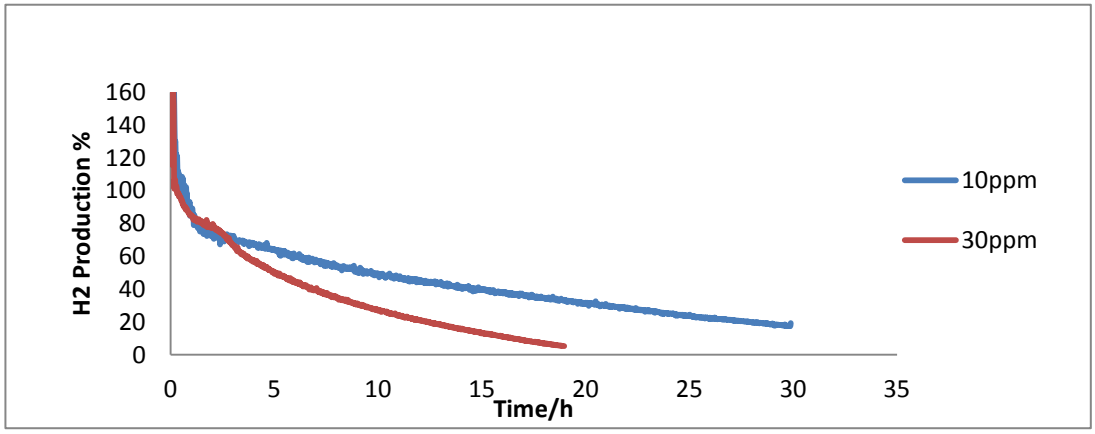

Fig 5-21- Hydrogen yield for 2:1 CH_4:CO_2 reforming reaction over 1-NiLCZ at 700° C with different concentrations of H_2S

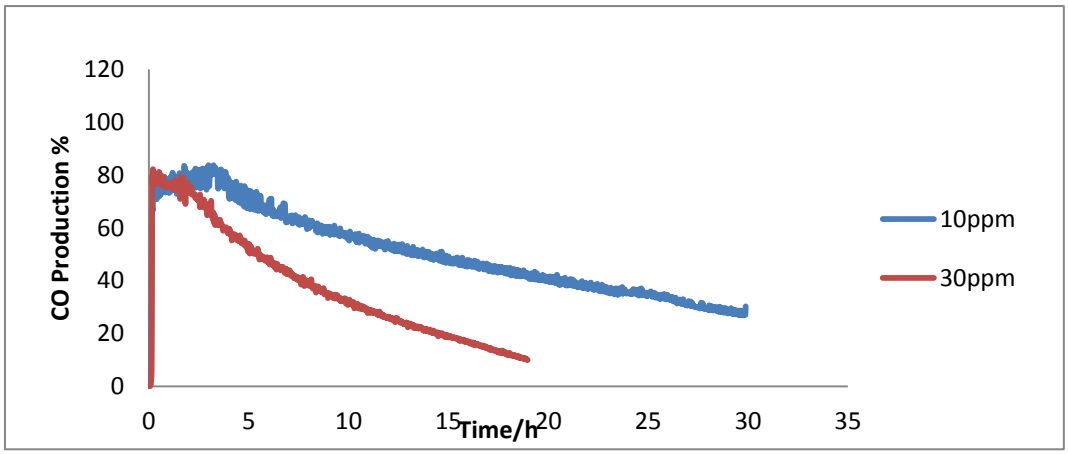

Fig 5-22- Carbon monoxide yield for 2:1 CH_4:CO_2 reforming reaction over 1-NiLCZ at 700°C with different concentrations of H_2S

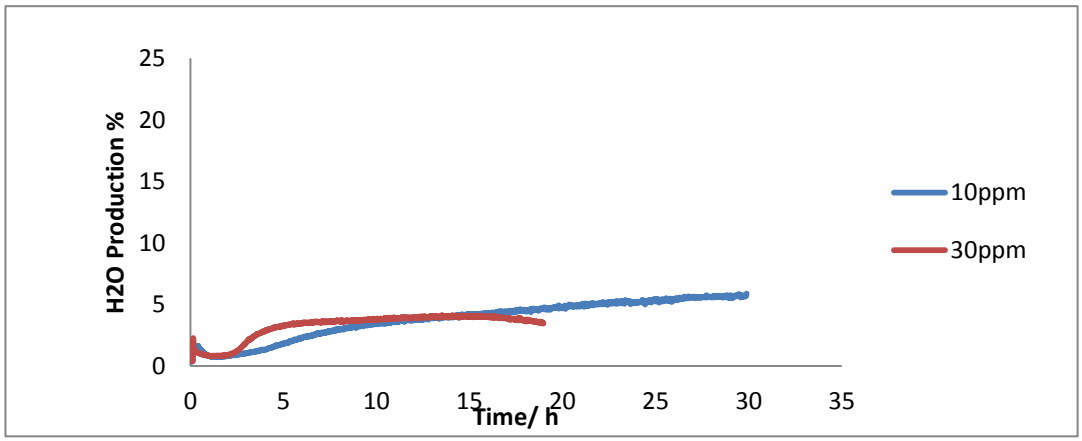

Fig 5-23- Water production for 2:1 CH_4:CO_2 reforming reaction over 1-NiLCZ at 700° C with different concentrations of H_2S

As can be seen from the CH_4 conversion profile (fig 5-19), for both concentrations, the initial amount of CH_4 conversion was higher than expected for around 3 hours, where at 10 ppm and 30 ppm H_2S the CH_4 conversions were about 30% and 10% higher than the equilibrium ratio respectively. In general, Ni catalysts are rapidly deactivated and poisoned by sulphur compounds, but the presence of H_2S in methane over Ni-LCZ pyrochlore catalysts represents a significant advantage, where the presence of a small amount of H_2S at lower temperatures seems to have a catalytic effect on the methane decomposition reaction. This catalytic effect may be based on the formation of intermediate HS* radicals, which, attack the methane molecules to produce methyl radicals followed by decomposition to H_2 and carbon.[16] The higher amount of H_2 in the first period of reaction could confirm this suggestion. Interestingly the amount of CO in both concentrations in the first period of reaction was lower by 20% than expected. This lowering in amount could be due to the Boudouard reaction which is thermodynamically favourable at this temperature.
In spite of the different amounts of H_2S in the reaction, the same catalytic behaviour was seen for around 3h and after that a continual decline in reforming was seen with a faster rate of decay for 30 ppm of H_2S. The presence of water in the reaction may be because of the CO reduction reaction (eq9).

5.4 The effect of Ni concentration on the catalyst performance

To study the effect of the amount of Ni on the performance of the catalyst, experiments were carried out with 30 ppm H_2S at both high (900°C) and low temperatures (700°C).

5.4.1.1 The effect of Ni concentration at low temperature (700 °C):-

The effect of Ni concentration on the catalyst performance at a low temperature are shown in fig 5- 24 to 28

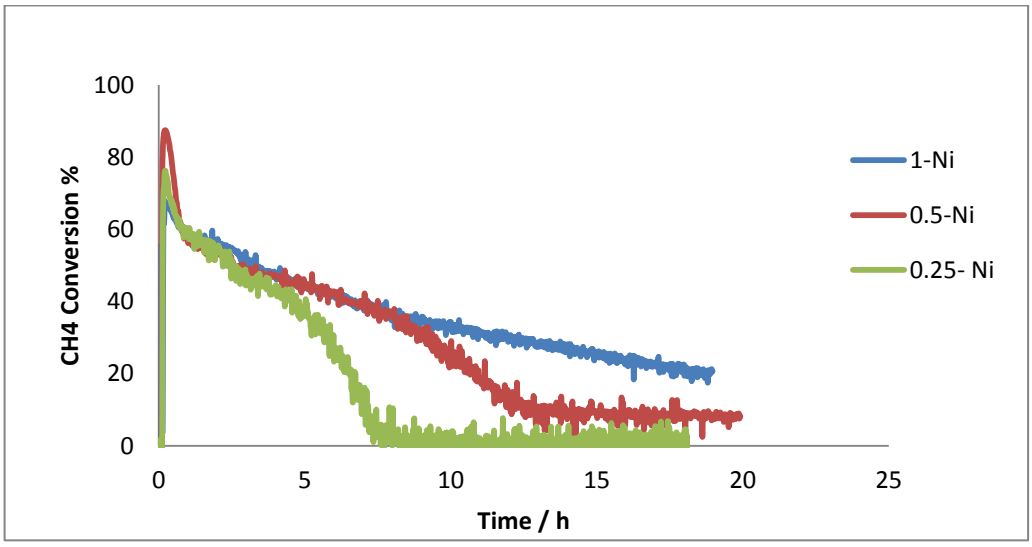

Fig 5-24- methane conversion for 2:1CH_4: CO_2 reforming reaction in presence of 30 ppm H_2S at 700°C with different concentrations of Ni

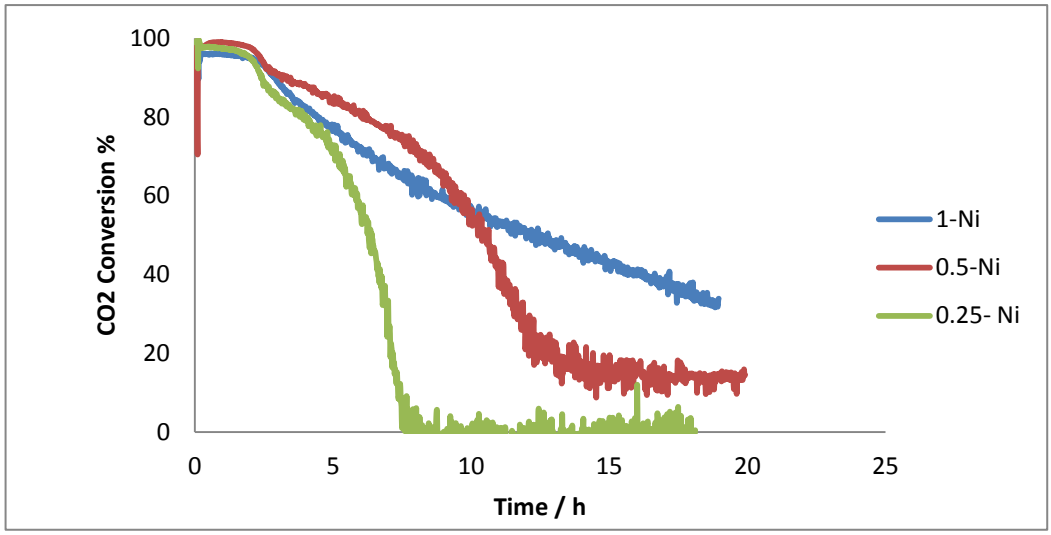

Fig 5-25- carbon dioxide conversion for 2:1CH_4:CO_2 reforming reaction in presence of 30 ppm H_2S at 700°C with different concentrations of Ni

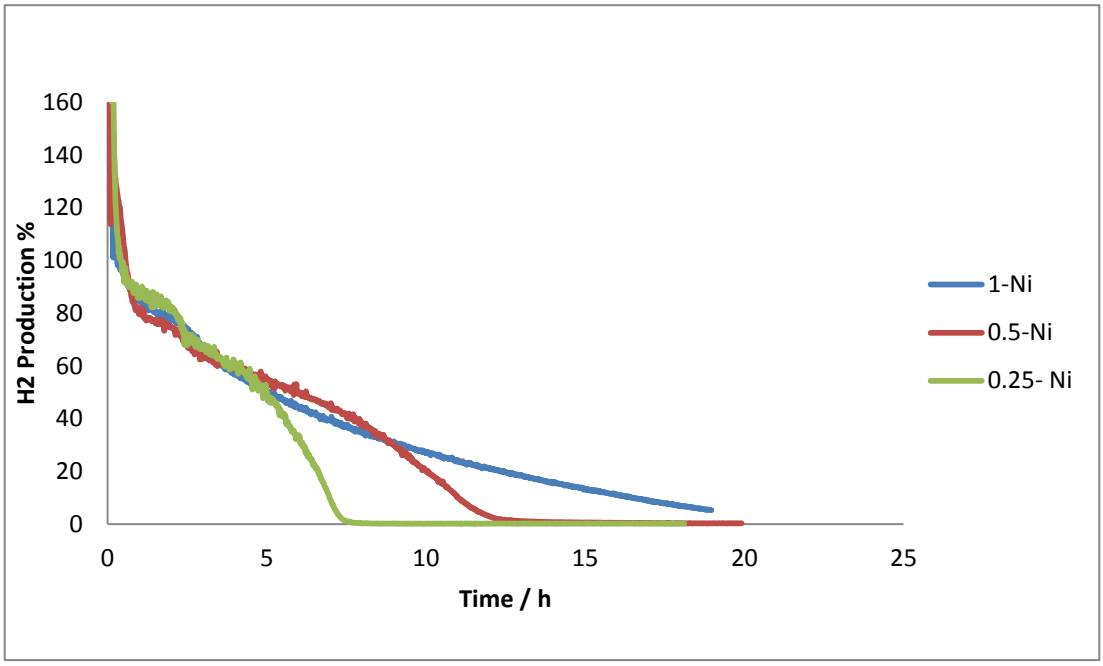

Fig 5-26- Hydrogen yield for 2:1CH_4:CO_2 reforming reaction in presence of 30 ppm H_2S at 700°C with different concentrations of Ni

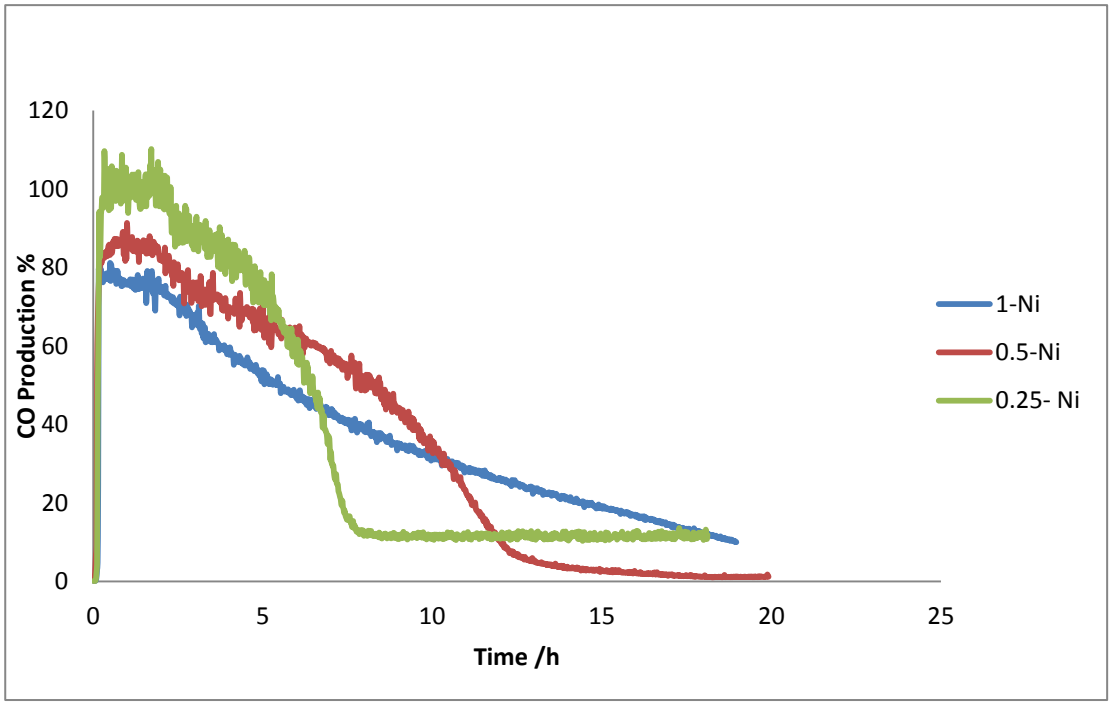

Fig 5-27- Carbon monoxide yield for 2:1CH_4:CO_2 reforming reaction in presence of 30 ppm H_2S at 700°C with different concentrations of Ni

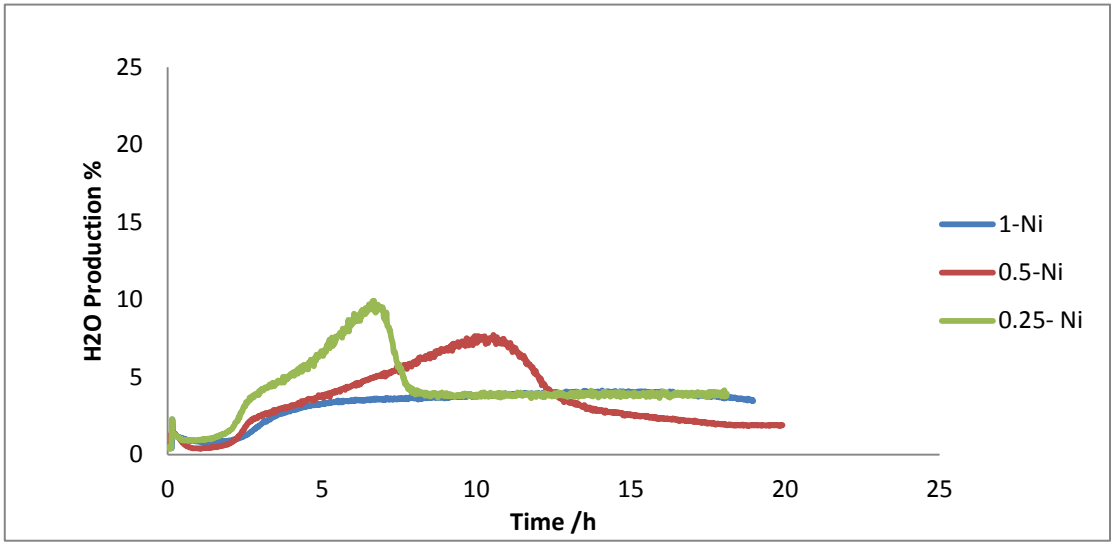

Fig 5-28- water production for 2:1CH_4:CO_2 reforming reaction in presence of 30 ppm H_2S at 700°C with different concentrations of Ni

As can be seen from fig 5- 24 to 28, the activity of the catalyst increased on increasing the content of nickel. The catalyst 1-NiLCZ did not show complete deactivation during 20 h of reaction and the CH_4 conversion decreased gradually in one step, with the amount of CH_4 conversion at the end of 20 h of reaction being about 20% while the amount of CH_4 conversion for 0.5-Ni and 0.25-Ni were about 10% and 5% respectively at the end of the reaction. A two-phase loss of reforming activity was clearly seen for the 0.25Ni and 0.5Ni catalysts, where the first phase was accelerated by decreasing the amount of nickel and this may be due to a larger number of sites for reforming available in the 0.5Ni sample in comparison with the 0.25-Ni sample. It is important to note, that the presence of H_2S had the same catalytic effect on methane conversion in all three catalysts at the beginning of reaction for around 3 hours, where all three catalysts had nearly the same amount of methane conversion despite the differing nickel amounts. In the case of CO_2 conversion, the amount of CO_2 decreased in the same trend as for CH_4 and at the end of reaction time the percentage of CO_2 conversion was around 35% for 1-Ni, while the amount of CO_2 conversion for 0.5- Ni and 0.25Ni were about 15% and less than 5% respectively. Important information that can be observed from fig 5- 27 is the higher amount of CO for

the 0.25-Ni sample, which does not correlate well with CO_2 conversion. In addition, there was a higher level of cycling in comparison with other catalysts at the beginning of the reaction. This suggests the availability of free Ce in the form of CeO_2 is higher in the material as ceria can promote redox reactions and reacts with carbon according to the Boudouard reaction to form CO as shown in the following reaction

$2CeO_2+C \leftrightarrow Ce_2O_3+CO$……eq12

Formation of Ce_2O_2S in 0.25-NiLCZ is most likely the reason for water being at a higher amount as shown in reaction eq (2)

The following observation can be concluded from the effect of Ni concentration

1-the amount of methane decomposition as a result of H_2S catalytic promotion was higher than expected in all three catalysts at the beginning of the reforming reaction

2-All the Ni-catalysts have the same period of stability before showing a decline in activity

3-The deactivation rate increased by decreasing the amount of Ni

4- Lowering the amount of Ni increases the amount of free ceria in the structure resulting in an increase in the amount of CO and H_2O

5-The second level of deactivation becomes clearer on decreasing the amount of Ni

6- A decrease in the amount of carbon is observed resulting from Boudouard interaction by reducing the amount of Ni in the catalyst structure

5.4.1.2 Carbon deposition:-

As can be seen from fig 5- 29, the lowest amount of carbon deposition was observed in the TPO profile of the 0.25-Ni catalyst and the amount of carbon deposition was at the highest level in the 1-Ni catalyst. Therefore, by increasing the amount of Ni, the amount of carbon deposition increased because of the higher amount of Ni sites available for carbon to deposit on. The lower amount of Ni also had an important role in increasing the amount of CeO_2 in the structure resulting in lowering the amount of carbon (eq12), as was discussed in the previous section.

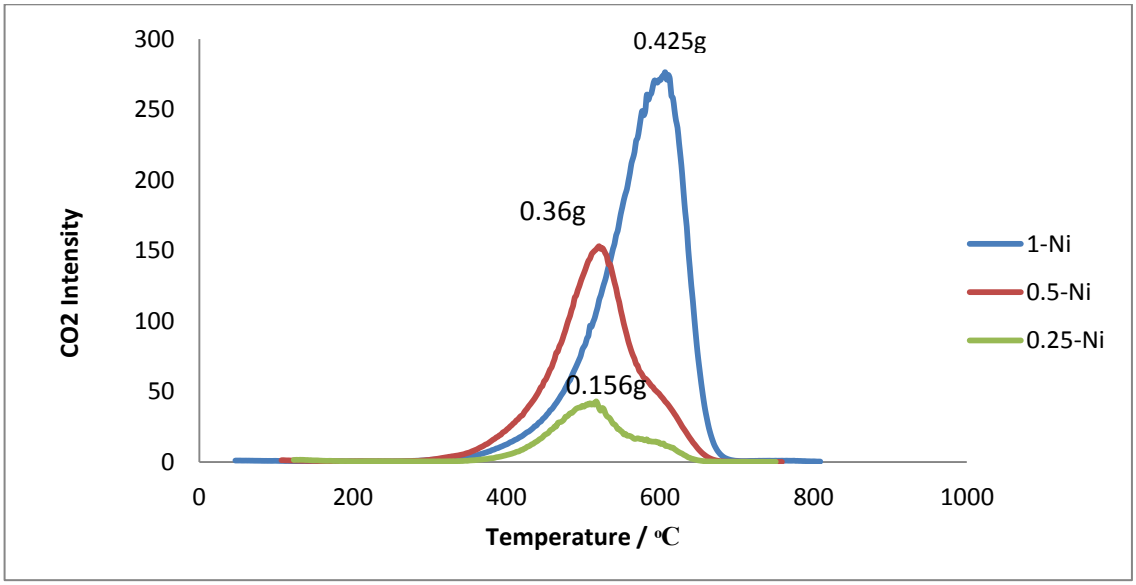

Fig 5-29- TPO for 2:1CH_4:CO_2 reforming reaction in presence of 30 ppm H_2S at 700° C with different concentrations of Ni

5.4.2.1 The effect of Ni concentration at high temperature (900 °C):-

The effect of Ni concentration on the catalyst performance at high temperature are shown in fig 5- 30 to 34

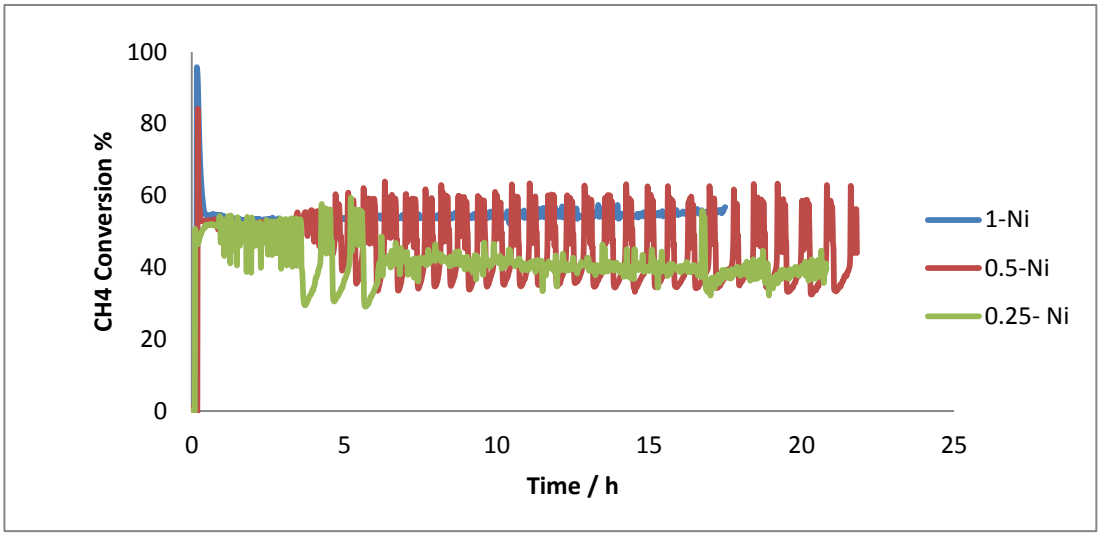

Fig 5-30- methane conversion for 2:1CH_4:CO_2 reforming reaction in presence of 30 ppm H_2S at 900°C with different concentrations of Ni

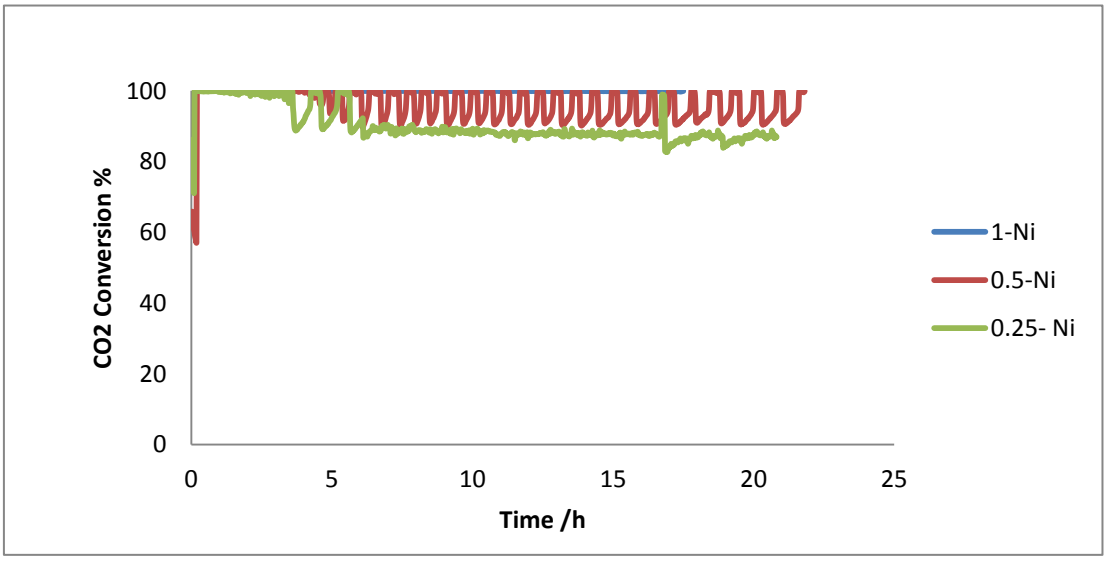

Fig 5-31- Carbon Dioxide conversion for 2:1CH_4:CO_2 reforming reaction in presence of 30 ppm H_2S at 900°C with different concentrations of Ni

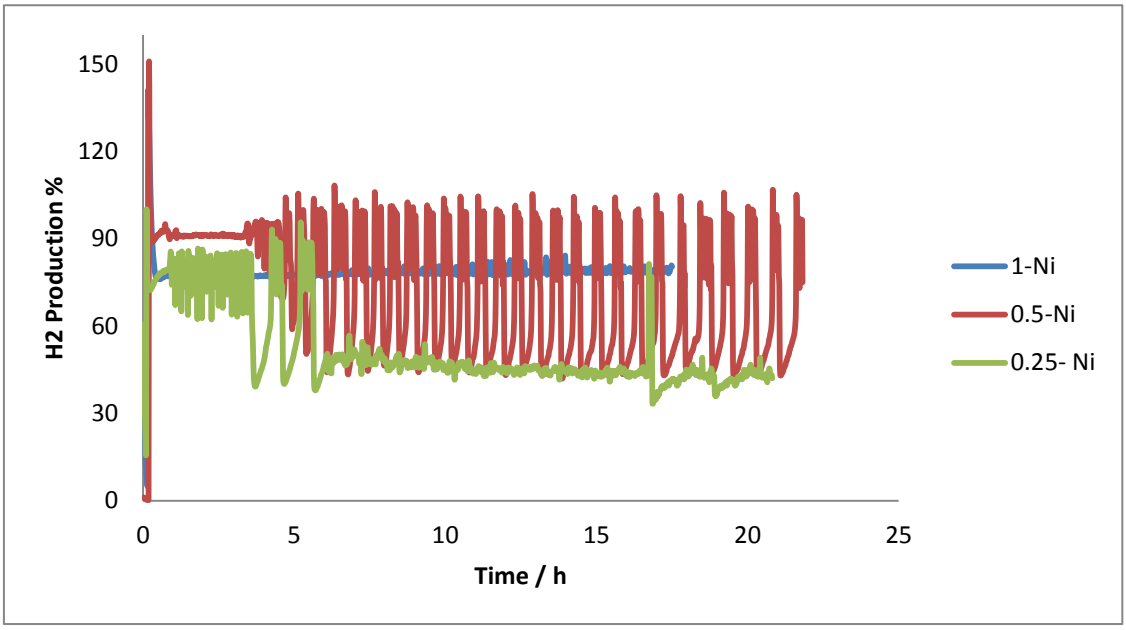

Fig 5-32- Hydrogen yield for 2:1CH_4:CO_2 reforming reaction in presence of 30 ppm H_2S at 900℃ with different concentrations of Ni

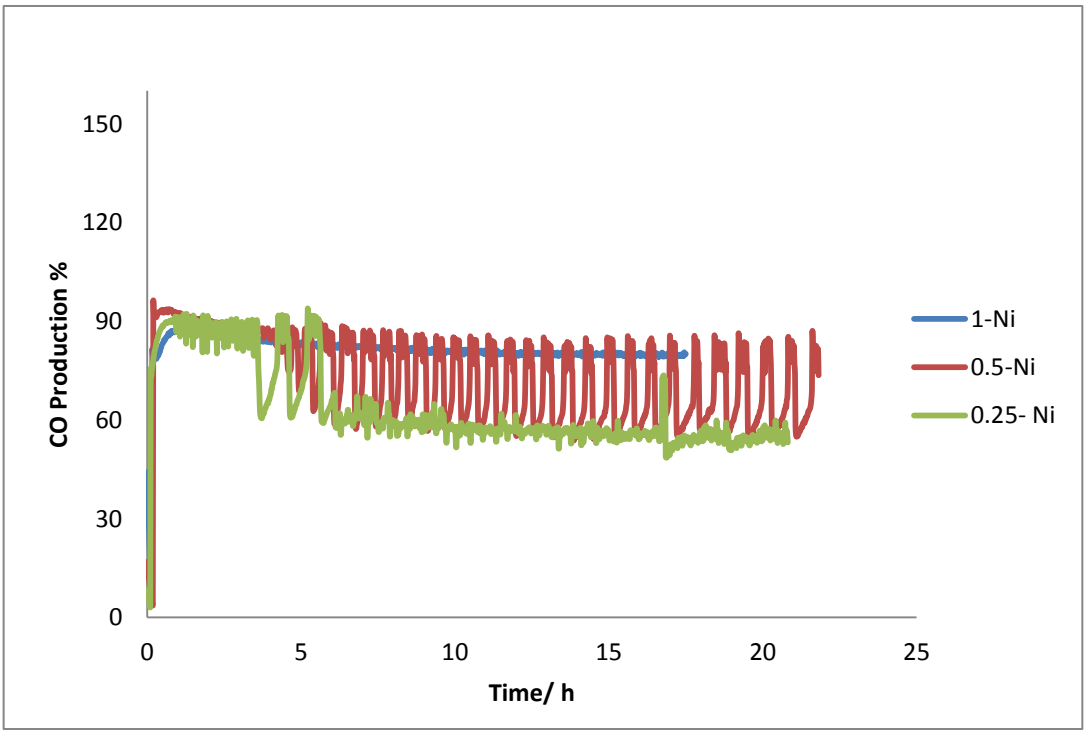

Fig 5-33- Carbon monoxide yield for 2:1CH_4:CO_2 reforming reaction in presence of 30 ppm H_2S at 900°C with different concentrations of Ni

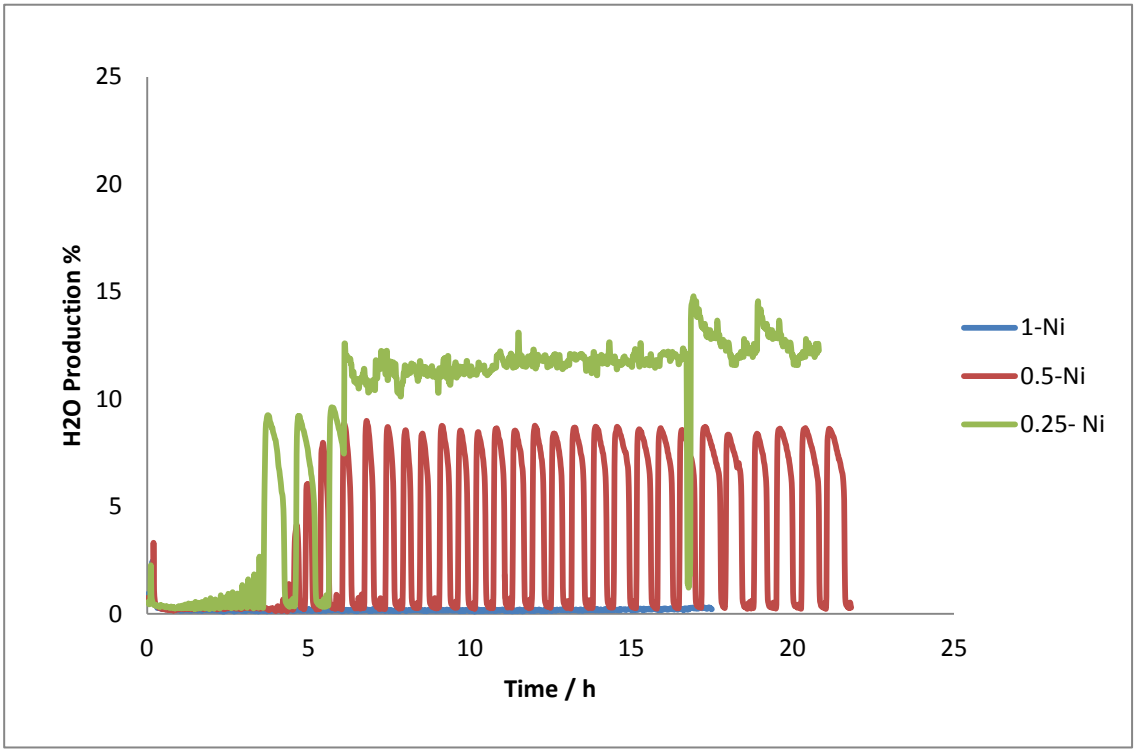

Fig 5-34- Water production for 2:1CH_4:CO_2 reforming reaction in presence of 30 ppm H_2S at 900°C with different concentrations of Ni

As shown in Fig 5- 30 to 34, at 900 ° C and 30 ppm H_2S, the stability and tolerance toward sulphur were increased by increasing the amount of Ni. As seen from fig 5- 30, the cycling behaviour in the first period of reaction was increased by reducing the amount of Ni in the catalyst. The cycling behaviour for the 0.25 Ni, 0.5Ni and 1Ni catalyst started after the times of 2, 5 and 10 hours of the reaction respectively.

Since the amount of Ni in this catalyst (0.25-NiLCZ) is at the lowest level, the free Ni which is not within the pyrochlore structure will also be low and as a consequence, the amount of free CeO_2 will be higher due to there being not enough Ni on surface of CeO_{2-x}. Therefore an excessive amount of ceria simply acts as a sulphur adsorbent and as Karjalainen et al. showed from the thermodynamical calculation, Ceria has the tendency to

form $Ce_2(SO_4)_3$ and Ce_2O_2S species[17]. Ceria will also react with H_2S and carbon to produce a higher amount of H_2O and CO as was shown in eq 2 and 12.

As the reaction progressed and the amount of free CeO_x decreased, the cycling decreased in magnitude and a nearly stable conversion of methane continued for the rest of the reaction time. A low level of cycling could be due to the redox properties of ceria. In 0.5 Ni-LCZ and 1-NiLCZ, the amount of free Ni increased and since the $La_2Zr_2O_7$ pyrochlore has limited capacity for doping, this amount of free nickel will react with free cerium and the probability of formation of Ce_3Ni, Ce_5Ni and Ce_{10} Ni will be increased. Because the amount of free Ce was decreased, an increased stability at equilibrium ratios can be seen at the beginning of the reaction and this stability was twice the duration for the1-NiLCZ pyrochlore catalyst. It was noticeable in the 0.5-NiLCZ catalyst that, after 5h of stable reforming, an organized cycling period of adsorption and desorption occurred for the rest of the reaction time, unlike the 0.25-Ni catalyst, which showed a long stable reforming period after the period of adsorption and desorption or oxidation and reduction as a form of cycling. As observed for the 0.25-NiLCZ catalyst, it can be concluded that, in the presence of higher amount of H_2S and at the temperature of 900^{o}C, an excessive amount of cerium in comparison with Ni in the pyrochlore structure, increases the cycling behaviour and as a consequence lowers the amount of carbon deposition.

5.4.2.2 Carbon deposition:-

As can be seen from fig 5-35, and as was expected, the lowest amount of carbon deposition was observed on the 0.25-NiLCZ pyrochlore catalyst. The reason was attributed to ceria's OSC properties, where the presence of a higher amount of unconnected cerium in the structure, had the ability to oxidize the carbon that formed on the Ni surface.

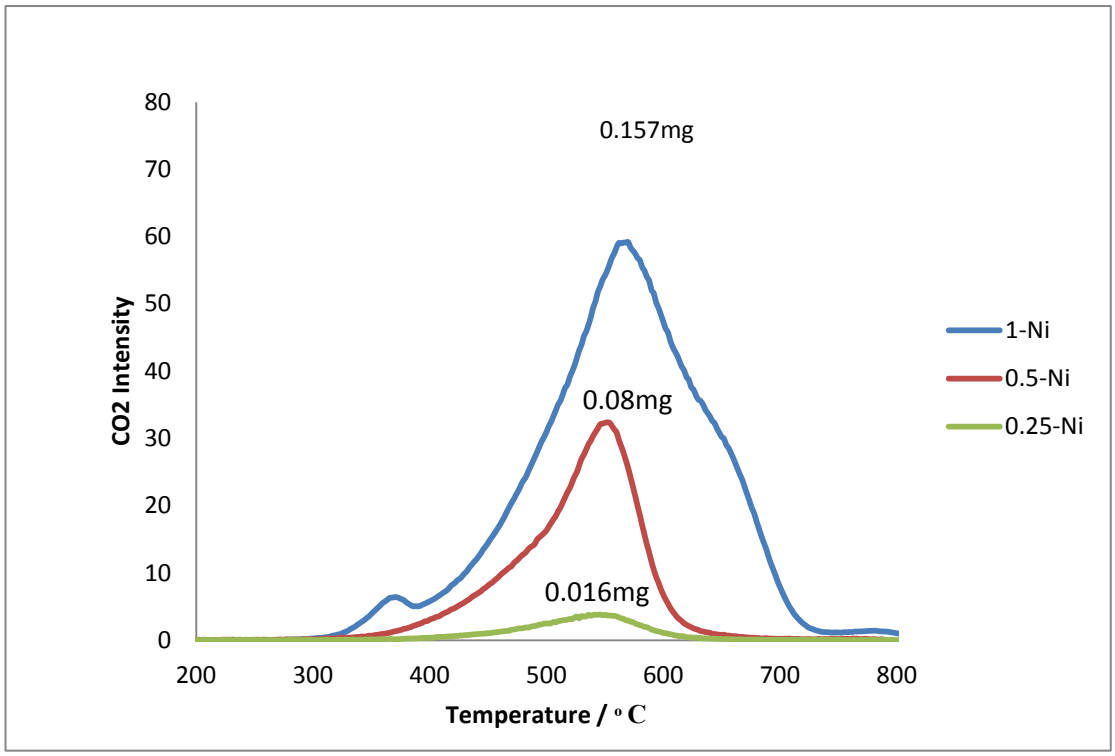

Fig 5-35- TPO for 2: 1CH_4:CO_2 reforming reaction in presence of 30 ppm H_2S at 900° C with different concentrations of Ni

5.5.1 Long term stability study on various NiLCZ pyrochlore catalysts prepared by the hydrothermal method

To evaluate the influence of a low concentration of H_2S on the behaviour and stability of the catalysts, the experiments were performed at 10 ppm H_2S at 850°C on LCZ pyrochlore catalyst with different amounts of nickel. The results are shown in fig 5- 36 to 40

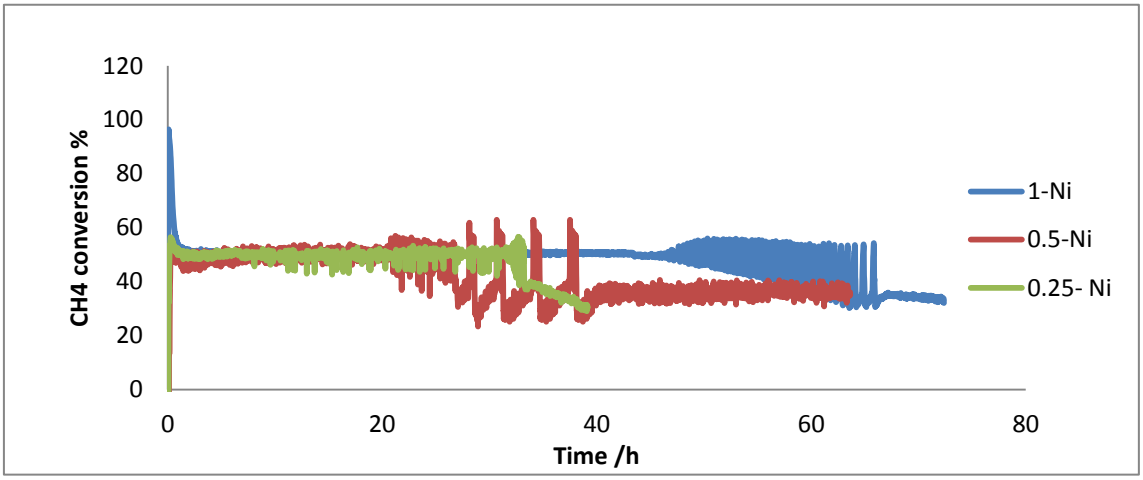

Fig 5-36- methane conversion for 2:1CH_4:CO_2 reforming reaction in presence of 10 ppm H_2S at 850°C with different concentrations of Ni

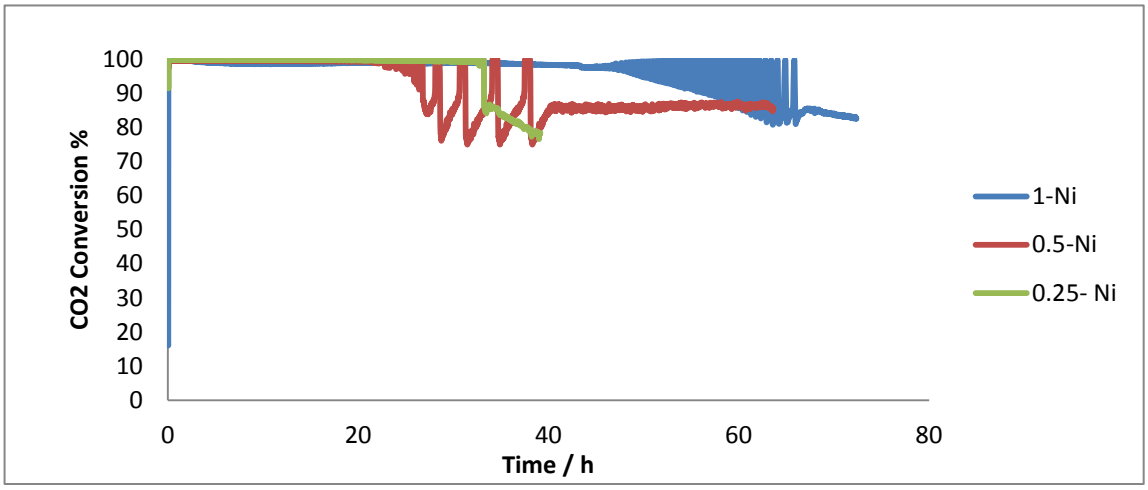

Fig 5-37- carbon dioxide conversion for 2:1CH_4:CO_2 reforming reaction in presence of 10 ppm H_2S at 850°C with different concentrations of Ni

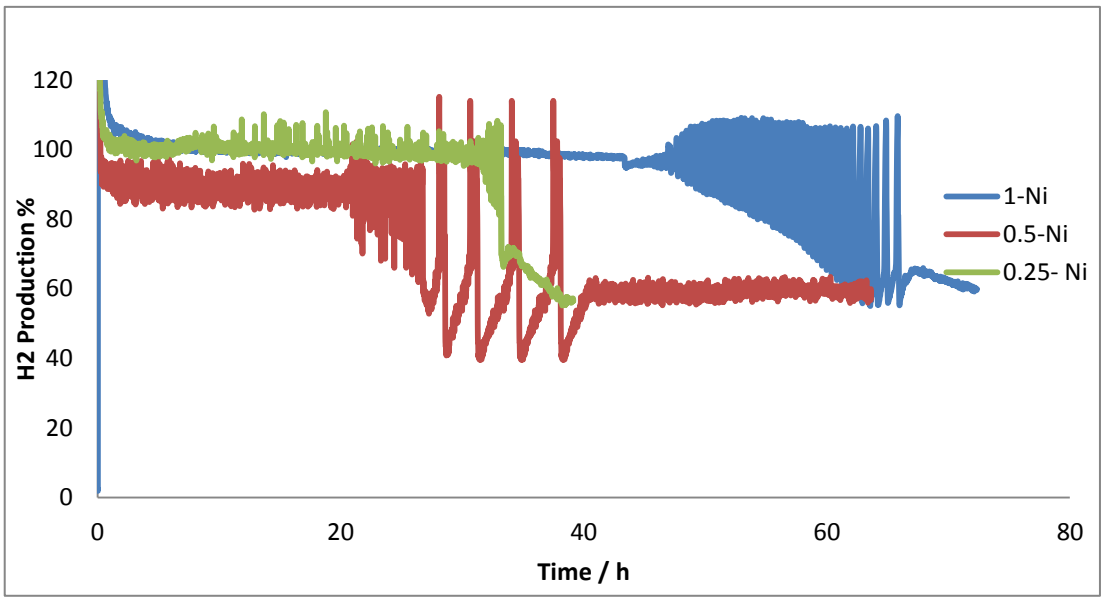

Fig 5-38- Hydrogen yield for 2:1CH_4:CO_2 reforming reaction in presence of 10 ppm H_2S at 850°C with different concentrations of Ni

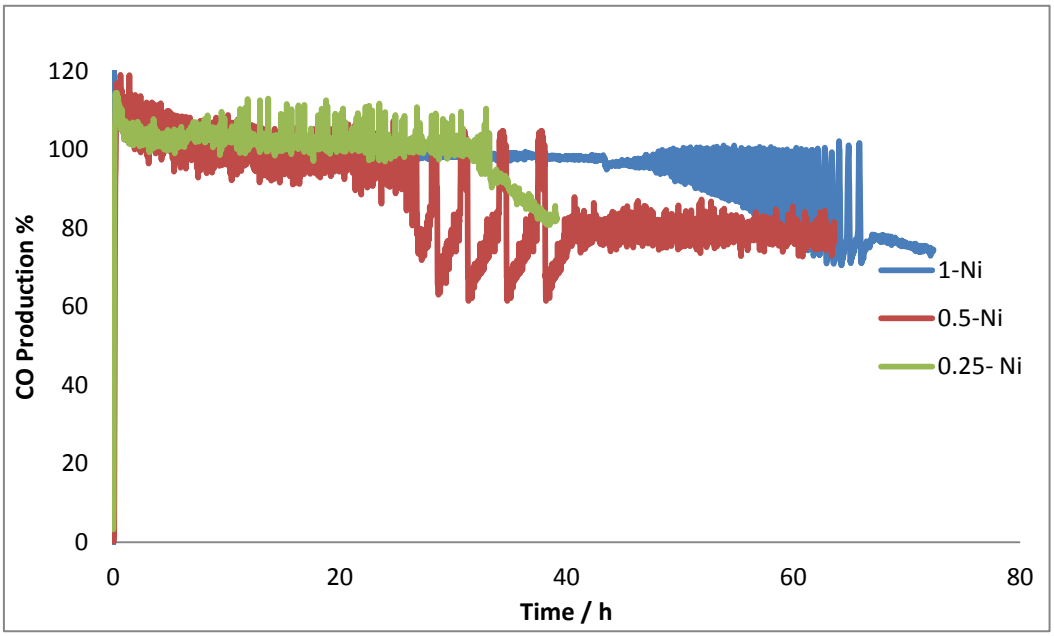

Fig 5-39- Carbon monoxide yield for 2:1CH_4:CO_2 reforming reaction in presence of 10 ppm H_2S at 850°C with different concentrations of Ni

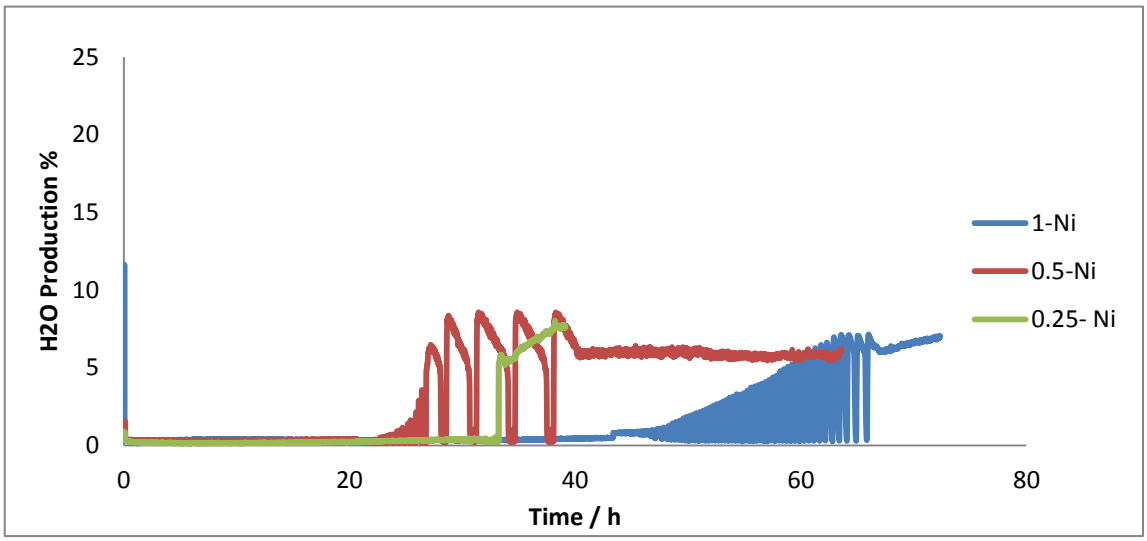

Fig 5-40- water production for 2:1CH_4:CO_2 reforming reaction in presence of 30 ppm H_2S at 850°C with different concentrations of Ni

As can be clearly seen from the results, the catalyst with the higher amount of Ni showed more stability and resistance to sulphur poisoning. All three catalysts had the same initial methane conversion as the equilibrium state dry reforming reaction. The stability in performance of the 0.25Ni catalyst was for a period of 30 hours, whereas, the 1-NiLCZ catalyst showed performance losses after 70 hours of reaction. In all three catalysts, levels of cycling were observed, and a more linear loss of activity was seen in the final phase of reaction. It was important to note that no complete deactivation was observed in all three catalysts, and all three catalysts had nearly the same reforming activity by the end of reaction (30%). The amount of CO_2 in all three catalysts displayed relatively good correlation with the CH_4 conversion which means no methane decomposition, or other side reactions occurred except some water gas shift reaction. The cycling loss behaviour of the reforming activity before a linear loss of activity could be due to the H_2S adsorption-desorption on the cerium oxide surface and formation of Ce_2O_2S which was accompanied by water formation as is clear in figure 5-40. At the end period of reaction, a steady

reforming activity was seen despite the presence of H_2S and this could be due to the formation of a sulphide ceria protective layer, which protects the nickel from poisoning.

5.5.2 Carbon deposition:-

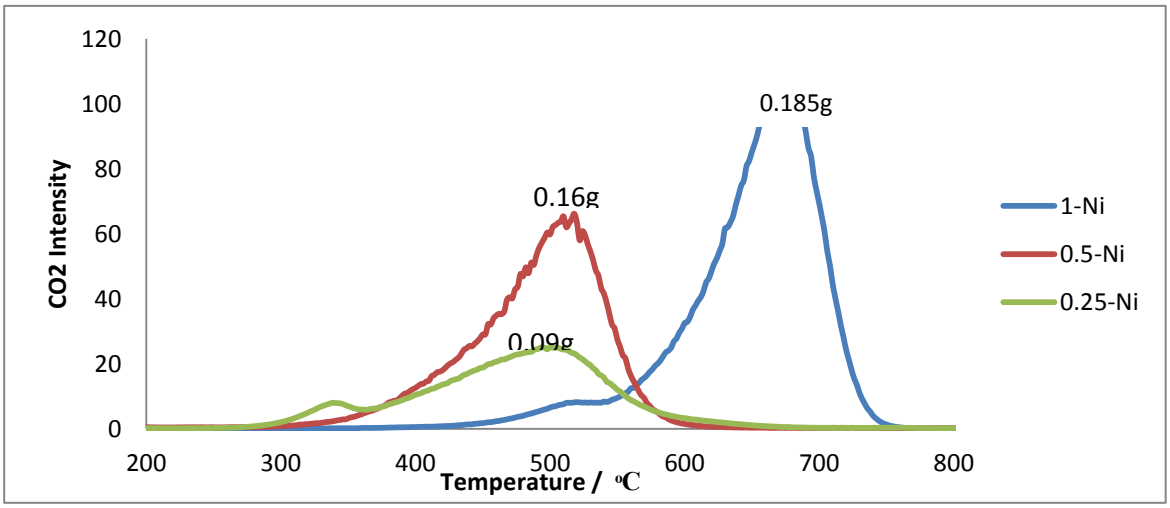

Fig 5-41- TPO for 2:1CH_4:CO_2 reforming reaction in presence of 10 ppm H_2S at 850° C with different concentrations of Ni

As can see from fig 5-41, the lowest amount of carbon deposition can be observed at the lowest nickel doping. The type of carbon formed during the reaction was altered to a higher temperature form by increasing the amount of Ni to 1-NiLCZ. Except for the 0.5-NilCZ catalyst which has one form of carbon, two distinct peaks were seen for the 0.25NiLCZ and 1-NiLCZcatalysts. These two peaks may be due to deposition of carbon at different parts of the catalyst, with the peak at the lower temperature of 320° C in 0.25-NLCZ suggesting the presence of a relatively reactive polymeric carbon species, which is located on or very near the active metal, and the peak at the higher temperature of 650° C for 1NiLCZ, due to the carbon accumulated on the oxide surface[19]. The peak observed at 510° C for all three catalysts, can be attributed to the carbon present at the metal-LCZ interface. [20].

5.6 The effect of preparing catalysts using the Pechini method

5.6.1.1 The influence of temperature on the Pechini 1Ni-LCZ pyrochlore catalyst

To study the effect of preparation method on the performance of Ni-pyrochlore catalysts, 1Ni-LCZ was prepared by the Pechini method. Methane-rich dry reforming reactions were carried out at various temperatures in the range of 700° C-900° C and in presence of 30 ppm H_2S. The results are shown in fig 5- 42 to 46.

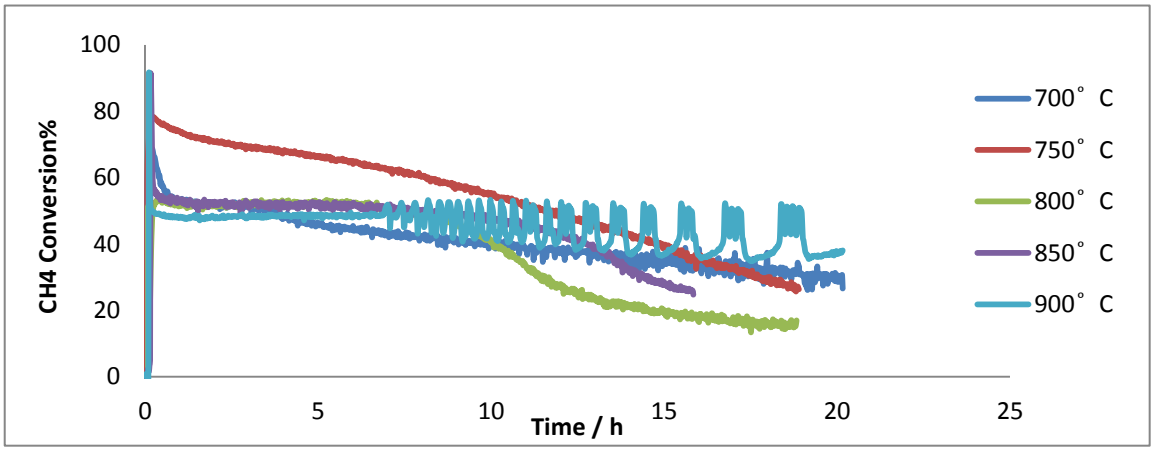

Fig 5- 42- percentage of methane conversion at different temperatures methane-rich dry reforming over Pechini 1Ni-LCZ in presence of 30 ppm H_2S

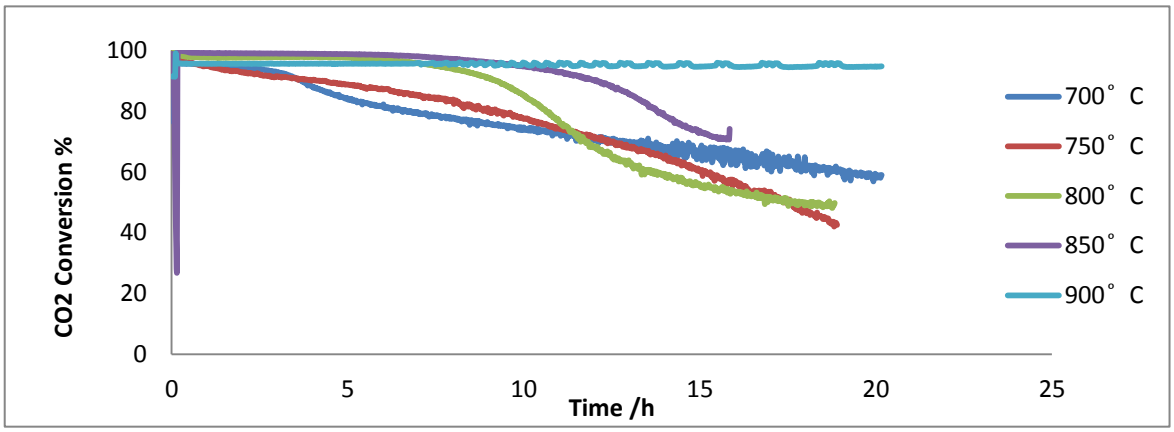

Fig 5- 43- percentage of CO_2 conversion at different temperatures of methane-rich dry reforming over Pechini 1Ni-LCZ in presence of 30 ppm H_2S

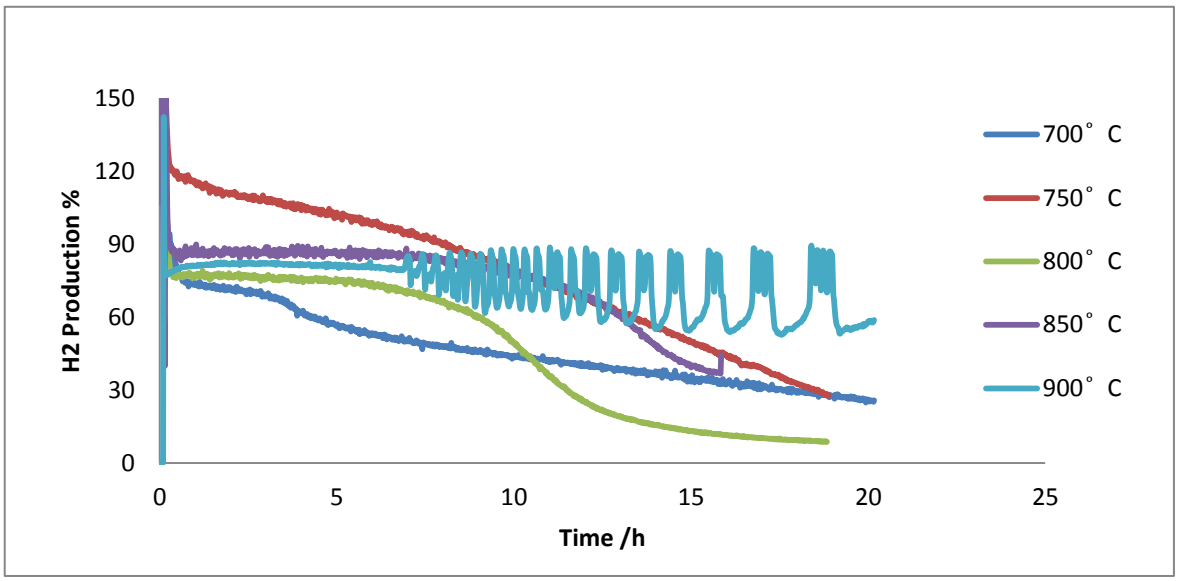

Fig 5-44- percentage of hydrogen yield at different temperatures methane-rich dry reforming over Pechini 1Ni-LCZ in presence of 30 ppm H_2S

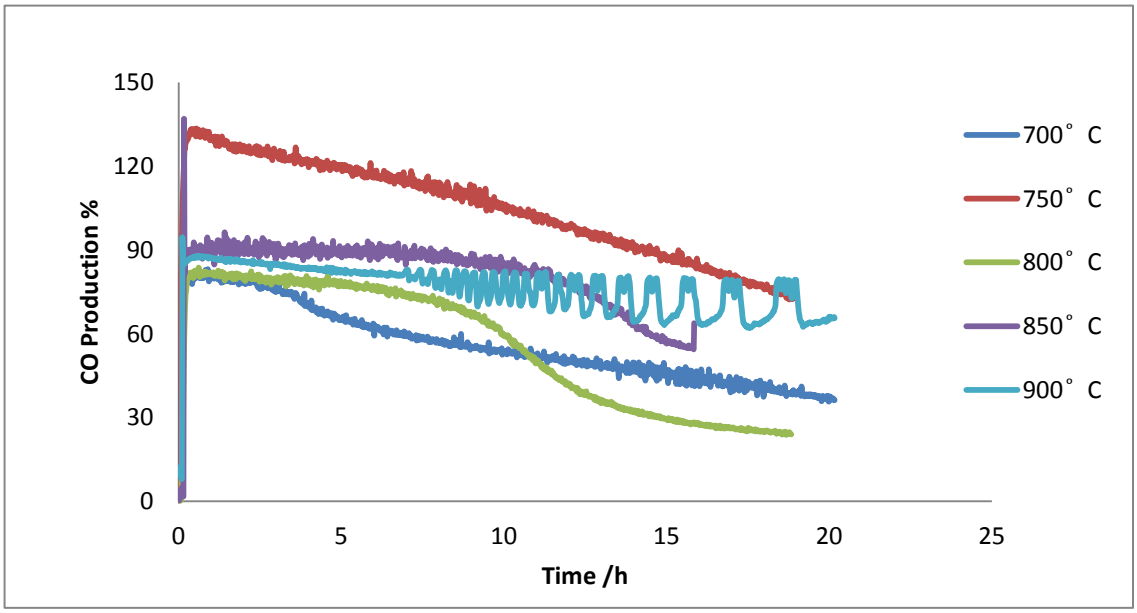

Fig 5-45- percentage of carbon monoxide yield at different temperatures of methane-rich dry reforming over Pechini 1Ni-LCZ in presence of 30 ppm H_2S

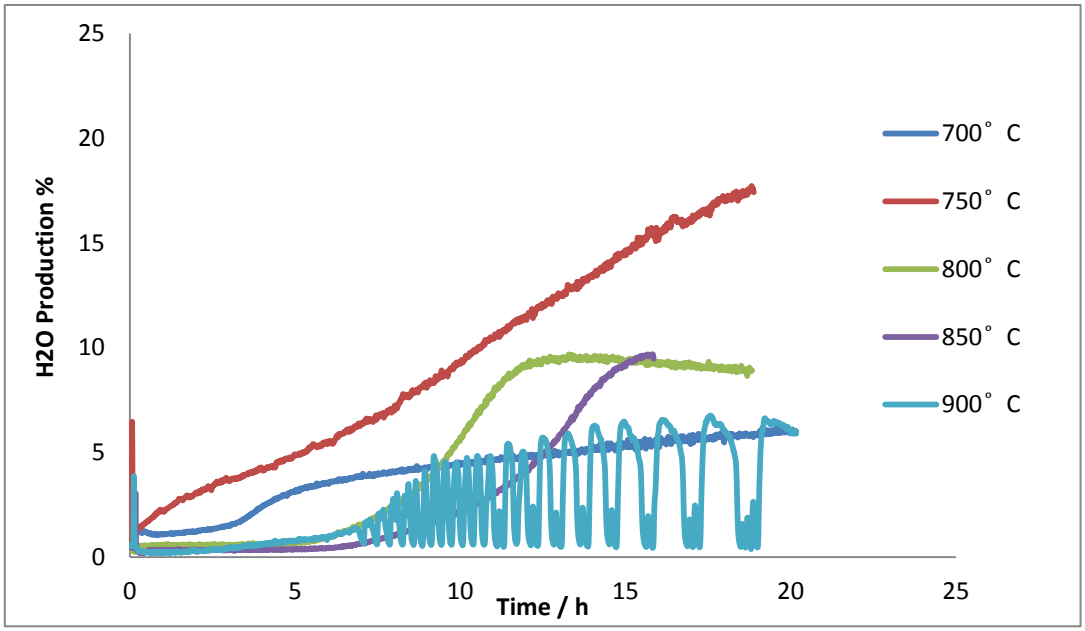

Fig 5-46- percentage of H_2O production at different temperatures of methane-rich dry reforming over Pechini 1Ni-LCZ in presence of 30 ppm H_2S

At a temperature of 700° C, the catalyst showed a stable equilibrium value of methane conversion for about 4 hours before showing a gradual decrease in conversion with time. The decrease in conversion could be because of the loss of active metallic sites , as a result H_2S poisoning. The carbon dioxide conversion correlated with the methane conversion in all periods of reaction. The higher amount of carbon monoxide in comparison with hydrogen was due to the water gas shift reaction and an increase in the amount of water after 8h confirmed this reaction as shown in fig 5- 46. The lower initial amount of CO was because of the Boudouard reaction. As the temperature was increased to 750° C, the amount of methane conversion became higher than expected and the percentage conversion was as high as 80 percent in the initial period of reaction. The reason could be because of CH_4 decomposition in the presence of H_2S which seems to have a catalytic effect on the methane decomposition by formation HS* radicals that attack the methane molecules.[16] The presence of a higher amount of H_2 provides support for this reaction. As

can be seen from fig 5- 45, the amount of CO was higher than expected and did not correlate with the CO_2 conversion. This could be because of the effect of CeO_2 in the structure. At this temperature CeO_2 can react with carbon formed from methane decomposition (eq12). A rapid decrease in the amount of H_2 in comparison with CO was because of the water gas shift reaction, as shown in fig 5- 46. Two-stages of poisoning can clearly be seen at the temperature of 800 °C. The stability in methane conversion was for 10h at equilibrium ratio. As can be seen from fig 5- 42, the amount of methane conversion in the second phase became constant at 20% for the remainder of the reaction time. The amount of CO_2 conversion correlated well with the amount of methane conversion but noticeably the amounts of H_2 and CO were lower than expected. The amount of CO and H_2 at the beginning of the reaction decreased at the same level of decline by 20%. Therefore, this decrease can be attributed to the CO reduction reaction (eq 9). Since there is no evidence of water in this period of the reaction, the presence of cerium in the structure in the form of Ce_2O_3 can play a critical role. The following mechanism can be suggested for this behaviour:

$H_2 + CO \leftrightarrow H_2O + C$……eq 9

$Ce_2O_3 + H_2O \leftrightarrow 2CeO_2 + H_2$……..eq 13

$2CeO_2 + C \leftrightarrow Ce_2O_3 + CO$…….eq 12

The higher amount of CO_2 conversion during the second stage of poisoning in comparison with the methane conversion, and the reason for the amount of CO in the second stage being higher than hydrogen is most likely due to the reaction of CO_2 with H_2S (eq6).

Similar behaviour was observed by increasing the reaction temperature to 850 °C, but there was a significant difference in the length of the reaction, which increased as expected. The reason for this is that sulphur adsorption is not favourable at high temperature. With a temperature rise to 900 ° C steady stability was observed for approximately 9 hours followed by a large level of cycling reforming, which can be related to the redox properties

of ceria in addition to the sulphur adsorption-desorption. These levels of cycling became more organized over time, and at 15 hours after the reaction started, the highest amount of CH_4 conversion was nearly 50% and the lowest amount was about 40%, or in other words, the reduction in methane conversion was 10%. Moreover, it was observed that the rate at which the catalyst remains at the highest level of methane conversion in each cycle increases over time. More steady behaviour in CO_2 conversion was observed in comparison with the CH_4 conversion.

The following observation can be concluded from this section:

1- A second poisoning stage was observed by increasing the reaction temperature.

2- The lifetime of the first stage increased on decreasing the reaction temperature.

3- The second phase of poisoning is most likely because of the presence of ceria in the form of Ce_2O_3

4- The conversion of methane increased by decreasing the reaction temperature due to H_2S catalytic activity at the beginning period of the reaction

5.6.1.2 Carbon deposition: -

As can be seen from fig 5- 47, the highest level of carbon deposition was observed at 700° C. At this temperature the probability of the Boudouard reaction occurring is high. Although the possibility of the Boudouard reaction at 750° C exists, the presence of CeO_2 which reacts with deposited carbon becomes more effective and as result, the amount of carbon deposition decreased significantly in comparison with that at 700° C. No carbon deposition was observed at 800° C as was expected because of Ce_2O_3, which at this temperature has an important catalytic role as was discussed previously. When the temperature was increased to 850 ° C, the amount of carbon deposition increased dramatically in comparison with 800 ° C. The reason could be because of methane decomposition, which is more likely at higher temperatures. A significant reduction in carbon deposition was observed at 900 ° C in spite of the methane decomposition. This noticeable decrease could be because of the oxygen storage capacity of ceria which increases at 900° C, and most likely suppressed the amount of carbon deposition

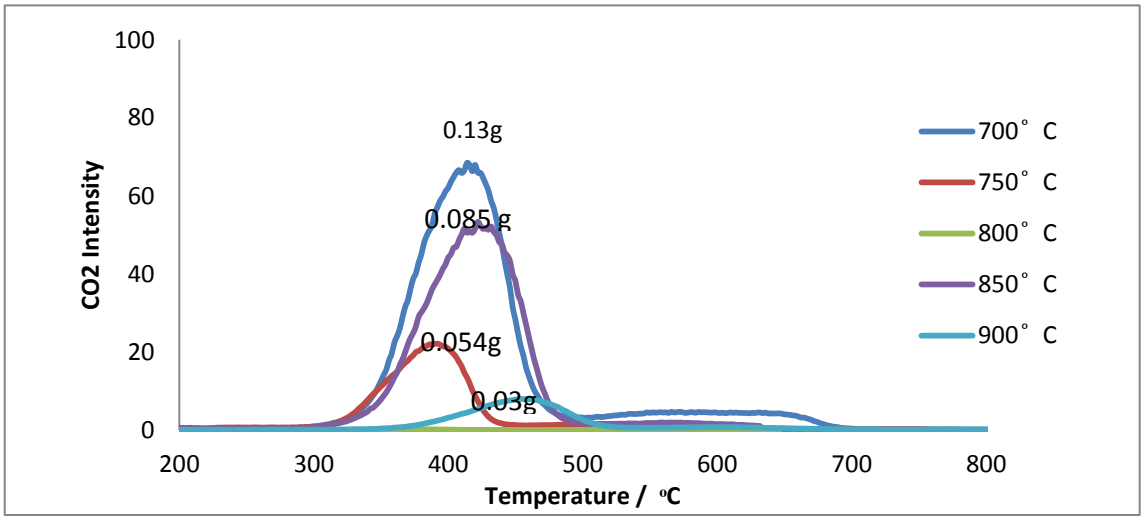

Fig 5-47- TPO profile at different temperatures of methane-rich dry reforming over Pechini 1Ni-LCZ in presence of 30 ppm H_2S

5.6.2.1 The influence of H_2S concentration on the Pechini 1Ni-LCZ pyrochlore catalyst

To determine the effect of H_2S concentration on catalyst performance, reactions were performed at 850 °C and at concentrations of 10 ppm and 30 ppm. As was expected, the increase in H_2S concentration increased the extent of 1Ni-LCZ catalyst poisoning. The results are shown in Fig 5- 48 to 52 during the reaction of a 2: 1 mixture of CH_4: CO_2 at 850 ° C.

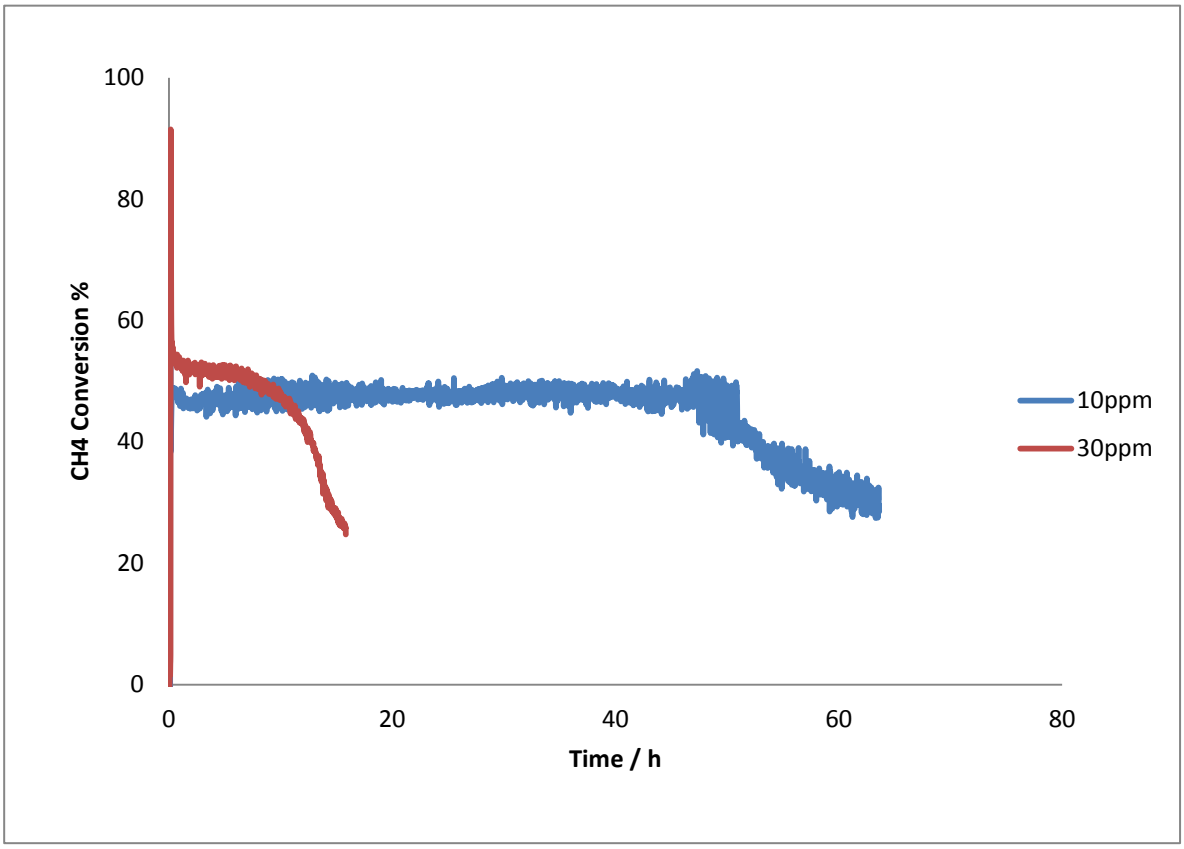

Fig 5-48- methane conversion for 2:1 CH_4:CO_2 reforming reaction over 1-NiLCZ at 850° C with different concentrations of H_2S

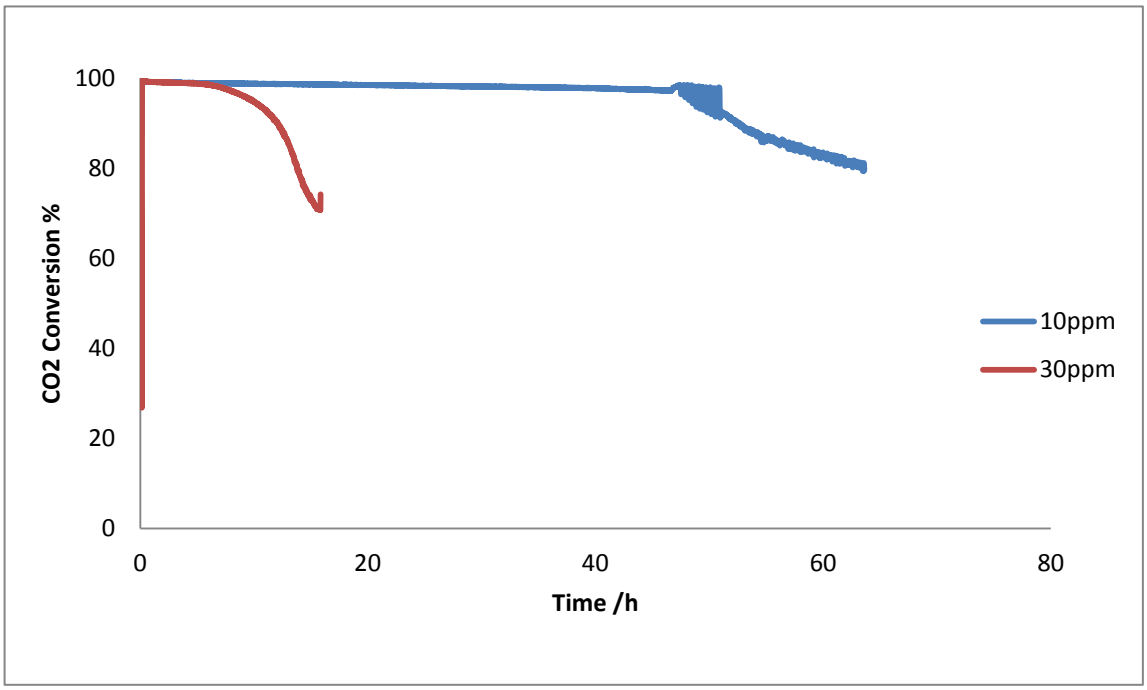

Fig 5-49- carbon dioxide conversion for 2:1CH_4:CO_2 reforming reaction over 1-NiLCZ at 850°C with different concentrations of H_2S

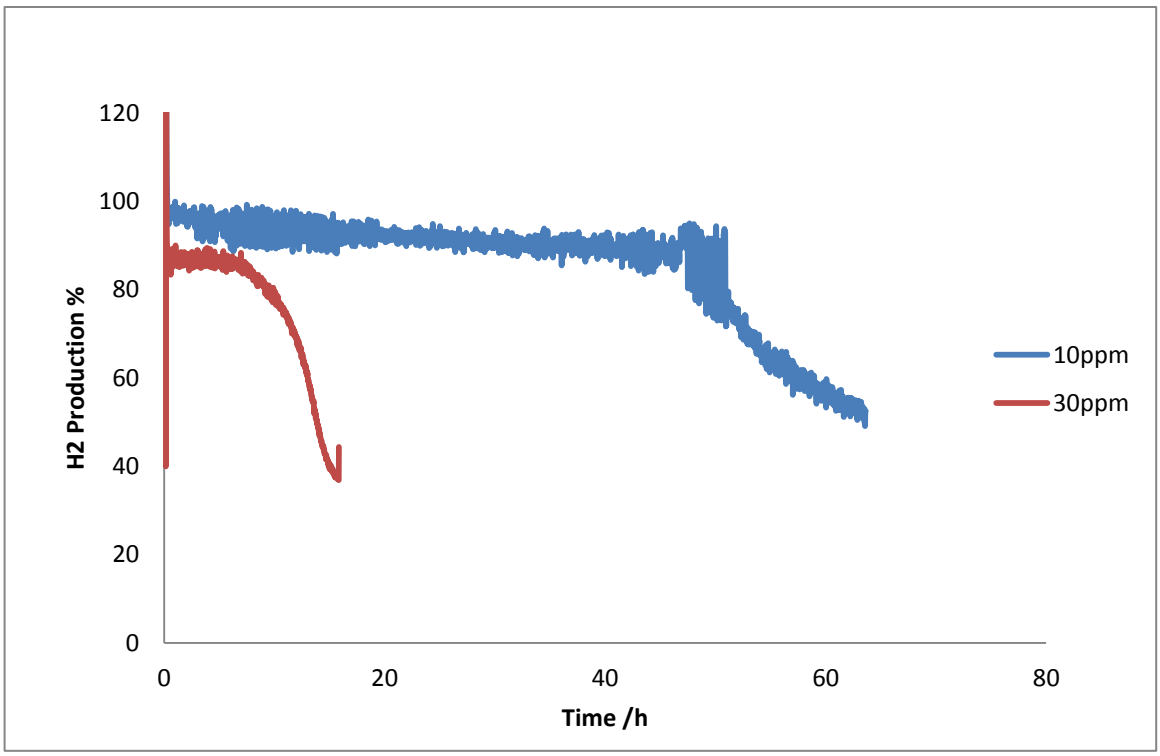

Fig 5-50- hydrogen yield for 2:1CH_4:CO_2 reforming reaction over 1-NiLCZ at 850°C with different concentrations of H_2S

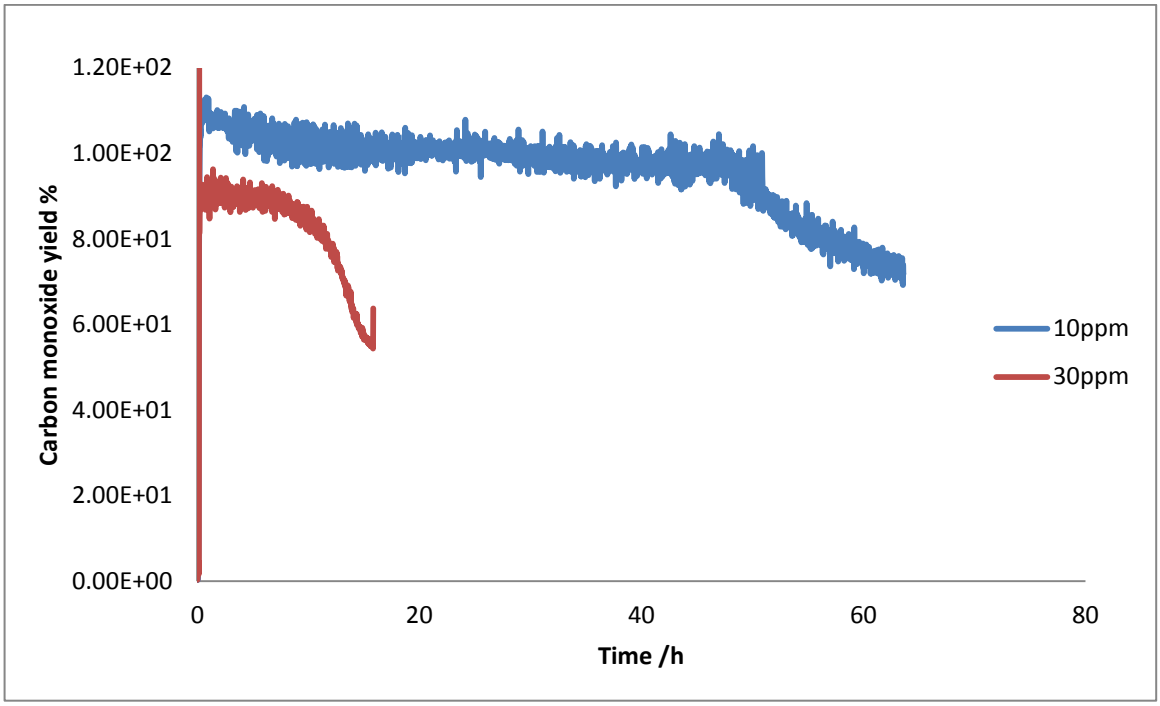

Fig 5-51- carbon monoxide yield for 2:1CH_4:CO_2 reforming reaction over 1-NiLCZ at 850° C with different concentrations of H_2S

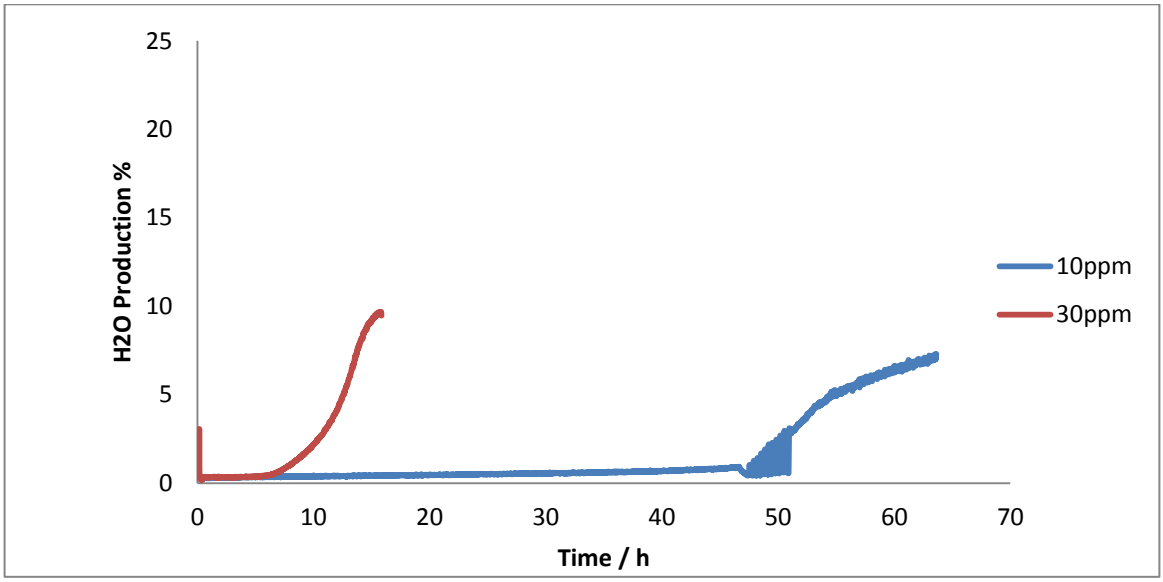

Fig 5-52- water yield for 2:1CH_4:CO_2 reforming reaction over 1-NiLCZ at 850° C with different concentrations of H_2S

As can see from fig 5- 48, the methane conversion at 10 ppm H_2S was stable for around 45 hours. However, after that, some level cycling was observed followed by a fairly linear decrease in the methane conversion as a result of sulphur poisoning. Increasing the sulphur

concentration to 30 ppm increased the rate of poisoning where the catalyst showed stability only for around 10 hours before a sharp decrease in its activity. At 30 ppm a slightly higher percentage of CH_4 conversion was seen for the first 5 hours of the reaction. This behaviour could be due to H_2S acting to encourage methane decomposition through the distribution of S across the catalyst surface. In the case of CO_2 conversion, both catalysts showed good correlation with the CH_4 conversion. The amount of CO in both catalysts was higher than the amount of H_2, and therefore the H_2S had a catalytic effect on the carbon dioxide reduction (eq 6). The obvious difference between the two catalysts in addition to the lifetime was in the amount of H_2 and CO yields where, as was seen, the amount of CO and H_2 at 30 ppm H_2S was lower than 10 ppm H_2S by 20%. The reasons may be attributed to the CO reduction reaction in the presence of Ce_2O_3 and as was discussed before.

5.6.2.2 Carbon deposition

As seen from fig 5- 53, the amount of carbon deposition increased with increasing the H_2S concentration. The reason could be due to the adsorbed sulphur blocking the lattice oxygen from oxidising the deposited carbon species. The presence of two TPO peaks at 270 °C and 375 °C for the 10ppm H_2S indicates two kinds of carbon species were present on the surface, which have similar reactivity. This carbon could be polymeric in nature deposited near the metal site in the pyrochlore structure. By increasing the concentration of H_2S to 30 ppm, only one TPO peak at 412 °C is observed.

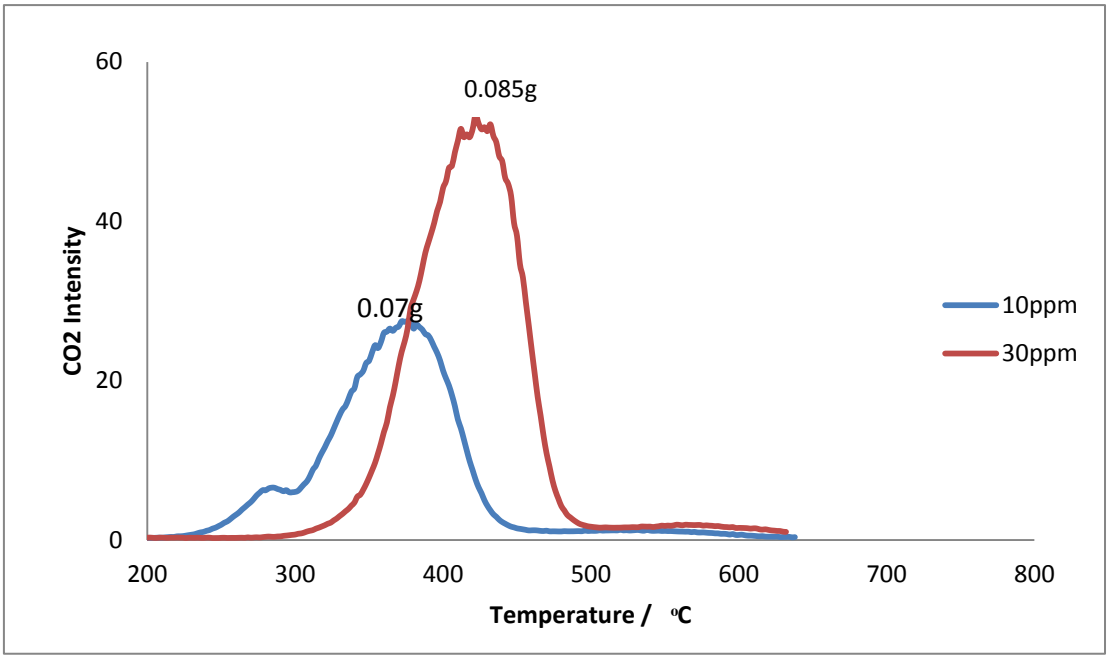

Fig 5-53- TPO profile at different concentration of H_2S during methane-rich dry reforming over Pechini 1Ni-LCZ at 850°C

5.7 The effect of H_2S on the 0.5Ru-LCZ-pyrochlore catalyst: -

5.7.1.1 The influence of temperature on the hydrothermal 0.5Ru-LCZ pyrochlore catalyst: -

To study the effect of doping with a noble metal on the performance of LCZ pyrochlore catalyst, 0.5Ru-LCZ was prepared by the hydrothermal method. Methane-rich dry reforming reactions were carried out at various temperatures in the range of 700°C-850°C and in the presence of 30 ppm H_2S. The results are shown in fig 5- 54 to 58.

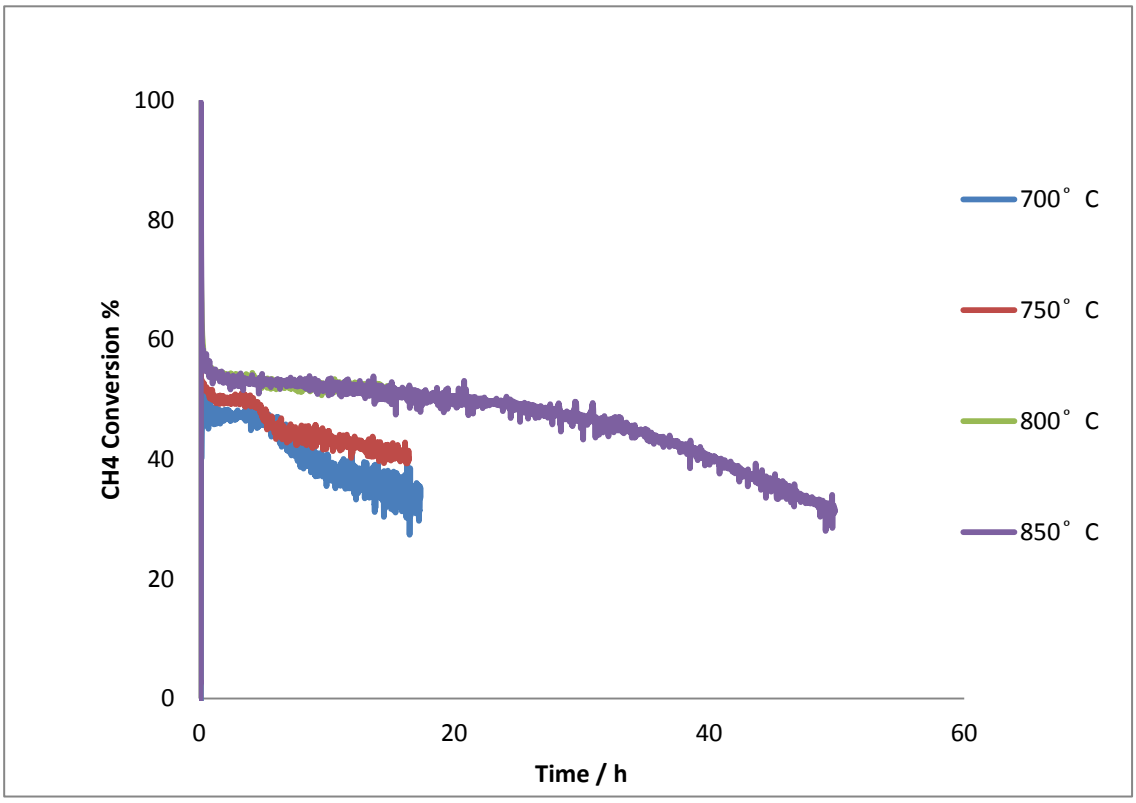

Fig 5- 54- percentage of methane conversion at different temperatures during methane-rich dry reforming over 0.5Ru-LCZ in presence of 30ppm H_2S

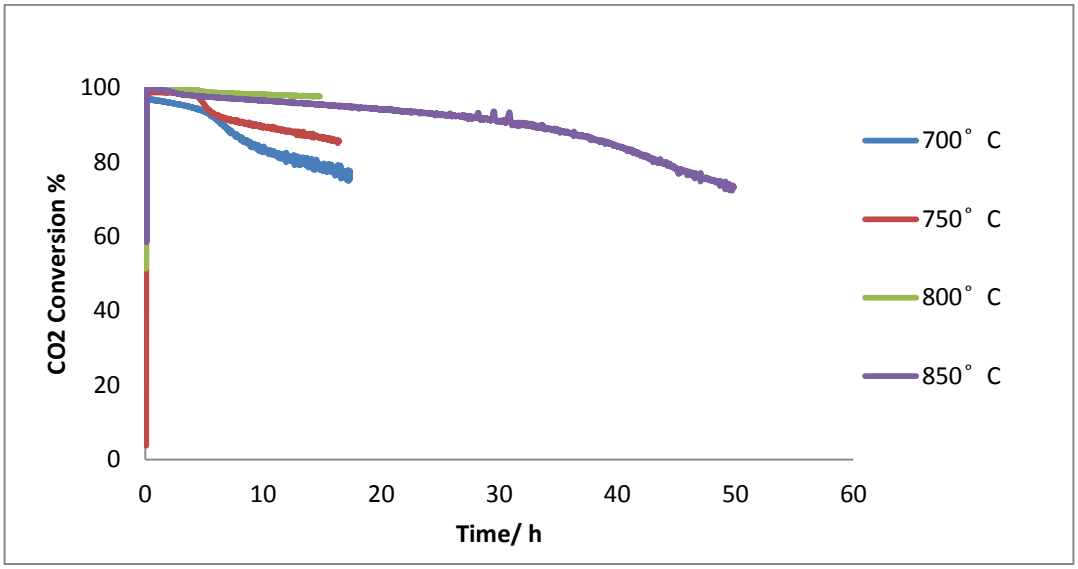

Fig 5- 55- percentage of carbon dioxide conversion at different temperatures during methane-rich dry reforming over 0.5Ru-LCZ in presence of 30 ppm H_2S

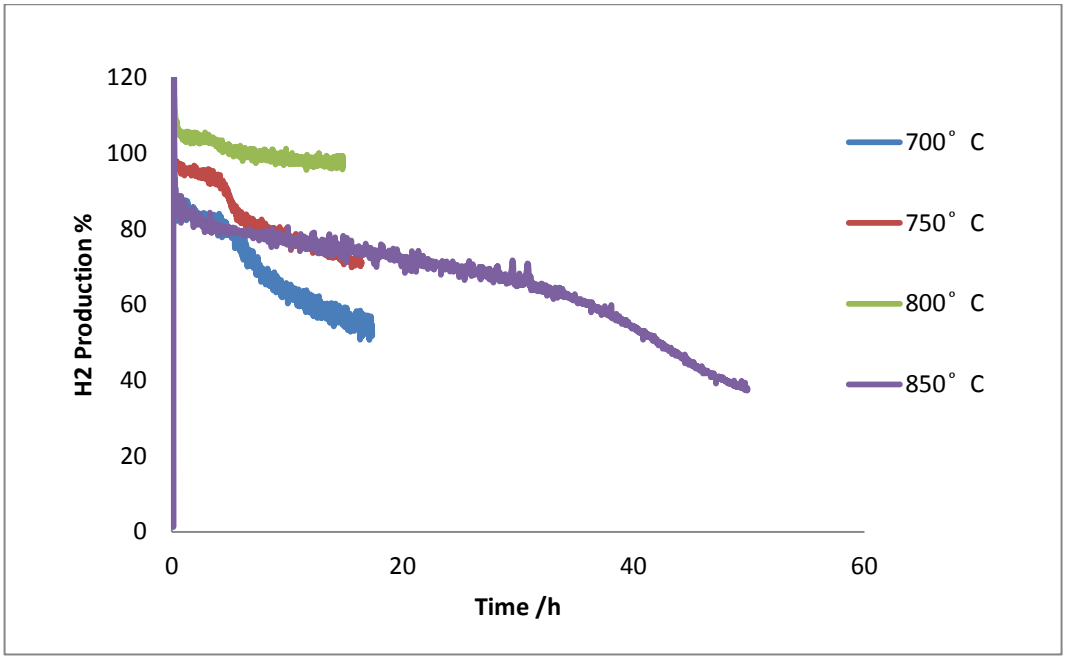

Fig 5- 56- percentage of hydrogen yield at different temperatures during methane-rich dry reforming over 0.5Ru-LCZ in presence of 30 ppm H_2S

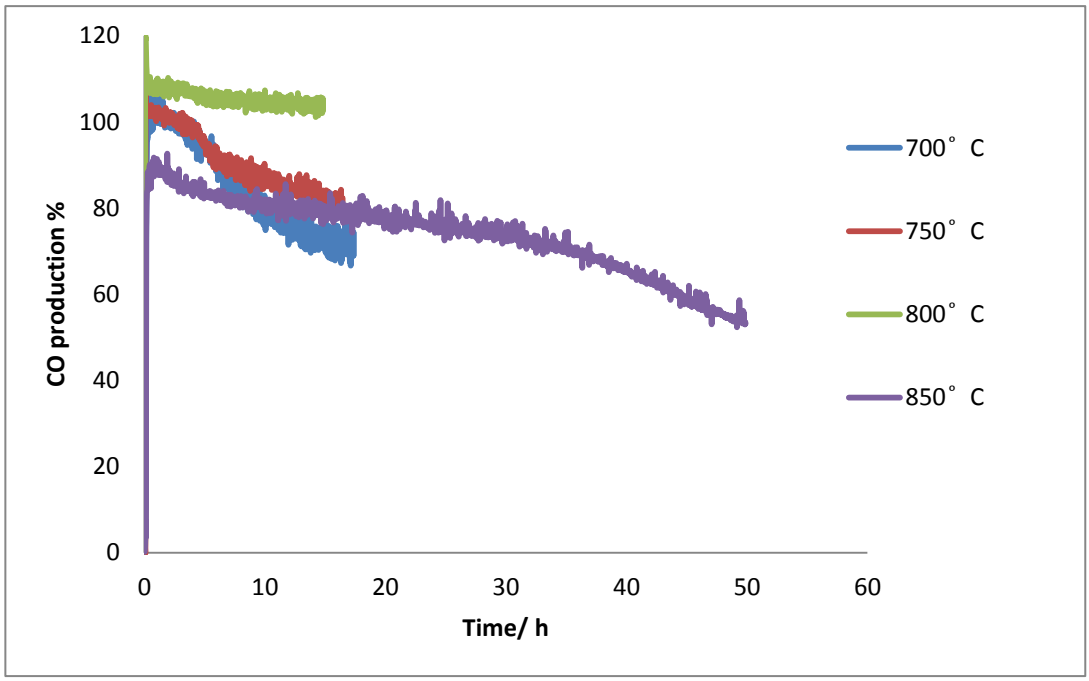

Fig 5- 57- percentage of carbon monoxide yield at different temperatures during methane-rich dry reforming over 0.5Ru-LCZ in presence of 30 ppm H_2S

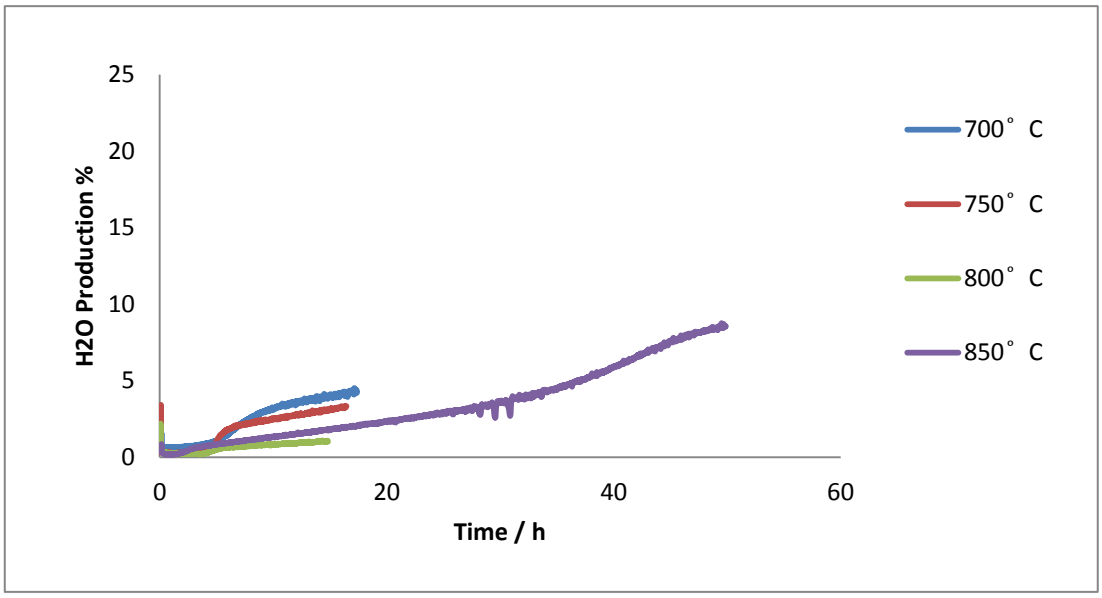

Fig 5- 58- percentage of water yield at different temperatures during methane-rich dry reforming over 0.5Ru-LCZ in presence of 30 ppm H_2S

In the case of CH_4 and CO_2 conversion, as can be seen from fig 5- 54 and 55, there is a direct inverse relationship between sulphur poisoning and the temperature of reaction for the Ru-LCZ pyrochlore catalyst. The reason is because the sulphur adsorption is thermodynamically favoured at lower temperature. At 700 ^{o} C there is a lower amount of H_2 in comparison with CO because of the water gas shift reaction (eq7). An increased amount of H_2O compared with other temperatures at the beginning of the reaction confirms this reaction. By increasing the temperature to 750 ° C, the rate of the first stage of the deactivation increased slightly because sulphur attacks more than one active site at the same moment. At 800 ° C, the amount of H_2 increased significantly and this is due to methane degradation (eq 10). The higher amount of CO is because of the presence of ceria in the structure which reacts with the adsorbed carbon (eq12). Increasing the temperature to 850 ^{o} C, the rate of deactivation decreased and the CO_2 conversion showed the same trend of CH_4 conversion. The initial amount of CO and H_2 was similar and less than expected by 20%. This decrease in the amount could be because of the CO reduction reaction (eq 9) and since no evidence of water was observed in the first period of the reaction it is suggested that the cause is due to the presence of ceria in the structure in the form of Ce_2O_3 as shown in the following:-

$H_2 + CO \leftrightarrow H_2O + C$……..eq 9

$Ce_2O_3 + H_2O \leftrightarrow 2CeO_2 + H_2$…….eq 13

$2CeO_2 + C \leftrightarrow Ce_2O_3 + CO$……eq 12

The presence of the higher amount of CO in comparison with H_2 in the second period of poisoning is because of the reaction between the CO_2 and H_2S at the higher temperatures. Two-stage of poisoning with no complete loss of reforming activity were observed at all temperatures and the reason could be due to the interaction of ceria with sulphur which is more favourable thermodynamically than the reaction between Ru and sulphur.[18]

The increase in the amount of water in the second stage of deactivation could be attributed to the reaction of ceria with H_2S where this amount increases with temperature increasing. (eq 2)

5.7.1.2 Carbon deposition: -

As shown in fig 5- 59, at 700 ° C, and due to Boudouard reaction, the amount of carbon deposited was at its highest level. The increase in temperature to 750 °C led to a reduced Boudouard reaction, resulting in a reduced amount of carbon deposition. Increasing the temperature further, caused a greater increase in the amount of carbon deposition. This may be due to methane degradation at high temperatures.

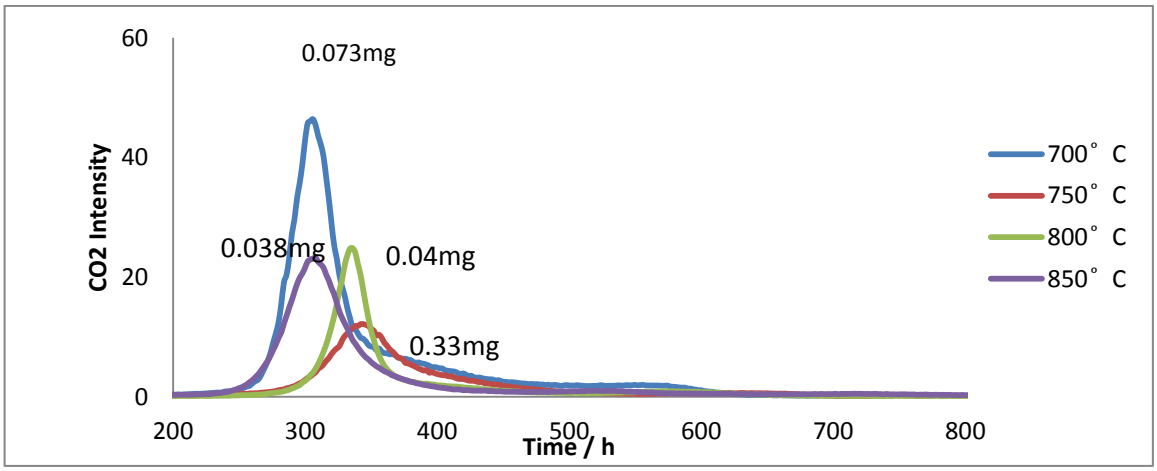

Fig 5-59- TPO profile of 0.5Ru-LCZ at different temperatures during methane-rich dry reforming in presence of 30ppm H_2S

The impact of poisoning temperature on Ru-LCZ can be concluded as below:

1- First stage of deactivation increases by increasing the temperature
2- The occupation of Ru atoms by sulphur, shift from one Ru atom at the lowest temperatures to binding two atoms as the temperature is increased
3- The amount of methane decomposition increases with increasing poisoning temperature.

4- At temperatures of 700° C and 850° C, the lower amount of H_2 is because of the water gas shift reaction and CO reduction reaction respectively.

5- A significant increase in the amount of H_2 at 800° C is because of methane decomposition.

6- The reaction of carbon dioxide increases with sulphur by increasing the temperature.

5.7.2.1 The influence of H_2S concentration on the hydrothermal 0.5Ru-LCZ pyrochlore catalyst: -

To evaluate the performance of the catalyst under various concentrations of H_2S (10 ppm and 30 ppm), the dry reforming reactions were carried out at 850° C. As expected, the increase in H_2S concentration increased the extent of 0.5-RuLCZ catalyst poisoning. The results are shown in Fig 5- 60 to 64 during the reaction of a 2:1 mixture of CH_4: CO_2 at 850 ° C.

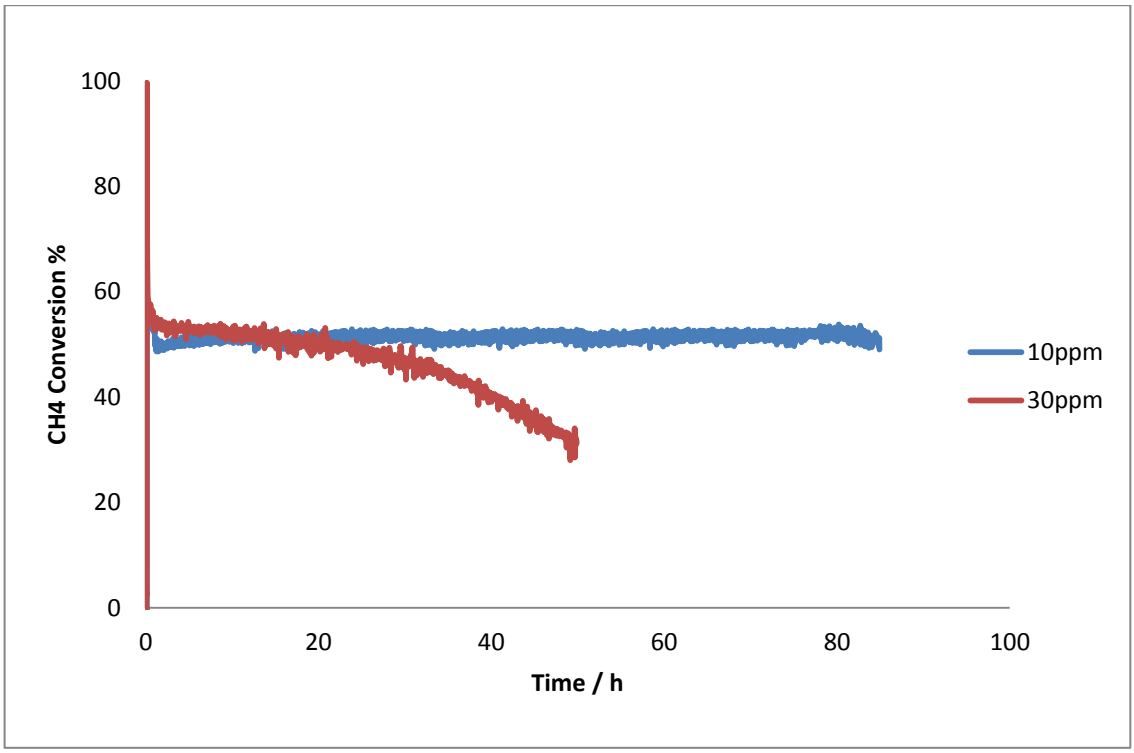

Fig 5-60- percentage methane conversion for 2:1CH_4:CO_2 reforming reaction over 0.5-Ru-LCZ at 850°C with different concentrations of H_2S

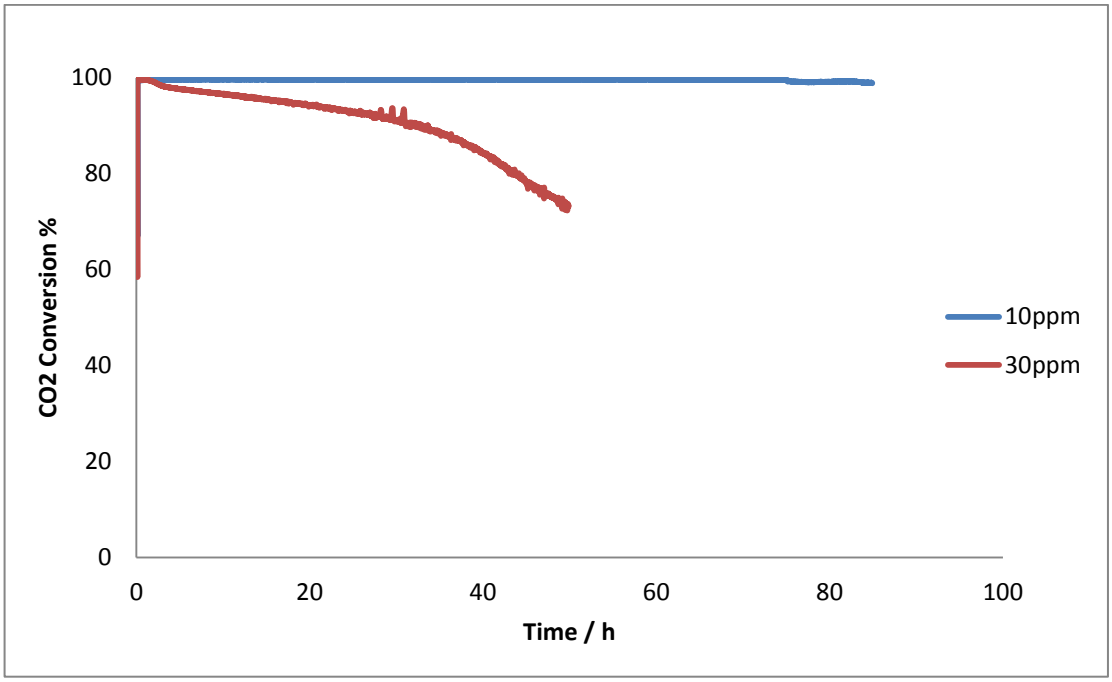

Fig 5-61- percentage carbon dioxide conversion for 2:1CH_4:CO_2 reforming reaction over 0.5Ru-LCZ at 850°C with different concentrations of H_2S

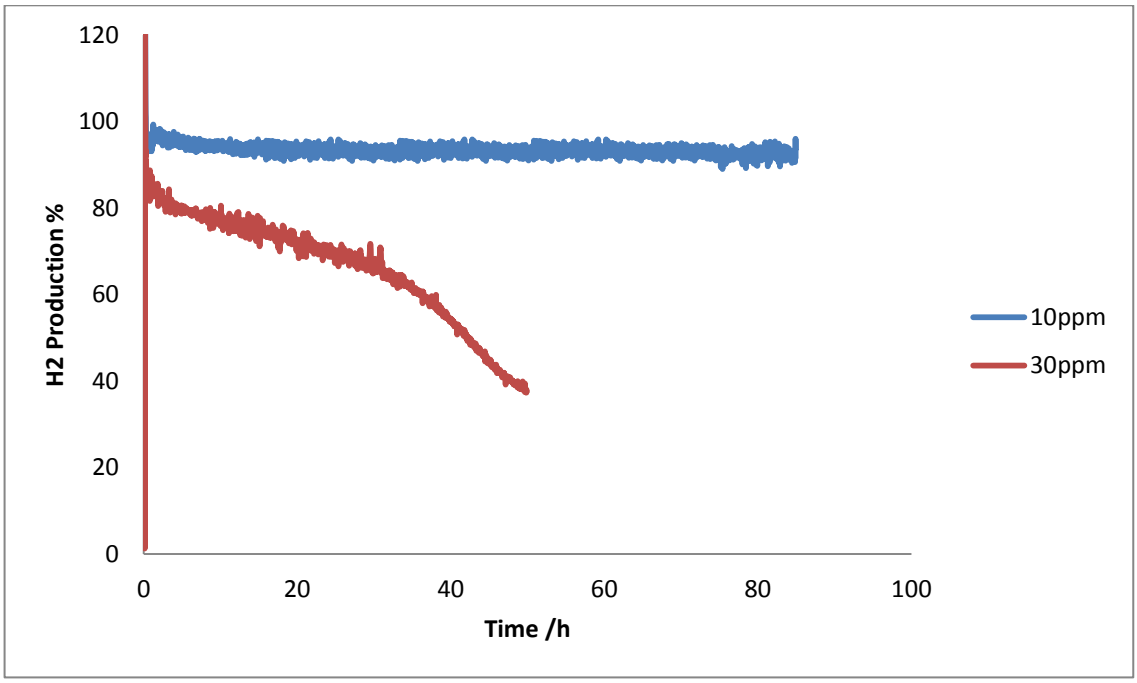

Fig 5-62- percentage hydrogen yield for 2:1CH_4:CO_2 reforming reaction over 0.5Ru-LCZ at 850°C with different concentrations of H_2S

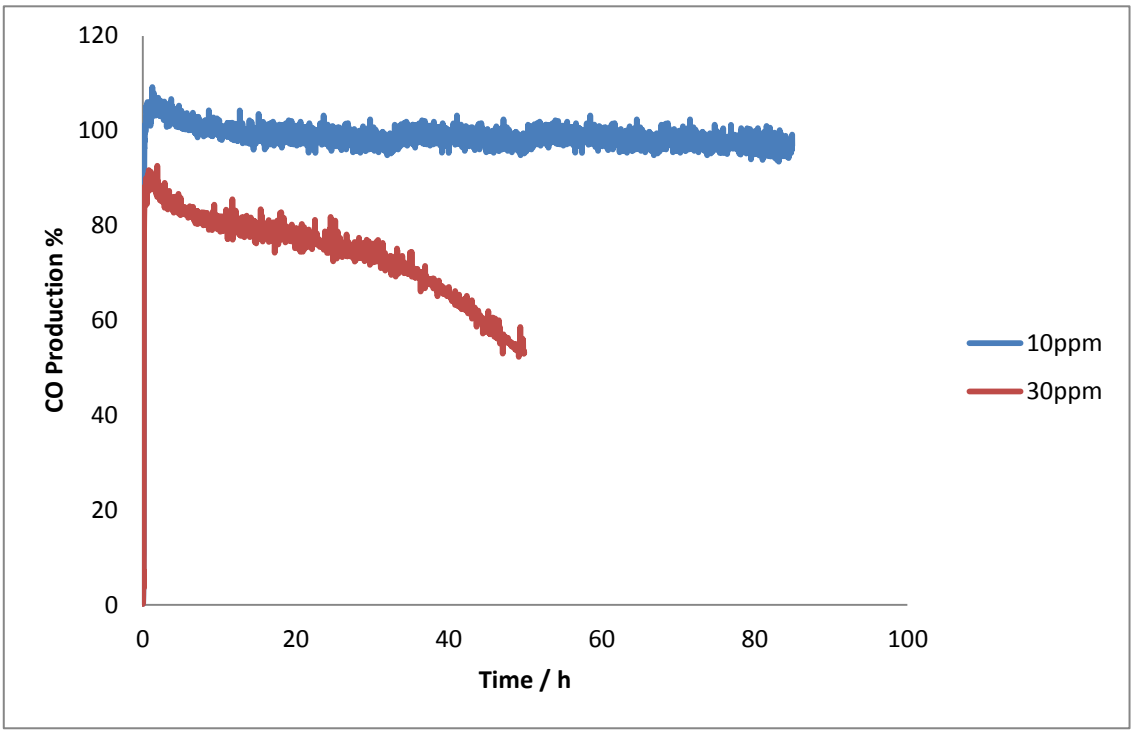

Fig 5-63- percentage carbon monoxide yield for 2:1CH_4:CO_2 reforming reaction over 0.5Ru-LCZ at 850°C with different concentrations of H_2S

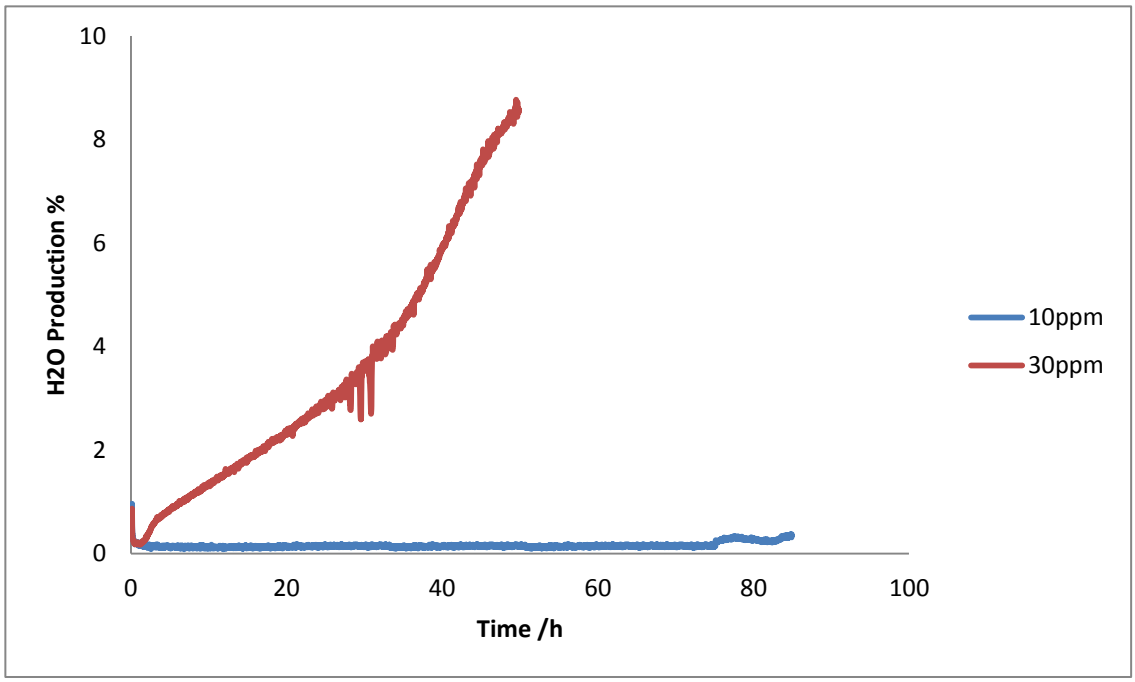

Fig 5-64- percentage water yield for 2:1CH_4:CO_2 reforming reaction over 0.5Ru-LCZ at 850°C with different concentrations of H_2S

At a concentration of 10 ppm, a highly stable reforming activity was observed over time. At this concentration the 0.5Ru-LCZ catalyst did not show any reduction in its activity for 80 hours. The amount of all conversion and production of gases was comparable with the equilibrium state. When 30 ppm of H_2S was added to the reactant stream, a slightly higher conversion was observed for methane in the first 10 hours of reaction. The reason could be because of the catalytic promotion by H_2S, but over the same time a gradual decrease in CO_2 conversion was noticeable. The `reason could be because of the presence of ceria in the structure of the Ru-catalyst ,where in the higher concentration of H_2S, the amount of ceria was decreased due to the interaction of ceria with sulphur, and as a result there was a decrease in the amount of CO_2 conversion by ceria. The lower amount of H_2 at 30 ppm H_2S by 20% could also be attributed to the CO reduction reaction in the presence of Ce_2O_3 as was discussed before. The presence of a larger amount of water at 30 ppm H_2S compared to 10 ppm H_2S provides support for this suggestion.

It can be concluded that the presence of ceria in an excess amount of H_2S has a dual function. On one side, at the beginning of the reaction, it increases the methane conversion capacity by maintaining a clean surface, in addition to decreasing the amount of H_2O, C and the CO_2 conversion. On the other hand, in the second stage of deactivation, ceria delays the poisoning of the Ru and increases the amount of water through its reaction with sulphur. (eq2)

5.7.2.2 Carbon deposition:-

As can be seen from the TPO profile of deposited carbon in fig 5-65, there was a decreasing trend of carbon deposition with the amount of H_2S concentration. At 30 ppm H_2S, more carbon deposition was suppressed due to the formation of Ce_2O_2S which acts as protective cover. At 10 ppm H_2S, more sites are available for reaction with more carbon and it was also noticeable from the TPO profile that an increase in H_2S concentration did

not change the type of carbon that formed during the reforming reaction. Therefore, it could be suggested that the carbon deposition occurs in the first phase of deactivation and the nature of carbon is likely to be graphitic as the Boudouard reaction is unlikely at high temperature.

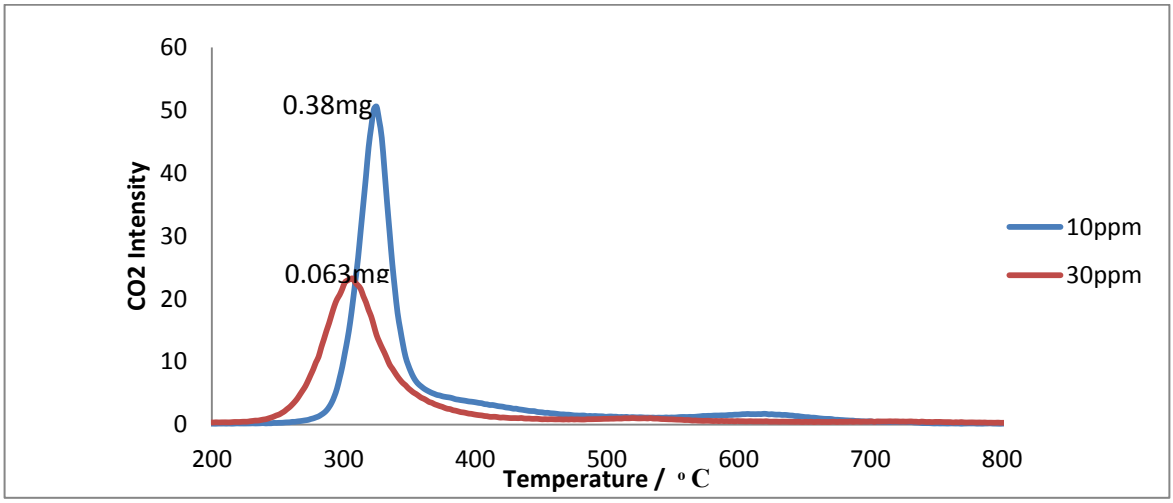

Fig 5-65- TPO profile of 0.5Ru-LCZ at 850 C during methane-rich dry reforming in different H_2S concentration

The impact of H_2S concentration on Ru-LCZ can be concluded as below:

1- The lifetime of the reforming reaction increased by decreasing the H_2S concentration
2- A high amount of H_2S has catalytic promotion on methane conversion and on CO reduction reaction at the beginning of the reaction
3- Increasing the H_2S concentration decreases the amount of carbon deposition over time through the formation of a protective cover in the form of Ce_2O_2S at the second stage of poisoning

5.8 The effect of metal and preparation method on sulphur poisoning during methane-rich dry reforming at one glance

In this section, due to the global warning of CO_2 and the need for clean and renewable fuel, the effect of metal and catalyst preparation method was studied on CO_2 conversion and H_2 production during methane rich dry reforming, including an investigation in the presence of H_2S.

5.8.1.1-The effect of poisoning temperature:

The amount of CO_2 conversion and H_2 yield were compered on Ni-LCZ catalyst prepared by hydrothermal and Pechini methods and 0.5 Ru-LCZ pyrochlore catalyst prepared by the hydrothermal method in the temperature range 700°C to 850°C in the presence 30 ppm of H_2S.

As can be seen from the results in fig 5- 66 and 67, 0.5 Ru-LCZ shows the best reforming activity at all temperature when compared with the Ni-LCZ catalysts. This higher resistance to sulphur poisoning was attributed to the potential for the Ru to resist H_2S binding. The 1Ni-LCZ catalyst showed the same trend of deactivation and the difference was in the lifetime, where the catalyst prepared by the Pechini method showed higher hydrogen production and CO_2 conversion in comparison to those by the hydrothermal preparation method. The better performance of the catalyst prepared by the Pechini method could be because of greater Ni dispersion on LCZ.

Analysis of the deposited carbon showed a high level of carbon deposition resulting from the Boudouard reaction at 700°C and low levels of carbon in the Ni-LCZ catalysts at 800°C, is as a result of Ce_2O_3 formation which acts as a protective cover. Also, as can be seen from fig 5- 68, a higher amount of carbon was deposited on the 1-NiLCZ catalyst, which was prepared by hydrothermal method and the temperature of carbon deposition was also at higher temperatures in comparison with other catalysts.

The amount of carbon deposition for the Pechini method sample was nearly at the same level as the Ru catalyst at low temperatures and, as can be seen, the carbon deposited on the Ru catalyst was at a lower temperature in comparison with other catalysts

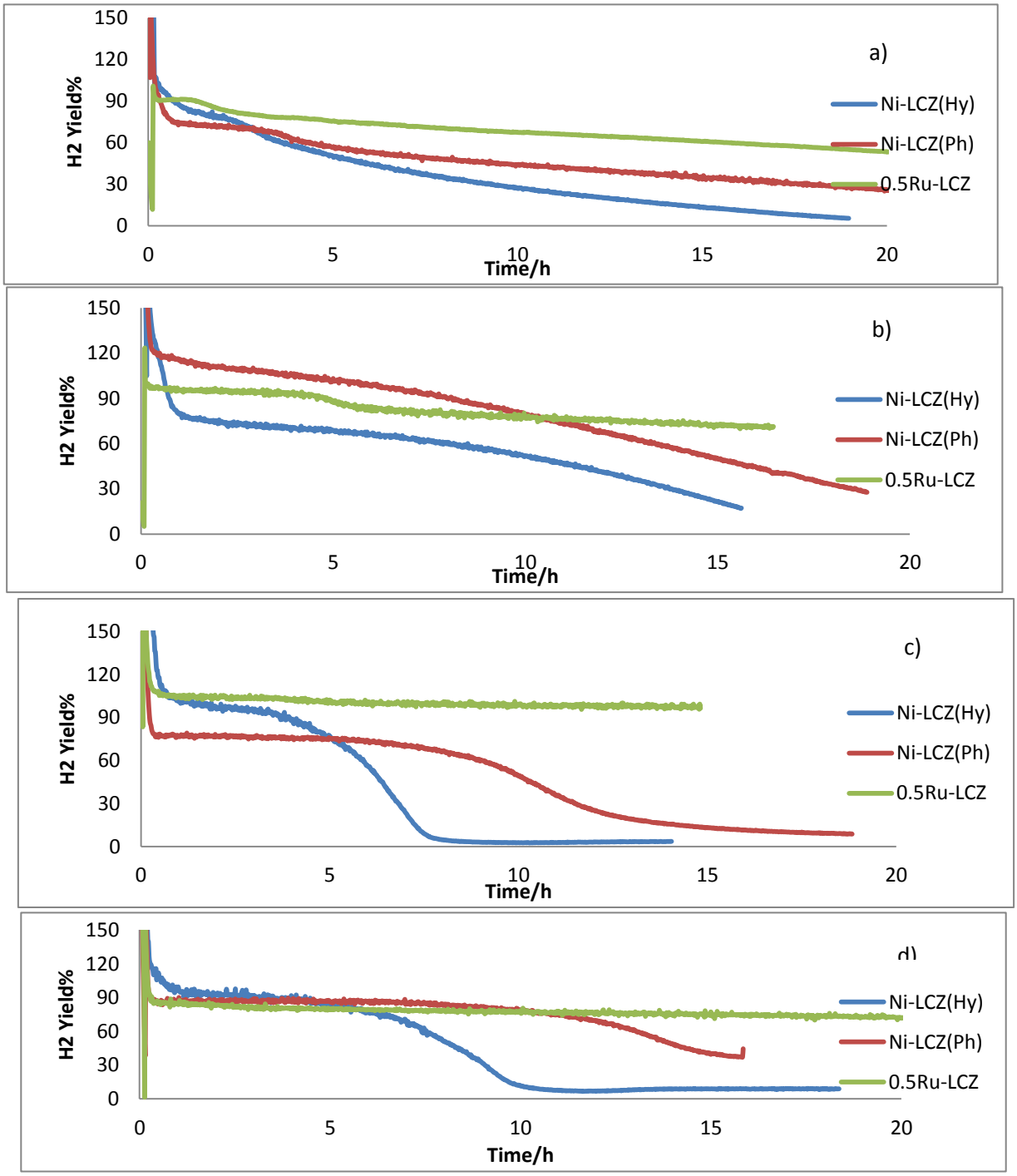

Fig 5- 66- Effect of temperature on H_2 yield at a)700° C b)750° C c)800° C d)850° C in various catalyst in presence of 30 ppm H_2S

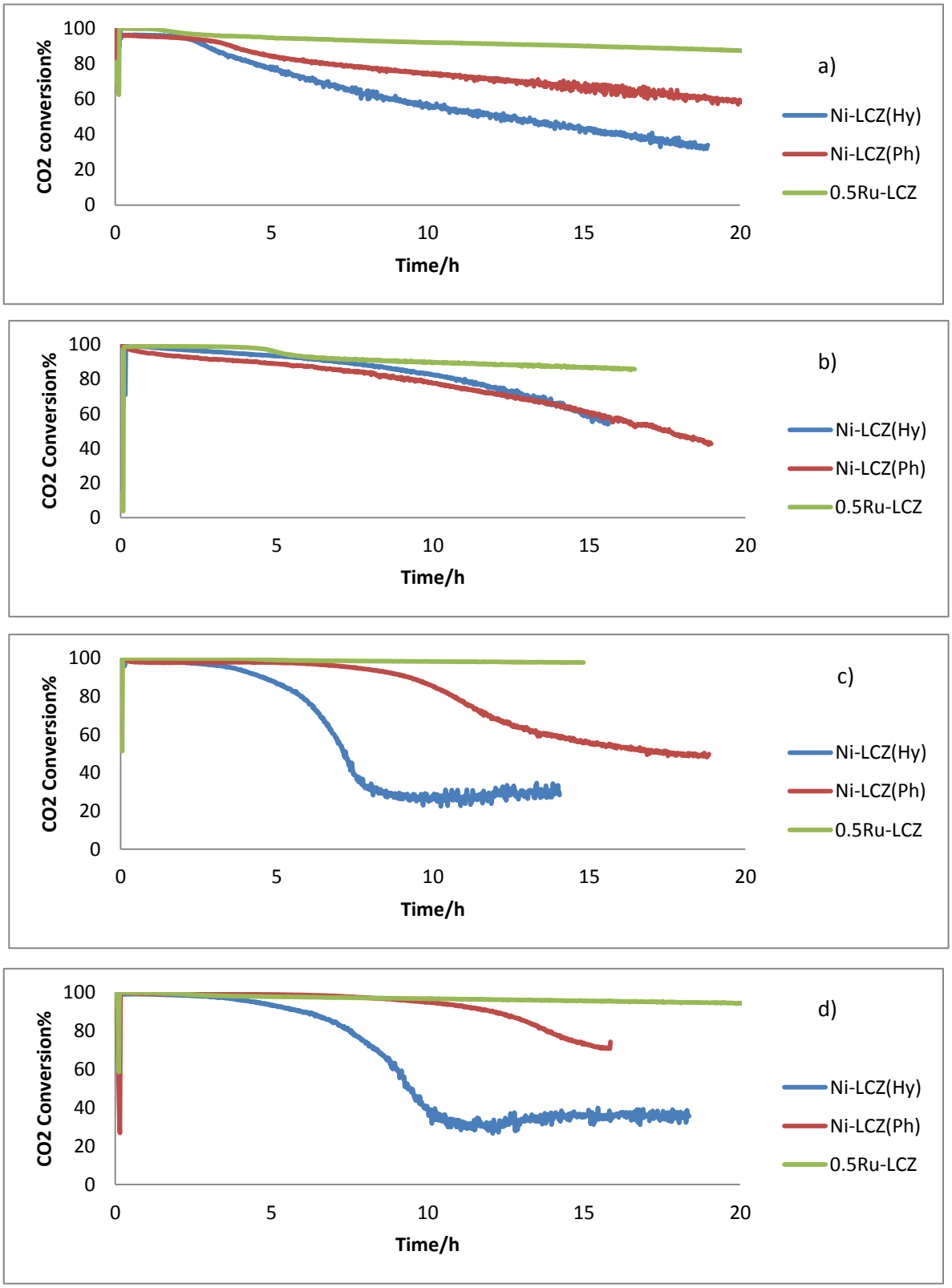

Fig 5-67- Effect of temperature on CO_2 conversion at a)700°C b)750°C c)800°C d)850°C in various catalyst in presence of 30 ppm H_2S

5.8.1.2 Carbon deposition:-

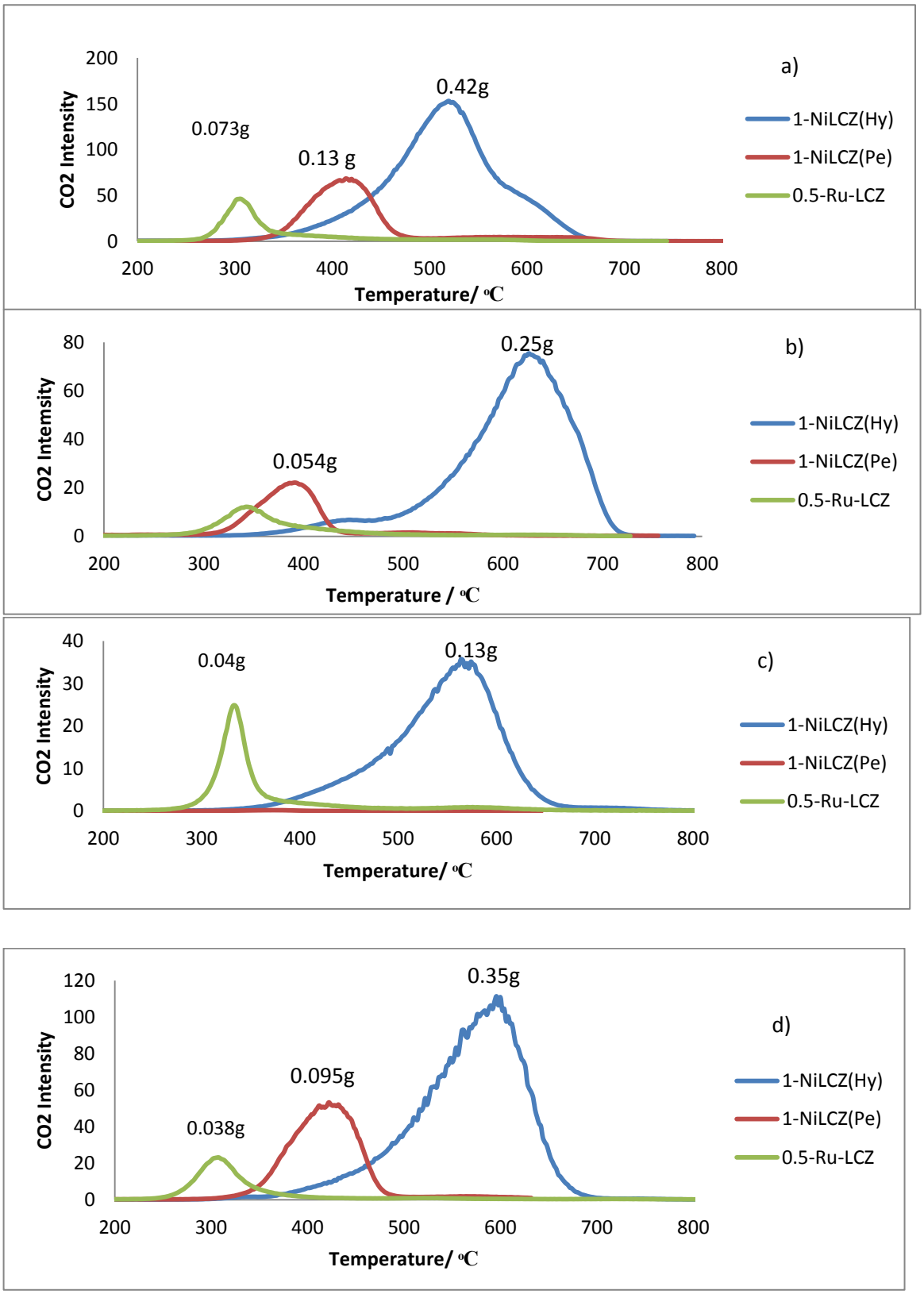

Fig 5-68- TPO profile at a)700° C b)750° C c)800° C d)850° C in various catalysts in presence of 30 ppm H_2S

5.8.2 Long term stability

To evaluate the effect of H_2S at a low concentration on materials prepared by different methods and with different metals, the reactions were performed at a temperature of 850°C and in 10 ppm of H_2S.

As can be seen from fig 5-65, at 10 ppm H_2S both the Ni catalysts showed nearly the same trend and nearly the same percentage of H_2 production and CO_2 conversion during the 50 hours of the reaction. During the end period of reforming activity, the hydrothermal method catalyst showed more cycling behaviour before a linear loss in activity in comparison to the Pechini method catalyst. The Ru-catalyst did not show any loss in activity at this level of concentration. The amount of H_2 yield at the end of 70 hours in the hydrothermal method was 10% higher than the Pechini method but the percentage of CO_2 conversion in both Ni catalysts was nearly the same and lower than the Ru catalyst by 20%.

In the case of the carbon deposition, both Ni catalysts had the same kind of TPO profile but with a difference in temperature of deposition, which was higher for the hydrothermal method. Only one sharp carbon peak was seen for the Ru-catalyst at the low temperature of 335°C.

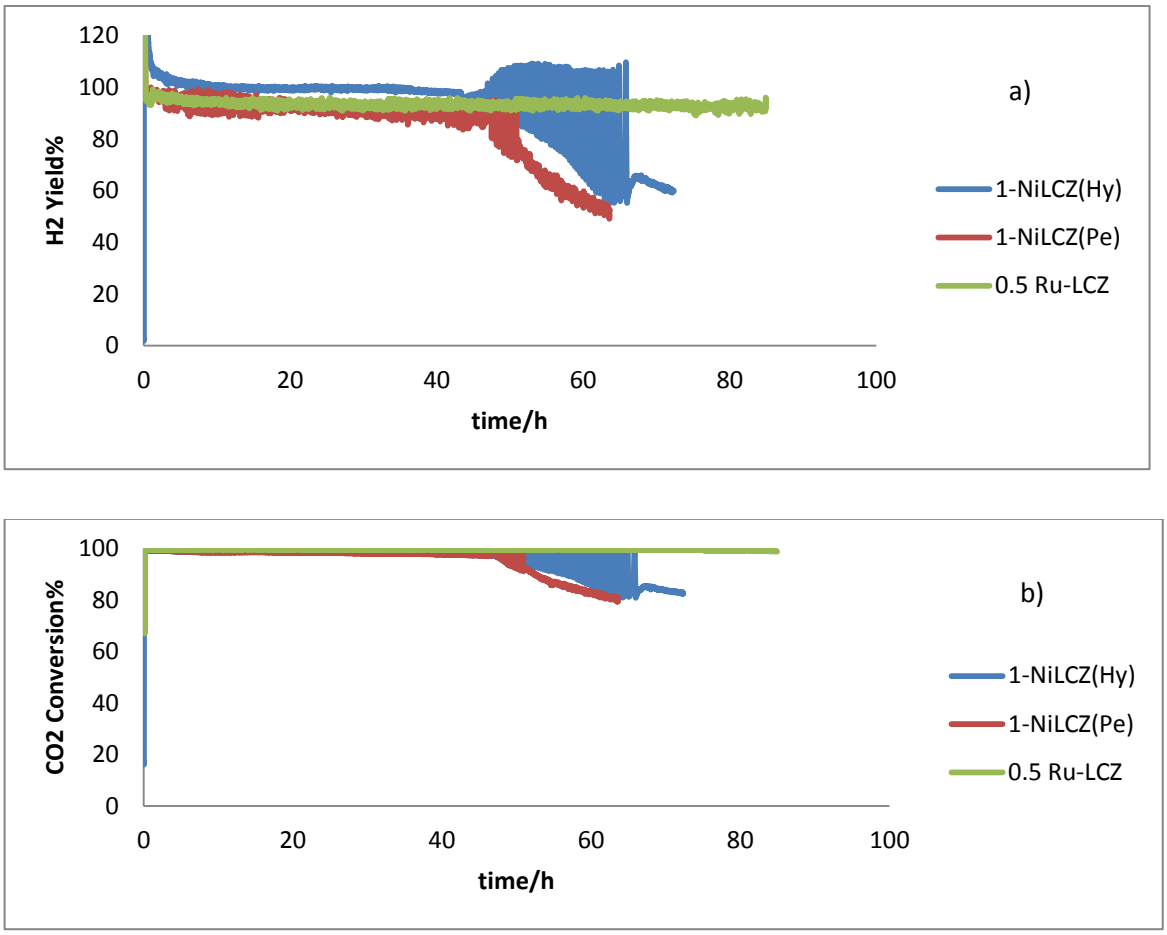

Fig 5-69- percentage of a) H_2 yield and b) CO_2 conversion for three difference catalyst at 850°C and in presence of 10 ppm H_2S during 2:1 CH_4:CO_2 dry reforming

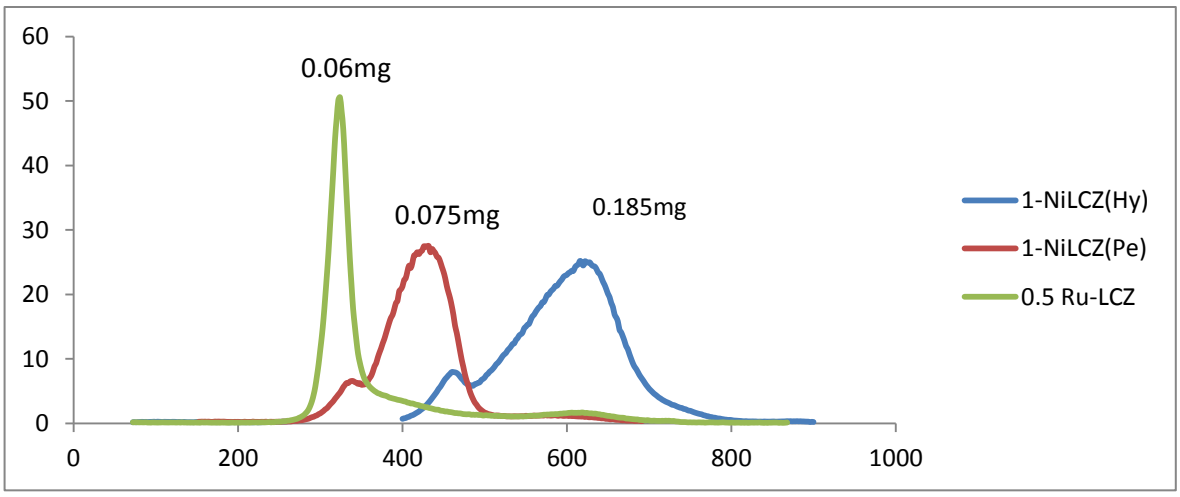

Fig 5-70-TPO profile for various catalyst at 850°C and in presence of 10 ppm H_2S during 2:1 CH_4:CO_2 dry reforming

5.9 Conclusion:-

All pyrochlore catalysts in this work regardless of the preparation method and the type of doped metal have shown two stages of loss of reforming activity. The first stage is because of dissociative chemisorption of H_2S and the second stage of deactivation is linked to the formation of bulk metal sulphide species.

The first stage of deactivation is affected by the amount of Ni in the catalyst, preparation method, type of metal, initial H_2S concentration and the temperature of the poisoning reaction.

The first stage deactivation was accelerated by decreasing the amount of Ni in the catalyst with 0.25 Ni-LCZ having less active Ni sites and therefore showing faster deactivation. Generally, the Pechini preparation method showed higher resistance to deactivation than the hydrothermal method. The first stage of deactivation was delayed significantly at the higher temperatures and this resistance may be due to the structure of the catalyst. Because of the high activation energy for the catalytic process for Ru in comparison with Ni, the first stage deactivation was not observable during 20 hours at 800 and 850 ^{o}C. The loss of reforming activity was significantly lower than Ni catalysts.

By increasing the temperature, the first stage deactivation accelerates in all materials. This can be attributed to the reaction of one sulphur with more than one active site at a time. The first deactivation stage was significantly faster in 30 ppm than 10 ppm due to a dramatic decrease in active sites.

The CO_2 conversion was in good correlation with the CH_4 conversion for the Ru catalyst, while all Ni-doped pyrochlore catalysts showed higher CO_2 conversion. This can be attributed to the reaction of cerium oxide and CO_2 with H_2S.

All Ni-doped catalysts encouraged the CO reduction reaction that decreased the amount of H_2 and increased water formation.

Cycling behaviour in the reforming profile was affected by the Ni amount, catalyst preparation method, concentration of H_2S, temperature and the nature of the metal-dopant. By increasing the poisoning temperature, the cycling behaviour increased in both Ni Pechini and low content Ni hydrothermal catalyst. The decrease in the H_2S concentration increased the cycling behaviour as a result of redox properties of cerium oxide. The Ru catalyst showed high stability in its reforming profile at the high temperatures and in the low H_2S concentration.

In the Ni materials, the amount of carbon deposition increased with decreasing temperature, unlike the Ru catalyst that showed a direct relationship.

In the case of the Ni catalysts, the amount of carbon deposition increased with increasing H_2S concentration, while higher carbon was deposited on the Ru catalyst in the low H_2S concentration.

Increasing the amount of nickel led to increasing carbon deposition amount.

A lower amount of carbon was deposited on the Pechini catalyst than the hydrothermal method. At the lower temperature, the amount of carbon deposition was nearly at the same level as the Ru catalyst.

5.10 References: -

1-Ashrafi, M., Pfeifer, C., Pröll, T. and Hofbauer, H., 2008. Experimental study of model biogas catalytic steam reforming: 2. Impact of sulfur on the deactivation and regeneration of Ni-based catalysts. *Energy & Fuels*, *22*(6), pp.4190-4195.

2-Rostrup-Nielsen, J.R., Sehested, J. and Nørskov, J.K., 2002. Hydrogen and synthesis gas by steam-and C02 reforming.

3-Nasri, N.S., Jones, J.M., Dupont, V.A. and Williams, A., 1998. A comparative study of sulfur poisoning and regeneration of precious-metal catalysts. *Energy & fuels*, *12*(6), pp.1130-1134.

4-Rostrup-Nielsen, J.R., 1968. Chemisorption of hydrogen sulfide on a supported nickel catalyst. *Journal of Catalysis*, *11*(3), pp.220-227.

5-Hansen, J.B. and Rostrup-Nielsen, J., 2009. Sulfur poisoning on Ni catalyst and anodes. *Handbook of Fuel Cells–Fundamentals, Technology and Applications*, *6*, pp.1-13.

6-Niakolas, D.K., 2014. Sulfur poisoning of Ni-based anodes for solid oxide fuel cells in H/C-based fuels. *Applied Catalysis A: General*, *486*, pp.123-142.

7-1-Izquierdo, U., García-García, I., Gutierrez, Á.M., Arraibi, J.R., Barrio, V.L., Cambra, J.F. and Arias, P.L., 2018. Catalyst Deactivation and Regeneration Processes in Biogas Tri-Reforming Process. The Effect of Hydrogen Sulfide Addition. *Catalysts*, *8*(1), p.12.

8- Boldrin, P., Ruiz-Trejo, E., Mermelstein, J., Bermúdez Menéndez, J.M., Ramírez Reina, T. and Brandon, N.P., 2016. Strategies for carbon and sulfur tolerant solid oxide fuel cell materials, incorporating lessons from heterogeneous catalysis. *Chemical reviews*, *116*(22), pp.13633-13684.

9- Lohsoontorn, P., Brett, D.J.L. and Brandon, N.P., 2008. Thermodynamic predictions of the impact of fuel composition on the propensity of sulphur to interact with Ni and ceria-based anodes for solid oxide fuel cells. *Journal of Power Sources*, *175*(1), pp.60-67.

10- Devianto, H., Yoon, S.P., Nam, S.W., Han, J. and Lim, T.H., 2006. The effect of a ceria coating on the H2S tolerance of a molten carbonate fuel cell. *Journal of Power Sources*, *159*(2), pp.1147-1152.

11- He, H., Gorte, R.J. and Vohs, J.M., 2005. Highly sulfur tolerant Cu-ceria anodes for SOFCs. *Electrochemical and Solid-State Letters*, *8*(6), pp.A279-A280.

12- Kurokawa, H., Sholklapper, T.Z., Jacobson, C.P., De Jonghe, L.C. and Visco, S.J., 2007. Ceria nanocoating for sulfur tolerant Ni-based anodes of solid oxide fuel cells. *Electrochemical and solid-state letters*, *10*(9), pp.B135-B138.

13- Gorte, R.J., Kim, H. and Vohs, J.M., 2002. Novel SOFC anodes for the direct electrochemical oxidation of hydrocarbon. *Journal of Power Sources*, *106*(1-2), pp.10-15.

14-Laycock, C.J., Staniforth, J.Z. and Ormerod, R.M., 2011. Biogas as a fuel for solid oxide fuel cells and synthesis gas production: effects of ceria-doping and hydrogen sulfide on the performance of nickel-based anode materials. *Dalton Transactions*, *40*(20), pp.5494-5504.

15-Evans, S.E., 2017. *Catalytic reforming of biogas using nickel based perovskite materials* (Doctoral dissertation, Keele University).

16- Fidalgo, B., Muradov, N. and Menéndez, J.A., 2012. Effect of H2S on carbon-catalyzed methane decomposition and CO2 reforming reactions. *international journal of hydrogen energy*, *37*(19), pp.14187-14194.

17-) Laosiripojana, N., Charojrochkul, S., Kim-Lohsoontorn, P. and Assabumrungrat, S., 2010. Role and advantages of H2S in catalytic steam reforming over nanoscale CeO2-based catalysts. Journal of Catalysis, 276(1), pp.6-15.

18- Hennings, U. and Reimert, R., 2007. Noble metal catalysts supported on gadolinium doped ceria used for natural gas reforming in fuel cell applications. Applied Catalysis B: Environmental, 70(1-4), pp.498-508

19-Gaur, S., Pakhare, D., Wu, H., Haynes, D.J. and Spivey, J.J., 2012. CO2 reforming of CH4 over Ru-substituted pyrochlore catalysts: effects of temperature and reactant feed ratio. *Energy & Fuels*, *26*(4), pp.1989-1998.

20-Kumar, N., Roy, A., Wang, Z., L'Abbate, E.M., Haynes, D., Shekhawat, D. and Spivey, J.J., 2016. Bi-reforming of methane on Ni-based pyrochlore catalyst. *Applied Catalysis A: General*, *517*, pp.211-216.

6. Catalyst recovery from sulphur poisoning:

6.1 Introduction:-

Sulphur compounds present in biomass syngas decrease the reforming activity of the catalyst due to the strong chemisorption of sulphur on the metal surface[1-3]. As Ni surface chemisorption of sulphur is reversible, the catalyst can recover its activity in a reducing environment at high temperature.[4] The problems with this treatment are that they involve consuming a large volume of sulphur free reducing gas in addition to a slow sulphur removal rate that decreases exponentially with time. In industry, sulphur poisoned reforming catalysts are regenerated by steam treatment via the following reaction:-

$Ni\text{-}S + H_2O \leftrightarrow NiO + H_2S$……..eq1

$H_2S + 2H_2O \leftrightarrow SO_2 + 3H_2$…..eq2

$Ni + H_2O \leftrightarrow NiO + H_2$……..eq3

After sulphur removal, the nickel oxide is reduced in H_2 and then put back to the reforming system. The major disadvantage of this process is its long-time treatment that requires 2-3 days.

Four steps regenerations including 1-oxidation at 750 °C in 1% O_2, 2-decomposition at 900 ^{o}C in an inert gas, 3-reduction at 900^{o}C in 2% H_2 and 4-reaction at 900^{o}C under reforming conditions was reported in Liyu for restoring catalytic activity in a more effective and time –efficient manner[5].

Under the right conditions of temperature, time and concentration of initial poisoning [6-9], the catalyst can recover its activity after sulphur desorbs into the gas form as SO_2, CS_2 or H_2S[10-12].

Ashrafi observed that the initial activity can be recovered partially by removing hydrogen sulphide and in comparison with a temperature of 700°C; the activity was stable at 900°C in the presence of H_2S[11].

Shakouri examined the effect of preparation method on regeneration. Their results showed that the catalyst made by impregnation was more active than that by a coprecipitation method.[12]

In comparison between cermet materials and Ni-doped perovskites the recovery after H_2S removal treatment increased by increasing the concentration of sulphur, despite all materials showing no activity at the first period of recovery. At a high concentration of H_2S, the Ni cermet recovered its activity much less than the Ni-doped perovskite, while at the low concentration, the difference was negligible. The study also showed the effect of recovery temperature on catalyst reforming activity. Generally, Ni-doped perovskites recovered activity slightly faster than the Ni cermet catalyst. At 900°C, all three catalysts showed rapid recovery while no evidence of recovery at 700°C was observed.[13]

In this chapter, regeneration behaviours of LCZ pyrochlores have been investigated with different metal dopants and preparation methods. The effect of the initial concentration of H_2S and temperature on the recovery was determined after H_2S removal under the conditions of 2:1 methane to carbon dioxide.

6.2 -Effect of temperature:

To investigate the effect of temperature on catalyst recovery, the catalyst was poisoned at 850°C, and 10 ppm H_2S. After losing activity, the H_2S was removed from the reaction stream and the recovery experiment was performed at three different temperatures. The

first temperature was at 850° C. This starting temperature was selected to illustrate how only the H_2S removal would be sufficient to recover the catalyst. After 20 hours of recovery at 850 °C, the temperature was dropped to 800 °C and the reaction was performed for 72 hours. To study the effect of high temperature on recovery, the experiment was performed at 900 °C for 20 hours. The aim of these variable temperature changes was to find the stability of the catalyst, its ability to recover and the best recovery temperature

6.2.1 Recovery of 0.25 NiLCZ catalyst (Hydrothermal method)

Fig 6- 1 displays both the poisoning and recovery phase over 0.25 Ni-LCZ catalyst. As can be seen the catalyst did not reach full H_2S poisoning and at the end of 2 hours of poisoning the catalyst showed steady reforming activity. At this point, the H_2S source was removed and cycling reforming behaviour was seen in two kinds of micro and macro cycling patterns.

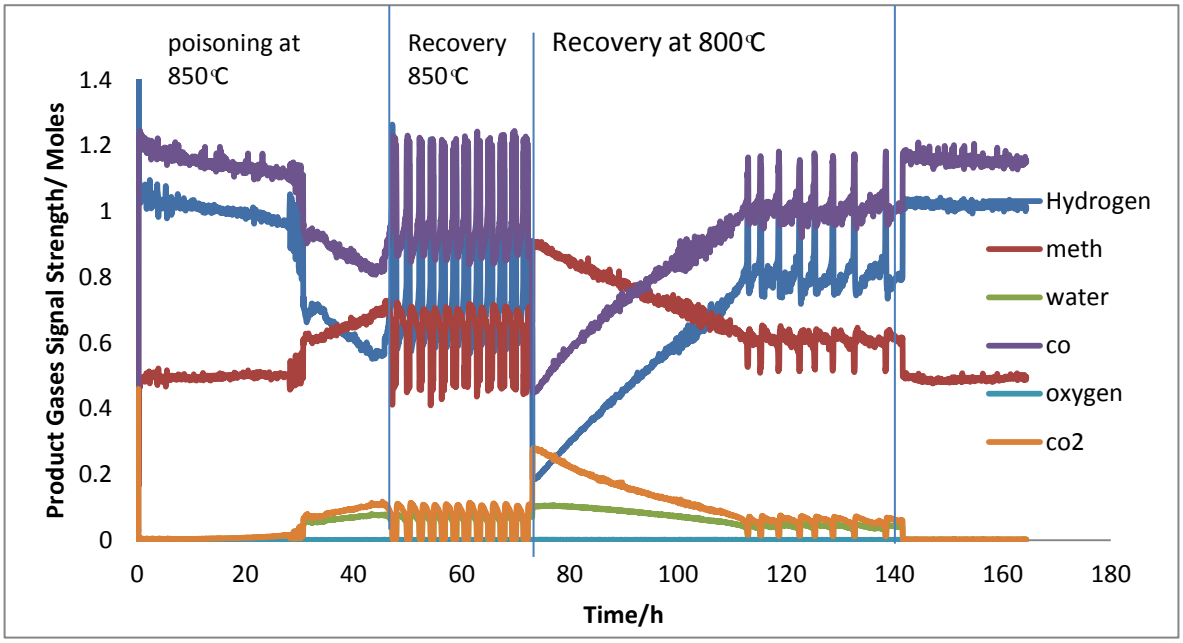

Fig 6-1- sulphur poisoning -recovery reaction profile of 2:1 CH_4/CO_2 ratio passed over 0.25NI-LCZ at various temperatures and initial poisoning temperature of 850℃ with 10 ppm H_2S

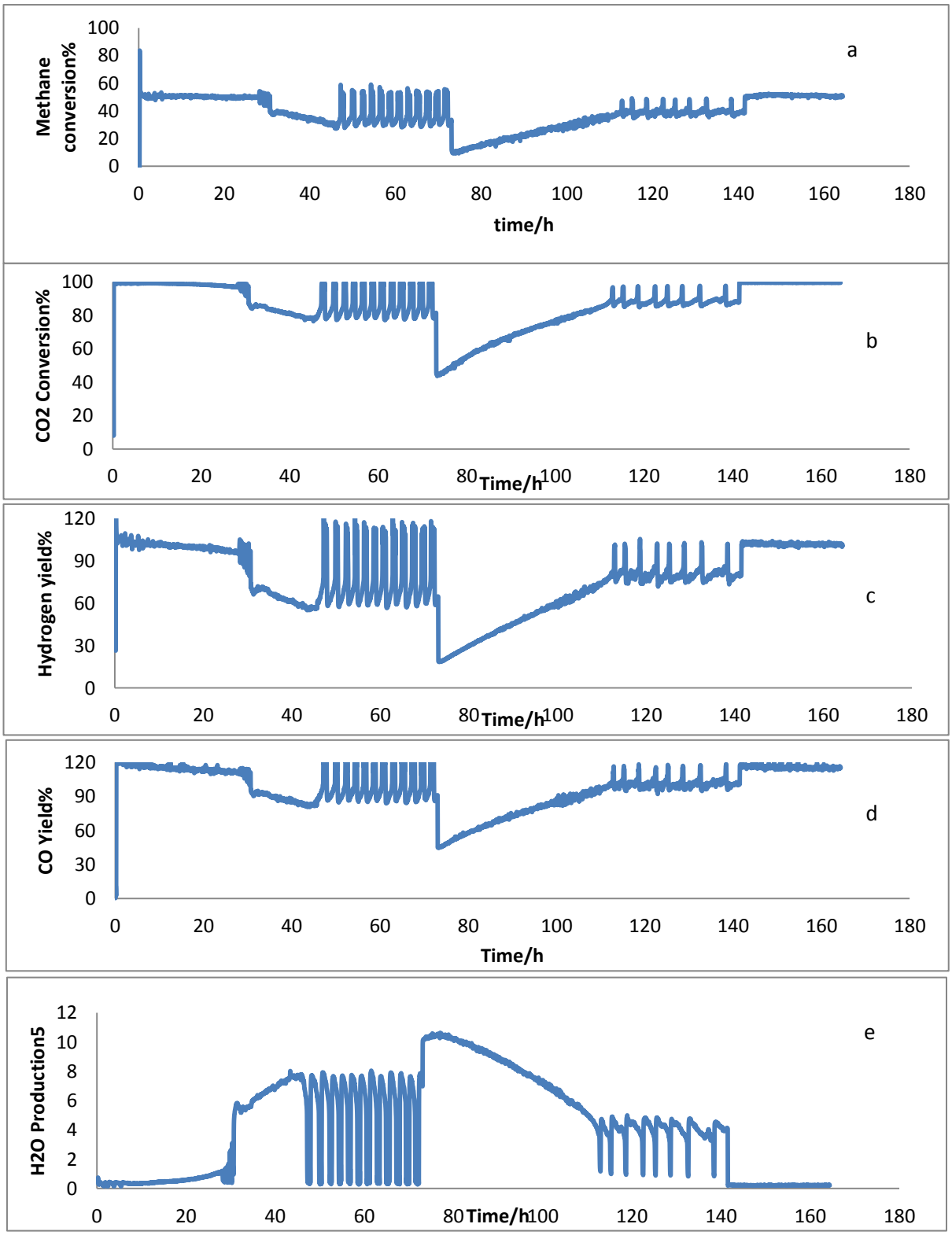

Fig 6- 2-sulphur poisoning- recovery profile of a) CH_4 conversion, b) CO_2 conversion, c) H_2 yield, d) CO yield and e) water production using 2:1 CH_4/CO_2 dry reforming with 10 ppm H_2S at initial poisoning temperature of 850°C and recovery at various temperatures

As was discussed previously; the last period of poisoning was combined with the formation of a protective layer of Ce_2O_2S. The amount of methane conversion was stable at approximately 30% and no more loss of catalytic activity was seen up to the end of the poisoning time. At 850^{o}C and after removing H_2S from the stream, the amount of Ce_2O_2S decreased gradually and the catalytic activity increased due to the cleaning of active sites from sulphur

Complete catalyst recovery was seen with several micro cycles because of transient oxidation and reduction of CeO_2. The presence of CeO_2 resulted in increased catalytic activity, while subsequently reduced Ce_2O_3 is inactive for methane reforming. When the amount of Ce_2O_3 increased over time, the following equation shifted to the right again resulting in a loss of catalytic activity.

$Ce_2O_3 + H_2S \leftrightarrow Ce_2O_2S + H_2O$……..eq2

This macro cycling behaviour due to adsorption-desorption of H_2S was continued in the shape of regular organizing patterns. The higher amount of CO by 20% during the recovery phase also could be attributed to the ability of ceria to oxidise the carbon which forms on the nickel surface from the methane decomposition step, which results in an increase in the amount of CO as follows: -

$2CeO_2 + C \leftrightarrow Ce_2O_3 + CO$…….eq3

Since the recovery step follows a reduction in the amount of H_2S throughout the progress of the reaction, as a result, total linear recovery can be expected without the macro cycling behaviour. When the recovery temperature dropped to 800 ° C, the catalyst lost its activity significantly. This severe deactivation can be attributed to H_2S adsorption, as it becomes more favourable thermodynamically at lower temperatures. The absence of Ce_2O_2S as a protective layer could also be the cause. After this sharp deactivation, the catalyst started to regenerate its activity gradually with no cycling behaviour observed. The amount of methane conversion reached 40%, with no more increase in activity seen and regular

cycling behaviour appearing in this step. By increasing the temperature to 900°C, the catalyst recovered its activity immediately. There was no evidence of cycling behaviour and the efficiency of reforming was 100%, with side reactions observed in this recovery stage.

It can be concluded that no damage occurred due to poisoning of the catalyst. The catalyst recovered its total activity by increasing the temperature. As can be seen in all reaction durations the amount of CO was higher by 20%. This can be attributed to the OSC properties of ceria which provides the O_2 to oxidize any carbon which is deposited on the nickel surface.

6.2.2 Recovery of 1- NiLCZ (Pechini method)

Fig 6-3 shows the poisoning and recovery profile of 1-NiLCZ which was prepared by the Pechini method. Poisoning at 10ppm of H_2S at 850°C followed by recovery at three different temperatures (80, 850 and 900°C) were investigated.

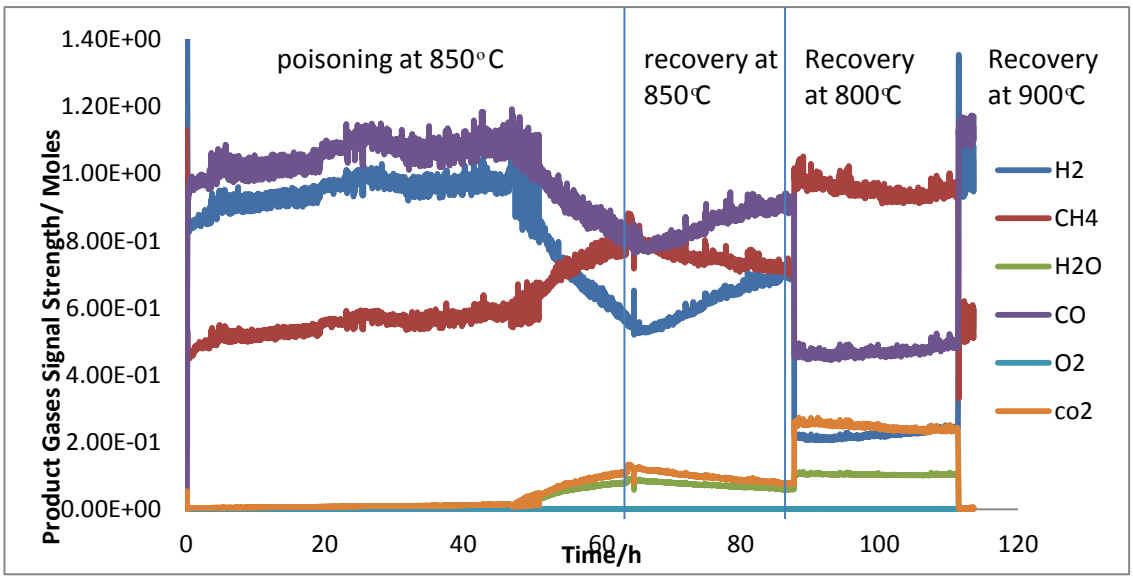

Fig 6-3- sulphur poisoning -recovery reaction profile of 2:1 CH_4/CO_2 ratio passed over 1NI-LCZ(Pechini.) at various temperatures and initial poisoning temperature of 850° C with 10ppm H_2S

Some stability was seen in the reforming reaction after 62 hours of poisoning. At this point, the H_2S source was removed and as is clear from fig 6- 3, that the CH_4 and CO_2 conversion increased quickly from the same endpoint of poisoning at a recovery temperature of 850°C. As the surface becomes covered by H_2S, desorption is energetically favourable by removing the H_2S and as a result a gradual increase in the reforming activity has occurred. As there is no evidence of a plateaued reaction, full recovery can be expected. The fact, that the amount of CO is higher than H_2 cannot be attributed to the reverse CO reduction reaction as the amount of water decreased over time. Therefore, the reason could be due to the presence of ceria in the structure in the form of Ce_2O_2S as shown by the following reactions.

$Ce_2O_2S + H_2O \leftrightarrow Ce_2O_3 + H_2S$…….eq4

$Ce_2O_3 + C \leftrightarrow 2Ce_2O + CO$……....eq5

A quick drop in reforming activity can be seen when the temperature of recovery was altered to 800°C. The absence of significant recovery in the methane conversion could be attributed to the thermodynamic and kinetic sulphur removal which becomes slower and less favourable at lower temperatures. Interestingly, although the amount of methane conversion was about 10%, the amount of CO_2 conversion was higher by 50%. The reason may be because of the reaction of CO_2 with H_2S

$H_2S + CO_2 \leftrightarrow H_2O + CO + 1/2S_2$…….eq6

This reaction can give a clear explanation of the fact that the water content is stable at 10% and the amount of CO is higher than H_2. At 900°C, rapid recovery of the reforming activity was seen due to the metal sulphide species being unstable at this reaction temperature. Complete recovery with a low level of cycling due to the presence of ceria was expected, and because of the reaction of carbon with oxygen, the amount of CO was higher by nearly 20%.

At the poisoning temperature of 850° C, no complete deactivation occurred, and the amount of methane conversion was about 20%, while at the recovery temperature of 800° C, this amount of CH_4 conversion dropped instantly at the beginning of recovery without any significant improvement in its recovery profile. This means that cerium even at the poisoning stage has an important protecting role on the Ni surface at the higher temperatures.

At 900° C, the catalyst recovered its total activity, so, it can be concluded that H_2S has no permanent effect on the performance of the catalyst and the catalyst is highly stable.

6.3 The effect of Ni content on recovery: -

After finding the best temperature for recovery, it is time to see how the amount of nickel would affect the recovery process. The experiments were performed on three Ni catalysts of (0.25-Ni, 0.5Ni, 1-Ni) LCZ at a poisoning temperature of 700° C with 30 ppm H_2S. After 20 hours of poisoning; the recovery process was applied by removing the H_2S from the stream and increasing the temperature to 900° C.

As can be seen from fig 6- 4, the catalyst with a higher amount of Ni, had lower recovery activity. This is because there is a greater amount of sulphur adsorbed on the larger amount of Ni and this resulted in a longer time to recovery.

As the second stage of poisoning on 0.25 Ni-LCZ occurred faster than on 0.5 Ni-LCZ, the cerium oxide sulphide did not have sufficient time to protect the Ni surface from sulphur poisoning. This led to a delay in the time of recovery in comparison with the 0.5 Ni-LCZ catalyst. After the recovery reached its equilibrium state of methane-rich dry reforming, all three catalysts showed the recovery behaviour in the shape of micro and macro cycling at all periods of recovery time. Macro cycling, as was discussed before, was due to the conversion of Ce_2O_2S to Ce_2O_3 and micro cycling was because of redox properties of

ceria. Generally, it is clear from all reaction profiles of reactant and product , that decreasing the amount of Ni in the catalyst improves the efficiency of recovery.

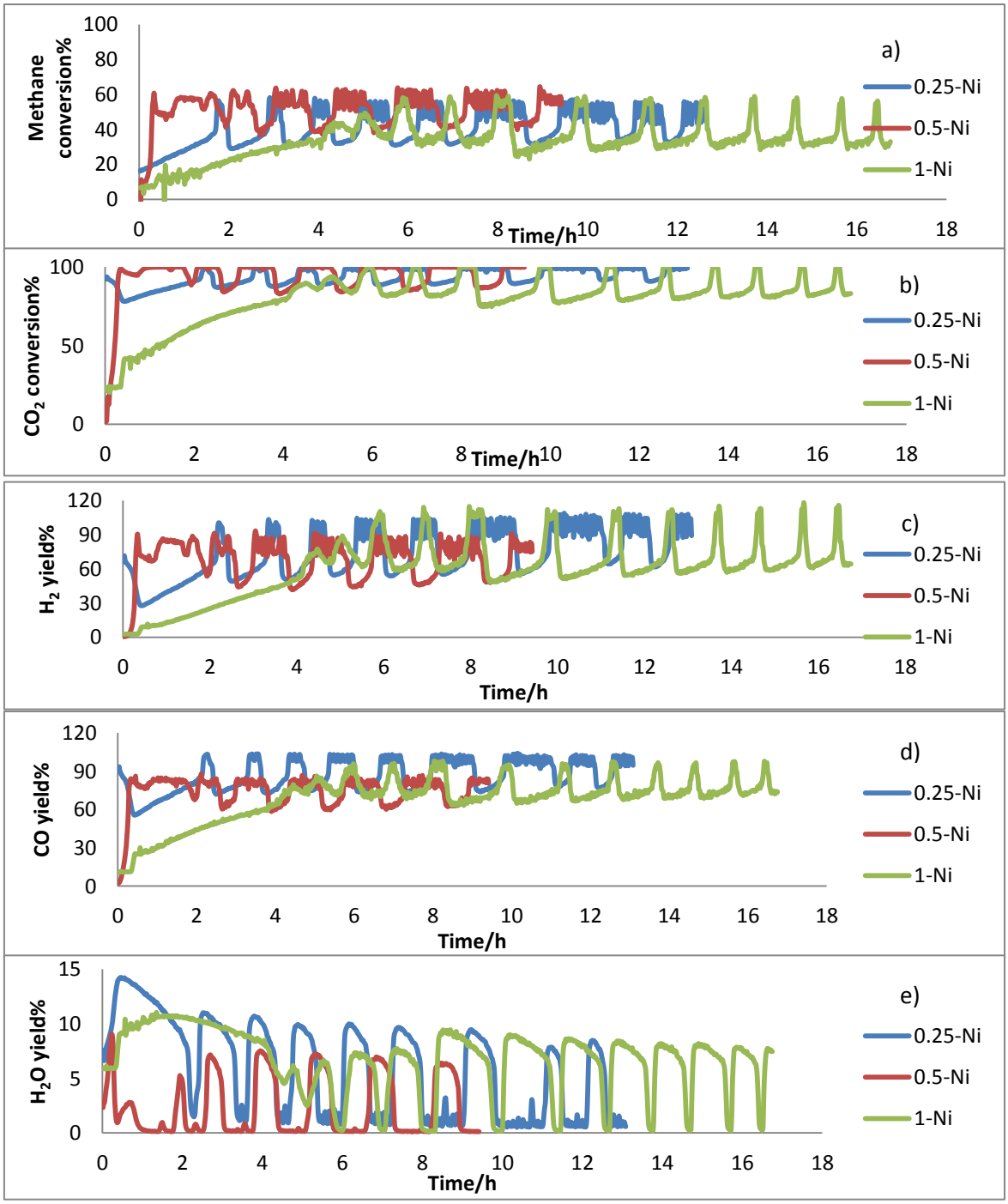

Fig 6-4 recovery profile of a) CH_4 conversion, b) CO_2 conversion, c) H_2 yield, d) CO yield and e) water production using 2:1 CH_4/CO_2 dry reforming with 30 ppm H_2S at initial poisoning temperature of 700℃ and recovery at 900℃

6.4 The effect of initial H_2S concentration on recovery

To investigate the influence of initial H_2S concentration on the recovery behaviour of the Ni-LCZ pyrochlore, experiments were carried out at different initial concentrations of H_2S (10 ppm and 30 ppm). The catalyst deactivation was achieved under the condition of CH_4: CO_2 =2:1 and the temperature of 700° C. After the poisoning reaction, the H_2S was removed from the reaction stream and the reaction temperature was increased to 900°C.

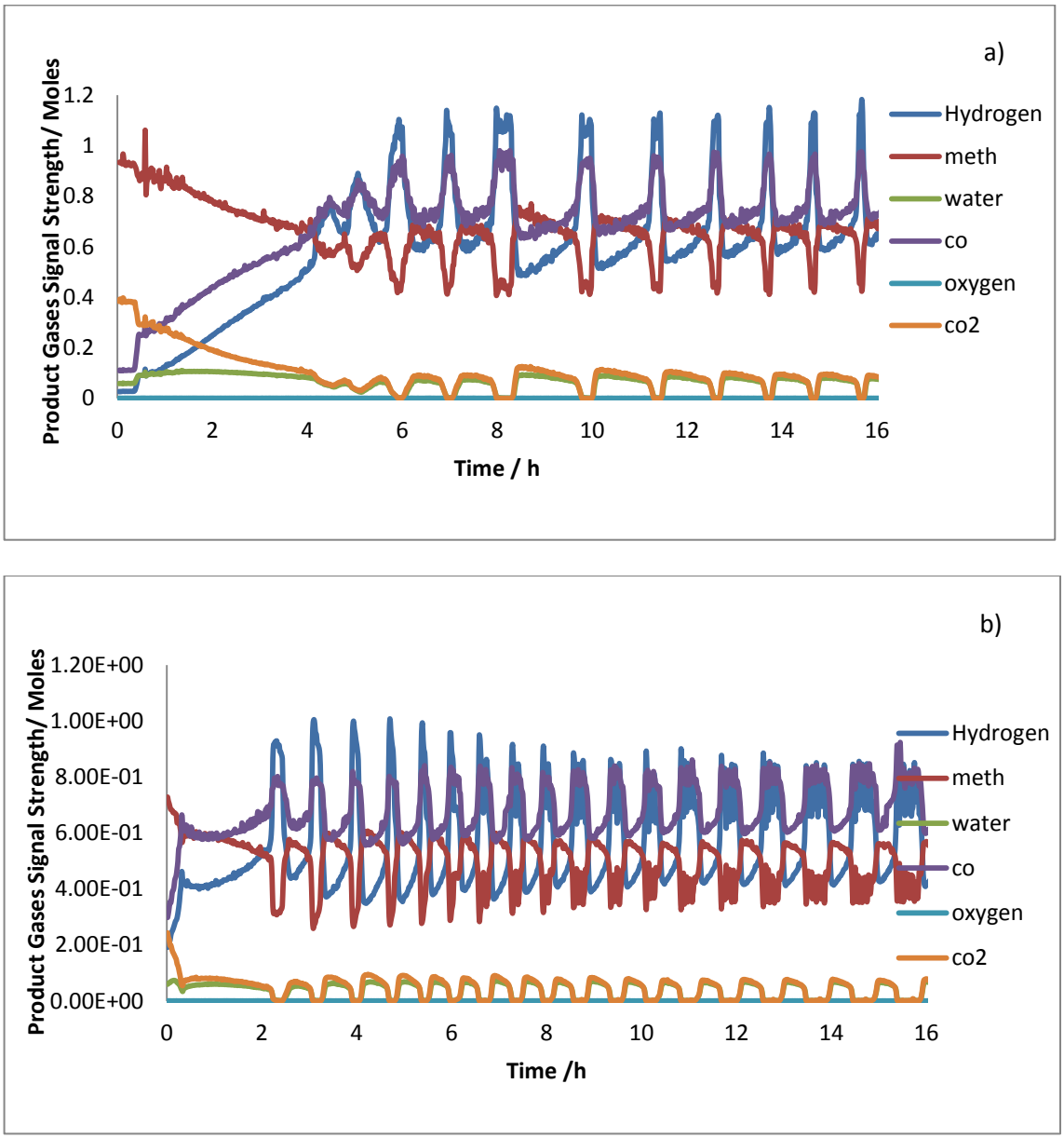

Fig 6-5- sulphur recovery reaction profile of 2:1 CH_4/CO_2 ratio passed over 1Ni-LCZ (Hy.) at temperature of 900°C and initial poisoning temperature of 700°C with a) 30 ppm b) 10 ppm

As can be observed from fig 6- 5, both catalysts have almost the same recovery trend. The main difference is in the time it took for recovery to reach the equilibrium state. The recovery time took longer when the H_2S concentration was greater. Both catalysts showed an instant linear recovery but the starting point for 10 ppm H_2S was higher by 20%. The catalyst exposed to 10 ppm H_2S reached its equilibrium state after 2 hours, while the other one took 4 hours. Both catalysts after reaching their equilibrium state showed cycling recovery behaviour. The last 10 hours of the recovery profile for 30 ppm H_2S exposure was very similar to the period of 2 to 7 hours of the 10 ppm H_2S profile. The extent of each macrocycle increased with time and the length of each cycle decreased where, linear behaviour would be expected. In both sulphur concentrations, the amount of CO was higher than the amount of H_2 and interestingly at the stage of micro cycling; the amount of H_2 was higher. This behaviour reversed over time and at both micro and macrocycles, the amount of CO became greater. This micro and macro cycling behaviour, as explained before, is due to the redox and H_2S adsorption-desorption properties of ceria.

It can be concluded that when the concentration of H_2S is high, more time will be needed for the catalyst to recover completely.

.

6.5 The effect of preparation method and metal on recovery

To determine how the recovery from H_2S poisoning is affected by the preparation method and the kind of active metal, experiments were performed on three catalysts: Ru-LCZ and 1-NiLCZ prepared by both the hydrothermal and Pechini method. Each catalyst was poisoned with 30 ppm H_2S under the reaction temperatures of 700° C and 850° C. The recovery temperature was 900° C and was applied after the poisoning stage.

6.5.1 Recovery from low initial poisoning temperature (700 ° C)

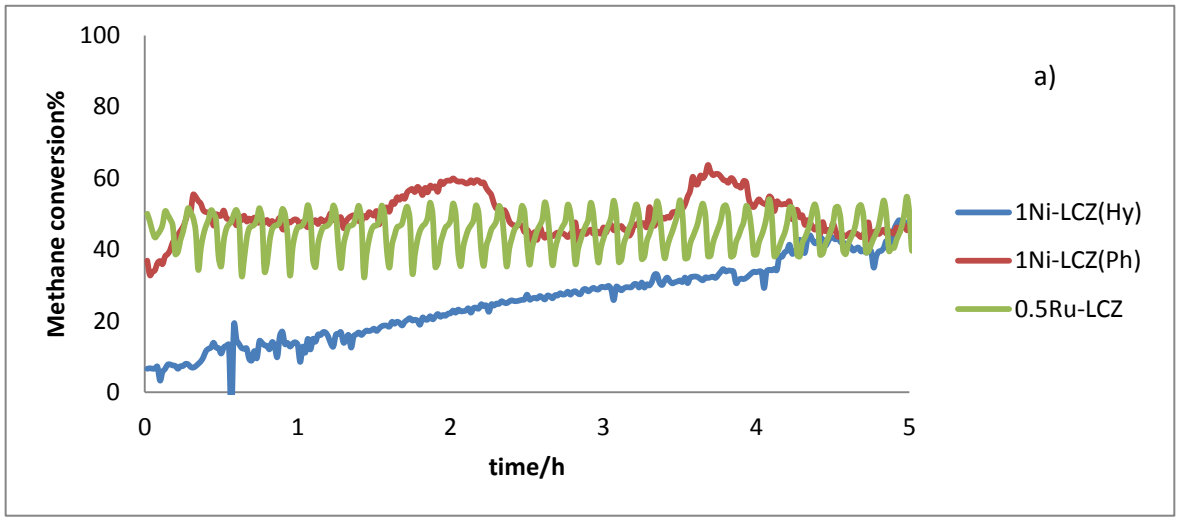

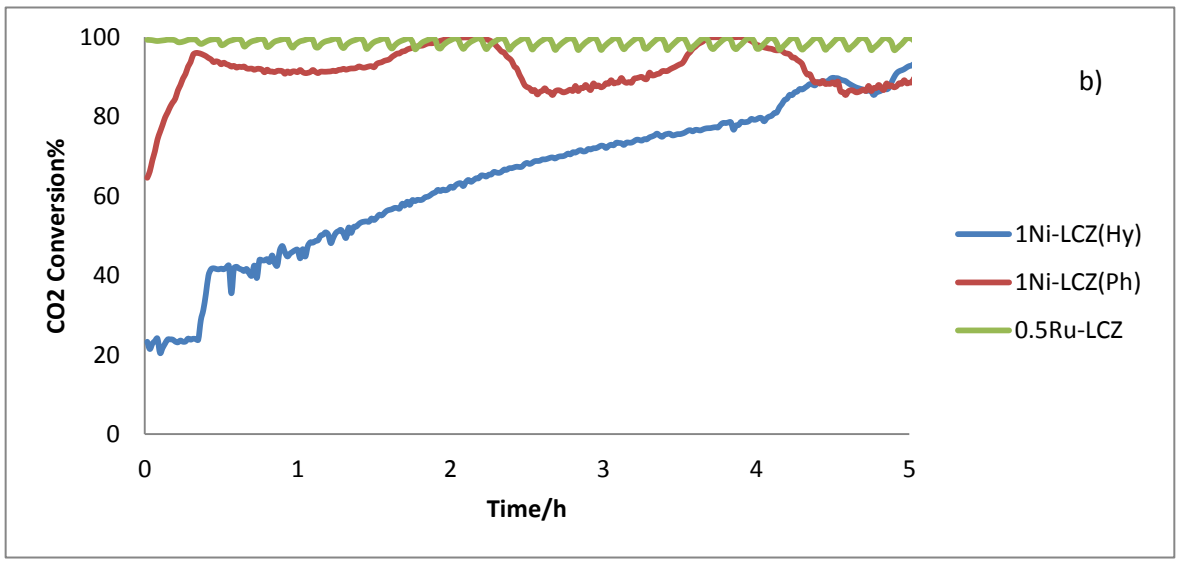

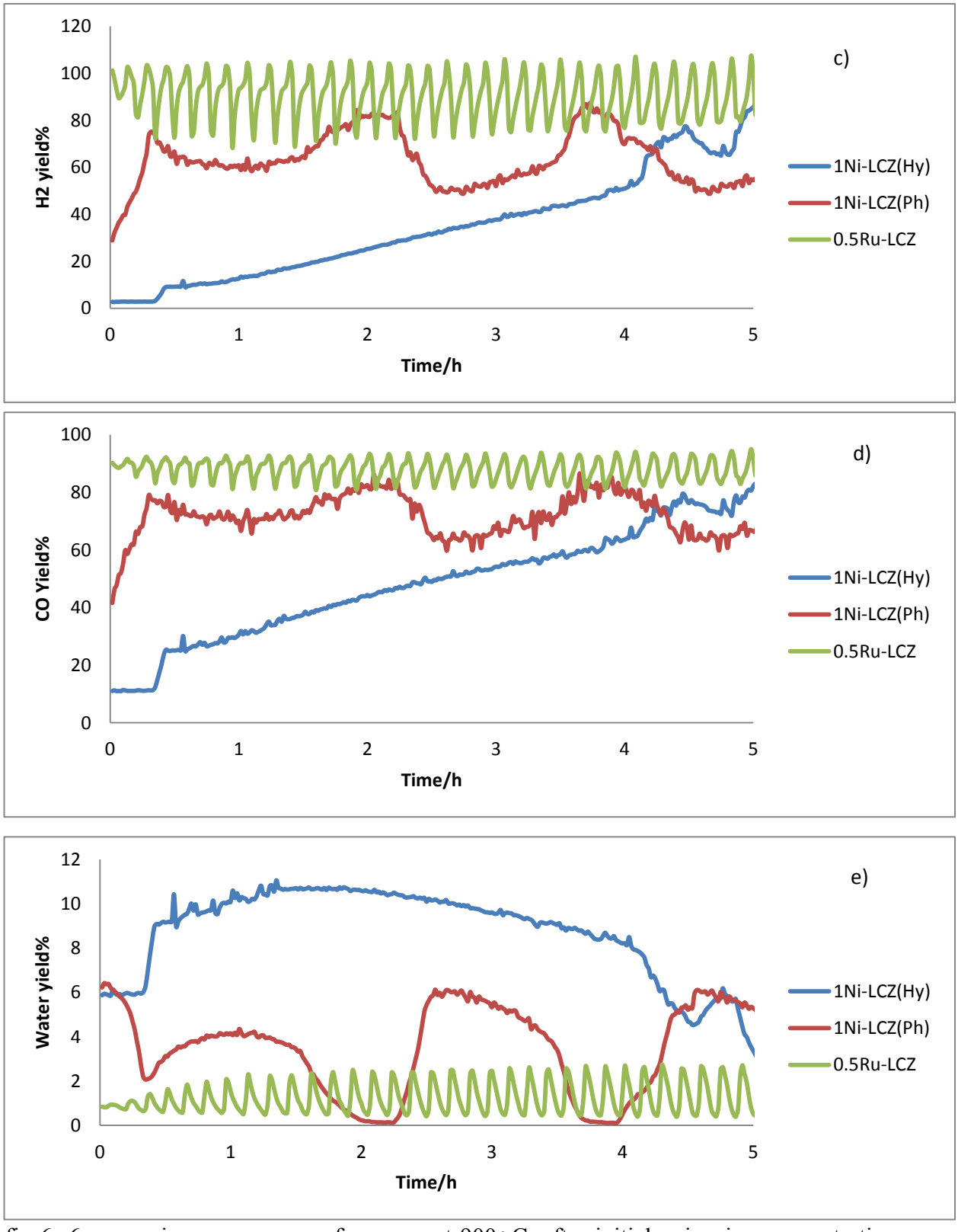

fig 6- 6-comparison recovery performance at 900° C, after initial poisoning concentration of 30ppm H_2S and reaction temperature of 700° C. a) Methane conversion b) CO_2 conversion c) H_2 yield d) CO yield e) H_2O yield

Regardless of the cycling behaviour, it was no surprise that the 0.5Ru-LCZ showed an immediate recovery and at a starting point of 50% CH_4 conversion, but what was interesting was the recovery performance of the 1NiLCZ, which was prepared by the Pechini method. Although this catalyst contains Ni metal in its structure, the initial starting point was 40% methane conversion and in less than an hour it reached a state of equilibrium of 50% and showed wide cycling behaviours, unlike the Ru catalyst, which showed severe cycling behaviours.

The starting methane conversion point of 1 Ni-LCZ (hydrothermal method) was less than 10%. A slow gradual linear increase was seen in the recovery process where after about five hours the catalyst reached its equilibrium state in the form of cycling behaviour. In the case of CO_2 conversion, all catalysts showed a good relationship with methane conversion. The H_2 and CO yields correlated well with the CH_4 and CO_2 conversions for the catalysts Ru-LCZ and Ni-LCZ (hydrothermal method). As observed from Fig 6-6(c, d), the amount of H_2 and CO yield of the Ni-LCZ (Pechini) was lower than expected by 20% at all recovery periods. The CO reduction reaction could be the cause of this decrease in addition to the water gas shift reaction.

$H_2 + CO \leftrightarrow H_2O + C$…...eq7

$H_2 + CO_2 \leftrightarrow H_2O + CO$…eq8

It can be concluded that, in the case of the methane conversion, all three catalysts reached their total conversion ratio in the form of cycling. As was proved before, this cycling behavior will diminish over time as Ce_2O_2S is the reason for this behavior. In the case of the H_2 yield the Ni-LCZ (Pechini) catalyst showed a 20% lower amount than expected, unlike other catalysts that showed a good relationship with CH_4 conversion. The nickel catalyst, prepared by the hydrothermal method, took more time to reach its equilibrium state.

6.5.2 Recovery from high initial poisoning temperature (850 ° C)

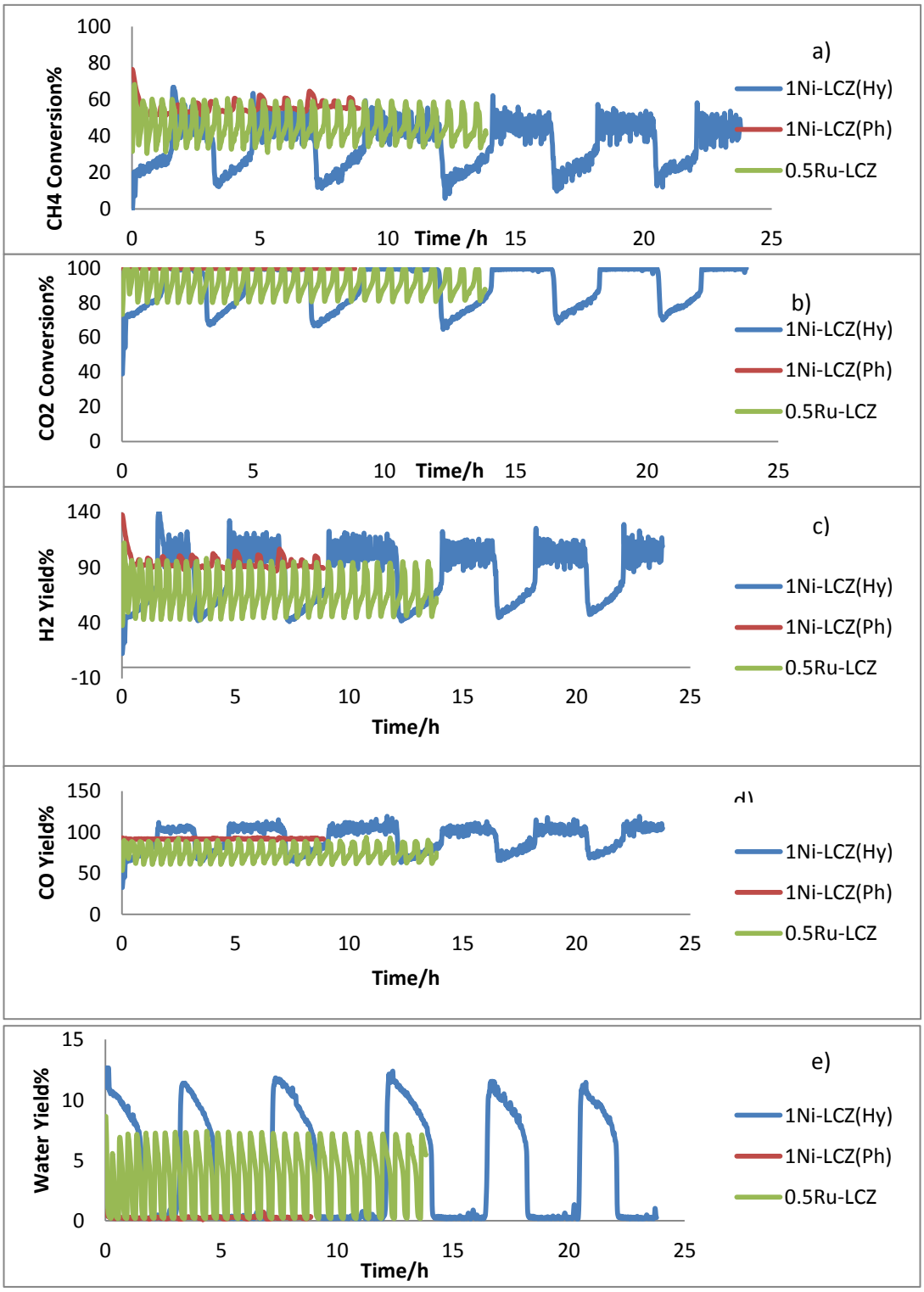

Fig 6- 7-comparison recovery performance at 900° C, after initial poisoning concentration of 30 ppm H_2S and reaction temperature of 850° C. a) Methane conversion b) CO_2 conversion c) H_2 yield d) CO yield e) H_2O yield

As can be observed from the recovery profiles of all three catalysts (fig 6-7), the Pechini preparation method showed more stability in its recovery behaviour. The starting point of the CH_4 conversion was as high as 70% and this amount decreased sharply in half an hour to 50%, and the recovery continued in the form of some low-level unorganized cycles and with an average methane conversion of 55%. The amount of CO_2 conversion for this catalyst was 100% and the average H_2 and CO yields were 97% and 90% respectively. The lack of water in the reaction confirms that the efficiency of the Ni-LCZ (Pechini) towards recovery is higher than for other catalysts.

There was also marked difference when the method of preparation was changed to the hydrothermal method. The starting point of methane conversion was 20% and regular cycling behavior was seen over time and the average of the methane conversion was 35%. The amount of CO_2 conversion was 90% which was higher than expected by 20%. The CO yield was 92% which was in good correlation with the CO_2 conversion. The presence of a higher amount of hydrogen by 15% in spite of the lower amount of CH_4 conversion could be because of the presence of Ce_2O_2S as a protective layer. In the presence of H_2S the main reaction in the second period of poisoning was $Ce_2O_3 + H_2S \leftrightarrow Ce_2O_2S + H_2O$, therefore by stopping sulphur from the stream the reaction shifted to the left. As H_2S at high temperature can dissociate and react with CO_2, the amount of CO_2 conversion increased in addition to the H_2.

$H_2S + CO_2 \leftrightarrow H_2O + 1/2S_2 + CO$……..eq6

$H_2S \leftrightarrow 1/2S_2 + H_2$……eq9

The Ru-catalyst showed severe regular cycling recovery behaviour. The average methane conversion was 45% and the CO_2 conversion was in good correlation with the CH_4 conversion. As can be observed from the H_2 and CO yields, this catalyst produced the lowest amount of H_2 and CO (68% and 75% respectively). The CO reduction reaction could be behind this decrease as the amount of CO and H_2 decreased in the same trend and

nearly in the same amount. The higher amount of CO in comparison to H_2 by 10% is because of the presence of Ce_2O_2S as was explained previously.

From all the above discussion, it can be shown that the Pechini preparation method has a positive effect on the recovery process and the presence of cerium in the catalyst has an impact on recovery behaviour. At high temperature, the Ru containing catalyst encouraged CO reduction reaction resulting in a reduced H_2 yield.

6.6 Conclusion:-

As one important property of the catalyst is the ability to recover, this chapter has focused on the ability of Ni, Ru LCZ pyrochlores to recover from H_2S poisoning with the aim of using these materials as the anode in a SOFC or as a biogas reforming catalyst.

The recovery at 900 °C after poisoning with 10 ppm H_2S was faster than with 30 ppm H_2S. The starting point of the methane conversion was 35%, and the catalyst reached its equilibrium state after 2 hours. No methane conversion was seen at the beginning of the reaction with 30ppm H_2S and it took 5 hours to reach its equilibrium state. After H_2S removal, the equilibrium state was in the form of cycling at both concentrations.

After poisoning with 30 ppm H_2S at 700 °C, 0.25Ni-LCZ showed higher methane conversion than 1NiLCZ by 10%, while 1 Ni-LCZ reached the equilibrium state after 6h that was later than 4h in comparison with 0.25-NiLCZ. However, the best recovery profile was seen in the 0.5 Ni-LCZ catalyst, that only took 30 minutes.

The Ru catalyst showed immediate recovery reaching equilibrium state in the form of severe organised cycling after poisoning in 30 ppm H_2S at 700 °C. The Pechini 1-NiLCZ showed better stability with wider cycling after 30 minutes from H_2S removal, while the hydrothermal 1- NiLCZ took more than 5 hours to reach the equilibrium state. H_2 was in good correlation with CH_4 in both the Ru and the hydrothermal catalyst while it was 20% lower in the Pechini method prepared catalyst.

The effect of recovery temperature was determined after poisoning in 10 ppm H_2S at 850 °C. At 850 °C, the hydrothermal catalyst showed immediate recovery reaching the equilibrium state in the form of organised cycling behaviour. At 800 °C, a gradual increase

in recovery was observed for 30 hours followed by cycling behaviour. Immediate recovery with no cycling was seen at 900^{o}C.

The effect of recovery temperature on the Pechini catalyst was different than the hydrothermal catalyst. Despite both catalysts showing direct recovery relationships with temperature, at 850^{o}C, the recovery increased gradually, and more than 30 hours was needed to reach its equilibrium state. At 800^{o}C, no significant recovery was seen for 20 hours, while at 900^{o}C, immediate recovery was observed in the form of low cycling behaviour.

6.7 References:-

1-Torres, W., Pansare, S.S. and Goodwin Jr, J.G., 2007. Hot gas removal of tars, ammonia, and hydrogen sulfide from biomass gasification gas. *Catalysis Reviews*, *49*(4), pp.407-456

2-Yung, M.M., Jablonski, W.S. and Magrini-Bair, K.A., 2009. Review of catalytic conditioning of biomass-derived syngas. *Energy & Fuels*, *23*(4), pp.1874-1887

3-Ma, L., Verelst, H. and Baron, G.V., 2005. Integrated high temperature gas cleaning: tar removal in biomass gasification with a catalytic filter. *Catalysis Today*, *105*(3-4), pp.729-734.

4-Rostrup-Nielsen, J.R., 1971. Some principles relating to the regeneration of sulfur-poisoned nickel catalyst. *Journal of Catalysis*, *21*(2), pp.171-178.

5-Li, L., Howard, C., King, D.L., Gerber, M., Dagle, R. and Stevens, D., 2010. Regeneration of sulfur deactivated Ni-based biomass syngas cleaning catalysts. *Industrial & Engineering Chemistry Research*, *49*(20), pp.10144-10148

6- Birss, V.I., Deleebeeck, L., Paulson, S. and Smith, T., 2011. Understanding performance losses at Ni-based anodes due to sulphur exposure. *ECS Transactions*, *35*(1), pp.1445-1454.

7- Smith, T.R., Wood, A. and Birss, V.I., 2009. Effect of hydrogen sulfide on the direct internal reforming of methane in solid oxide fuel cells. *Applied Catalysis A: General*, *354*(1-2), pp.1-7.

8- Nixon, D.J., 2013. Catalytic behaviour of nickel-based catalysts operating on simulated biogas: optimisation through oxygen addition, temperature variation and catalyst modification (Doctoral dissertation, Keele University).

9- Zha, S., Cheng, Z. and Liu, M., 2007. Sulfur poisoning and regeneration of Ni-based anodes in solid oxide fuel cells. *Journal of the Electrochemical Society*, *154*(2), pp.B201-B206.

10- Offer, G.J., Mermelstein, J., Brightman, E. and Brandon, N.P., 2009. Thermodynamics and kinetics of the interaction of carbon and sulfur with solid oxide fuel cell anodes. *Journal of the American Ceramic Society*, *92*(4), pp.763-780.

11- Brightman, E., Ivey, D.G., Brett, D.J.L. and Brandon, N.P., 2011. The effect of current density on H2S-poisoning of nickel-based solid oxide fuel cell anodes. *Journal of Power Sources*, *196*(17), pp.7182-7187.

12- Y. Matsuzaki, *Solid State Ionics*, 2000, **132**, 261–269.

13- Evans, S.E., 2017. *Catalytic reforming of biogas using nickel based perovskite materials* (Doctoral dissertation, Keele University).

7- Conclusion and future work: -

The aim of this work was to prepare new Ru and Ni-doped pyrochlore catalyst to be used as biogas reforming catalysts. The effect of preparation method on the reforming performance was evaluated, as the nature of the catalyst closely depends on the preparation method. The Ni-doped catalysts were prepared by the hydrothermal and the Pechini method while the Ru catalyst was prepared only by the hydrothermal method.

To find out whether the new Ni-doped pyrochlore catalysts could be promising catalyst for industry, they were compared with a Ru doped pyrochlore catalyst that has high activity and good resistance toward methane reforming conditions. The performance of all catalysts was evaluated based on their ability to suppress carbon formation and to resist sulphur poisoning, which are considered to be the most important issues in the biogas reforming process.

All catalysts were characterised by the XRD, TPR, SEM and BET techniques. From the XRD results, it can be concluded that all of the four catalysts contain a pyrochlore phase in their structures. However, the Ni pyrochlore catalysts prepared by the hydrothermal method showed spilt peaks that belonged to the mixture of Pyrochlore and $La/CeZrO_4$ oxide phases. The effect of Ni ratio on the phase formed within the catalyst was clear in the form of higher fluorite phase availability in the lower Ni loading catalyst in comparison with Pyrochlore phase. This may be because of cerium, which is no longer needed to balance the catalyst charge. All Ni pyrochlore catalysts showed an impurity in the form of NiO, which on increasing the amount of Ni loading made the peak easier to observe. The Ru containing catalyst, unlike the hydrothermal Ni catalyst, did not show the $La/CeZrO_4$ oxide phase in its profile.

TPR analysis showed all four catalysts are reducible and in comparison with the fresh catalyst, the reduction peak was shifted to higher temperature in the case of the hydrothermal Ni catalysts, while for the Pechini method the reduction peak shifted to lower temperature indicating some level of sintering. As-synthase Ru pyrochlore catalyst had higher reduction temperature in comparison with the used catalyst.

BET analysis showed that the Ni containing hydrothermal catalysts have a larger surface area in comparison with the catalyst prepared by the Pechini method and the Ru catalyst has the biggest particle size with the lowest surface area.

From SEM analysis, it was found that the hydrothermal method produces irregular agglomerate particles while the Pechini method generates rigid triangular plate particles with regular spherical uniform particles on the surface.

The temperature programmed reaction for the methane-rich dry reforming conditions showed that the 0.25Ni-LCZ has a lower starting temperature in comparison with the 0.5 and 1Ni-LCZ catalyst ratio by about 100 ℃. This was similar to both Ni-Pechini and Ru doped pyrochlore catalysts. In terms of the isothermal study at the temperature between 650 and 900 ℃, the 0.25-Ni catalyst showed high activity at 650 ℃ and the conversion of methane was in excess of what could be achieved by a 2:1 methane to carbon dioxide ratio. Higher methane conversion in the low Ni catalyst was likely due to the reaction of ceria with methane illustrating that Ceria showed the specific effect on lower Ni loading condition at the low temperature.

Generally, Ni-hydrothermal catalysts showed cycling behaviour in their dry reforming profiles. However, this behaviour decreased at the low reforming temperatures <800℃, and at the high ratio of Ni-doped (1Ni-LCZ). The amount of hydrogen increased with increasing the temperature and the amount of Ni in the catalyst, due to the thermodynamic

favourability and higher amount of activating sites for CH_4 conversion. CO reduction as a side reaction plays a significant role in decreasing the amount of H_2 at the low temperatures in both the 0.25 and 0.5 Ni-LCZ catalysts. At 850^o C, as DRM became more thermodynamically favourable, the yields became higher, giving almost 100% yields for all the Ni-hydrothermal catalysts.

All three catalysts showed a decrease in carbon deposition trend with temperature, as CO hydrogenation and the Boudouard reaction are thermodynamically more favourable at the lower temperatures.

At the low temperatures, a significant difference in the amount of deposited carbon was seen by increasing the amount of Ni in the pyrochlore structure. The 0.25-NiLCZ pyrochlore had the lowest amount of deposited carbon due to fewer nickel sites present for reaction with carbon, that formed as a result of Boudouard reaction. In addition the presence of higher CeO_2 increases the ability of the catalyst to oxidise carbon at the lower temperatures. At higher temperatures >700 °C, the deposited carbon was suppressed significantly, and the amount of nickel had no significant impact on carbon deposition. The presence of ceria increases the potential for carbon oxidation through increased oxygen availability.

In terms of the long stability experiments at 750 ℃ under methane-rich dry reforming conditions, the amount of CH_4 and CO_2 conversion were close to the stoichiometric ratio for both the 0.25 and 1-Ni-LCZ hydrothermal pyrochlore catalysts. The main difference between 0.25- NiLCZ and 1-NiLCZ was in the amount of syngas emission, where it was higher by nearly 20% for 1-Ni-LCZ. The decrease in the amount of CO and H_2 in comparison with 1-NiLCZ could be because of some side reactions from CO reduction (CO-R). During the DRM, the amount of H_2 was lower than CO because of the reverse water gas shift reaction. In addition, ceria can chemisorb large amounts of H_2 and CO. Both catalysts showed stability in performance without any deactivation over 3 days of reaction.

The amount of carbon deposition showed no real increase with time for both 0.25 and 1-Ni-LCZ catalysts, while increasing the amount of Ni at 750^{o}C did not show any effect on deposited carbon. One visible difference between the two catalysts is that the carbon peak shifts to higher temperature for 1-Ni-LCZ, indicating the presence of traces of carbonaceous species, while one major TPO peak at 500 °C for 0.25 -NiLCZ corresponds to a soft type of carbon since it can be oxidised under relatively mild conditions. This presence of soft carbon supports the hypothesis that small Ni domains available at the catalyst surface during the reaction. Therefore, the Ni particles of 0.25-NiLCZ remain small and well dispersed on the surface. The agglomeration of Ni clusters would lead to more graphitic carbon.

In the methane-rich dry reforming, both the hydrothermal and the Pechini Ni catalysts showed slightly higher CH_4 conversions than the Ru catalyst at the lower temperature. As the CO_2 conversion for both Ni catalysts decreased at the lower temperature, it suggests that the Boudouard reaction is occurring and is more likely on Ni catalysts than the Ru catalyst. As the amount of CO_2 increased due to the Boudouard reaction, the probability of methane conversion increased at the lower temperature. The selectivity of H_2 and CO in both Ni catalysts is lower than for the Ru catalyst at 650^{o}C due to the Boudouard reaction and CO reduction reaction causing an increase in water production. Ni containing catalysts prepared by the Pechini method showed the lowest syngas selectivity at the middle temperature. The Ru containing catalyst showed a 3% reduction in selectivity at 850^{o}C in contrast with other Ni containing catalysts due to the carbon deposition.

The hydrothermal 1Ni-LCZ pyrochlore catalyst has the highest amount of carbon deposition because of the Boudouard reaction and hydrogenation of CO at the lower temperature. The amount of carbon deposition was not significantly different at various temperatures on the Ni containing catalysts prepared by the Pechini method. At 850^{o}C, the Ru catalyst showed a low level of carbon deposition due to methane decomposition which affects catalyst activity.

The highest level of deposited carbon did not affect the Ni catalysts activity. It can be concluded that the amount of Ni that is not incorporated within the pyrochlore structure in the hydrothermal method was the reason for promotion of the Boudouard reaction and high activity of the catalyst at the middle temperature. The presence of cerium and the form and structure of the catalyst play an essential role in catalyst activity. Ru containing catalysts support methane decomposition and Ni containing catalyst support the Boudouard and CO reduction reactions. By decreasing the ratio of Ni in the hydrothermal LCZ catalysts, the amount of carbon deposition decreased and it can be said that the hydrothermal preparation method had no adverse effect at the lower temperature, however controlling the Ni amount has to be done carefully to achieve the best results.

The reactions over time at different temperatures under stoichiometric conditions for the 0.25, 0.5 and 1Ni-LCZ catalysts showed almost similar patterns.

In the isothermal reactions, generally, 0.5Ni-LCZ showed higher activity in comparison with the others. At the low temperature, because of the low loading of Ni in the 0.25Ni-LCZ catalyst, the CH_4 conversion was lower than other catalysts. However, the 0.5Ni-LCZ catalyst had higher conversion than the 1Ni-LCZ catalyst due to the more significant amount of deposited carbon on 1Ni-LCZ that blocks the Ni active sites.

Due to the lowest loading of Ni, the 0.25Ni-LCZcatalyst had the lowest amount of deposited carbon at all temperatures. At 800^{o} C, despite the amount of CH_4 and CO_2 conversion in 0.25 Ni-LCZ being the same as for the other catalysts, the amount of synthesis gas showed a dramatic decrease. The CO reduction reaction could be the reason for this decrease and the amount of carbon deposition at 750 °C and above is negligible for all three catalysts.

Despite the highest levels of carbon deposited being on the Ni-hydrothermal catalysts, in comparison with other catalysts, the Pechini Ni catalyst had the lowest productivity at all temperatures for 1:1 CH_4: CO_2. The Pechini Ni catalyst promotes the RWGS reaction significantly, in addition to the methane coupling reaction. In the stoichiometric condition, the Ni containing hydrothermal catalyst showed almost similar activity with the Ru containing catalyst.

The Ru containing catalyst did not show significant carbon deposition at any temperatures while both Ni containing catalysts showed noticeable carbon at 650 ℃ and the catalyst prepared by the Pechini method contained 10 times less deposited carbon than the hydrothermal Ni pyrochlore catalyst.

While all prepared catalysts did not show significant deactivation because of the carbon deposition , it was important to show their ability to resistance sulphur impurities present in hydrocarbon fuels to be promising commercial anodes for SOFC.

Deactivation is affected by the amount of Ni in the catalyst and accelerated by decreasing the amount of Ni in the catalyst. For example 0.25Ni-LCZ, due to having less active Ni sites showed faster deactivation. Generally, the Pechini preparation method showed higher resistance to deactivation than the hydrothermal method. This resistance may be due to the morphology of the catalyst. Because of the high activation energy for the catalyst process with Ru in comparison with Ni, the loss of reforming activity was significantly lower than in the Ni catalysts.

All pyrochlore catalysts in this work regardless of the preparation method and the type of doped metal have shown two stages of reforming activity loss. The first stage is because of dissociative chemisorption of H_2S and the second stage of deactivation is linked to the formation of bulk metal sulphide species. By increasing the temperature, generally, the first stage deactivation accelerates in all materials due to the reacting of one sulphur with more

than one active site at a time. The first deactivation stage was significantly faster in 30 ppm H_2S than 10 ppm due to a dramatic decrease in active sites.

The CO_2 conversion correlated well with the CH_4 conversion in the Ru catalyst, while all the Ni-doped pyrochlore catalysts showed higher CO_2 conversion due to the reaction of cerium and CO_2 with H_2S. All Ni-doped catalysts encouraged the CO reduction reaction that decreased the amount of H_2 and increased water formation.

The cycling behaviour in the reforming profiles were affected by the Ni amount, catalyst preparation method, concentration of H_2S, temperature and the metal-dopant. By increasing the poisoning temperature, the cycling behaviour increased in both the Ni-Pechini and low content Ni-hydrothermal catalysts. The decrease in the H_2S concentration increased the cycling behaviour because of the redox properties of cerium. The Ru catalyst showed high stability in its reforming profile at the high temperatures and in the low H_2S concentration.

In the Ni containing materials, the amount of carbon deposition increased with decreasing temperature, unlike the Ru containing catalyst that showed a direct relationship. In the case of the Ni containing catalysts, the amount of carbon deposition increased with increasing H_2S concentration, while higher carbon was deposited on the Ru containing catalyst in the low H_2S concentration. A lower amount of carbon was deposited on the Pechini method catalyst than the hydrothermal method. At the lower temperature, the amount of carbon deposition was nearly at the same level as the Ru containing catalyst.

As one important property of the catalyst is the ability to recover, the recovery results after deactivation by sulphur showed that complete recovery can be achieved in all materials by H_2S removal at 900 °C. The recovery at 900^{o}C after poisoning with 10 ppm H_2S was faster

than with 30 ppm. After H_2S removal, the equilibrium state was in the form of cycling for both concentrations.

After poisoning in 30ppm H_2S at 700 °C, 0.25Ni-LCZ showed higher methane conversion than 1NiLCZ by 10%., while 1 Ni-LCZ reached the equilibrium state after 6h, which was 4h later than for 0.25-NiLCZ. However, the best recovery profile was seen in 0.5 Ni-LCZ that only took 30 min.

The Ru catalyst showed immediate recovery reaching the equilibrium state in the form of severe organised cycling after poisoning in 30ppm H_2S at 700 °C. The Pechini 1-NiLCZ catalyst showed better stability with wider cycling after 30min from H_2S removal, while the hydrothermal 1-NiLCZ catalyst took more than 5h to reach the equilibrium state. H_2 was in good correlation with the CH_4 in both the Ru and the hydrothermal Ni containing catalysts while it was 20% lower in the Pechini method catalyst.

The effect of recovery temperature was determined after poisoning in 10ppm H_2S at 850 °C. At 850 °C, the hydrothermal catalyst showed immediate recovery reaching the equilibrium state in the form of organised cycling behaviour. At 800 °C, a gradual increase in recovery was observed for 30h followed by cycling behaviour, whilst immediate recovery with no cycling was seen at 900 °C.

The effect of recovery temperature on the Pechini catalyst was different from the hydrothermal catalyst. Despite both catalysts showing a direct recovery relationship with temperature, at 850 °C the recovery increased gradually and more than 30 h was needed to reach its equilibrium state. At 800 °C no significant recovery was seen for 20h, while at 900 °C immediate recovery was observed in the form of low cycling behaviour.

Generally, the Ru containing catalyst did not show complete deactivation for more than 20 h under any conditions even at the low temperature of 700°C and high concentration of 30ppm

H_2S. This material could be a unique catalyst that shows this high resistance in comparison with other literature materials in this condition and therefore may be promising as a SOFC anode.

For decreasing the cost of catalyst, using the Ni-LCZ catalyst is an alternative to the Ru containing catalyst at 900℃ in the presence of 30ppm H_2S.

Future works: -

- As cycling behaviour is closely dependent on the presence of ceria in the structure of the catalyst, it would be useful to study the effect of ceria ratio on cycling behaviour to limit it.
- As increasing the amount of Ni, led to increase the performance of the catalyst without a significant increase in the carbon deposition at the temperatures higher than 800 ℃, it would be useful to increase the amount of Ni in the structure and study the catalytic performance and stability.
- Evaluate the catalytic performance by using real biogas from landfill sites that have a different ratio of CH_4: CO_2 in addition to natural contaminants.
- Testing the electrical and ionic conductivity of the materials as an anode in solid oxide fuel cells.
- Further study into the characterization and understanding of the structure and the kind of the impurity phases and how dopants can be full incorporated into the structure.
- Testing other reforming reactions such as partial oxidation, steam reforming, bi and tri reforming.